# HOW TO ACHIEVE FUNCTIONAL THERAPEUTIC ANGIOGENESIS: LESSONS FROM IN VIVO GENE TRANSFER USING AAV VECTORS

**PhD thesis**
**SISSA/ISAS**
**2005**

*Serena Zacchigna*

Supervisor: Prof. Mauro Giacca
External examiner: Prof. Peter Carmeliet

# INDEX

# 1. SYNOPSIS

The work described in this thesis has been mainly focused on the dissection of some of the fundamental mechanisms underlining new blood vessel formation in vivo. More precisely, a gene transfer approach, based on Adeno-Associated Virus (AAV) vectors, has been exploited for the sustained and prolonged expression of several factors involved in angiogenesis and arteriogenesis.

Bearing in mind the key role of Vascular Endothelial Growth Factor (VEGF) in the angiogenic process, we decided to thoroughly investigate the morphology and the functional performance of the VEGF-induced vasculature, by taking advantage of molecular imaging techniques, such as PET and SPECT, which allowed a non invasive assessment of vascular function over time. Starting from the observation that VEGF single gene transfer is not sufficient to drive the formation of functional blood vessels, we showed that the simultaneous delivery of Angiopoietin-1 (Ang1) allowed an improved remodeling and maturation of the newly formed vasculature. This finding is of particular interest in a clinical perspective, suggesting that the delivery of a proper combination of growth factors, which is feasible and particularly straightforward with the use of AAV vectors, is probably required to fulfill the goal of therapeutic angiogenesis.

By studying the in vivo effect of VEGF, particular emphasis was attributed to the distinct biological effect specifically exerted by the two main VEGF isoforms, composed of 121 and 165 aminoacids, respectively. Since the main structural difference between the two isoforms consists of their diverse ability to bind the co-receptor NP-1, we also assessed the effects induced by the overexpression of Semaphorin 3A (Sema3A), a well known NP-1 ligand in the developing nervous system. Collectively, these data provided convincing evidence of a massive recruitment of mononuclear cells from the bone marrow to the sites of neoangiogensis through NP-1. Although these cells did not seem to directly participate to new blood vessel formation through transdifferentiation, they turned up to have a key role in promoting arteriogenesis.

A schematic representation of the molecules studied in this work, and their ability to bind to the relative receptors, is shown in Figure 1.1.

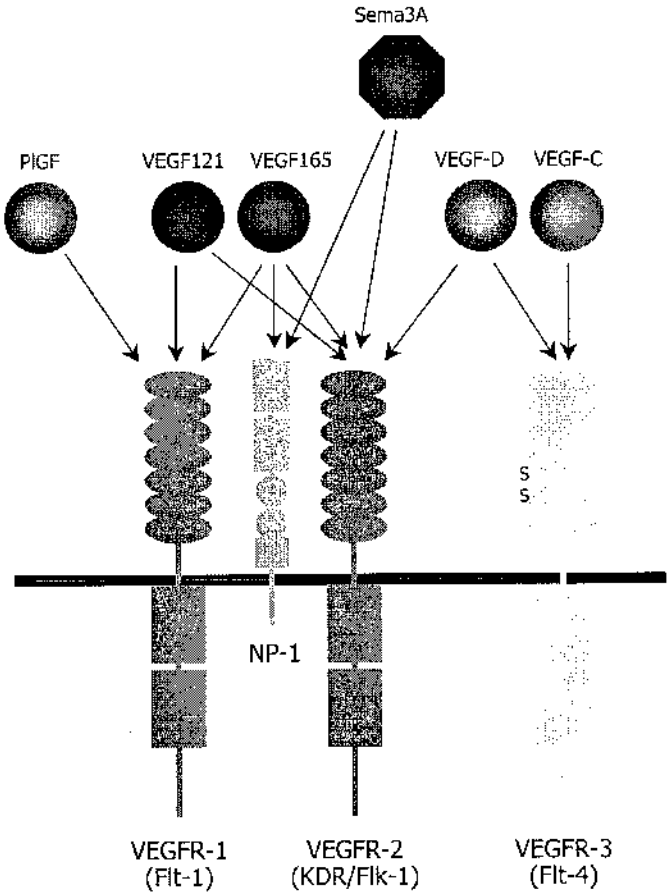


**Figure 1.1. Main ligands and TKRs involved in angiogenesis.** The picture schematically describes the most important interactions of the factors studied in this work with their receptors. In dark red are the molecules, whose cDNA have been cloned in AAV vectors to dissect their biological effect in vivo.

# 2 . INTRODUCTION

## 2.1 MECHANISMS OF BLOOD VESSEL FORMATION

The vascular system in all vertebrate species is composed of an extensive and complex network, which is spatially organized to provide the finest exchange of gas and metabolites from blood to tissues throughout the body.

At least two mechanisms exist to explain the de novo formation of blood vessels (Isner, 1999) (Figure 2.1). During embryonic development, a process called vasculogenesis involves the formation and the fusion of multiple blood islands that ultimately coalesce giving rise to the yolk sac capillary network. In the blood islands, the cells destined to generate the blood elements (hematopoietic stem cells, HSCs), are located into the center, while endothelial progenitor cells (EPCs), or angioblasts, are more peripheral. In addition to this special association, HSCs and EPCs share a series of antigenic determinants, including VEGFR-2, Tie-2, Sca-1 and CD34 (Asahara, 2004). These progenitor cells are consequently thought to derive from a common precursor, putatively named "hemangioblast".

In the following phases of development this primary endothelial plexus expands via angiogenesis, which is a complex process involving sprouting, bridging and branching of pre-existing vessels. The subsequent vascular remodeling, with the recruitment of smooth muscle cells and/or pericytes as well as with trimming of excess vessels, finally gives rise to the complex and hierarchical vascular system, which is highly conserved among vertebrates (Herzog, 2002). The most important function of pericytes in medium-sized vessels and of smooth muscle cells (SMCs) in larger vessels is probably the synthesis of a peculiar extracellular matrix (ECM)l which stabilizes the capillary endothelium. Angiogenesis is also considered the main process by which new blood vessels can arise during the adult life, during a wide series of physiological and pathological conditions.

A third process, called arteriogenesis, is probably responsible for the growth of collateral arteries from pre-existing arteriolar anastomoses in conditions of chronic ischemia (Herzog, Sager, 2002). This process, which occurs independently from angiogenic sprouting, probably represents the main adaptive response in patients with progressive arterial occlusive diseases (Fig. 2.1).

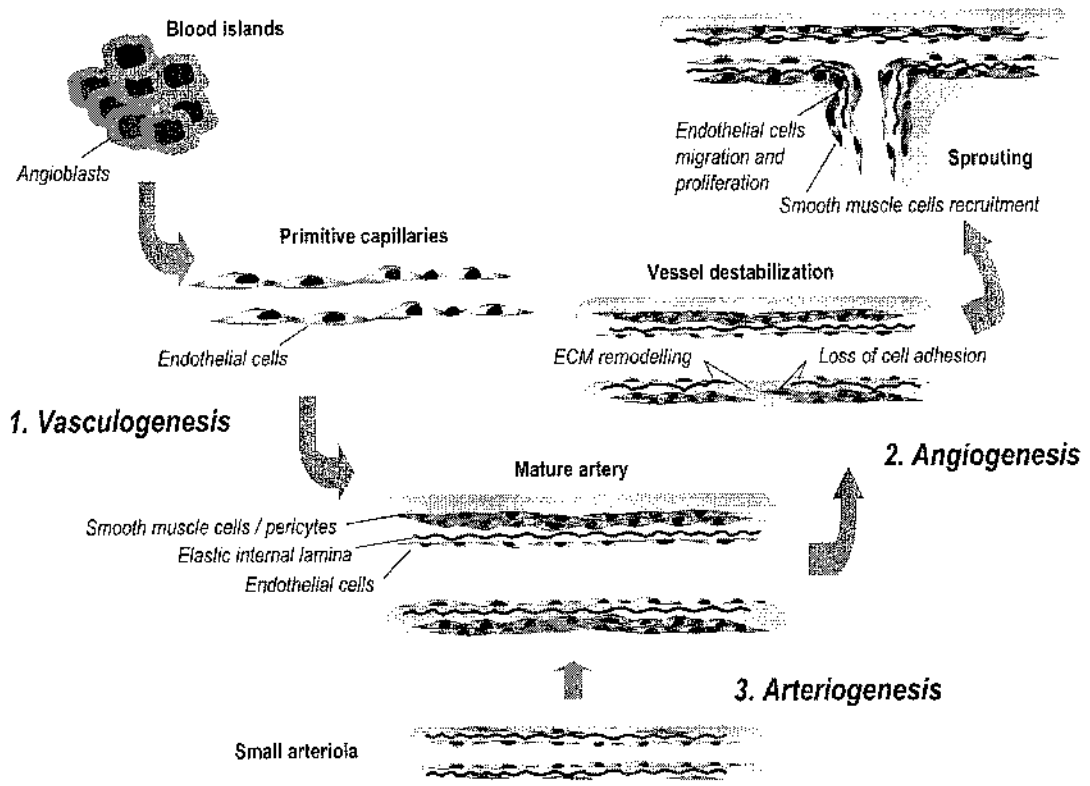


**Figure 2.1. Mechanisms of neovascolarization.** Blood vessels can arise by three main mechanisms: vasculogenesis, angiogenesis and arteriogenesis. During embryonic development, a population of endothelial cell precursors (angioblasts) start to proliferate within the blood islands, forming a primitive capillary network. The subsequent establishment od cell-to-cell contacts, with the recruitment of pericytes, gives rise to functionally competent vessels. On the contrary, angiogenesis is the main process by which blood vessels can form in adult life, and consists of endothelial sprouting from pre-existing vessels. A transient destabilization of the vessel wall, with extensive extracellular matrix (ECM) degradation and remodeling is required for angiogenesis to start. The latter stages of the process involve the strenghtening of endothelial cell adhesion to ECM components and the enrollment of smooth muscle cells. Arteriogenesis also exclusively occurs in adults, usually as a consequence of a major arterial narrowing, and consists in the remodeling of pre-existing arteriolae to form larger arteries, thus providing a compensatory collateral network during ischemic conditions.

Hypoxia was identified as a major stimulus for angiogenesis during embryonic development, leading to the induction of several growth factors and receptors responsible for the different stages of vascular development (Ikeda, 1995). The most important growth factors involved in the early phases originate from the VEGF and FGF family. Indeed, VEGF mRNA levels are rapidly increased by exposure to low oxygen conditions in a variety of normal and transformed cells. In particular, a 47-bp regulatory element located about 1 kb upstream to the VEGF transcription start site appears to be involved in the activation of VEGF transcription in hypoxic cells. This element includes a binding site for the transcription factor hypoxia-inducible factor (HIF-1) (Jiang, 1996) (Figure 2.2).

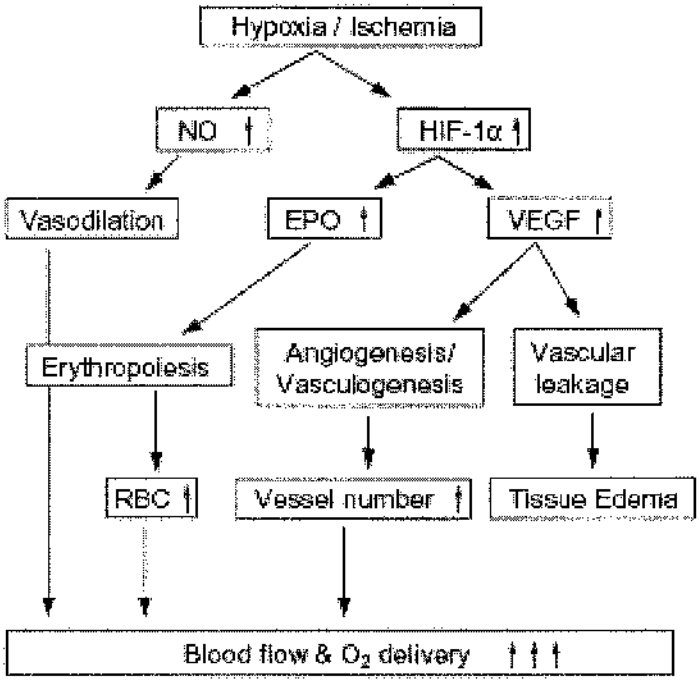


**Figure 2.2. Tissue responses to hypoxia.** The best described tissue hypoxia response system is the oxygen sensitive degradation of the transcription factor HIF-1α, which induces the transcription of more than 40 known genes, including erythropoietin (EPO), and VEGF. This triggers a cascade of events that ultimately leads to increased blood flow and oxygen deliver to the hypoxic tissue.
*Figure adapted from Cao et al., Cardiovascular Research 2005*

As a result of hypoxia, HIF-1 helps to restore oxygen homeostasis by inducing the expression of a number of genes involved in glycolysis, erythropoiesis and angiogenesis. In fact, beside VEGF, HIF-1 also promotes the transcription of a cascade of growth factors and relative receptors that cooperate during the different phases of the angiogenic process. For instance, vessel maturation occurs as the newly formed tubules recruit and become coated by mural cells, such as smooth muscle cells and pericytes. The observation that during embryogenesis mural cells become associated with the forming vessels at later stages of development (Hungerford, 1996) has led to the suggestion that endothelial cells may govern vessel layer acquisition. The exact mechanism by which endothelial cells recruit mural precursors, likely from lateral mesenchyma, and induce their differentiation into smooth muscle cells is largely unknown. However, this heterotypic cell-cell interaction renders both cells quiescent and plays an integral role in the stabilization of the vessel. Members of the Angiopoietin family appear to be particularly important during this phase, being responsible for the reinforcement of intercellular junctions between endothelial and smooth muscle cells, as well as with ECM components

(Figure 2.3). In particular, Angiopoietin-1 (Ang-1) acts by binding to the Tie2 tyrosine kinase receptor. Targeted inactivation of the Ang-1 gene renders embryos unable to form a complex vascular network, with decreased vessel support by mural cells (Suri, 1996). Null mutation of the Tie2 gene gives rise to a similar phenotype (Dumont, 1994). Since Tie2 was thought to be largely specific to endothelial cells, it has been suggested that Ang-1 activates the Tie2 receptor on endothelial cells, which then produce other factors that recruit mesenchymal cells to the newly formed vessels and promote their differentiation into mural cells.

Hallmark of vessel maturation, recruitment of perivascular cells seems to depend, at least in part, on yet another family of growth factors, platelet-derived growth factors (PDGFs) (Lindahl, 1997). However, recent work has shown that Ang-1, in concert with VEGF, could act directly on mural cells and their precursors, which express Tie2, to stimulate their migration, thus promoting vessel maturation (Metheny-Barlow, 2004). An important role in the induction of smooth muscle phenotype in mesenchymal precursors was also attributed to TGF-β (Hirschi, 1998).

As described in the following paragraphs in more detail, all these factors, naturally involved in the process of vascular growth, have been extensively used for therapeutic purposes, with the aim to induce new blood vessel formation in ischemic tissues.

Although a wealth of information has been accumulated in the past years about the molecular mechanisms underlying both vasculogenesis and angiogenesis, little is known about the final remodeling step that leads to the formation of a mature and functioning vascular network. In particular critical issues on how the vessels choose and follow specific paths to reach their correct targets still remain to be explored. This might have particularly important implications for the successful development of therapeutic interventions. Indeed, proper vascularization of organs and tissues requires not only the growth of new blood vessels, but also arterio-venous differentiation and an appropriate patterning of the vascular network (Autiero, 2005).

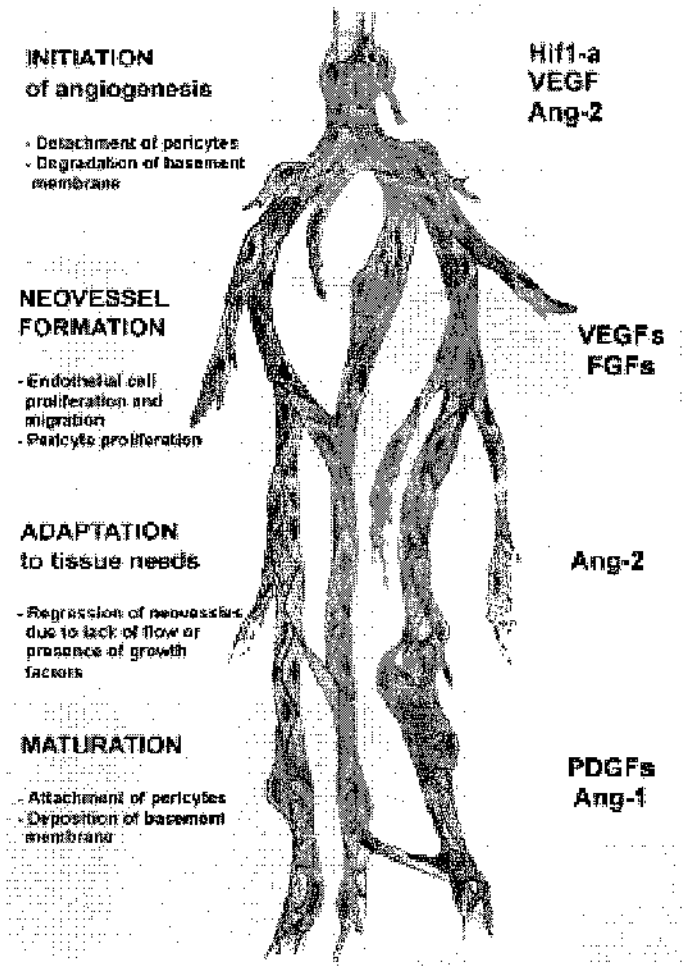


**Figure 2.3. A selection of growth factors from the nature's own angiogenesis tool box can be used for therapeutic purposes.** Angiogenesis is a complex multi-step complex, in which every step requires the coordinated action of a mixture of growth factors. The natural trigger for angiogenesis is hypoxia, which induces the expression of a variety of molecules (VEGF, Ang-2) able to induce transient vascular regression, with proliferation and migration of endothelial cells and pericytes. Excessive neovessel network is then trimmed to adapt to the metabolic needs of the tissue.
*Figure adapted from Markkanen et al., Cardiovascular Research 2005*

Leading from the striking anatomical parallel in the patterning of nerves and blood vessels, several studies in mice and in zebrafish suggest that common pathways are shared between neural and vascular cells to find the way and reach their target tissues during development (Carmeliet, 2003; Autiero, De Smet, 2005). Indeed, both the vascular and the nervous systems are highly branched networks, which arise from a central core and distally extend to reach almost all the cells in the organism. Moreover, in both systems a bidirectional transport may be identified, allowing $O_2$ delivery or $CO_2$ elimination through arteries and veins, and electrical impulse propagation through afferent sensory or efferent motor neurons.

Accordingly, both systems develop by following a similar pattern. As in the vascular system, neural development initially involves the differentiation of progenitors cells

into neurons, with the subsequent formation of central structures, such as the neural tube and dorsal root ganglia. From these neural structures, sprouting axons detach to reach the more distal targets in a very conserved and predictable manner, thus forming a complex and interconnected nervous network (Tessier-Lavigne, 1996). Moreover, vessels extending and interconnecting throughout the body coalign with the nerve pathways, raising the question whether the molecular signals that govern the branching of these two systems are related and interdependent (Shima, 2000) (Figure 2.4).

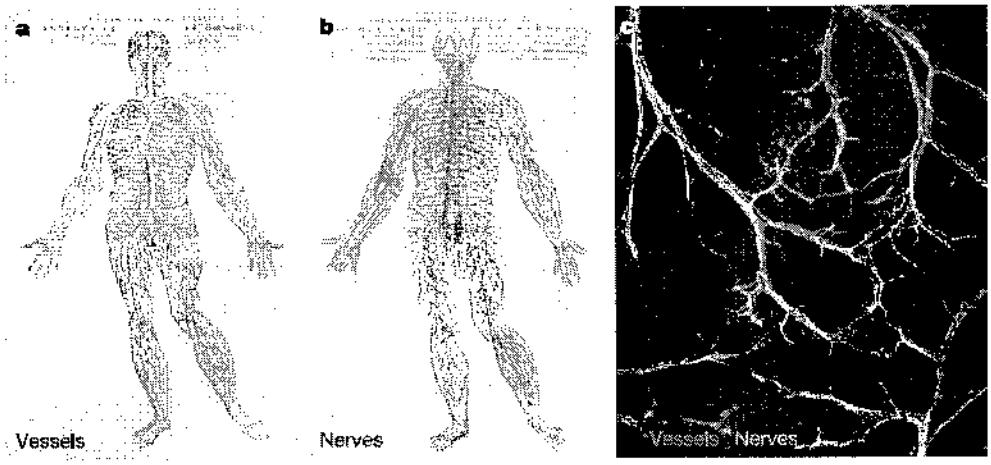


**Figure 2.4. Similarities in vascular and neural networks.** The first two panels (**a** and **b**) reproduce drawings of Andreas Vesalius, from which emerge the similarities between the human vascular network and the peripheral nervous system. In **c** is shown a magnification of vessels (in red) extending in parallel and in close proximity to nerves (in green).
*Figure reproduced from Carmeliet et al., Nature 2005*

Recent evidence actually prooved that similarities between the nervous and the vascular systems extend at the molecular level. For instance, Eph receptors and their ligands, the ephrins, were first characterized as mediators of repulsive guidance events crucial for correct navigation of neuronal growth cones and neural crest cells (Holder, 1999). Their unexpected role in vascular development was revealed when mutant mice that lacked either ephrin B2 or its cognate receptor EphB4 were shown to die during embryogenesis due to cardiovascular disfunction (Wang, 1998; Gerety, 1999). Consistent with this observation, ephrin B2 and EphB4 exhibit a reciprocal expression pattern in arterial and venous endothelial cells (Wang, Chen, 1998).
As described later in detail, another example of a cell surface receptor whose function is required for the development of both the cardiovascular and the nervous system is provided by the neuropilins. These are multifunctional transmembrane

proteins capable of binding to distinct ligands belonging to completely unrelated protein families: the semaphorins and the vascular endothelial growth factors (VEGFs). The most interesting aspects of the structure and the function of these molecules will be discussed in the following paragraphs.

**The VEGF family**

The various forms of the growth factors belonging to the VEGF family (VEGF-A, PlGF, VEGF-B, VEGF-C, and VEGF-D) act as inducers and modulators of vasculogenesis, angiogenesis and vascular remodeling in vivo (Ferrara, 2003). The active forms of the VEGF members form homodimers or heterodimers with other VEGF family members (Keck, 1989; Leung, 1989; DiSalvo, 1995). Their biological effects are mainly mediated by the receptor tyrosine-kinases VEGFR-1 (flt-1), VEGFR-2 (KDR/flk-1) and VEGFR-3 (flt-4), whose relative affinity and distribution mediate the biological effect (Carmeliet, 1999) (Figure 2.5).

In particular, VEGF-A exhibits high affinity for VEGFR-1 and VEGFR-2, which are abundantly exposed on the surface endothelial. Both these receptors have 7 immunoglobulin repeats in the extracellular region, a transmembrane domain, and an intracellular tyrosine kinase domain, essential for autophosphorylation and signal transduction that ultimately results in endothelial cell proliferation and migration. VEGF-B mainly binds to VEGFR-1 and seems to be particularly expressed in the cardiac tissue. On the contrary, VEGF-C and VEGF-D display selective affinity for VEGFR-3 (VEGF-D is actually able to bind both VEGFR-2 and VEGFR-3), thus having a key role in the formation as well as in the regulation of lymphatic vessels.

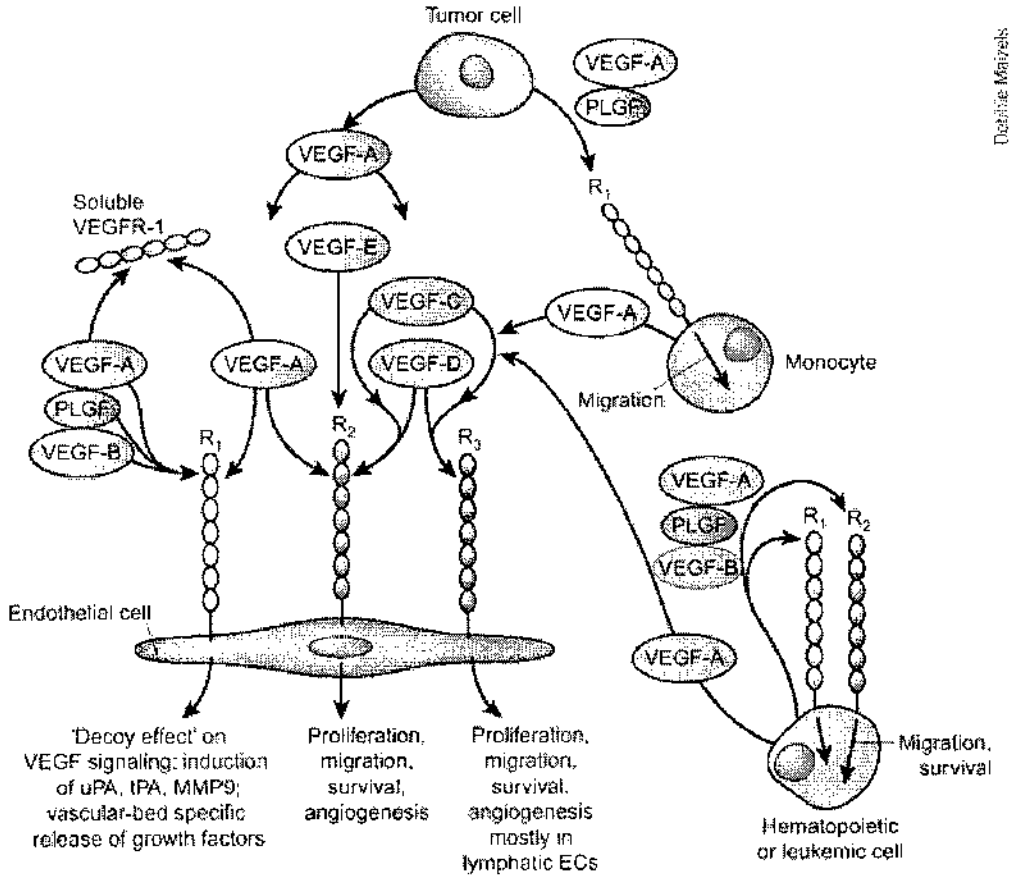


**Figure 2.5. Role of the VEGF receptor tyrosine kinases in different cell types.** VEGFR-1 and VEGFR-2 are expressed on the surface of most blood endothelial cells. Instead, VEGFR-3 is largely restricted to lymphatic endothelium. VEGF-A binds both VEGFR-1 and VEGFR-2. In contrast, PLGF and VEGF-B interact only with VEGFR-1. The orf-virus-derived VEGF-E is a selective VEGFR-2 agonist. VEGFC and VEGFD bind VEGFR-2 and VEGFR-3. There is much evidence that VEGFR-2 is the major mediator in angiogenesis. In contrast, VEGFR-1 seems not able to mediate an effective mitogenic signal and it perform a "decoy" role by sequestering VEGF, thus preventing its interaction with VEGFR-2. However, VEGFR-1 has an established signaling role in mediating monocyte chemotaxis, as well as a survival signal in hematopoietic stem cells (HSC) or leukemic cells.
*Figure adapted from Ferrara et al, Nature Medicine 2003*

VEGF-A (herein VEGF) is an endothelial cell agonist and is essential for vasculogenesis, angiogenesis, and wound healing and plays a role in tumor growth. It was originally isolated by virtue of its ability to stimulate endothelial cell growth and to increase vascular permeability (Lobb, 1985; Leung, Cachianes, 1989). Remarkably, the targeted disruption of the VEGF gene, even in heterozygous conditions, severely compromises angiogenesis and results to be lethal *in utero* at day 11.5, indicating that a correct level of VEGF *in vivo* is critical for the development of the cardiovascular system (Carmeliet, 1996; Ferrara, 1996). Five VEGF isoforms ranging from 121 to 206 amino acids are created by alternative mRNA splicing in humans (Keck, Hauser, 1989; Leung, Cachianes, 1989). These isoforms differ

primarily for the presence or the absence of the heparin-binding domains encoded by exons 6 and 7 (Ferrara, Gerber, 2003). Likewise, other VEGF family members, such as PlGF, are also expressed in several forms that differ in their heparin and heparan-sulfate binding ability (the peptide encoded by exon 6 is found only in PlGF-2 and confers a heparin binding ability that is not present in PlGF-1) (Maglione, 1993).

Recent studies also indicate that VEGF might exert its effect on a variety of cell types, stimulating their survival and/or proliferation, independently from angiogenesis. For instance, VEGF appeared to be critical to prevent motor neuron degeneration, not only because it was essential to maintain sufficient perfusion, but also because it had a direct trophic effect on neuronal survival (Oosthuyse, 2001; Carmeliet, 2002; Azzouz, 2004). An interesting role of VEGF as an important modifier of amyotrophic lateral sclerosis (ALS) has been recently reported, also implicating VEGF as a possible therapeutic molecule in neurodegenerative disorders (Lambrechts, 2003; Storkebaum, 2004).

By adding complexity to its pleiotropic effect, we and others recently observed a potent effect of VEGF in promoting survival and regeneration of skeletal muscle cells (Germani, 2003; Arsic, 2004).

In addition, VEGF was shown to stimulate bone repair, through the induction of angiogenesis, but also having an autocrine role on osteoblast differentiation and bone turnover (Street, 2002).

Finally, a relevant role of VEGF on the survival of several types of stem cells, including endothelial and neural progenitor cells, hematopoietic stem cells and embryonic stem cells has been recently described by different investigators (Rabbany, 2003; Schuch, 2003; Wang, 2004; Brusselmans, 2005)

**Classical VEGF receptors**

All VEGF isoforms bind to VEGFR-1 and to VEGFR-2. Both receptors are essential for fetal angiogenesis, and mouse embryos null for either of the two receptors die in utero between day 8.5 and 9.5 (Fong, 1995; Shalaby, 1995). Compelling evidence indicates that VEGFR-2 is the major mediator in VEGF-induced angiogenesis, despite both receptors have high affinity binding to VEGF. The binding of VEGF to VEGFR-2 initiates intracellular signal transduction and is correlated with the induction of endothelial cell proliferation, migration, and in vivo angiogenesis (Millauer, 1994;

Waltenberger, 1994). Whereas VEGFR-2 is mostly expressed on endothelial cells, VEGFR-1 is expressed by a variety of cell types, including hematopietic, myelomonocytic and smooth muscle cells (Barleon, 1996; Clauss, 1996; Mitola, 1997; Wang, 1998).

By contrast, the activation of VEGFR-1 does not seem to result in an important angiogenic response, although it seems able to enhance cell migration (Seetharam, 1995; Barleon, Sozzani, 1996; Clauss, Weich, 1996). Interestingly, a regulatory loop by which VEGF controls survival of haematopoietic stem cells has recently been described, revealing a function for VEGFR-1 signaling during haematopoiesis (Gerber, 2002).

Hypoxia has been proposed to play an important role also in the regulation of VEGFR gene expression. Accordingly, VEGFR-1 and VEGFR-2 mRNA were substantially up-regulated throughout the heart following myocardial infarction, as well as in the lung vasculature after exposure of the animals to acute or chronic hypoxia (Tuder, 1995; Li, 1996). However in vitro studies on endothelial cells clearly demonstrated that only VEGFR-1 is directly up-regulated by hypoxia through the activation of a hypoxia-inducible enhancer element in its promoter. In contrast, VEGFR-2 mRNA levels do not change, or even decrease, when endothelial cells are exposed to a hypoxic environment, suggesting that the up-regulation of VEGFR-2 observed in vivo is probably mediated by a paracrine factor released by ischemic tissues (Brogi, 1996; Gerber, 1997).

Both receptors play pivotal roles in embryonic vasculogenesis and angiogenesis. Embryos lacking the VEGFR-2 gene die before birth because differentiation of endothelial cells does not take place and blood vessels do not form (Shalaby, Rossant, 1995). In contrast, the homozygous disruption of the gene encoding VEGFR-1 does not prevent the differentiation of endothelial cells, but the development of functional blood vessels is severely impaired, still causing embryonic lethality. In particular, overgrowth of endothelial cells and disorganized blood vessels seems to be the cause of death in these animals, providing additional evidence that VEGFR-1 can serve as a competitive inhibitor of VEGFR-2 mitogenic signaling during vascular remodeling (Fong, Rossant, 1995). A puzzling observation is that mice that retain the extracellular and trans-membrane domains of VEGFR-1 but lack the signaling tyrosine-kinase domain develop normally (Hiratsuka, 1998). It is unclear how the extracellular domain of VEGF is able to restore the normal embryonic development of mice. It is possible that it is required for VEGF sequestration, so as

to limit the activity of VEGF. Such a decoy function might be particularly attributed to a soluble form of VEGFR1, which arises by an alternative processing of the molecule. However, recent studies using PlGF gene disruption, indicate that the direct activation of VEGFR-1 by PlGF, through the phosphorylation of specific tyrosine residues, can amplify the angiogenic activity of VEGF and even promote arteriogenesis, with a monocyte-mediated mechanism (Carmeliet, 2001; Autiero, 2003; Pipp, 2003). Alternatively, as discussed in the following paragraph, it may associate with other membrane proteins to form a signaling holo-receptor.

**Neuropilins and plexins**

Beside the canonical VEGF receptors, endothelial cells also contain two other co-receptors, which bind VEGF165 but not VEGF121 (the shortest isoform that lacks a heparin-binding domain) (Soker, 1996). Several types of prostate and breast cancer-derived cell lines were found to express unusually large amounts of one of these isoform-specific receptors, which resulted to be the product of the neuropilin-1 (NP-1) gene (Soker, 1998). Although originally identified as receptors for class-3-semaphorins mediating neuronal guidance, NP-1 and NP-2 were subsequently found to form complexes with both VEGFR-1 and VEGFR-2. In particular, expression of NP-1 in endothelial cells enhances the affinity of VEGF165 to VEGFR-2 and the subsequent endothelial chemotaxis (Miao, 1999). By directly associating with VEGFR-2, NP-1 thus serves as a VEGF165 co-receptor that increases the ability of the growth factor to activate its main receptor. In contrast, when complexed with VEGFR-1, NP-1 prevents the binding of VEGF to VEGFR-1 (Fuh, 2000). Interestingly, it was subsequently observed that the heparin-binding form of PlGF (PlGF-2) and VEGF-B, are also able to bind to NP-1 (Migdal, 1998; Makinen, 1999). As discussed later, when the role of NP-1 as a VEGF receptor was discovered, it was already known that NP-1 functions in the nervous system as a receptor for Sema3A that causes repulsion of growing tips of axons (He, 1997; Kolodkin, 1997). More precisely, NP-1 is part of a gene family that includes the closely related receptor NP-2 and both proteins were originally found to function as receptors for several class 3 semaphorins that mediate repulsive axon guidance during the development of the nervous system (He and Tessier-Lavigne, 1997; Kolodkin, Levengood, 1997). Sema3A binds only to NP-1, while Sema3B, Sema3C and Sema3F bind to both NP-1 and NP-2, functioning as

agonist at NP-2 sites on sympathetic neurons and as antagonists of NP-1 sites on DRG neurons (Chen, 1997; Chen, 1998; Giger, 1998; Takahashi, 1998). In particular, NP-2 activation by Sema3F also induces axon repulsion (Chen, Chedotal, 1997). On the vascular side, NP-2 is able to bind VEGF165 and PlGF-2 but not VEGF121. However, unlike NP-1, NP-2 is also able to interact with VEGF145, which lacks the peptide encoded by exon 7 (included in VEGF165) but contains instead the heparin-binding domain encoded by exon 6 of the VEGF gene (Gluzman-Poltorak, 2000).

As further discussed later, *np-1* mutant mice exhibit defects in projections of spinal and cranial nerves, and die at the embryo stage due to severe cardiovascular dysfunction (Kitsukawa, 1995; Kitsukawa, 1997; Kawasaki, 1999). In contrast, mice lacking functional NP-2 receptors are viable, with no evidence of cardiovascular defects (Chen, 2000; Giger, 2000).

It was shown that both NP-1 and NP-2 can both form homodimers and heterodimers (Chen, He, 1998). In fact, the neuropilins have a short intracellular domain and are unlikely to function as independent receptors. Indeed, no biological response to VEGF165 can be observed in cells expressing either NP-1 or NP-2 but no other VEGF receptors (Soker, Takashima, 1998; Gluzman-Poltorak, Cohen, 2000). These findings suggest that for the transduction of VEGF signaling the neuropilins have to associate with other membrane proteins. Beside the well known ability to form complexes with VEGFR-2, both neuropilins have been shown to be able to associate with VEGFR-1 (Fuh, Garcia, 2000; Gluzman-Poltorak, 2001).

In accordance, the binding of Sema3A to NP-1 is not sufficient for the induction of Sema3A-mediated growth cone collapse. It was indeed found that it forms complexes with members of a highly conserved family of single pass transmembrane receptors known as plexins and that these complexes mediate the biological response to the majority of semaphorins (Tamagnone, 1999). Moreover, the NP-1-plexinA1 complex exhibits an enhanced binding affinity for Sema3A as compared with NP-1 alone (Takahashi, 1999).

In humans, there are at least nine plexins, most of which have been shown to mediate neuronal cell adhesion and contact, fasciculation, and axon guidance. Plexin-semaphorin interactions now have been implicated in a host of responses, including loss of cell-cell contacts and branching morphogenesis in epithelium, regulation of angiogenesis, growth and metastasis of tumors, and immune responses.

The plexin family was originally identified through homology in their extracellular domains to the scatter factor receptors, the prototype of which is c-Met, the receptor for HGF (also called scatter factor-1). c-Met activation by its ligand, HGF, promotes branching morphogenesis and axonal guidance in neuronal tissues, and proliferation, enhanced cell motility, and metastasis in many tumor cells (Zhang, 2003). In addition to sharing structural homology, plexins and scatter factor receptors mediate similar responses in target tissues, such as survival of sensory neurons, outgrowth of motor neuron axons, and induction of cell migration, proliferation, and branching morphogenesis, known as the "scatter phenotype," in epithelium (Zhang and Vande Woude, 2003). HGF itself exerts well-known pro-angiogenic effects on blood vessels, stimulating chemotaxis, protease production, proliferation, and capillary formation in endothelial cells in a VEGF-independent manner (Dong, 2001). HGF also induces proliferation of smooth muscle cells and pericytes during the maturation of developing microvasculature. Furthermore, there are some hints that class III semaphorins cooperate with HGF in endothelial cell motility and capillary sprouting and in the induction of invasive growth in tumor metastasis. Nonetheless, plexins and scatter factor receptors may be functionally linked because it has been observed recently that on Sema4D binding, plexin-B1 interacts through its extracellular domain with c-Met, which is then phosphorylated and activated in a step required for successful plexin-B1 signaling (Giordano, 2002).

In contrast to the extracellular segment, the cytoplasmic region of the plexins has no homology with the Met tyrosine kinase cytoplasmic domain or with any other known protein, but is highly conserved within and across species.

As a general rule, class 3 semaphorins bind to plexin-A, but only when associated in a complex with members of the neuropilin class of cell surface receptors, neuropilin-1 and neuropilin-2. Conversely, Sema4D appears to bind plexin-B1 directly (Oinuma, 2004; Conrotto, 2005).

Plexin-B1 is highly expressed in nervous tissues, where it provides repelling cues for the axon guidance during development of the nervous system, inhibition of axon growth after injury and maintenance of established neural pathways in the adult, but its gene expression profile shows that plexin-B1 transcripts are detectable in many adult tissues, among which endothelial cells. This evidence suggests that Sema4D-plexin-B1 interaction might play a crucial role in the regulation of the biological functions of endothelial cells, specifically in the control of angiogenesis. Indeed, it was recently reported that Sema4D-mediated activation of plexin-B1 induces

tubulogenesis and migration of endothelial cells and angiogenesis in vivo (Basile, 2004).

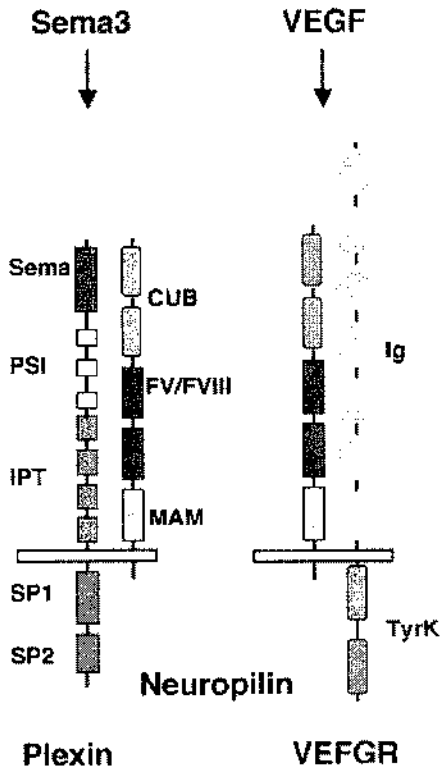


**Figure 2.6. Simplified model of signaling through Neuropilin receptor complexes.** Functional association of NP-1 and NP-2 receptors with Plexin-signaling receptors transduce Sema3 signals. NP-1 is known to bind Sema3A and Sema3C, while NP-2 binds Sema3C and Sema3F. This mode of signaling is thought to signal axon repulsion in the nervous system. In the vascular system, NPs associate with VEGF tyrosine kinase receptors to transduce VEGF signals. IN particular, signal transduction of VEGF165 through VEGFR-2 is enhanced in the presence of NP-1.
*Figure adapted from Eichmann et al., Genes and Deveoplment, 2005*

### Neuropilin-1 (NP-1)

NP-1 is a single spanning transmembrane glycoprotein of 130-140 kDa, with a large extracellular domain and a very short cytoplasmic tail of 40 amino acids (Gu, 2002) (see Figure 2.7). It was first identified in the optic tectum of Xenopus laevis and subsequently in the developing human brain (Kawakami, 1996). As already mentioned, NP-1 mainly localizes to axons and was originally described as the

receptor for Sema3A, a secreted axon guidance molecule that repels axons and collapses growth cones of dorsal root ganglia.

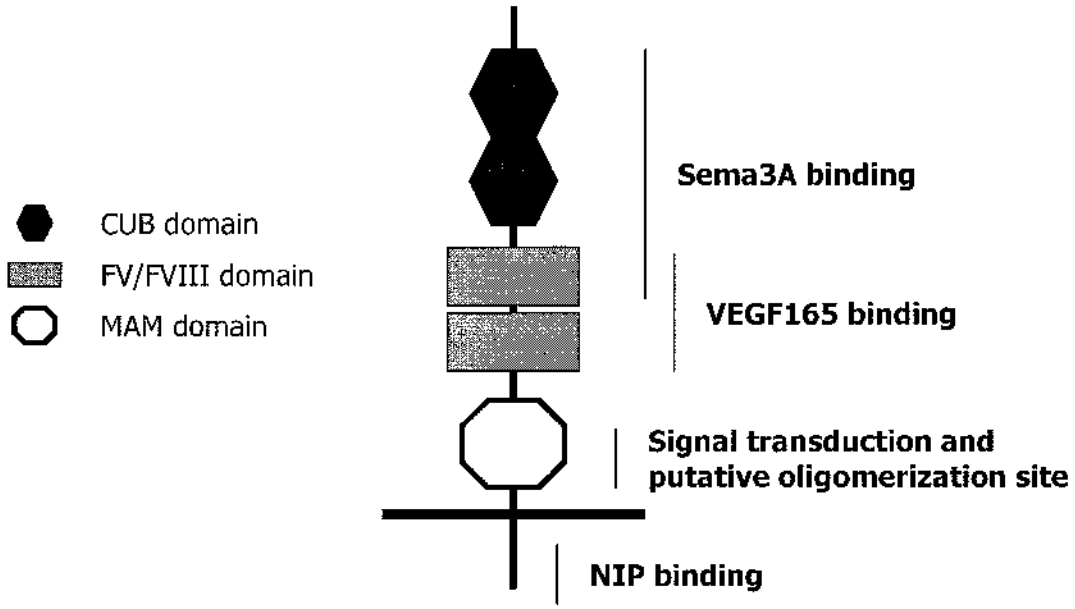


**Figure 2.7. Schematic representation of the NP-1 structural and functional domains.** Shown are the different domains identified in the NP-1 protein and their specific role for the receptor function. NIP: neuropilin interacting protein.

Structure-function analysis has revealed that the amino-terminal CUB (complement-binding protein homology) domain functions as a Sema binding site (Chen, He, 1998; Giger, Urquhart, 1998; Nakamura, 1998). The transmembrane and cytoplasmic domains are not required for Sema signaling through NP-1. Instead, the extracellular juxtamembrane MAM (meprin, A5, μ) domain is crucial, implicating a second transmembrane protein as the transducing element for Sema3A action. The identity of this transducing protein has recently been identified in the plexin family (Takahashi, Fournier, 1999), as well as the downstream intracellular mediators CRMP (collapsing response mediator protein) and the monomeric GTP-binding protein Rac-1 (Goshima, 1995; Jin, 1997). In addition, intracellular cGMP (guanosine 3', 5-cyclic monophosphate) levels influence growth cone steering by Sema3A (Song, 1998).
In addition, NP-1 has been recently reported to be also a functional receptor for VEGF165 in physiological as well as in tumor-associated angiogenesis: mainly by increasing the affinity of VEGF165 for VEGFR-2 on endothelial cells, it enhances all

the VEGF effects transduced through VEGFR-2, such as chemotaxis, endothelial cell survival, and angiogenesis (Yamada, 2001). Of interest, NP-1 can support VEGF autocrine function and cell migration in tumor cells that lack expression of VEGFR-1 or VEGFR-2, raising the possibility that NP-1 might either interact with other signaling receptors, such as NIP (Neuropilin interacting protein) or independently promote cell signaling (Soker, Takashima, 1998; Bachelder, 2001; Bachelder, 2003). In accordance, endothelial cells transduced with a chimeric fusion receptor composed of the extracellular domain of epidermal growth factor and the intracellular domain of NP-1, have recently been shown to migrate in response to the specific ligand (Miao, 2000).

Consistent with NP-1 playing an important role in regulating VEGF availability and function, NP-1-deificent mice die during mid-gestation with defects in the heart, vasculature, and nervous system (Kawasaki, Kitsukawa, 1999). Transgenic mice overexpressing NP-1 also exhibited abnormalities in the cardiovascular and nervous system, contributing to embryonic lethality (Kitsukawa, Shimono, 1995). NP-1 knockin mice expressing NP-1 mutants that bind either VEGF or class 3 semaphorins demonstrated that VEGF/NP-1 signaling is required for vascular development, whereas Sema3A/NP-1 signaling is required for neuronal, but not vascular development (Gu, 2003). In addition, the marked vascular abnormalities observed in endothelial cell-specific NP-1-null mice provided strong evidence for a non-redundant role of NP-1 in normal vascular development (Gu, Rodriguez, 2003). However, it is currently unclear whether NP-1 continues to have an essential function in endothelial cells postnatally. Very recently, a unique role of NP-1 has been described, as a regulator of endothelial cells attachment to ECM proteins, which is essential to endothelial cell survival, growth, movement and angiogenesis (Murga, 2005).

Finally, an important role of NP-1 in artero-venous patterning has recently been proposed. In fact, while both neuropilins are co-expressed in yolk-sac endothelial cells during vasculogenesis (Herzog, 2001), at later stages, NP-1 is preferentially expressed in arterial endothelial cells, while NP-2 labels venous and lymphatic endothelium (Herzog, Kalcheim, 2001; Moyon, 2001).

**The Semaphorin family**

The semaphorins (abbreviated Sema) are a large family of phylogenetically conserved molecules, which were originally identified based on their ability to

provide both attractive and repulsive axon guidance cues during neural development (Kolodkin, 1993). The more than 30 semaphorins identified to date share a conserved N-terminal extracellular Sema domain and have been classified into eight subgroups based on their species of origin and sequence similarity (Raper, 2000). The final classification proposed by the Semaphorin Nomenclature Committee is defined in Figure 2.8.

According to these rules, subclasses are designated by an Arabic number (with the exception of the viral subclass), and within each subclass semaphorins are assigned a letter, based on the date of availability in public databases such as GeneBank or EMBL. Classes 1 and 2 are found in invertebrates, classes 3 to 7 are found in vertebrates, and class V is found in viruses.

Though semaphorin function was initially addressed with respect to neuronal guidance, it is becoming clear that they exert a number of effects in vivo, ranging from cell migration to vascular morphogenesis, and including immunological modulation and neoplastic transformation.

Among the vertebrate semaphorins, the class 3 semaphorins are the most thoroughly investigated (Kolodkin, Levengood, 1997; Takahashi, Fournier, 1999). They are secreted proteins with potent axon repulsive activity that can abruptly collapse growth cones of dorsal root ganglia (DRG) (Luo, 1993). A repulsive role for Sema3A in vivo is supported by the excessive peripheral DRG axon growth seen in Sema3A-/- mice (Taniguchi, 1997). However, Sema3 proteins are also involved in different processes such as immune modulation (Hall, 1996), organogenesis (Behar, 1996), neuronal apoptosis (Gagliardini, 1999), and drug resistance (Yamada, 1997).

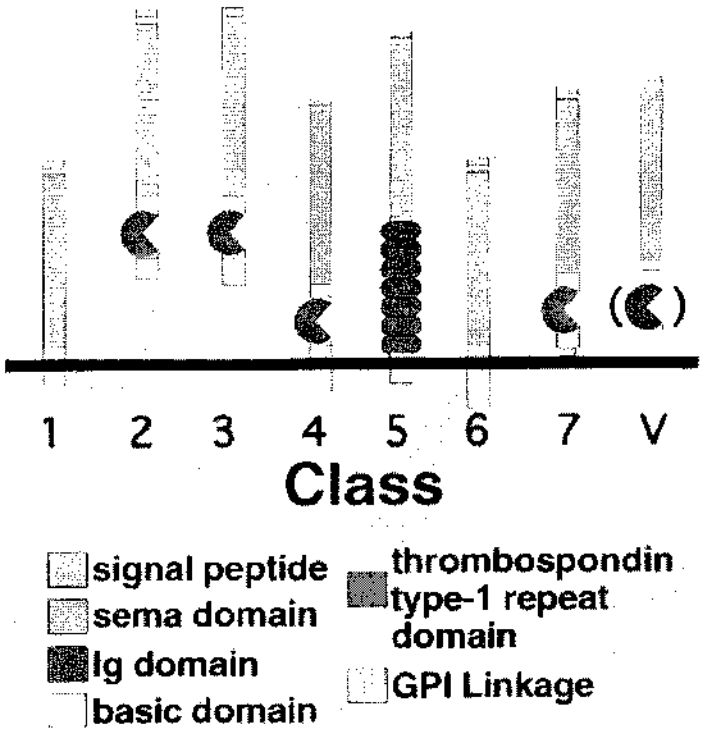


**Figure 2.8. The eight subclasses of the Semaphorin family.** 1) Sema domain, transmemebrane (TM) domain, and short cytoplasmic domain (invertebrate). 2) Sema domain, immunoglobulin domain (Ig), secreted (invertebrate). 3) Sema domain, Ig domain, short basic domain, secreted (vertebrate). 4) Sema domain, Ig domain, TM domain, and short cytoplasmic domain. 5) Sema domain, seven thrombospondin repeats, TM domain and a short cytoplasmic domain (vertebrate). 6)Sema domain, TM domain, and a cytoplasmic domain (vertebrate). 7) Sema domain, Ig domain, and a GPI membrane anchor (vertebrate). V) Viral semaphorins, including to date a truncated secreted sema domain (SEMA VA) and a sema domain followed by an Ig domain shown in parentheses (SEMA VB); both secreted. *Figure adapted from Goodman et al, Cell 1999*

Class 3 semaphorins form complexes with two types of cell surface receptors: neuropilins (NP-1 and NP-2) and plexins (Tamagnone, Artigiani, 1999); Takahashi, 1999 #45; Rohm, 2000 #46]. As already described, neuropilins have been identified as high-affinity binding sites for class 3 semaphorins, whereas plexins are necessary for signal transduction (Maestrini, 1996; Winberg, 1998; Takahashi, Fournier, 1999). In particular, Sema3A has been the most studied protein of the Sema3 subclass, due to its widely recognized role in axon guidance. However, the observation that its main receptor, NP-1, is abundantly expressed on endothelial cells and forms complexes with different VEGF receptors, prompted to postulate the existence of a functional interplay between VEGF and Sema3A in the nervous as well as in the vascular system. In particular, it has been demonstrated that VEGF165 can antagonize the proapoptotic and inhibitory effects of Sema3A on axons, probably

because both proteins share the same binding domain on cell surface receptors (Gu, Limberg, 2002). On the other hand, porcine and rat aortic endothelial cell expressing NP-1 and VEGFR-2 respond to exogenously added Sema3A by decreasing their migratory capacity, as well as microvessel and lamellipodia formation. These effects are reversed by high doses of VEGF165 (Miao, Soker, 1999). A similar pattern is observed in medulloblastoma cells expressing NP-1 and VEGFR-1; in these cells Sema3A induces apoptosis, whereas VEGF165 antagonizes this effect by promoting cell proliferation and survival (Bagnard, 2001). Finally, comparable results could be obtained in breast carcinoma cells (Bachelder, Lipscomb, 2003). The existence of common receptors for both VEGF165 and Sema3A implies that these factors might compete for the same binding sites on the cell surface. Alternatively, the two factors might directly provide opposite and independent signals to the target cells. Aligned with this latter hypothesis, the class III semaphorins are now known to participate in vascular morphogenesis by promoting an autocrine chemorepulsive signal, in addition to their best-understood role in axon pathfinding (Bates, 2003; Serini, 2003; Shoji, 2003).

Additional recent data on other class 3 Semaphorins point to these molecules as having important function also in tumor and vascular development. For instance, Semaphorin 3B (Sema3B) is a site of very frequent allele loss and or promoter methylation in the early pathogenesis of lung and breast cancer (Sekido, 1996; Lerman, 2000) and has been shown to have direct tumor suppressor activity for lung cells (Tomizawa, 2001). Interestingly, Sema3B induces apoptosis in lung and breast cancer cells and this effect is reversed by the simultaneous expression of VEGF165 but not of VEGF121, suggesting an important role of NP receptors (Castro-Rivera, 2004). These results suggest that VEGF is an autocrine tumor cell survival or growth factor and that Sema3B might act through a VEGF-regulated system to mediate its tumor suppressor effects. These findings are in line with prior observations by Bachelder et al., showing that NP-1 supports a VEGF signaling pathway that is critical for breast carcinoma cell survival and that VEGF and SEMA3A are antagonistic NP-1 ligands regulating breast carcinoma cell migration (Bachelder, Crago, 2001; Bachelder, Lipscomb, 2003).

Recent evidence also show Sema3F and VEGF having opposite effects on cell attachment and motility in breast cancer cells, in which SEMA3F inhibited lamellipodia formation, membrane ruffling, and cell–cell contacts through interaction with NP-1, and VEGF counteracted all these effects (Nasarre, 2003).

Finally, Sema3E has been shown to control vascular pattern through PlexinD1 signaling, but independently from neuropilins (Gu, 2005). This unanticipated observation adds to the diversity of how Sema3s orchestrate tissue morphogenesis, with a particular reference to the vascular and the nervous system.

## 2.2 GENE TRANSFER TO THE CARDIOVASCULAR SYSTEM WITH VIRAL VECTORS

The wealth of knowledge generated over the past decades in the progressive understanding of the molecular pathways leading to new blood vessel formation, opened the possibility to exploit this information for therapeutic purposes.

Among the most promising approaches for the delivery of angiogenic factors is gene transfer, and in particular the use of recombinant vectors based on adenovirus (rAd) and Adeno-Associated virus (rAAV) (Guzman, 1993; Fisher, 1997). These two vectors share some similar features, such as the ability to transduce a variety of proliferating and quiescent cell types, including skeletal muscle fibers and cardiomyocytes. However they also possess their own unique set of properties that render them particularly attractive for different gene transfer applications. rAd vectors can accommodate larger inserts, mediate transient but high levels of protein expression, and can be easily produced at high titers, although their application in vivo is notably limited by their strong immunogenicity and the stimulation of a potent inflammatory response (Yang, 1996). In the gene therapy arena, major safety concerns about a wide use of these vectors have recently been raised by the death of young patient recruited in a gene therapy trial for the treatment of a rare metabolic disorder (OCT deficiency). The lethal event was most probably due to a systemic inflammatory response to the delivered adenoviral vectors (Lehrman, 1999). Starting for these considerations, we can predict that adenoviral vectors will probably find their specific niche only in cancer gene therapy, where a robust inflammatory response against adenoviral-transduced cells is highly desirable.

A constantly increasing number of pre-clinical and clinical gene therapy studies exploit vectors based on AAV, a parvovirus that owes its name to the fact that it has been originally discovered as a contaminant of an adenoviral preparation. The gaining popularity of AAV vectors can be attributed principally to their ability to mediate prolonged transgene expression in a variety of target tissues and to their

lack of pathogenicity (Favre, 2001). The safe profile of AAV vectors stems from two major properties: first, AAV have never been associated to any human diseases, and, second, they are completely replication-deficient.

Importantly, gene transfer technologies should be considered not only for their therapeutic applications, but also for their usefulness in basic research, since viral vectors represent a unique tool to investigate the molecular pathways responsible for different pathologic conditions. In this context, AAV vectors, allowing long-term transgene expression in the absence of inflammation, stand as an interesting alternative to the use of transgenic, knock-in and knock-out mice. AAV-mediated overexpression of a specific angiogenic factor in a normal or ischemic muscle is a simple and straightforward way to examine the biological effect of that molecule in vivo (Figure 2.9).

Moreover, these vectors offer the unique possibility to define possible synergistic, antagonistic or complementary effects exerted by different angiogenic molecules (Arsic, 2003). In fact, since they infect cells at high multiplicity, they allow the simultaneous delivery of several combinations of genes in the same tissue. In contrast, this goal would never be possible using genetically modified animals or other viral vector systems, such as retroviruses, whose genome is integrated in the host genome at a frequency of one copy per cell. The possibility to simultaneously or subsequently deliver different combinations of genes of interest is of great significance from both the biological and the clinical points of view. For instance, it will be possible to define which cocktail of cytokines has the greatest efficacy in the induction of a new functional vascular network, as well as the most appropriate timing for their administration (Athanasopoulos, 2000).

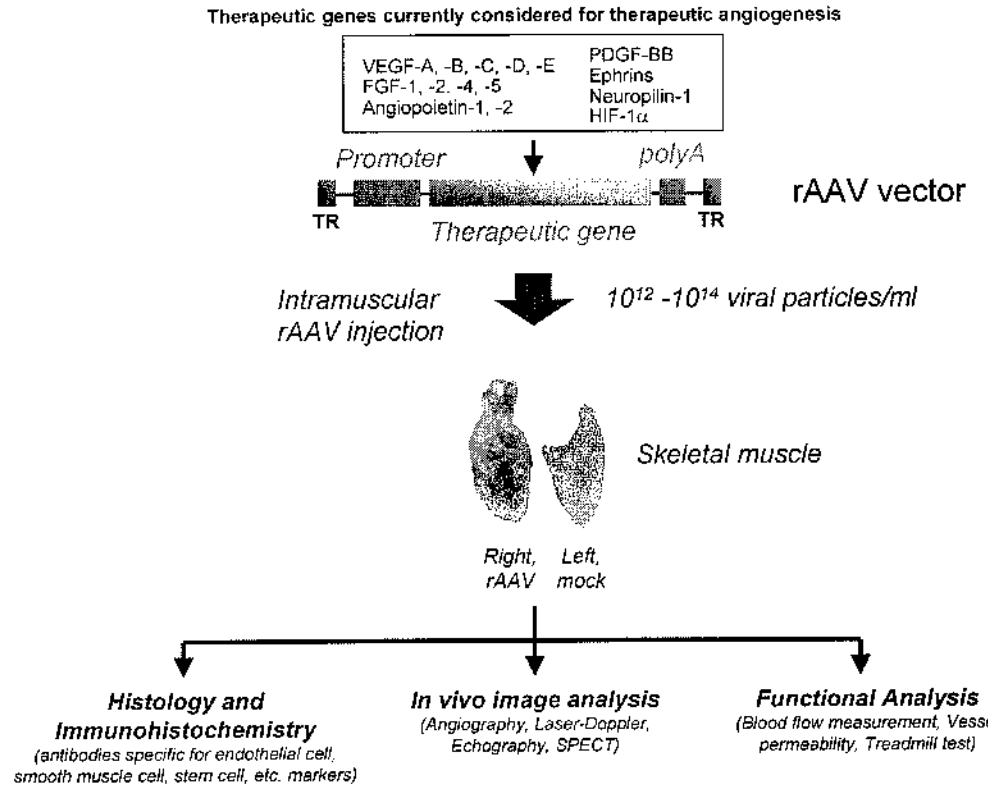


**Figure 2.9. AAV vectors as a tool to study therapeutic angiogenesis.** AAV vectors represent a potent tool to study the effect of several angiogenic molecules in vivo. The list in the top part show the main candidate genes currently considered for the induction of therapeutic angiogenesis. The cDNA of almost every interesting gene can be cloned in the AAV plasmid backbone to obtain high titer preparation of rAAV vectors, which are then suitable for in vivo administration. The high tropism of AAV for both skeletal and cardiac muscle cells offers the remarkable possibility to obtain sustained and prolonged transgene expression, thus allowing long-term functional studies. In particular, the transduction of skeletal muscle is suitable for the comparison of the effects of the AAV under investigation with those of an AAV expressing the reporter gene LacZ as an internal control.

## Molecular properties of AAV vectors

AAV is a small, helper-dependent human Parvovirus, whose linear single-stranded, non-enveloped 4.7 kb genome requires co-infection with adenovirus or herpes simplex virus to enter a lytic growth cycle and be packaged into particles of plus or minus polarity. Although AAV can replicate also in helper-free conditions, most frequently, and in the absence of superinfection, it preferentially integrates its DNA in a non-random manner into a 4 kb region of human chromosome 19, designated AAVS1, thus allowing a latent infection to occur. In this case, no AAV gene expression is required to maintain latency, and the provirus is stably propagated for several cell passages (Berns, 1995). This could be a very useful feature for a safe and long-term gene therapy in humans.

The viral genome contains two open reading frames (orf), whose expression is under the control of three promoters. From the first orf, four different transcripts are produced by alternative splicing, coding for the non structural Rep proteins. The two major forms of Rep (Rep78 and Rep68) bind to specific sites within the inverted terminal repeats (ITR), and are required for both viral DNA replication and site-specific integration. In addition, the AAV Rep proteins participate in the regulation of gene expression. In particular, Rep induces the up regulation of the homologous AAV promoters in the presence of adenovirus infection, while it exerts an inhibitory effect when adenovirus is absent. Other heterologous promoters, including viral and proto-oncogene promoters, are also down regulated by Rep, suggesting a pleiotropic effect of this protein on gene expression (Marcello, 2000). Another property if Rep is the inhibition of replication of a number of DNA viruses, such as adenoviruses, herpesviruses and papillomaviruses. This effect could partially be ascribed to the above mentioned down-modulation of transcription, but it is probably also due to a more general effect of Rep on DNA replication.

The 3' side of the AAV genome encodes for the capsid Cap protein. Because of the alternative usage of three different translation start sites and of a common polyadenylation signal, three capsid proteins are produced (VP1, VP2, VP3).

The whole coding region is flanked by two 145 bp interted terminal repeats (ITRs), which show complementarity within the first 125 bp and form a T-shaped hairpin at both ends of the genome. This palindromic sequence is the only cis-acting element required for all the major functions of AAV (viral DNA replication, assembly of the viral particles, integration/excision from the host genome).

The life cycle of AAV strictly depends on the presence or absence of a helper virus superinfection in the host cells. Under non-permissive conditions (i.e. without helper virus), the AAV genome mainly integrates into the AAVS1 region, where it establishes a latent infection for indefinite periods of time. A crucial role in latency persistence is played by Rep 68/78, which is synthesized at basal levels and negatively regulates AAV gene expression and DNA synthesis. The latency state, although not altering cell viability, does affect the phenotype as well as the expression of specific cellular genes, conferring more sensitiveness to UV-light, genotoxic agents and heat, enhancing serum requirement and reducing the cellular growth rate. It is assumed that all these effects are somehow related to a low-level production of the Rep protein (Marcello, Massimi, 2000).

Under permissive conditions (i.e. after superinfection with helper virus), the regulation of AAV gene expression becomes rather complex, depending upon both the helper virus and the presence of Rep68/78 proteins. In these circumstances, the integrated genome can be rescued from the host and packaged into infectious particles.

The mechanism underlying the integration process, depending on the specific recognition between AAV sequences and the AAVS1 region on chromosome 19, is not yet fully understood. Recent evidence indicates that this region is located close to the human troponin T gene, displaying an overall GC content of 65%, a 35-mer minisatellite tandemly repeated for 10 times and a putatively transcribed orf; but the putative role of these features in the integration process still remains unclear (Dutheil, 2000). A pivotal role in the integration and rescue mechanisms is exerted by the viral ITRs, and in particular by two short sequences (Rep Binding Site, RBS and Terminal Resolution Site, TRS) in the stem of the T-shaped structure. These sequences drive the binding of Rep 68/78 and the subsequent nicking of the viral DNA, a process essential for viral DNA replication. Since the same RBS and TRS are present also within the AAVS1 sequence, a model has been proposed which suggests the involvement of an oligomeric complex of Rep to juxtapose the RBS and TRS from the cellular and viral DNAs.

The exact elucidation of the molecular mechanisms underlying the site-specific AAV integration process is of extreme importance in the light of the utilization of these vectors for gene therapy purposes. However, it should be emphasized that site-specific integration is strictly dependent on the rep gene, or at least on one of its products, the Rep68 or Rep78 proteins. Since the gene coding for this protein is never present in the recombinant AAV vectors, it can be reasonably concluded that integration of vector DNA either occurs in a random manner or does not occur at all.

**Production of recombinant AAV vectors**

The characteristics of AAV life cycle, including its defectiveness and ability to persist in infected cells as a latent viral genome, early suggested that this virus could be an excellent tool for in vivo gene transfer. Since the AAV genome cloned into a plasmid is still infectious and able to produce viral particles, any exogenous gene (less than 4.5 kb in length) can theoretically be placed within the two 145 bp ITRs to obtain a

circular backbone suitable for vector production. Unlike other delivery systems that have evolved into several generations, the original composition of the AAV vector plasmid (a transgene expression cassette flanked by the two ITRs) is essentially the same as in the current version. The traditional method for rAAV production is based on co-transfection of the vector plasmid together with a second plasmid, supplementing the rep and cap gene functions, into helper-infected cells (usually HeLa or 293 cells) (Figure 3.10).

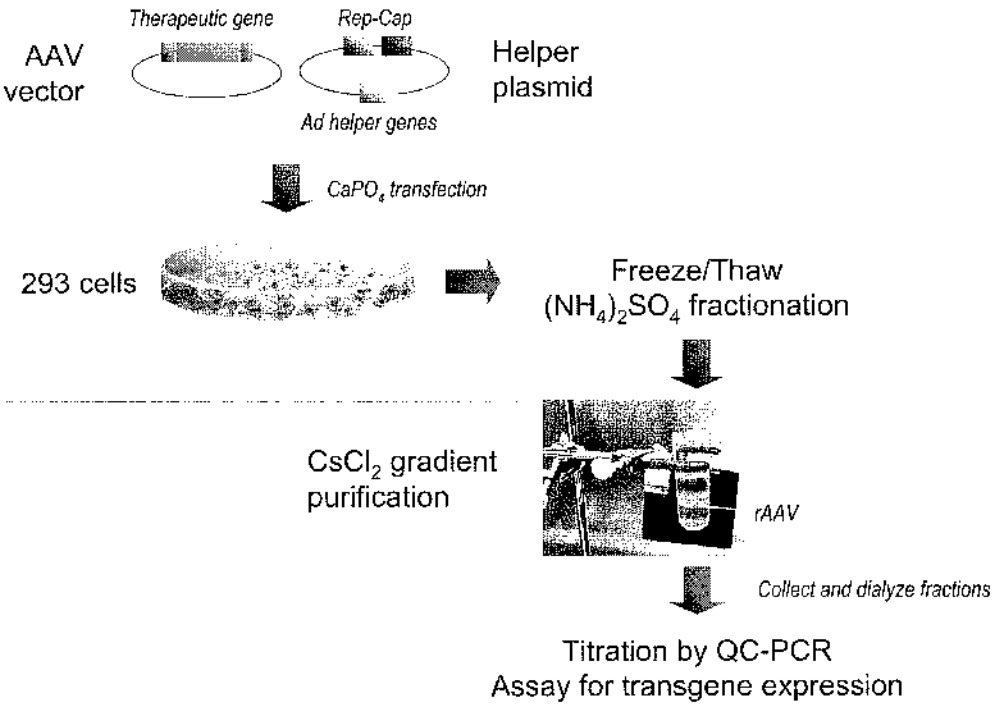


**Figure 3.10. Production of recombinant AAV vectors.** After co-transfection of the AAV vector plasmid (carrying the cDNA of the therapeutic gene), together with the helper plasmid (supplementing the rep and cap gene functions, as well as adenoviral genes with helper activity), HEK293 cell lysate is obtained by repeated freezing and thawing, and subsequently fractionated by $(NH_4)_2SO_4$ precipitation. rAAV particles are then purified by CsCl2 density gradient ultracentrifugation and dialyzed. Viral preparation stocks are finally titrated and assessed for transgene expression.

Packaging efficiency seems to depend principally on the cellular system used and on the size of the packaged genome. A "head-full" mechanism appears to be used by the packaging machinery, with upper and lower limits of 4.9 and 4.1 kb respectively for optimal packaging, even if constructs up to 5.2 kb are tolerated.

One of the most critical problems in the traditional AAV preparations is the presence of the contaminant helper virus, and occasionally also of wild-type AAV. Since recombinant particles are usually assembled in cells infected by adenovirus, they have to be purified, which may negatively interfere with the amount and the activity

of the recombinant particles. In fact, even marginal amounts of infectious adenovirus or adenoviral proteins can result in relevant host immune response, while the presence of the wild-type virus poses the risk of mobilization of the recombinant AAV vector (provided that simultaneous infection with a helper virus also occurs in the same organism). Several improvements of the conventional protocol for rAAV vector production have been proposed over the last few years, as a consequence of the growing understanding in the biology of the AAV life cycle (Grimm, 1998).

AAV vector particles are traditionally separated from adenovirus virions by repeated cesium chloride ($CsCl_2$) density gradient ultracentrifugation. However, this separation is far from perfect, having a negative impact on the success of rAAV production. To decrease toxicity from residual hyperosmotic $CsCl_2$, the substitution of density centrifugation with the iso-osmotic and inert iodixanol has recently been adopted. Alternatively, the identification of heparan sulfate proteoglycan as a cellular receptor for the attachment of the virions, has resulted in the transition to ligand affinity matrix chromatography purification as the standard of rAAV production in most core facilities.

The risk of adenovirus contamination has been recently solved by the identification of the adenoviral genes essential to provide helper activity to AAV replication in packaging cells. Actually, it is now clear that this effect is not direct. Proteins expressed from the adenovirus early region 4, open reading frame 6 (E4ORF6) stimulate still unrecognized cellular activities that are essential to stimulate AAV replication. This notion led to the development of new protocols that allow for vector manufacturing in a setting totally free of helper virus, based on plasmids containing part of the adenoviral genome. These plasmids are completely non-infectious, carrying only the subset of adenoviral genes that is essential for rAAV production. More recently, both the AAV and adenoviral genes were assembled on one plasmid, thus reducing the number of plasmids required to transfect for recombinant particles production (Grimm, Kern, 1998). In this way, it is now possible to obtain rAAV preparations free of contaminating helper virus and unwanted adenoviral protein at a yield even higher than that achieved by using infectious helper virus.

A particular goal in trying to overcome the dependency on transient transfection is the establishment of packaging cell lines, similar to those already developed for retroviral and adenoviral vector production, but stably containing multiple copies of the rep and cap genes. Expression of these genes would be moderate in basal conditions, but could be triggered by infection with adenovirus. Nonetheless, these

efforts have met very limited success so far, mainly due to the toxicity of the constitutive expression of Rep, which, even at very low levels, is very badly tolerated by proliferating cells. Therefore, transient transfection still remains the method of choice to obtain AAV vector preparation for both investigation and gene therapy purposes.

The increasing popularity of rAAV vectors relies on the results of a number of in vivo transduction experiments that have demonstrated efficient and long-term persistent infection of a series of tissues and organs in vivo (Xiao, 1996). For some still completely unexplored reasons, however, transduction occurs essentially only in cells of muscular origin (including skeletal and smooth muscle cells and cardiomyocytes), in neuronal cells (both in the central and peripheral nervous system and in the retina), in retinal pigmental cells, and, at a lesser extent, in hepatocytes. The reasons for this selective tropism are most likely unrelated to viral penetration into the cells, since AAV particles are able to efficiently bind and enter a large number of cells, due to the usage of widely expressed molecules as receptors, including heparan sulphate proteoglycans, FGFR-1 and $\alpha V\beta 5$ integrin (Bartlett, 2000). After infection, however, different and unknown cellular factors influence the outcome of viral transduction that limit the in vivo efficiency. In adenovirus-infected cells, AAV DNA co-localizes in the adenovirus replication centers within the nucleus. In contrast, in the absence of adenovirus, AAV essentially has a perinuclear localization, whereas it is quickly internalized in the nucleus after helper viral superinfection. A peculiar molecular event limiting the infection efficiency is the synthesis of the complementary strand of the viral genome, which converts the single-stranded AAV DNA into its transcriptionally active, double-stranded form (Ferrari, 1996). Intriguingly, this event often takes a long time to occur: even in highly permissive tissues, the maximum levels of transgene expression is detected only after several weeks, being preceded by a lag period during which some still not completely understood molecular events take place (Zentilin, 2001).

Current knowledge on AAV biology has been mainly accumulated by using serotype-2 vectors. However, a number of new AAV serotype vectors (from 1 to 9) have recently become available, with distinct tissue tropism and interacting with different cellular receptors. Of specific interest for future cardiovascular applications, AAV-1 and AAV-6 demonstrate particularly robust transduction of skeletal muscle. In contrast, AAV-8 seems to display the highest efficiency in crossing the blood vessel

barrier, thus attaining systemic gene transfer to both skeletal and cardiac muscles (Wang, 2005).

## 2.3 STRATEGIES FOR THE INDUCTION OF TISSUE NEO-VASCOLARIZATION

### Use of growth factor gene transfer for the induction of therapeutic angiogenesis: from animal studies toward clinical trials

The exceptional scientific progress achieved during the last decade in the vascular biology field, with the identification of a growing number of endogenous angiogenic factors, has led to the elaboration of the novel concept that new vessels can be grown to improve the perfusion of ischemic tissues.

In parallel, the same concepts were further substantiated by a number of studies in the field of tumor angiogenesis, as introduced by Judah Folkman in 1971 (Folkman, 1971) and by the development of a series of specific growth factor inhibitors, which displayed particular clinical efficacy for the treatment of chronic myelogenous leukemia and other tumors (Druker, 2002; Willett, 2004).

Likewise, the validity of therapeutic angiogenesis/collateral artery growth was successfully tested in a variety of preclinical models. The wealth of information inferred from animal studies was encouraging enough to gain regulatory approval for clinical testing, which actually started several years ago (Isner, 1996) and has been tremendously expanded over the last decade (Post, 2005).

After the identification of VEGF and FGF as powerful inducers of angiogenesis, a limited series of studies has been conducted in order to evaluate a possible therapeutic effect achievable by these factors when delivered as recombinant proteins (Takeshita, 1994; Takeshita, 1994; Sato, 2000; Post, 2001). Despite relatively good results obtained in animal models, this approach produced only modest success in clinical trials, as a consequence of the short half-life of these cytokines in vivo (Hendel, 2000; Henry, 2001) and severe hypotension reported after bolus injection of the proteins (Hariawala, 1996; Horowitz, 1997).

As a result, a larger number of investigations have assessed the feasibility of VEGF gene delivery by gene transfer via injection of plasmid DNA or adenovirus. Both of these delivery systems led to transient production of the protein and induce

angiogenic sprouting from pre-existing vessels in different animal models and in humans (Mesri, 1995; Muhlhauser, 1995; Isner, Pieczek, 1996; Magovern, 1997; Mack, 1998). Indeed, much enthusiasm has been generated by the preliminary results of clinical trials of cardiovascular gene therapy conducted over the last few years (Ferrara, 1999).

Many growth factors are at our disposal for therapeutic intervention, alone or in combination. Few have followed the entire evolution from in vitro to preclinical and clinical phase II studies. These factors include FGF-2, VEGF-A165 and FGF-4. Others, such as VEGF-A121, HGF and the transcription factor HIF-1a are either in phase I or phase II trials.

Historically, gene transfer for the induction of therapeutic angiogenesis entered the clinical scenario in 1994, in a group of patients with critical limb ischemia and no options for conventional revascularization (Isner, Pieczek, 1996). In this case, the treatment consisted of the injection of a plasmid coding for VEGF and its effect was evaluated by angiography and nuclear magnetic resonance, which revealed the formation of new collaterals and a significant improvement in perfusion in the VEGF-treated group (Baumgartner, 1998). The only major side effect was the occurrence of a remarkable edema of the leg, probably related to the potent permeabilizing effect of VEGF (Baumgartner, 2000).

After having established proof of concept in this population, additional clinical studies were extended to patients with myocardial ischemia (Losordo, 1998) and to the use of alternative delivery systems, such as liposomes and adenoviral vectors, which are in fact the most used vectors in the clinics, (Laitinen, 1998), with several hundreds patients treated so far .

Table I presents an overview of the design and the results of the larger clinical trials of therapeutic angiogenesis already closed. What can we conclude? Actually, despite the consistent success in different animals models, clinical experience has been less successful in demonstrating benefits of therapeutic neovascularization. While the initial series of open label studies testing VEGF 165, FGF-1 and FGF-2 all showed significant improvement in myocardial perfusion and function, a similar improvement was seen in placebo groups in larger randomized double blind trials (Simons, 2002; Henry, 2003; Cao, 2005). The variable success of trials concluded to date might depend on a few recurrent reasons, including choice and formulation of growth factors, short exposure, route of administration and selection of patients.

As a preliminary consideration, which stems from the deeper understanding of the complexity of the angiogenic process, one major concern regards the evident inadequacy of a single agents to form a mature and functional vascular network. More importantly, the observation that the poor architecture and function of tumor vessels can be at least in part attributed to the imbalanced production of VEGF raised several concerns about the functional performance of the VEGF-induced neo-vasculature. Conversely, the combination of an angiogenic factor, such as VEGF, with a pro-maturation factor, such as Angiopoietin-1, could represent a rational approach to improve the remodeling and the stability of the newly formed vessels.

| Trial | Therapeutic agent | Disease target | n | End point | Results | Reference |
|---|---|---|---|---|---|---|
| VIVA Trial | rVEGF protein | CHD | 178 | ETT at 60 d | Negative | Henry et al., 2003 |
| FIRST Trial | rFGF-2 protein | CHD | 337 | ETT at 90 d | Negative | Simons et al., 2002 |
| TRAFFIC Trial | rFGF protein | PAOD | 190 | ETT at 90 d | Positive | Lederman et al., 2002 |
| AGENT Trial | Adenovirus-FGF-4 | CHD | 79 | ETT at 4 w | Positive* | Grines et al., 2002 |
| VEGF Peripheral Vascular Disease Trial | Adenovirus-VEGF165 Plasmid/liposome-VEGF165 | PAOD | 54 | Vascular density at 3 months (angiography) | Positive | Makinen et al., 2002 |
| KAT Trial | Adenovirus-VEGF165 Plasmid/liposome-VEGF165 | CHD | 103 | Improved myocardial perfusion at 6 months | Positive (adenovirus group only) | Hedman et al., 2003 |
| REVASC Trial | Adenovirus-VEGF121 | CHD | 67 | Time to 1 mm ST segment depression on ETT at 26 w | Positive | Stewart, 2002 |
| RAVE Trial | Adenovirus-VEGF121 | PAOD | 105 | Peak walking time at 12 w | Negative | Rajagopalan er al., 2003 |
| Euroinject One Trial | Plasmid VEGF165 | CHD | 74 | Improved myocardial perfusion at 3 months | Negative | Kastrup, 2003 |

**Table I. Phase II/III clinical trials addressing the efficacy of therapeutic angiogenesis.**
CHD, coronary heart disease; PAOD, peripheral vascular disease
* Only one dose group showed positive results, a larger phase-III trial has been recently stopped

An additional explanation for the poor clinical outcome of the clinical trials for the induction of therapeutic angiogenesis conducted so far stems from the low doses of VEGF that have been probably achieved with the use of plasmid DNA or of

adenoviral vectors. In fact, while plasmids can be spontaneously internalized by muscle cells, their transfection efficiency is still very low. On the other hand, as already discussed above, adenoviral vectors promote a potent inflammatory response, which rapidly switch off transgene expression.

In this context, the ability of AAV vectors to ensure a prolonged and sustained expression of the therapeutic genes in the absence of inflammation, together with the possibility to combine different vectors for the simultaneous expression of different growth factors, appear extremely appealing for the development of successful approaches of therapeutic angiogenesis in the next future.

**Does vasculogenesis exist in adult life?**

Although angiogenesis has been traditionally considered the only possible mechanism of de novo blood vessel formation in adults, a potential role for a vasculogenesis-like mechanism in adult organisms has been recently proposed.

Stem cells from adult tissues have been traditionally thought to differentiate exclusively into cell types of their tissue of origin. However, evidence has been recently accumulated that at least some stem cells may differentiate down alternative pathways when introduced into a regenerative environment. This concept of adult stem plasticity has recently generated much excitement by some authors, but it has been disbelief by several others.

One of the first indication that transdifferentiation might occur came from bone marrow transplantation experiments, in which genetically-marked hematopoietic stem cells (HSCs) were found to contribute to muscle regeneration in adult organisms (Ferrari, 1998). Moreover, HSCs transplanted into the murine ischemic myocardium have been shown to transdifferentiate into cardiomyocytes and blood vessels, thereby improving heart function and survival (Orlic, Nature 2001). These works were rapidly followed by other reports that bone marrow-derived cells could differentiate into cardiomyocytes (Bittner, 1999), osteoblasts (Horwitz, 1999), liver cells (Petersen, 1999), neurons (Brazelton, 2000) and endothelial cells (Shi, 1998).

However, since the bone marrow contains a rich reservoir of many cell types, it is very difficult to identify which cells could account for multiple activities. Interestingly, recent studies indicate that vascular cell progenitors are still present in adult circulation and resident in the bone marrow, contributing to blood vessel formation during tissue repair and in pathological conditions. This process that would involve

the coalescence of circulating and marrow-derived precursors, is thought to more closely resemble embryonic vasculogenesis rather than angiogenesis (Springer, 1998; Jackson, 2001; Kocher, 2001).

Precursors of vascular endothelial cells in adults were firstly identified in peripheral blood (circulating endothelial progenitor cells or CEPs) and compelling evidence suggests that they play an essential role in several physiological and pathological conditions, including wound healing (Asahara, 1997; Asahara, 1999; Asahara, 1999; Crisa, 1999) and myocardial ischemia (Kalka, 2000; Iwaguro, 2002). In addition, the growth of certain tumors seems to be strictly dependent upon the recruitment of CEPs and HSCs to the tumor vasculature (Asahara, Masuda, 1999; Lyden, 2001; Marchetti, 2002). In summary, CEPs can be considered to be marrow-derived angioblasts that migrate and proliferate and have the capacity to differentiate into mature endothelial cells (Coffin, 1991).

While these data originally generated a great excitement about the potential use of HSCs (or other stem cells of bone marrow origin) for tissue regeneration and revascularization, the physiological significance of CEPs in the regulation of post-natal processes has been recently the subject of intense scrutiny. Ironically, although a variety of groups worldwide have already started clinical trials of autologous bone marrow transplantation into ischemic myocardium (Britten, 2003; Schachinger, 2004), fusion of transplanted stem cells with resident cardiomyocytes has been offered as an alternative explanation for previous claims of transdifferentiation (Alvarez-Dolado, 2003; Nygren, 2004). Moreover, a couple of clever studies have ultimately demonstrated that HSC transplanted into the ischemic myocardium are not able to transdifferentiate, while they still adopt mature hematopoietic fates (Balsam, 2004; Murry, 2004)

Finally, the mechanistic underpinnings of stem cell therapy appear to be far more complex than previously anticipated, since a beneficial effect of HSCs might occur also in the absence of transdifferention, being mediated by the release of angiogenic factor, protection from cardiomyocyte apoptosis, induction of myocardial cell proliferation or recruitment of putative cardiac stem cells (Figure 3.11).

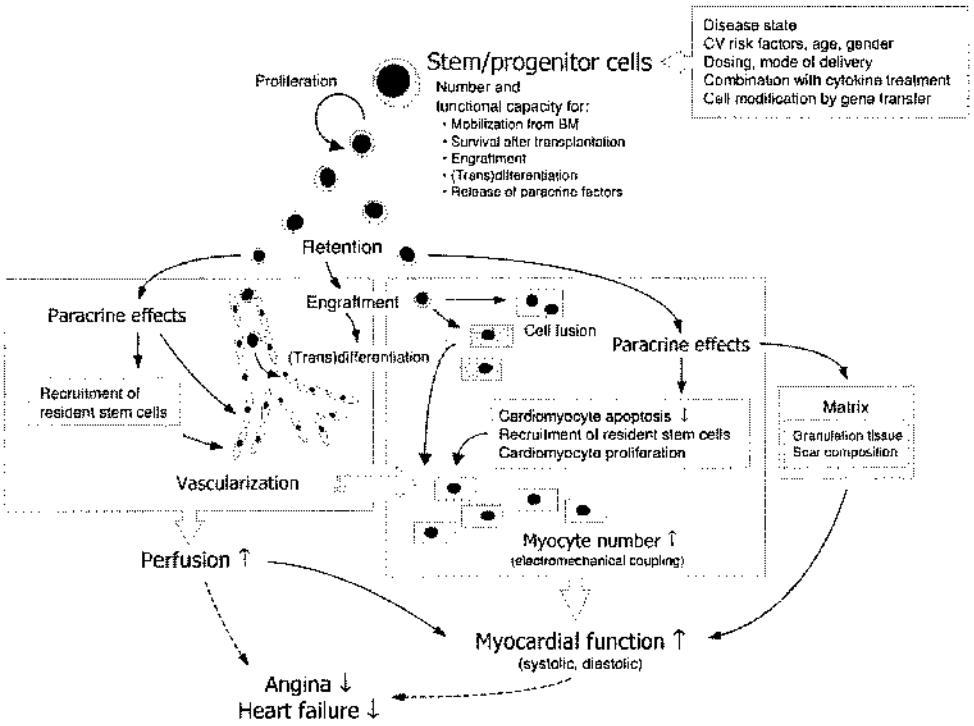


**Figure 3.11. Working hypothesis of therapeutic stem cell transplantation for the treatment of myocardial ischemia.** Stem and progenitor cells might have a favorable effect on tissue perfusion and contractile performance by promoting neovascularization and/or myocyte formation. Depending on cell type and local mileu, the relative contribution of cell incorporation (transdifferentiation and/or fusion) versus paracrine effects may vary.
*Figure adapted from Wollert et al., Circulation Research 2005*

So far, a flurry of small, mostly uncontrolled studies exploring the safety and feasibility of stem cell therapy for myocardial ischemia has been conducted. These trials have used a myriad of different cell types and preparations, each in a small number of patients, with different disease stages. Nevertheless, collectively, this preliminary clinical evidence suggest that stem cell therapy might work at some extent, and that the recruitment or transplantation of HSCs into ischemic tissues might have a favorable impact, probably through the paracrine secretion of growth and survival factors.

On this basis, several animal models have been developed, to study the mechanisms by which stem cells are mobilized from the bone marrow to particular organs, and the molecular mediators that orchestrate this process. The release of angiogenic factors and hematopoietic cytokines seems to have a major role in the mobilization of endothelial progenitors and subsets of HSCs. The exact identification of the molecular pathways that are essential in this process, as well as in the proliferation and differentiation of vascular stem cells, would open new avenues for accelerating neo-angiogenesis after vascular injury or ischemia.

In accordance with the works by Balsam and Murry (Balsam, Wagers, 2004; Murry, Soonpaa, 2004), among the several authors who tested whether circulating bone marrow–derived cells incorporate into collateral arteries after femoral artery ligation, many did not find any incorporation of bone marrow–derived cells in the endothelium and tunica media of growing vessels (Post and Waltenberger, 2005). However, they observed accumulations of bone marrow–derived cells in areas of collateral artery growth and capillary growth and identified these cells as fibroblasts, pericytes, and primarily leukocytes. These exciting data add another piece of evidence to the concept that apparently not mural, tissue-resident cells but other cell types play a more central role in vascular repair. However, given the diversity of blood leukocyte populations, the exact identity of these cells deserves careful consideration.

An increasing body of evidence suggests that an important role of inflammation as a trigger for neovascularization in the setting of ischemia. Among the players of the inflammatory response, monocytes and macrophages have been shown to accumulate in the ischemic area and positively modulate vessel growth (Arras, 1998; Heil, 2002). Accordingly, nude mice that lack all T cells or CD4+ T-lymphocyte-deficient mice exhibit a reduction in post-ischemic vessel growth, suggesting that T lymphocytes also are key mediators of neovascularization (Couffinhal, 1999; Stabile, 2003).

Inflammatory cells have been shown to promote neovascularization through various mechanisms, including production of angiogenic factors, secretion of pro-inflammatory cytokines that control the production of matrix metalloproteinases and, subsequently, ECM degradation (Sunderkotter, 1991; Silvestre, 2001; Mallat, 2002). Inflammatory cell infiltration is a feature of the post-ischemic neovascularization process. However, the mechanisms leading to leukocyte attraction to the sites of neovascularization are largely unknown. Classically, accumulation of leukocytes at inflammatory sites is regulated by a family of small, discrete chemotactic proteins, called chemokines, although a direct role of angiogenic factors in the recruitment of leukocytes cannot be excluded.

An important role of chemokine expression in the modulation of leukocyte trafficking to the neovascularization areas has been recently defined by the impairment in post-ischemic neovascularization observed in mice lacking the chemokine receptors CCR2 or CXCR3 (Heil, 2004; Waeckel, 2005) While CCR2 is mainly involved in monocyte recruitment, CXCR3 is a potent chemoattractant for T-lymphocytes. However,

monocyte infiltration is also severely affected in CXCR3-deficient mice (Waeckel, Mallat, 2005). Interestingly, the effect of CD4+ cells in vessel development are causally related, at least in part, to their capacity to attract monocytes/macrophages in the ischemic area, which subsequently trigger the neovascularization reaction (Stabile, Burnett, 2003). Collectively, these results support the concept that mechanisms contributing to the T cell-dependent neovascularization ultimately appear to reside in the ability of these cells to induce monocyte/macrophage accumulation.

Since VEGF does not only activate endothelial cells but also monocytes (Clauss, Weich, 1996), the mechanism by which VEGF can increase collateral growth could be mediated by both cell types. It is interesting to note that PlGF, a specific ligand for VEGFR1, which is the exclusive VEGF receptor identified in monocytes so far, seems not able to stimulate endothelial cell proliferation. Nevertheless, both gene knockout experiments and recombinant PlGF administration in an ischemic rabbit hindlimb model, clearly indicate a relevant role of PlGF in supporting collateral formation/arteriogenesis (Carmeliet, Moons, 2001; Pipp, Heil, 2003). Notably, monocyte depletion almost completely abolished the arteriogenic activity of PlGF, which is in agreement with the hypothesis that monocyte recruitment and activation is essentially involved in arteriogenesis.

# 3. RESULTS

### Efficient transduction of muscle tissues by AAV vectors

The tropism of AAV vectors for muscle tissues was assessed by injecting an AAV-LacZ in different muscle compartments of mice and rats, and evaluating transgene expression at different time points after transduction. In particular, to transduce skeletal muscle, 50μl of a vector stock (having a titer of $1 \times 10^{12}$ viral genome particles per ml) were injected into the distal part of the tibialis anterior muscle of mice, while 3 injections of 50μl were performed in the same muscle of rats. In the heart, two doses of 20 and 40 μl were injected intramyocardially in the mouse and rat, respectively. Transduction of the smooth muscle cells of blood vessels was only evaluated in a model of arterial restenosis in the rat, by injuring the common carotid artery with a Fogarty catheter and exposing the internal wall to the virus (50 μl) for 40 minutes before restoring blood flow (Ramirez Correa, 2004).

All the transduced tissues were analyzed for β-galactosidase expression by X-gal staining at 15 days, 1 month and 3 months after treatment. Transgene expression was found to be already high at two weeks after vector delivery and to persist, almost invariably, afterwards. A representative picture of a section of a rat skeletal muscle, a myocardium and a carotid artery 1 month after AAV-LacZ administration is shown in Figure 3.1.

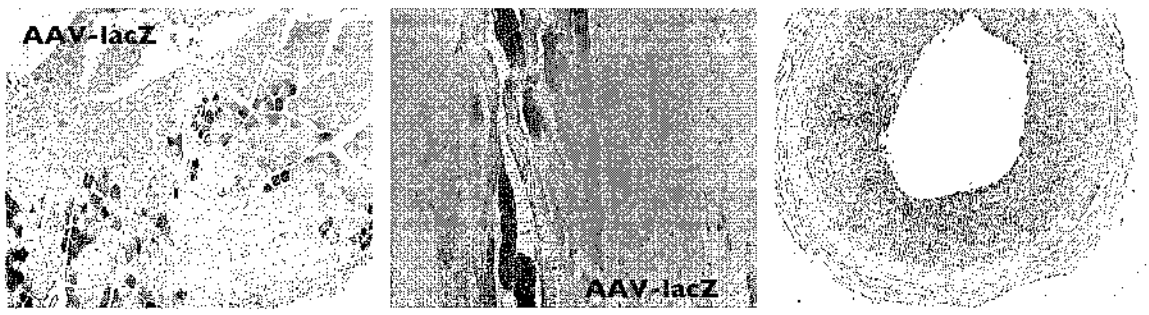


**Figure 3.1. AAV-LacZ transduction of skeletal muscle, myocardium and arterial smooth muscle cells in rodents.** Comparable amounts of AAV-LacZ ($2 \times 10^{10}$ - $2 \times 10^{11}$) were delivered into the different tissues of mice and rats to assess transgene expression by X-gal staining after 1 month.

**Long term VEGF165 gene expression is highly angiogenic in vivo**

To assess the biological effect of long term VEGF165 expression in vivo, an AAV-VEGF165 vector (see diagram in the synopsis) was injected in the right tibialis anterior muscle of normoperfused Wistar rats. Each animal also received an equal amount of AAV-LacZ or PBS in the same muscle of its left leg, as an internal control. When histological sections were examined 1 month after transduction, we observed a striking angiogenic effect, with the formation of an impressive number of new blood vessels. To start defining the phenotype of the newly formed vascular structures, we detected the presence of endothelial cells by an immunohistochemistry against the endothelial marker CD31. The number of CD31-positive cells was greatly increased in muscles transduced with AAV-VEGF165 (Figure 3.2).

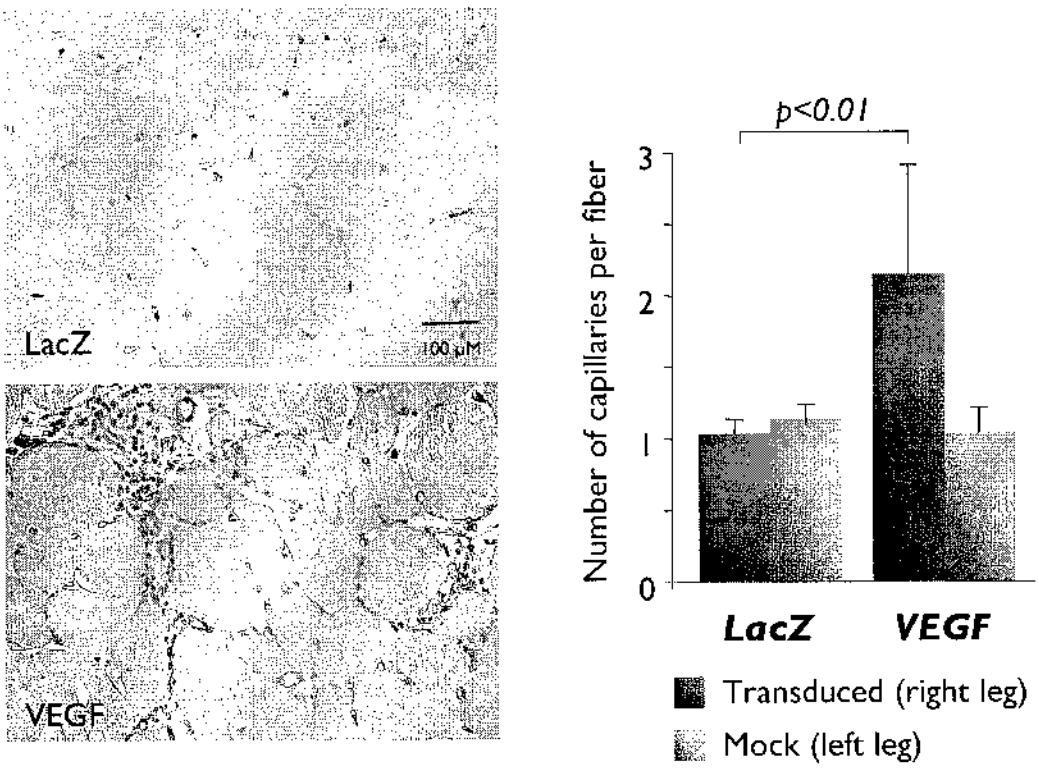


**Figure 3.2. The long term expression of VEGF165 into the skeletal muscle induced the formation of a great number of capillaries.** The prolonged expression of VEGF165 into the normoperfused skeletal muscle resulted in a 2-fold increase in the number of capillaries composed of CD31-positive endothelial cells, indicating an ongoing process of neo-angiogenesis.

The quantification of the number of capillaries (defined as 5-10 µm diameter vessels surrounded only by CD31-positive cells) revealed a 2-fold increase in the muscles

treated with VEGF165 compared to control. No significant difference in the number of capillaries was observed in animals sacrificed at earlier or later time points, although a progressive enlargement of the angiogenic area was detectable over time.

Even more impressive was the increase in the number of larger and more mature vessels, provided of a thick layer of cells expressing α-smooth muscle actin (α-SMA), a known marker of smooth muscle cells.

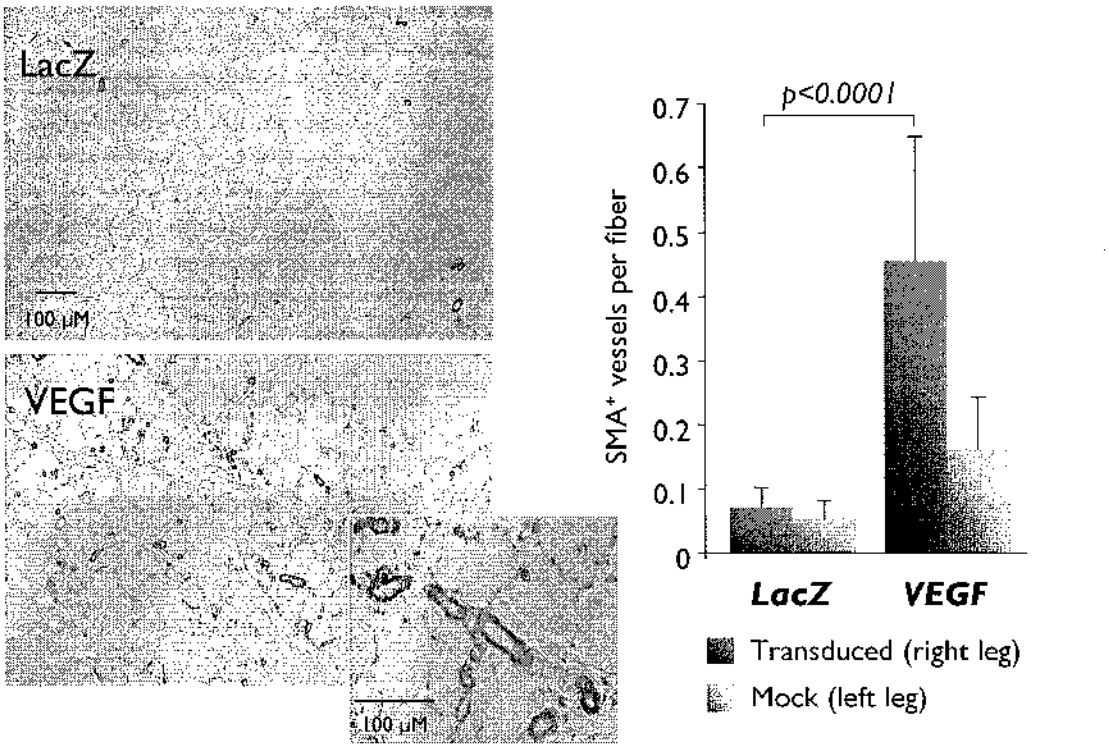


**Figure 3.3. The long term expression of VEGF165 into the skeletal muscle induced the formation of a great number of arteriolae.** The injection of an AAV-VEGF165 vector for the prolonged VEGF165 gene expression into the normoperfused skeletal muscle induced the formation of a great number of vessels positive for α-smooth muscle actin having a diameter of 20-120 μm. This resulted in an overall 6-fold increase in the number of arteriolae in the treated muscle compared to control.

As shown in the histogram of Figure 3.3, these arteriolae with a diameter in the 20-120 μm range were ~ 6-fold more abundant in the VEGF165-expressing muscles as compared to controls.

An identical histological pattern, with massive endothelial cell proliferation, capillary sprouting and formation of arteriolae, was observed in mice (not shown). As evident

from the enlargement of Figure 3.3, most of the newly formed arteriolae were filled of erythrocytes, suggesting their connection to the systemic circulation.

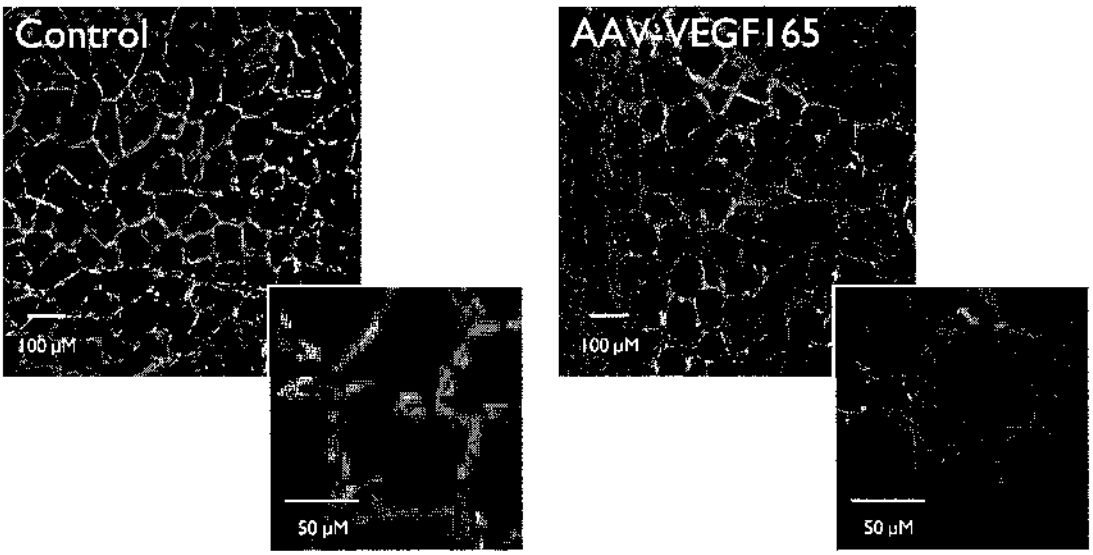


**Figure 3.4. In vivo perfusion with fluoresceinated lectin.** The vascular network formed in response to VEGF165 was reconstructed under the confocal microscope after in vivo perfusion of the animals with fluoresceinated lectin. Cellular nuclei are counterstained with Propdium Iodide and thus appear red.

In order to definitively prove this hypothesis, mice injected with AAV-VEGF165 in their right leg were in vivo perfused with fluoresceinated Lycopersicum Esculentum lectin, which strictly adheres to endothelial cells and monocytes, and therefore stably marks any perfused blood vessel. After animal sacrifice, 100µm thick cryosections of the treated and the untreated leg were subjected to confocal microscopy to obtain a 3D-reconstruction of the newly formed vessels. As evident from Figure 3.4, most of the vascular structures formed in response to VEGF165 overexpression resulted to be lectin-stained and thus appeared green, a direct indication of their functional connection to the circulatory system. Of particular interest was the observation that in the VEGF165-treated muscles only, some lectin-stained structures had the tendency to invade and substitute the muscle fiber parenchyma (see Figure 3.4, enlargement on the right).

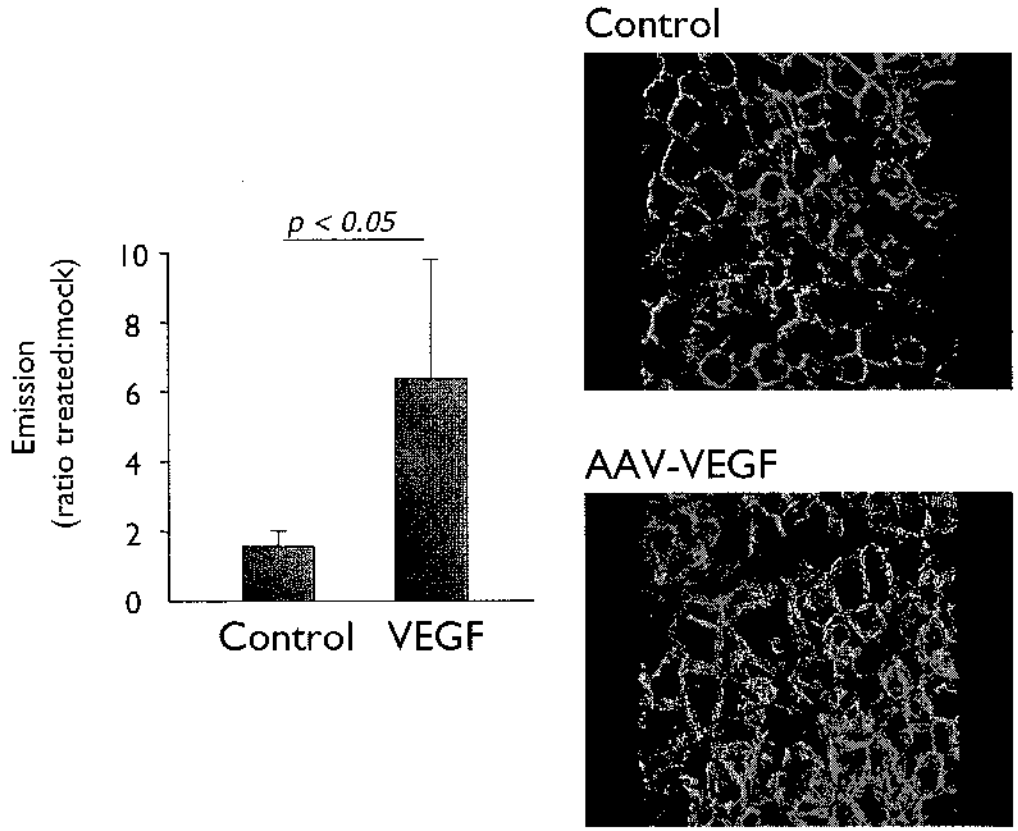


**Figure 3.5. In vivo perfusion with fluorescent microspheres.** Fluorescent microspheres injected i.v. into the animal were recovered from both the right (treated) and the left (untreated) tibialis anterior muscle, and quantified by fluorimetric analysis. Shown are means and standard deviations of the ratios between the two measurements, together with a 3D-reconstruction of the vascular network in each muscle.

As expected, the prominent angiogenic response induced by VEGF165 resulted in a marked increase in the blood volume of the treated muscle, as assessed by in vivo perfusion of the animals with a bolus of fluorescent microspheres. By the use of this technique we could obtain a quantitative measurement of the perfusion of the treated muscle relative to the controlateral untreated one, as well as a 3D-view of the vascular network that was present in each muscle. Both data are presented in Figure 3.6, showing that the treatment with VEGF165 resulted in a marked increase in the blood volume (~ 6-fold), with the formation of a network of vessels that appeared abnormally large and poorly organized.

Collectively, these results indicated that the sustained an prolonged expression of VEGF165 by AAV gene transfer was highly angiogenic in the normoperfused skeletal muscle of rodents, with the formation of a great number of new capillaries and arteriolae. These new vessels accounted for an increase in the overall blood volume of the treated muscle, a result that might suggest an increased perfusion of the

muscle fibers. However, in the same muscles we also observed the formation of several abnormal vascular lacunae, almost invariably filled of red blood cells, which had the tendency to invade and substitute the muscle fibers themselves (Figure 3.6). This unexpected phenomenon was quite impressive and led us to further characterize the functional performance of the newly formed vessels.

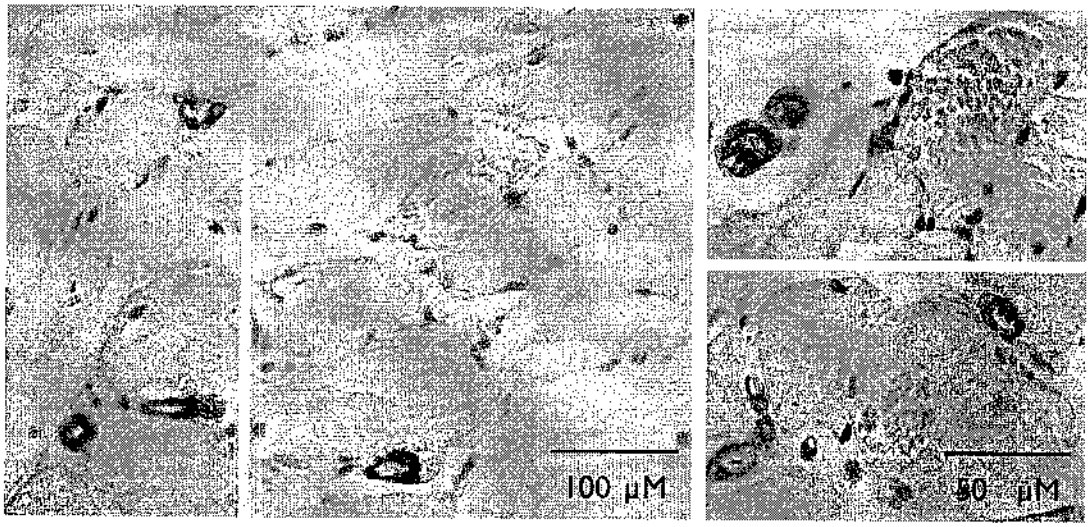


**Figure 3.6. Vascular lacunae formed in response to the prolonged expression of VEGF165.** Shown are sections from AAV-VEGF165-injected muscles, in which some of the muscle fibers appear substituted by large vascular lacunae. As clearly highlighted in the enlargements on the right, most of these abnormal vascular structures were almost completely filled of erythrocytes.

### Assessment of vascular permeability: a favorable effect of Ang1 on VEGF-induced vascular leakiness

The abnormal morphology of some vascular structures formed upon AAV-VEGF165 gene transfer suggested that they probably were not completely mature and therefore they might be not perfectly functional. In fact, the complexity of the angiogenic process is a strong indication that more than one growth factor is likely needed in order to obtain a properly organized and functional vascular network. In particular, several concerns have been raised about the widely recognized permeabilizing effect of VEGF, mainly due to the induction of endothelial fenestrations and resulting in edema formation.

To start understanding the functional competence of the VEGF-induced vessels, we analyzed vascular leakiness by an adaptation of the Miles test, after systemic

injection of a bolus of Evans blue into the jugular vein. As evident from Figure 3.7, muscles expressing VEGF165 were remarkably (approximately 6 times) more leaky than controlateral controls (visually shown in the upper panel and quantified by spectrophotometric analysis in the histogram) at both 1 and 3 months after treatment. However, this effect was consistently counteracted by the simultaneous delivery of an equal amount of a distinct AAV vector carrying the cDNA for Angiopoietin-1 (AAV-Ang1). The combination of the two factors resulted in an almost complete normalization of the vascular leakiness in the treated muscles. The expression of Ang1 alone had no effect on vascular permeability at any time point, nor it induced any visible angiogenic response (not shown).

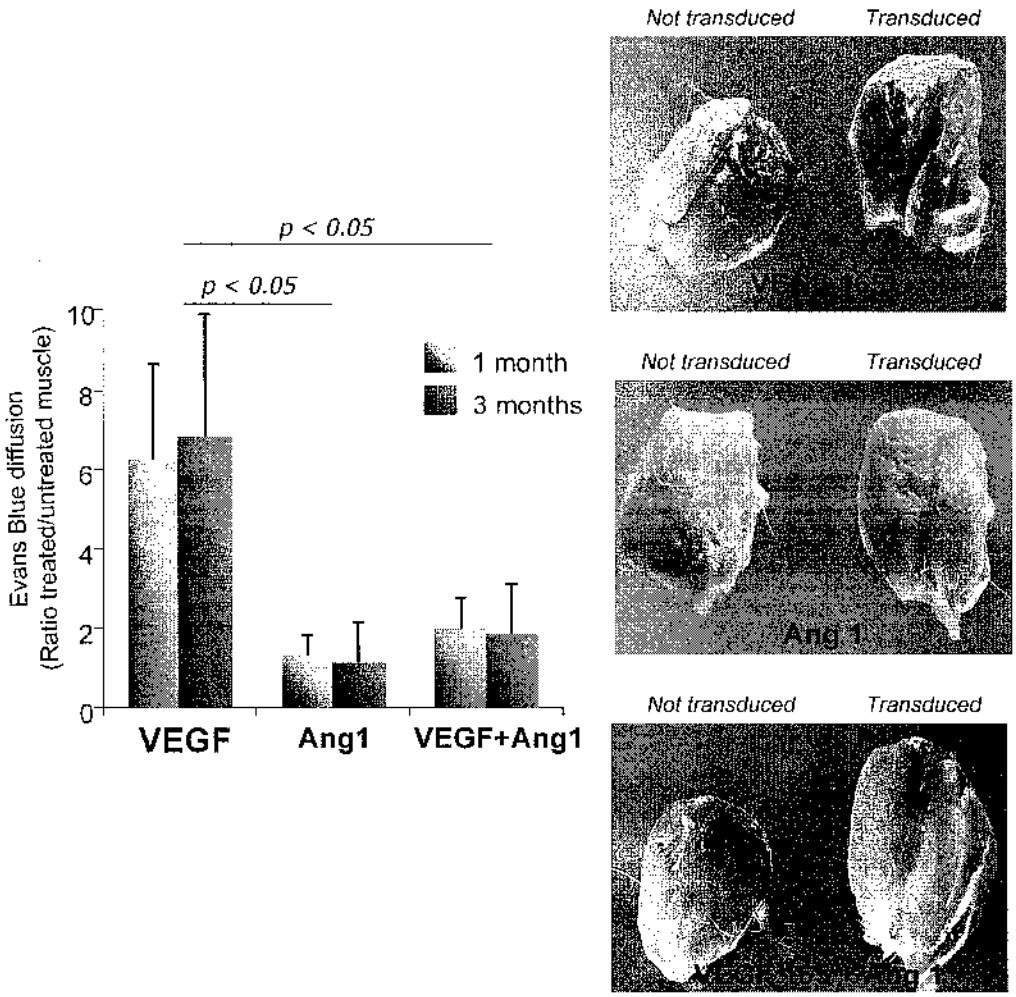


**Figure 3.7. Miles assay for vascular permeability assessment.** At 1 and 3 months after treatment, a bolus of Evans blue was injected into the jugular vein and both tibialis anterior muscles were harvested 30 minutes later. The histogram reports spectrophotometric quantification of the dye infiltrated in each muscle, expressed as a ratio between treated and mock-treated legs (shown are means and standard deviations obtained from 6 animals per group).

**Functional evaluation of the effect of AAV-VEGF165 and AAV-Ang1 transduction on muscle perfusion by PET**

Given the significant effect of Ang1 on VEGF165-induced vascular leakiness, we wanted to assess whether this also resulted in an improvement of vascular functional competence. Therefore, we set up a model to study muscle perfusion by PET, in both resting conditions and after muscle exercise. The general outline of the whole study is schematically shown in Figure 3.8.

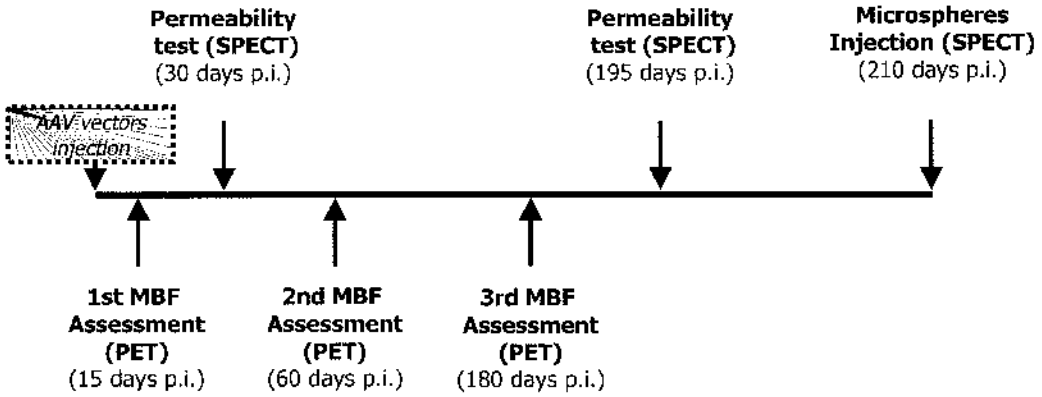


**Figure 3.8. Experimental flow chart.** All the animals injected with either AAV-LacZ, AAV-VEGF, AAV-Ang-1, or a combination of AAV-VEGF and AAV-Ang1, were subjected to PET imaging for the assessment of muscle blood flow, as well as to SPECT scanning for the sequential measurement of vascular permeability and of artero-venous shunting.

Rats were randomly divided into four experimental groups, which were all injected in their right hindlimb with an equal amount of different vector preparations (AAV-VEGF165, AAV-Ang1, AAV-VEGF165+AAV-Ang1 or AAV-LacZ), and with PBS in their left hindlimb, as an internal control; n=21 per group. All the animals were repeatedly subjected to PET imaging at different times after treatment up to 6 months, by measuring an index of muscle perfusion, bilaterally. More precisely, each PET session included two measurements of muscle blood flow (MBF), either in resting condition or after 20 min of pacing-induced bilateral muscle activity. After two weeks from the last PET experiment, all the animals were injected with $^{99}$Tc-labeled DTPA to assess vascular permeability by SPECT. Finally, after two additional weeks, they were evaluated for the presence of artero-venous shunts by the injection of radio-labeled macroaggregates into the abdominal aorta.

A representative PET image of a rat at 6 months after AAV-VEGF injection is shown in Figure 3.9. From the left panel, taken in resting conditions, is evident that, in contrast to our expectations, the prolonged expression of VEGF alone did not increase MBF as compared to the control leg. Even more surprising was the result obtained after exercise (right panel). In these conditions, vasodilation occurred in most organs, including heart, brain, kidney as well as in the left, control leg. In contrast, the VEGF-treated leg was completely unable to respond to the increased flow demand.

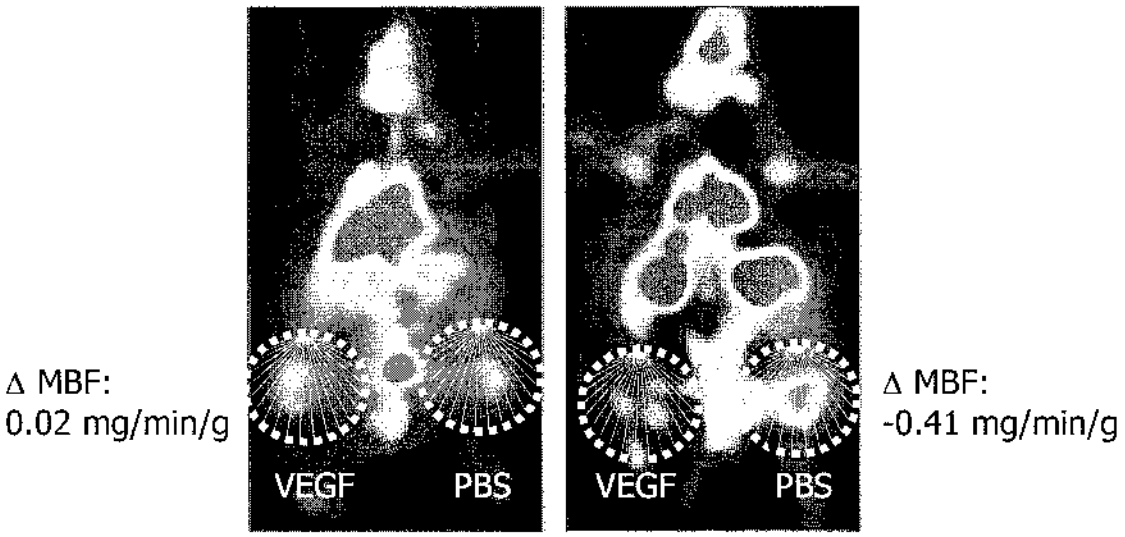


**Figure 3.9. PET image of a rat treated with AAV-VEGF165 in its right leg.** The relative perfusion of the different tissues is represented by an artificial color scale. While most organs, including the untreated controlateral leg, underwent a physiological vasodilation during muscle activity, the VEGF165-expressing muscles seemed not able to respond to the increased flow demand.

The results obtained in the whole set of animals at three time points after vector delivery are shown in Figure 3.10, expressed as ΔMBF (difference between the flow of the treated and the untreated leg). The unexpected negative effect of VEGF165 on muscle perfusion after exercise was already detectable as early as 15 days after vector injection, and became even more evident at the later time points (MBF ratio between the treated and the untreated leg was 0.70±0.13, 0.66±0.02, 0.50±0.02 at 15 days, 2 months and 6 months, respectively, vs. 0.89±0.03 control; $p<0.05$ at every time point). In contrast to VEGF alone, the simultaneous administration of AAV-VEGF and AAV-Ang1 resulted in a clear improvement in MBF both at baseline and after exercise. Again, this result was already evident at 15 days (MBF ratio: 0.61±0.34 vs. 0.33±0.05; $p<0.05$ at rest; 1.20±0.24 vs. 0.82±0.06; $p<0.01$ after

exercise) and persisted over time, up to 6 months after treatment (1.17±0.42 and 1.16±0.09 at 2 and 6 months, respectively; $p<0.01$ vs. control at both times). The expression of Ang1 alone had no effect on MBF at any time point. Therefore, the animals treated with Ang1 were not further considered in the subsequent experiments of this study.

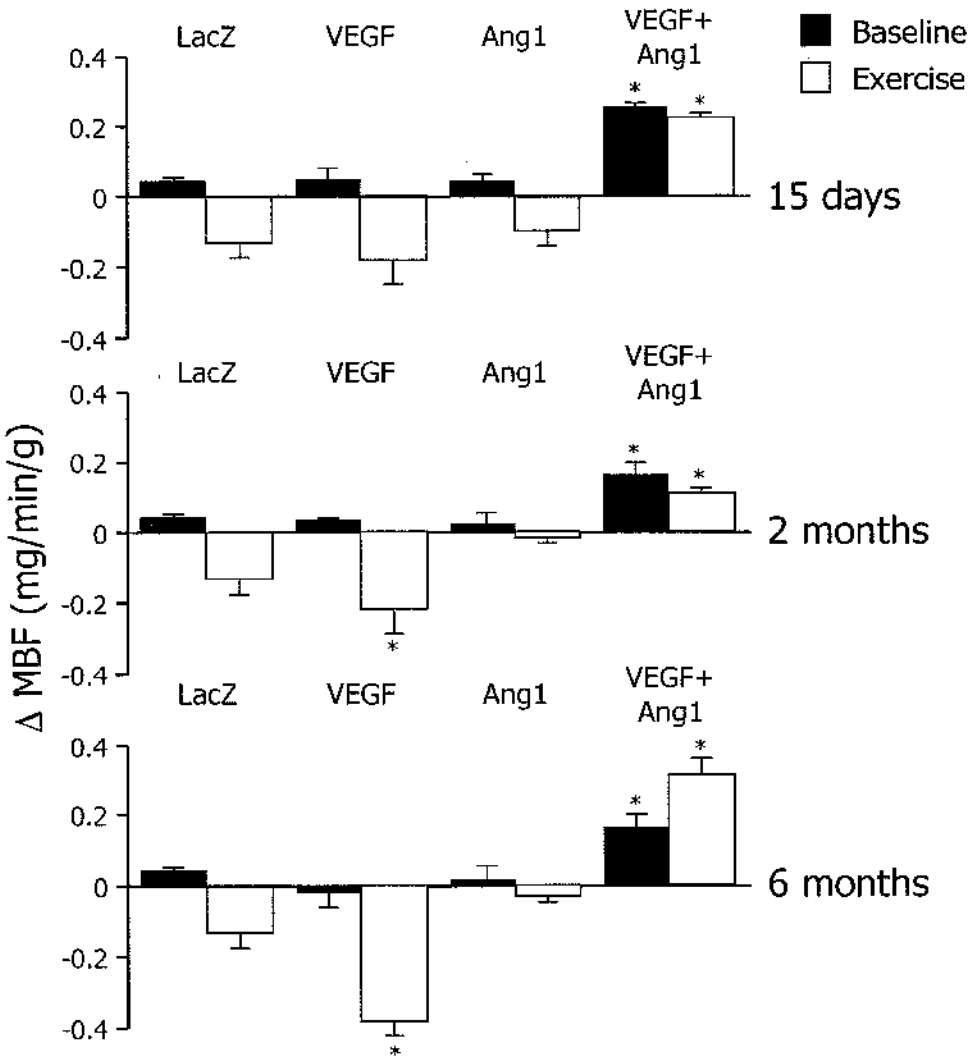


**Figure 3.10. PET analysis of MBF after VEGF165 and Ang1 gene transfer.** MBF assessment by PET revealed an unexpected drop in MBF in muscle transduced with VEGF165 after pacing-induced muscle activity. This negative effect was already detectable at 15 days and persisted up to 6 months after treatment. In contrast, the simultaneous overexpression of Ang1 resulted in a marked improvement in MBF both in resting conditions and after exercise. Asterisk denotes statistical significance over control.

**Expression of Ang1 improves functional maturation of the VEGF-induced blood vessels**

In order to start understanding the reason underlying the unexpected drop in MBF after AAV-VEGF165 transduction, we simultaneously analyzed the vascular volume and permeability of the treated muscles by the infusion of $^{99}$Tc-DTPA, in the same set of animals previously studied by PET. As expected, the delivery of AAV-VEGF165 was found to determine a remarkable increase in the blood volume of the treated leg, which was evident at 1 month (2.9±0.8 vs. 1.0±0.1, $p<0.05$) and further increased at 6 months after treatment (6.1±1.6 vs. 1.3± 0.2) (Figure 3.11). In contrast, the co-injection of AAV-Ang1 significantly counteracted this effect, although at 1 month a modest but not significant increase in vascular volume was still detectable relative to control.

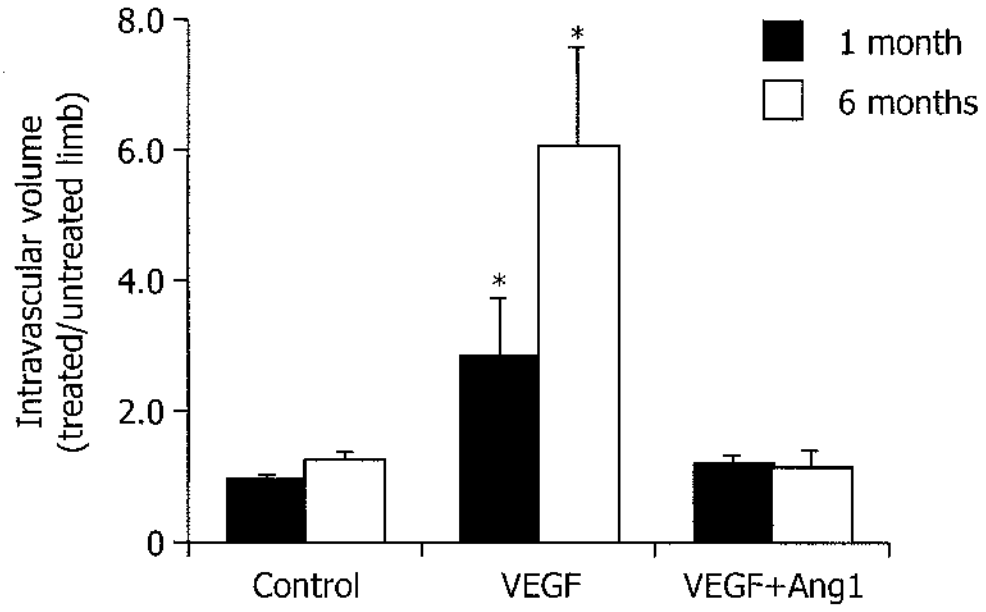


**Figure 3.11. Determination of intravascular volume by infusion of $^{99}$Tc-DTPA.** An index of the intravascular volume of the treated and the untreated legs was calculated by the systemic injection of $^{99}$Tc-DTPA. As evident from the histogram, muscle expressing VEGF165 displayed a remarkable increase in the overall blood content, while almost physiological levels were detected in muscle co-injected with AAV-VEGF and AAV-Ang1. Asterisk denotes statistical significance relative to control.

In the same set of experiments, an index of vascular permeability was also determined, as shown in Figure 3.12. In perfect agreement with the results of the

Miles test, obtained ex vivo up to 3 months after treatment, the injection of AAV-VEGF 165 caused a significant increase in the permeability of the treated leg, at both 1 and 6 months, while the simultaneous delivery of AAV-Ang1 resulted in a marked reduction of the VEGF-induced vascular leakiness, achieving an almost complete normalization after 6 months (1.4±0.1 vs 2.2±0.3 at 1 month and 1.1±0.1 vs 1.6±0.2 at 6 months, $p<0.05$).

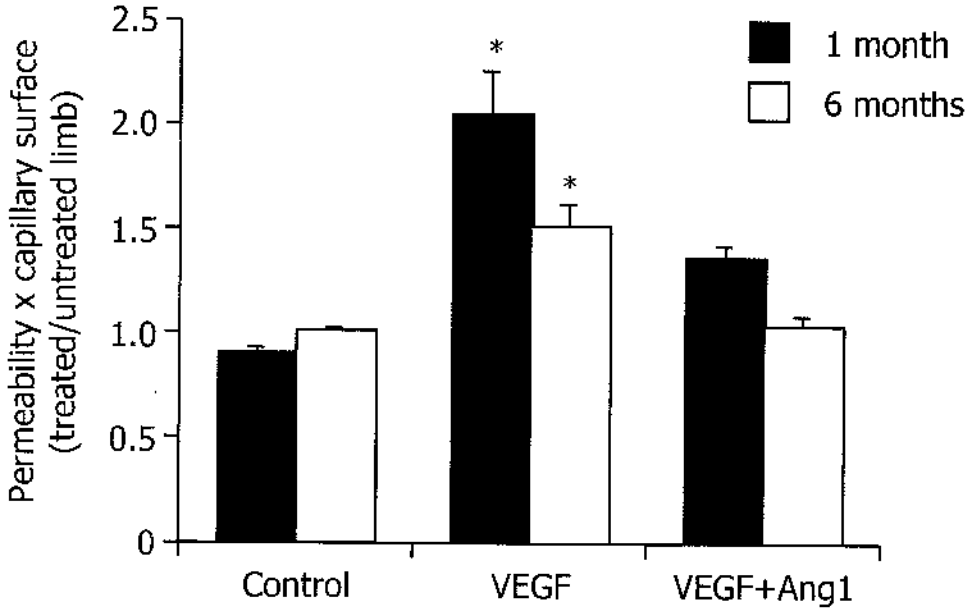


**Figure 3.12. Vascular permeability in vivo assessment by infusion of 99Tc-DTPA.** An index of vascular permeability for both the treated and the untreated leg was also determined after the systemic injection of 99Tc-DTPA. At 1 and 6 months after AAV-VEGF165 injection, the muscles resulted to be significantly more leaky than controls. In contrast, the simultaneous delivery of AAV-Ang1 efficiently counteracted this effect, accounting for an almost complete normalization of the permeability at 6 months after treatment. Asterisk denotes statistical significance

Overall, these functional experiments provided quite contradictory results. In fact, to our surprise, we found a drop in functional muscle perfusion by PET after AAV-VEGF165 gene transfer, but an increased intravascular volume, as assessed by both in vivo perfusion with fluorescent microspheres and $^{99}$Tc-DTPA injection.

As already mentioned, one possible explanation for the poor function of the VEGF-induced vessels could be their abnormal permeability, resulting in edema formation and subsequent hemodynamic impairment. In contrast, the significant effect of Ang1 on vessel maturation, through the reinforcement of the junctions between

endothelial cells, extracellular matrix and pericytes, is in prefect agreement with the observed improvement in MBF after the simultaneous delivery of AAV-VEGF165 and AAV-Ang1.

Alternatively, as already mentioned before, the documented formation of several large vascular lacunae might constitute a sort of blood reservoir, unable to efficiently flow through the vascular network and thus to actively provide oxygenated blood to muscle fibers. To start address this hypothesis, we wanted to further investigate the morphological details of the newly formed vascular structures in a subset of animals injected with AAV-VEGF165 or AAV-VEGF165 plus AAV-Ang1. Three animals for each experimental group were systemically perfused with a suspension of 0.2 μm red fluorescent microspheres, as already described for mice. After animal sacrifice, thick muscle sections (100 μm) were scanned, by acquiring at least 20 confocal planes for a 3D-reconstruction of the image. A planar view of a reconstruction for each experimental group is shown in Figure 3.13. In accordance with our previous findings on mouse muscles, the vessels formed in response to VEGF165 were found to be abnormally large and poorly organized, with a pronounced tendency to invade the muscle fiber parenchyma.

In contrast, more structured vessels were evident when Ang1 was expressed together with VEGF165 by the skeletal muscle. Interestingly, in the latter group, each muscle fiber appeared to be surrounded by a network of capillaries, each one being larger and more tortuous than those seen in the control.

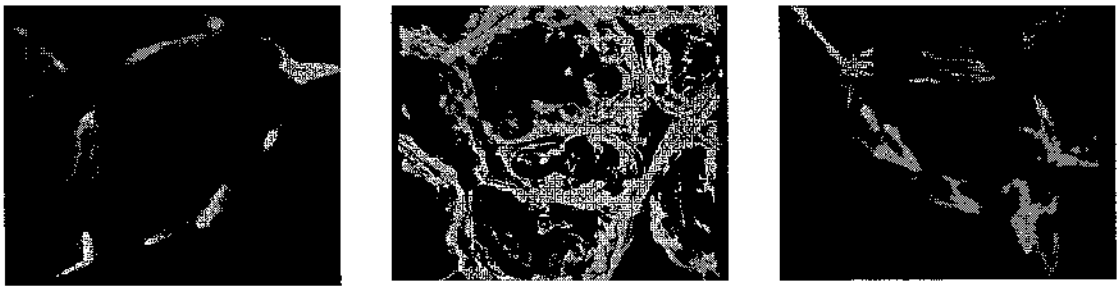


**Figure 3.13. Morphological evaluation of the capillary network formed in response to VEGF165 or VEGF165 + Ang1.** After in vivo perfusion of the animals with fluorescent microspheres, a 3D-reconstruction of the vascular network was obtained by confocal image scanning. As evident in the central panel, VEGF165 expression induced the formation of large vascular structures, invading the muscle fiber parenchyma. In contrast, the simultaneous expression of VEGF165 and Ang1 resulted in a more structured capillary network.

**Evaluation of the presence of artero-venous shunts after VEGF165 and Ang1 overexpression**

Considering the abnormal shape and size of the vessels formed by VEGF165, a possible explanation for their poor functional performance, alternative or additional to the permeability hypothesis, was to assume the formation of artero-venous shunts that might bypass the capillary system, thus not allowing a proper perfusion of the muscle fibers. In an attempt to verify this hypothesis, a bolus of radioactive macroaggregates in a 50-100 μm diameter range, was injected into the abdominal aorta to ensure their symmetrical distribution to the hindlimbs, bilaterally. The amount of radioactive spheres that were not trapped in the capillary bed and shunted to the lungs was detected by SPECT. As shown in Figure 3.14, a significant amount of radioactivity was found in the lungs of animals treated with AAV-VEGF, indicating the presence of an important artero-venous shunting (11.31±1.21% of abdominal aorta flow shunted to the lungs in the VEGF group vs. 3.6±0.44% in the control group, $p<0.01$), while the co-injection of AAV-Ang1 markedly reduced this phenomenon (6.19±0.61, $p<0.01$ vs. VEGF). A representative SPECT image of a rat for each experimental group is provided in the Figure, in which the histograms represent the means and standard deviations of the same animals previously considered in the perfusion and permeability experiments.

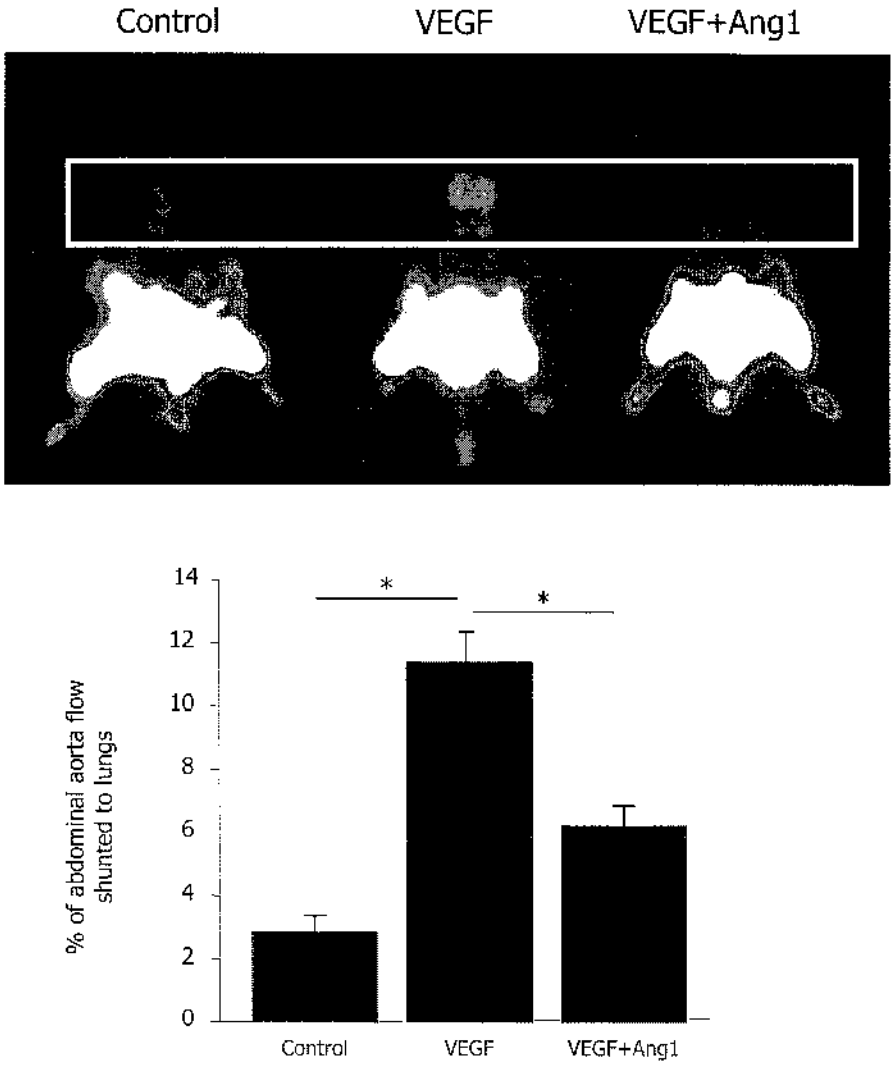


**Figure 3.14. Artero-venous shunting assessment.** The injection of radioactive macroaggregates into the abdominal aorta allowed the detection of artero-venous shunting activity. The presence of a significant amount of radioactivity in the lungs of animals treated with AAV-VEGF165 indicated the formation of an important number of artero-venous shunts, which resulted significantly reduced by the co-injection of AAV-Ang1. Asterisk denotes statistical significance.

**The overexpression of VEGF165 induces the recruitment of mononuclear cells from the bone marrow**

Beside the prominent angiogenic effect, the AAV-mediated overexpression of VEGF165 also induced a characteristic infiltration of mononuclear cells in the normoperfused skeletal muscle (Figure 3.15). These infiltrates definitely arise as a consequence of VEGF165 expression, since they were never observed in muscles injected with other AAV vectors expressing reporter genes (GFP, LacZ) or several other factors.

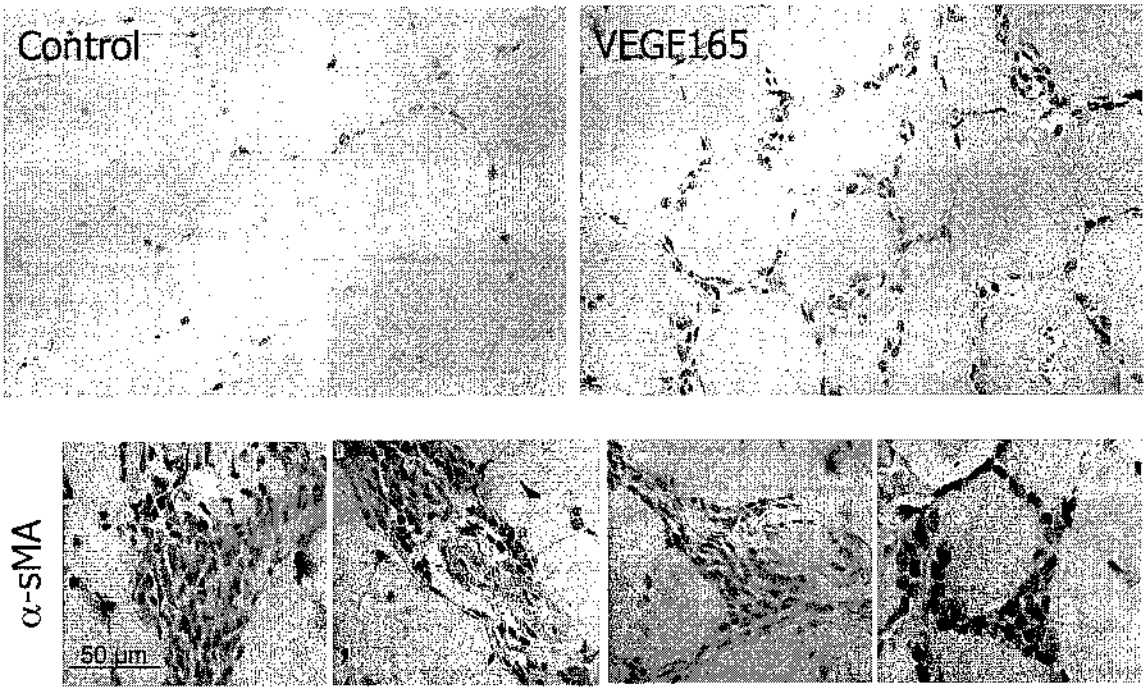


**Figure 3.15. AAV-VEGf165 induced the appearance of a massive cellular infiltrate.** Muscles expressing VEGF165 were characteristically infiltrated by a large number of mononuclear cells, in the interstitial space surrounding muscle fibers and in close proximity to the growing vessels.

Remarkably, these cellular infiltrations were always found in close proximity to the growing vessels, which are shown by α-SMA-immunohistochemistry in the enlargements of Figure 3.15 and in Figure 3.16. Of interest, these cells were already evident as soon as 3 days after AAV-VEGF165 injection. However, an inverse relationship between the entity of the cellular infiltration and the formation of

arteries could be observed over time, with the cells being more abundant at the earlier time points, when the arteries were not formed yet. Conversely, at 3 months after treatment, the appearance of arterial vessels was associated with a marked reduction in the number of infiltrating cells (no additional histological changes could be observed at later time points, up to several months after AAV-VEGF165 administration).

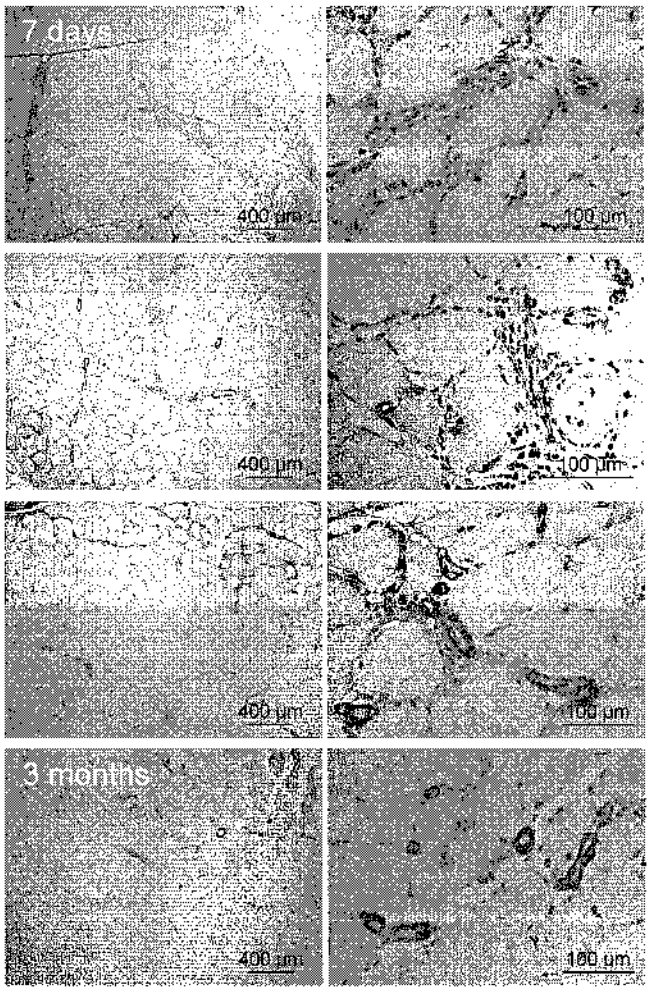


**Figure 3.16. Time course of the effect of VEGF165 overexpression.** An inverse relationship between the extension of the cellular infiltration and the formation of arterial vessels could be observed over time. While a massive infiltrate and no arteries could be detected soon after transduction, few cells were still present at the later time points, when several arteries became evident, interspersed between muscle fibers.

In order to start defining the origin of these cells, we undertook their extensive immunological characterization by immunofluorescence. As shown in the representative pictures reported in Figure 3.17, ~30% of the infiltrating mononuclear

cells were positive for CD31 and less than 10% for α-SMA, two markers of mature vascular cells. Of interest, ~20% of the infiltrating cells scored positives for the broad myelo/monocytic marker CD11b, with significant positivity also for the macrophage marker F4/80. Positive signals were also detected for Flk-1, Sca-1 and CD34, which are expressed by differentiated endothelial cells but also by progenitor cells of both endothelial and muscle lineages. Finally, a careful analysis also allowed the identification of rare c-kit positive cells.

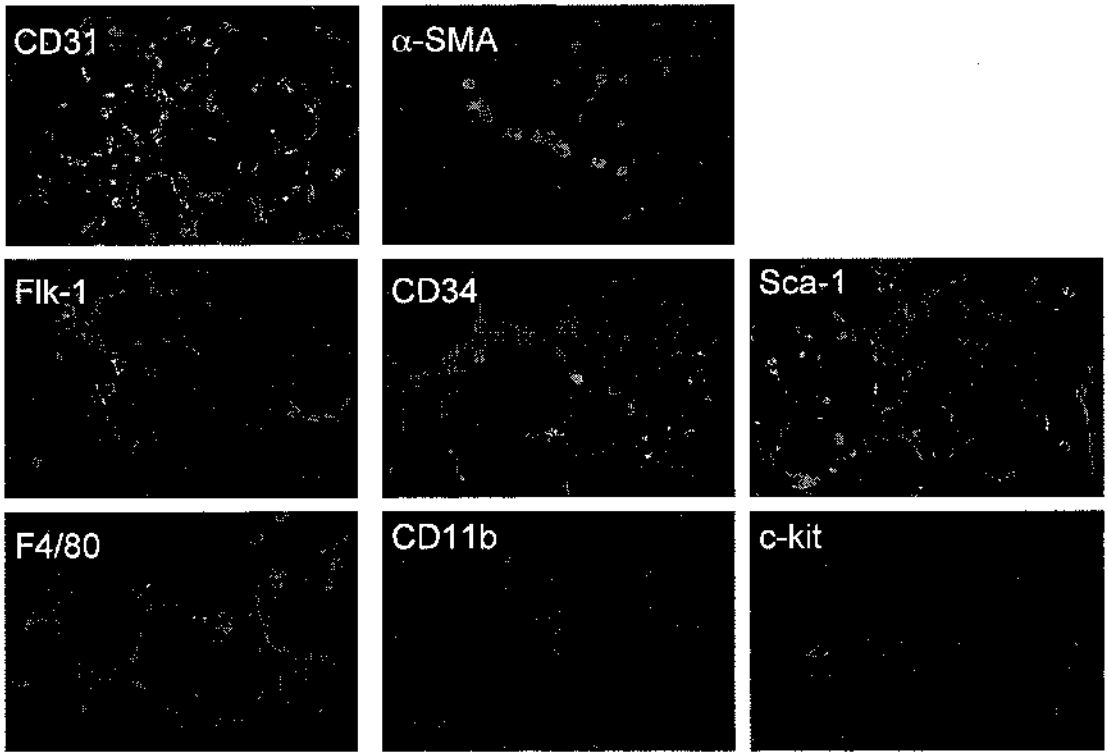


**Figure 3.17. Immunological characterization of the mononuclear cells infiltrating the foci of VEGF165-induced neovascularization.** Immunofluorescence staining was performed using CD31, α-SMA, Flk-1, CD34, Sca-1, F4/80, CD11b and c-kit specific antibodies, on histological sections of mouse tibialis anterior muscles injected with AAV-VEGF165 at 2 weeks after transduction. Positive cells are stained in red. Blue: nuclei stained with DAPI.

Taken together, these observations led to the fascinating hypothesis that the local expression of VEGF165 might trigger the recruitment and the subsequent differentiation of progenitor cells to the sites of new blood vessel formation.

As a first step to understand the origin of these cells and their contribution to the process of new blood vessel formation at the sites of VEGF165 overexpression, we

set up a bone marrow transplantation model as schematically described in Figure 3.18.

Unfractionated bone marrow cells from male Balb/c donor mice were transplanted into lethally irradiated syngenic female recipients, thus creating a Y-Balb/c chimeric mouse. The efficiency of engraftment was assessed by quantifying the copy number of donor-specific Y chromosome sequences by a competitive PCR assay and resulted to be >90%.

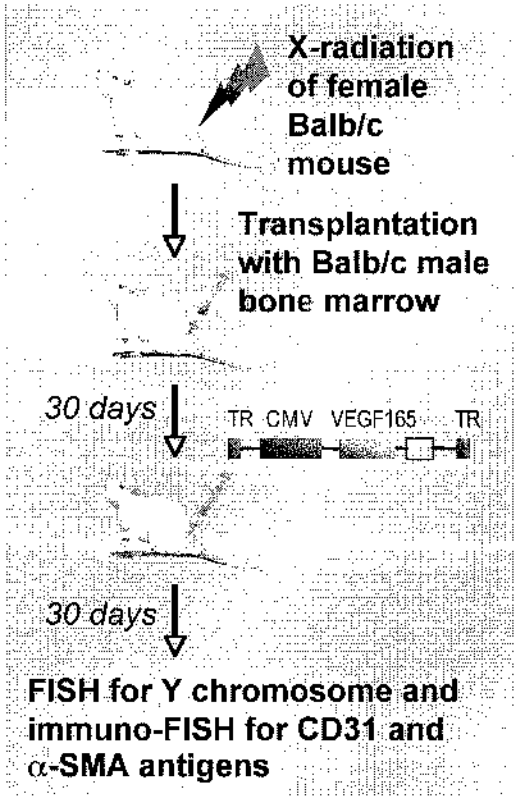


**Figure 3.18. Bone marrow transplantation model.** Female mice were lethally irradiated and subsequently transplanted with male bone marrow in order to have the Y-chromosome as a marker of bone marrow cellular origin. One month after bone marrow transplantation, the recipient females were injected with AAV-VEGF165 into the tibialis anterior skeletal muscle. The recruitment of bone marrow cells at the sites of neo-angiogenesis and their transdifferentiation into vascular structures were assessed by FISH and immunofluorescence.

After one month, the right tibialis anterior muscle of the transplanted female mice was injected with AAV-VEGF165. In this experimental system, the presence of male cells at the site of neo-angiogenesis was thus easily detectable by fluorescent in situ hybridization (FISH), by using a probe specific for the Y chromosome, as shown in the upper panels of Figure 3.19 on control male nuclei. In the same figure, the lower

panels show the cellular infiltrate recruited in a muscle of transplanted chimeric females upon AAV-VEGF165 injection.

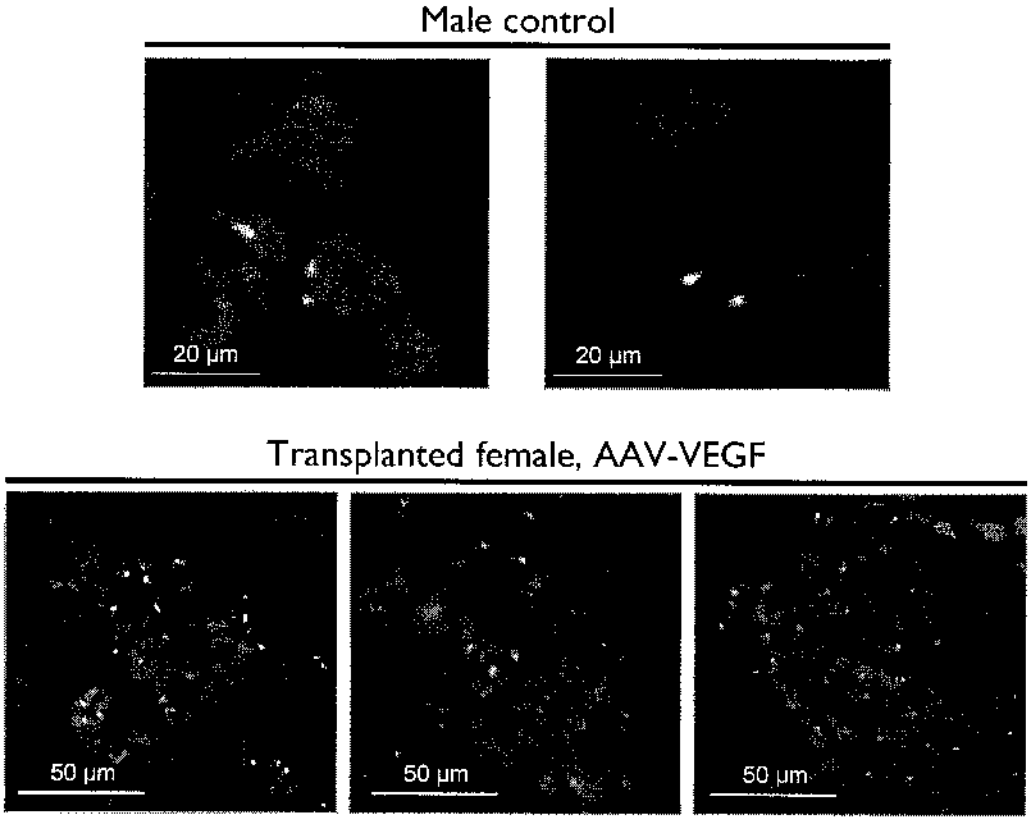


**Figure 3.19. FISH for the detection of the Y chromosome on tissue sections.** The upper panels show a control FISH for the detection of the Y chromosome (in green) within the nucleus of male muscle cells. Cellular nuclei are counterstained with Propidium Iodide and thus appear red. The lower panels show the cellular infiltration in muscles of female mice transplanted with male bone marrow and subsequently injected with AAV-VEGF165. Almost all the infiltrating cells seemed to react to the Y-chromosome probe, an observation that clearly indicate their bone marrow origin.

Here, the number of infiltrating cells bearing the Y chromosome ranged between 55 and 80% of the total cells, thus unequivocally indicating their bone marrow origin (it is noteworthy that this technique routinely detects 80% of Y- chromosome positive cells when performed on control male tissues).

**Bone marrow cells are not incorporated into the newly formed vessels**

At this point, we wanted to further explore the possible direct contribution of the recruited bone marrow cells to new blood vessels formation, by looking at their transdifferentiation into endothelial or smooth muscle cells. For this purpose, FISH analysis was combined to immunofluorescent staining of endothelial (CD31) or arterial ($\alpha$-SMA) markers. As shown in Figure 3.20, the vast majority of cells expressing either of the two markers were not found to contain a Y chromosome, an observation undoubtedly indicating their origin from the recipient and not from the transplant. Accordingly, most of the infiltrating cells, which were positive for the Y chromosome, did not express either of the two differentiation markers. Indeed, after careful observation, a few cells displaying the CD31 antigen and bearing a Y chromosome were occasionally detected within the bulk of mononuclear infiltrating cells. However, these were definitely very rare events. Out of 1,100 cells with a Y chromosome-positive nucleus, <1% was found to also express the CD31 marker. Additionally, most of these CD31/Y positive cells did not appear to be incorporated into the endothelial layer of vessels, even if they were found in close contact with the vascular wall (a few examples of these cells are shown in the enlargements at the bottom of the Figure).

No cells of donor origin and positive for the $\alpha$-SMA antigen were ever found in the tunica media of vessels after a serial examination of the treated muscles. Also, no major changes could be detected over time, from 15 days after transduction, up to three months.

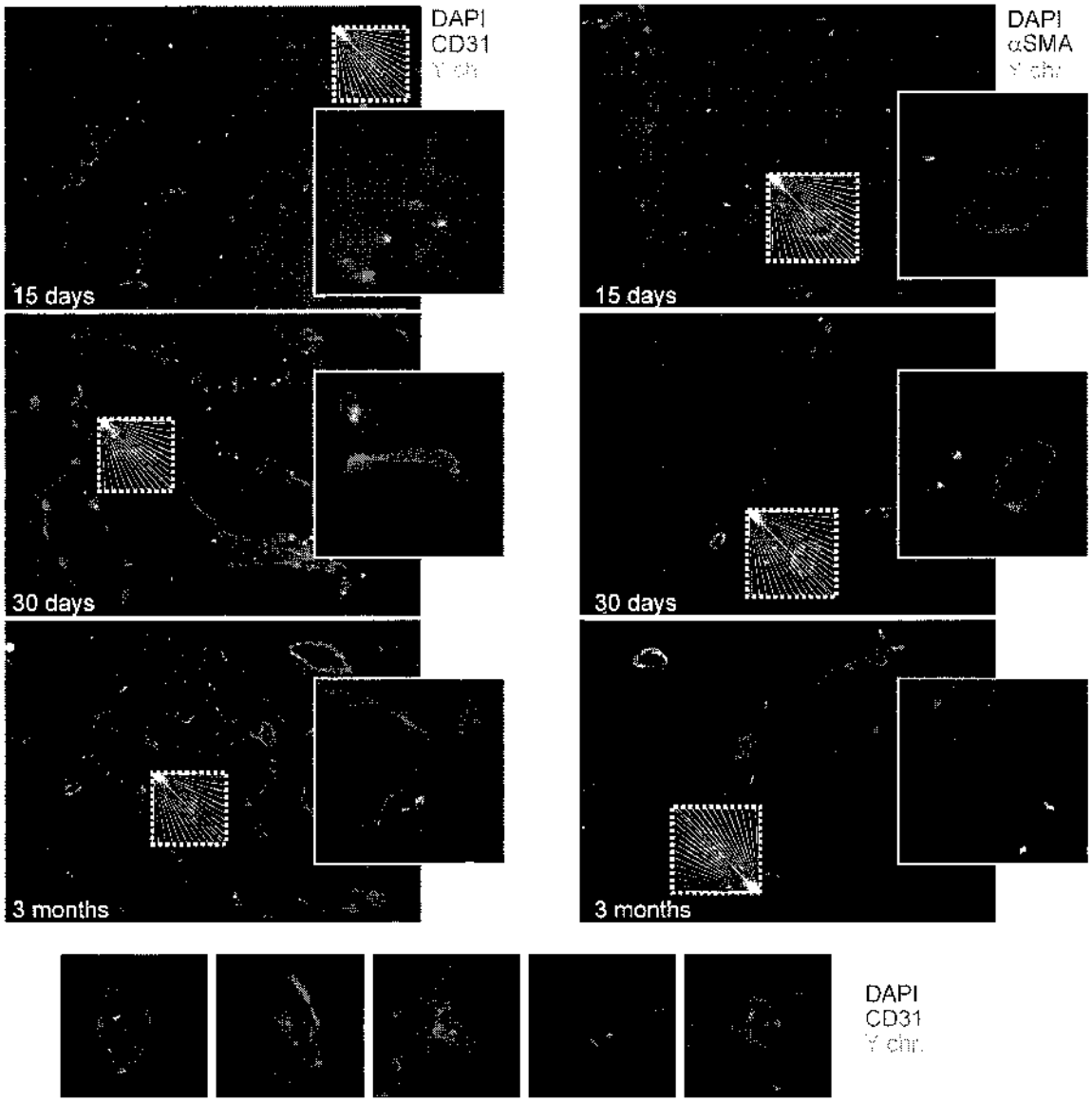


**Figure 3.20. Immunofluorescence staining for endothelial (CD31) and smooth muscle (α-SMA) antigens was combined with Y chromosome fluorescent in situ hybridization.** The vast majority of cells expressing either of the two markers were not found to contain a Y chromosome (left panels). Very rare cells (<1% of total Y chromosome-positive nuclei) were positive for CD31 and Y chromosome markers (shown in the enlargements on bottom); cells of donor origin and positive for the α-SMA antigen were never found in the tunica media of vessels.
Blu, nuclei stained with DAPI, Red, CD31 (left) and α-SMA (right) positive cells, Yellow, Y chromosome.

Collectively, these observations clearly indicated that VEGF165 induced a massive recruitment of bone marrow cells, mainly belonging to the myeloid lineage, to the sites of neo-angiogenesis, but also that these cells did not directly participate to new blood vessel formation. Therefore, the functional role of these cells still remained to be elucidated.

**Absence of cell recruitment and arterial formation upon VEGF121 gene transfer**

Some new insights on their possible function came from the study of the angiogenic effect exerted by the 121 aminoacid isoform of VEGF (VEGF121), which binds to the canonical receptors VEGFR1 and VEGFR2 but lacks the domain for binding the co-receptor NP-1. As expected, the injection of AAV-VEGF121 into the normoperfused skeletal muscle induced a massive capillary sprouting, as shown in the left side of Figure 3.21 at two different magnifications by immunofluorescent staining of frozen sections with an antibody against CD31.

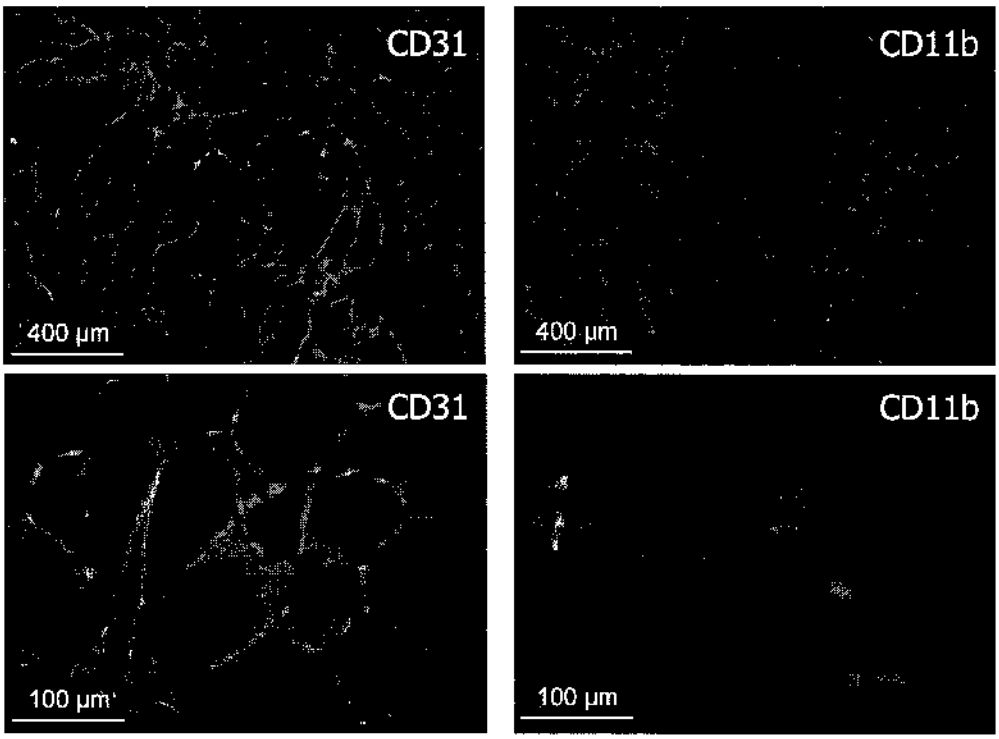


**Figure 3.21. Biological effect of AAV-VEGF121 into the normoperfused skeletal muscle.** The injection of an AAV vector coding for the 121 aa isoform of VEGF, which binds VEGFR1 and VEGFR2 but not NP-1, induced massive proliferation of CD31-positive endothelial cells in the absence of CD11b cells infiltration.

Interestingly, VEGF121 did not induce the huge infiltration of mononuclear cells observed after VEGF165 overexpression (right panels of Figure 3.21), strongly implicating a role of NP-1 in the recruitment of those cells.

Even more intriguing was the observation that the absence of bone marrow cell infiltration at the sites of neo-angiogenesis after VEGF121 gene transfer was

paralleled by poor formation of arterial vessels (shown in Figure 3.22 by anti-α-SMA immunohistochemistry at two different magnifications and at two different times after transduction).

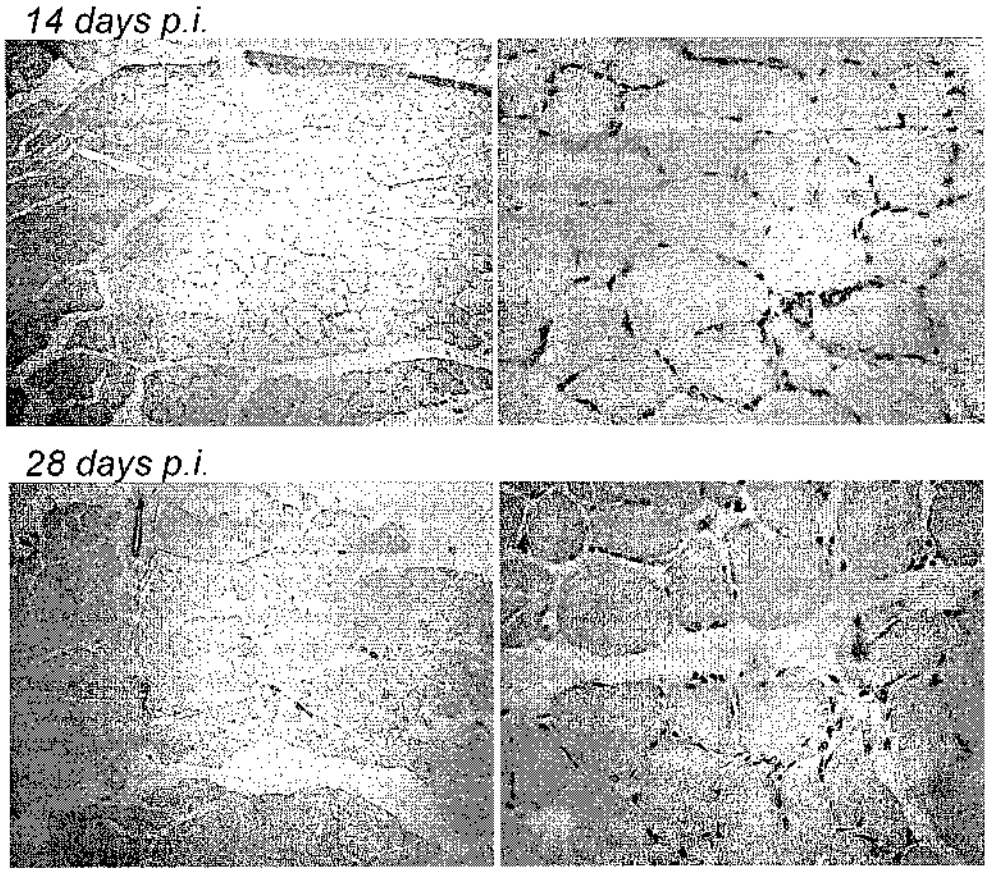


**Figure 3.22. Absence of arterial formation after AAV-VEGF121 gene transfer.** The inability of VEGF121 to recruit myeloid cells from the bone marrow correlated with its failure to form arterial vessels, as detected by immunostaining tissue samples with an antibody specific for the smooth muscle marker α-SMA.

Thus, the comparison between the angiogenic pattern induced by the two main VEGF isoforms, composed of 121 and 165 aminoacids respectively, revealed two important differences, with VEGF165 being able to recruit bone marrow cells and to form arteries and VEGF121 being incapable to sustain both events. Figure 3.23 summarizes these differences, by showing a representative CD31/α-SMA double-immunofluorescence on a muscle section for each of the two isoforms, as well as the quantification of the relative area occupied by cellular nuclei (DAPI staining), endothelial cells (CD31) and arterial smooth muscle cells (α-SMA) at 1 month after transduction.

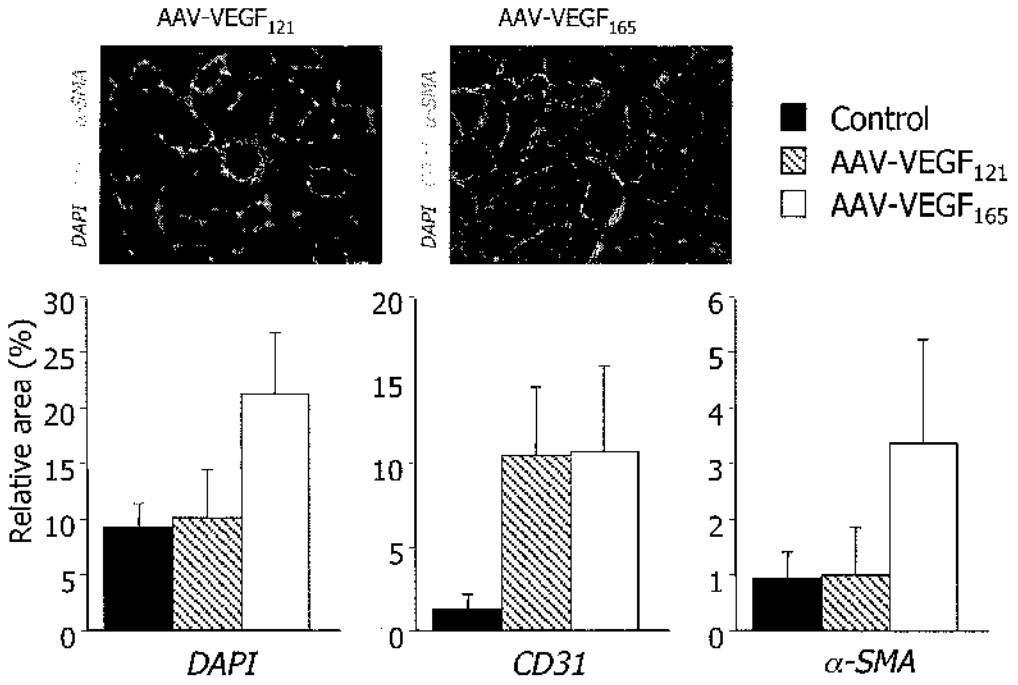


**Figure 3.23. Comparison between VEGF121- and VEGF165-induced angiogenesis.** While VEGF165 induced massive cell infiltration (DAPI nuclear staining) and arterial formation (α-SMA immunostaining), only capillary sprouting (CD31 immunostaining) could be detected after VEGF121 gene transfer. The histograms show the quantification of the relative area occupied by cellular nuclei (DAPI), CD31-positive cells and α-SMA-positive cells in tissue sections of muscles injected with AAV-VEGF121, AAV-VEGF165 or control vehicle at 1 month after transduction.

As already noted, the different angiogenic phenotype induced by VEGF121 and VEGF165 suggested a functional relationship between the recruitment of bone marrow cells and the formation of arterial vessels. In addition, the notion that the two isoforms mainly differ in term of NP-1-binding ability, prompted us to investigate further the role of NP-1 in bone marrow cell recruitment and arteriogenesis.

### Biological effect of AAV-Sema3A

For this purpose, we developed a new AAV vector for the expression of Sema3A, a well-known NP-1 ligand in the developing central nervous system. Surprisingly, the injection of AAV-Sema3A in the normoperfused skeletal muscle induced the appearance of a cellular infiltration very similar to the one observed upon VEGF165 gene transfer (a representative histological section at 1 month after transdcution is shown in Figure 3.24, left panel). However, no new blood vessels could be detected

in these muscles, as shown in the right panel of the same Figure by α-SMA immunohistochemistry. This latter observation is in perfect agreement with consistent literature data indicating a specific inhibitory effect of Sema3A on VEGF-induced endothelial cell activation (Miao, Soker, 1999).

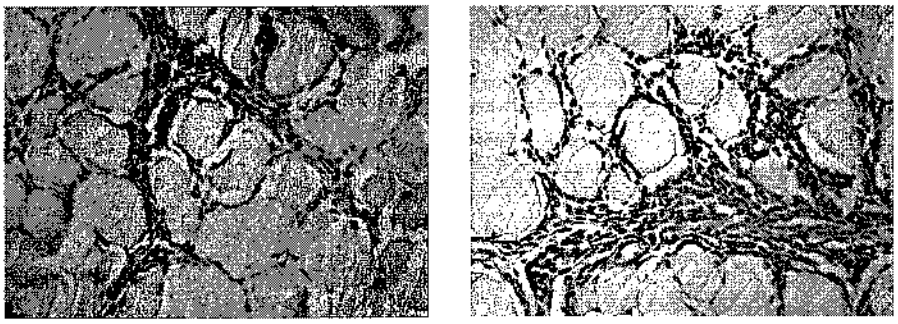


**Figure 3.24. Sema3A induces cellular infiltration but is not angiogenic.** The injection of AAV-Sema3A induced the appearance of a mononuclear cell infiltration very similar to the one recruited by VEGF65. However, no arterial formation could be detected in these muscles, as shown in the right panel by α-SMA immunohistochemistry.

Not only Sema3A was not able to drive an angiogenic response, but when AAV-Sema3A was co-injected with AAV-VEGF165, an impressive inhibition of VEGF165-induced angiogenesis was observed. This inhibitory effect was always evident, either by staining the vessels with an anti-CD31 antibody (Figure 3.25) or by using an anti-α-SMA antibody (Figure 3.26).

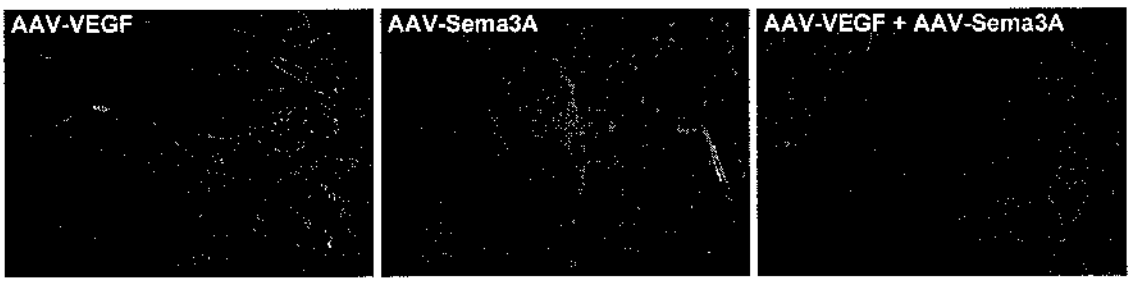


**Figure 3.25. Sema3A inhibits VEGF-induced angiogenesis.** In contrast to the massive endothelial cell proliferation and capillary sprouting observed upon AAV-VEGF165 injection, AAV-Sema3A was not angiogenic at all. In contrast, a specific inhibitory effect on VEGF165-induced neo-angiogenesis was observed when the two vectors were simultaneously injected into the skeletal muscle. Endothelial cells are stained in red by using an antibody against the endothelial marker CD31.

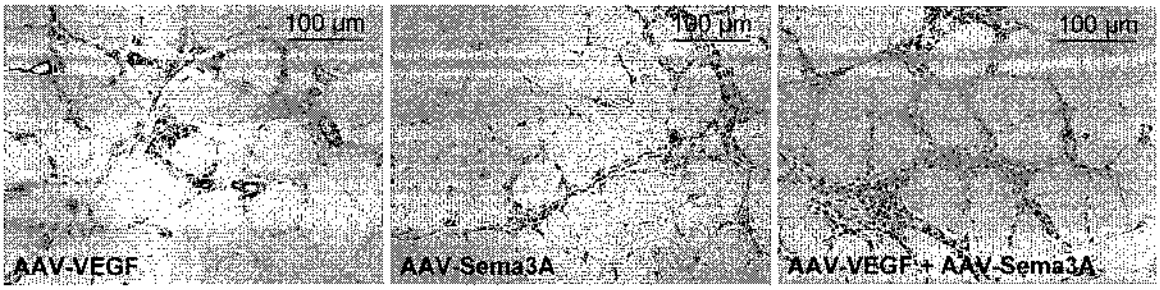


**Figure 3.26. Sema3A inhibits VEGF-induced arteriogenesis.** In accordance with the results of CD31 immunostaining, a peculiar inhibitory effect of Sema3A was also observed on the formation of arterial vessels induced by VEGF165 overexpression (arteries are decorated by α-SMA immunostaining)

In accordance with the histological data, the consistent inhibitory effect of Sema3A on VEGF-induced angiogenesis was also evident in functional assays, such as in vivo perfusion with fluorescent microspheres for the detection of intravascular volume, as well as in the Miles' test for vascular permeability assessment (Figure 3.27); n=6 per group in each experiment.

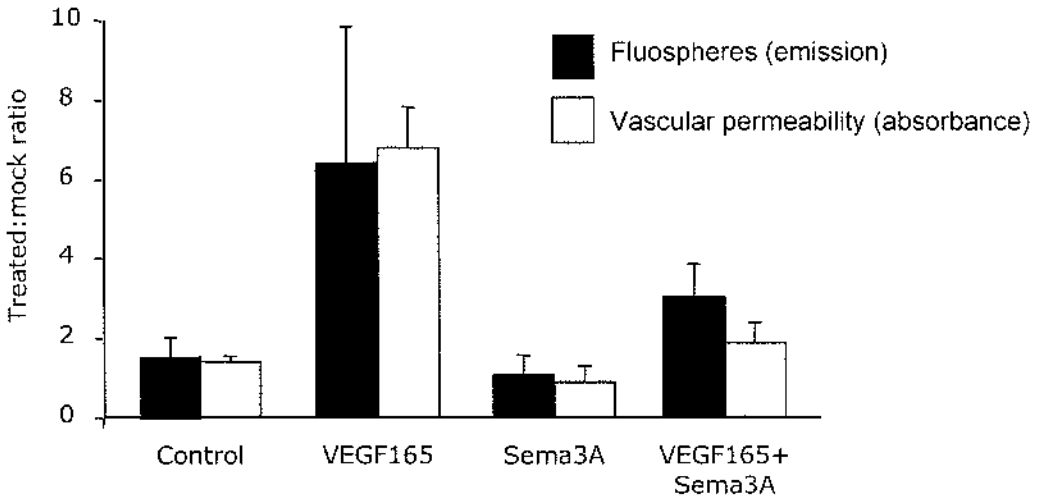


**Figure 3.27. Quantification of the inhibitory effect of Sema3A on VEGF165-induced angiogenesis.** Consistently with histological data, in vivo perfusion with fluorescent microspheres (black bars) confirmed the potent inhibitory effect of Sema3A on the observed increase in the vascular volume after VEGF165 overexpression. Similar results were obtained by the Miles' test for vascular leakiness quantification (white bars). Data are presented as a ratio between the value of emission (in case of fluospheres) or absorbance (in case of Evan's blue for the Miles' test) of the treated and the untreated leg for each animal.

As previously described, the systemic injection of a bolus of fluorescent microspheres in vivo, allowed the quantification of the intravascular volume in the treated right leg and in the control left leg, which thus represented an internal control in each experiment. The black bars of the histogram in Figure 3.27 show the results of these experiments at 1 month after transduction, indicating that the 6-fold increase in the intravascular volume observed after AAV-VEGF165 injection was significantly reduced by the simultaneous injection of AAV-Sema3A. Treatment with AAV-Sema3A alone seemed not to alter vascular volume.

Consistently, the co-injection of the two vectors showed a similar inhibitory effect of Sema3A on the VEGF-induced vascular leakiness. This might either point toward a specific role of Sema3A on vessel maturation, or simply reflect the anti-angiogenic activity of Sema3A (or a combination of both activity).

### Characterization of the cellular infiltrates recruited by VEGF165 and Sema3A

Considering the opposite biological and functional effects exerted by VEGF165 and Sema3A despite the recruitment of a very similar cellular infiltrate, we wanted to further investigate whether the two molecules actually attract the same cellular population. For this purpose, we repeated the bone marrow transplantation experiments as described above, but this time the female recipients were injected in their right leg with AAV-Sema3A.

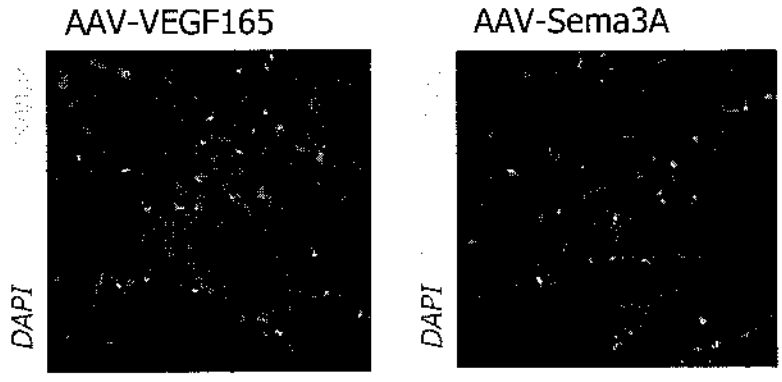


**Figure 3.28. Both VEGF165 and Sema3A recruit mononuclear cells from the bone marrow.** After bone marrow transplantation from male donor to female recipients, AAV-VEGF165 or AAV-Sema3A were injected into the right tibialis anterior. At 1 month, FISH analysis for the detection of the Y-chromosome on muscle sections revealed extensive infiltration of positive cells, suggesting that both factors were equally able to recruit mononuclear cells from the bone marrow.

As shown in Figure 3.28, FISH analysis of Sema3A-treated muscles revealed a pattern very similar the one induced by VEGF165, in which almost all the infiltrating cells were found positive for the Y-chromosome and thus appeared to be of bone marrow origin.

As expected, in both cases most of the infiltrating cells resulted to express the pan-leukocytic marker CD45 as well as the myeloid marker CD11b (Figure 3.29).

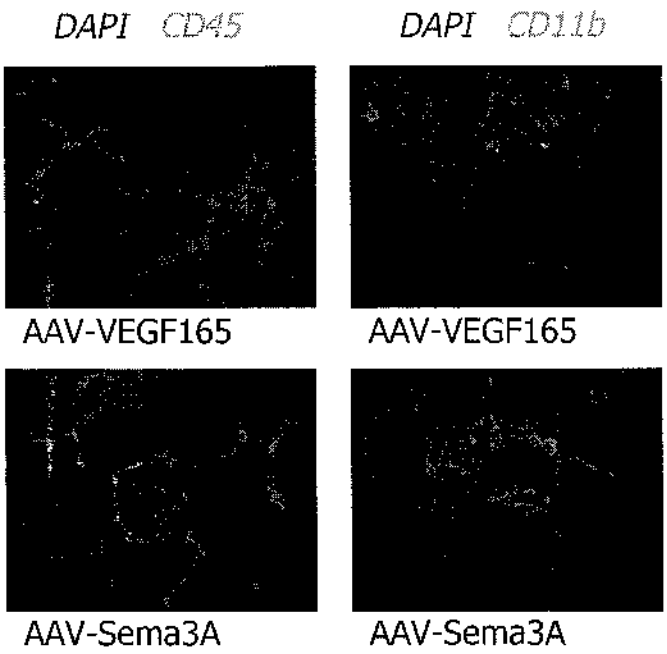


**Figure 3.29. Characterization of the cellular infiltrates recruited by VEGF165 and Sema3A.** As already described for VEGF165 (here shown again in the upper panels), the majority of the mononuclear cells recruited by Sema3A scored positive for the panleukocytic marker CD45 (detected by immunofluorescence in the left column) and for the myeloid marker CD11b (immunofluorescent staining in the right column).

Taken together, the results of FISH and immunofluorescence clearly suggested that the overexpression of both VEGF165 and Sema3A in the normoperfused skeletal muscle was able to recruit a population of bone marrow mononuclear cells having a myeloid phenotype. To further confirm this hypothesis, we set up an in vitro migration assay, in which CD11b+ cells were purified from mouse bone marrow and subsequently tested for their ability to migrate in response to increasing concentrations of recombinant VEGF165 or Sema3A. The results of these experiments are reported in Figure 3.30, which shows that both molecules behaved

as chemoattractants for CD11b+ cells in a dose-dependent manner. A representative picture of the migrated cells is also provided in the right part of the Figure.

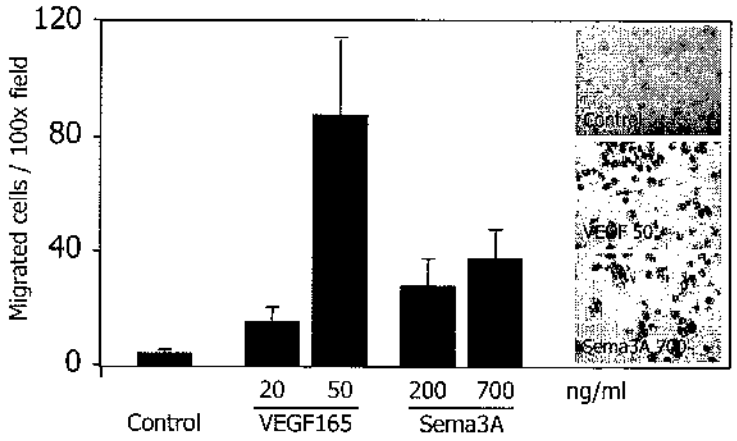


**Figure 3.30. VEGF165 and Sema3A induced CD11b+ cell migration.** Increasing doses of VEGF165 and Sema3A were used as chemoattractants in the lower compartment of a migration chamber. CD11b+ cells, purified from the bone marrow, were placed in the upper compartment and tested for their ability to migrate in response to both factors. The histogram shows mean number of migrated cells ± standard deviations of at least 8 fields per membrane. A representative picture of the cells migrated to the lower surface of the membrane is provided on the right for the most effective dose of each factor.

Collectively, these data pointed toward a common mechanism of recruitment of bone marrow CD11b+ cells by VEGF165 and Sema3A. Of interest, an important common feature of these two molecules is their ability to bind the co-receptor NP-1, while the shortest VEGF121 isoform, which does not bind NP-1, is not even capable to recruit cells from the bone marrow. This strongly suggests an important role of NP-1 in the recruitment of bone marrow cells.

As a first step to understand the role of the different receptors in bone marrow cell recruitment, a laser microdissection-capture technique was applied to the differently treated muscle sections, to isolate the cellular infiltrates formed upon VEGF165 or Sema3A gene transfer. The cDNA obtained from these samples was then used to quantify the expression levels of VEGFR1, VEGFR2 and NP-1, the three main receptors shared between VEGF165 and Sema3A. The result of this quantification is shown in the upper panel of Figure 3.31, in which a specific expression of VEGFR1 and VEGFR2 is detected only in the infiltrates of muscles treated with AAV-VEGF165, probably reflecting the presence of several proliferating endothelial cells. In contrast, a similar expression level of NP-1 was detected in the cells recruited by both factors.

As an additional experiment to substantiate the role of NP-1 in CD11b+ cell recruitment, the expression level of the three receptors was quantified also in purified CD11b+ cells. As shown in the lower panel of Figure 3.31, the transcript for all the three receptors was found to be present in CD11b+ cells, although NP-1 was clearly the most abundantly expressed.

These results are consistent with a model in which VEGF165 induces a cellular infiltration composed of both endothelial cells, which are probably locally in origin and stimulated to proliferate through VEGFR2 activation, and myeloid cells of bone marrow origin. In contrast, Sema3A is not angiogenic at all, and thus it is only able to attract a pure population of bone marrow myeloid cells. The fact the NP1 is equally expressed by the cells recruited by both factors, as well as by purified CD11b+ bone marrow cells, strongly suggested a relevant role of this receptor in CD11b+ cells recruitment.

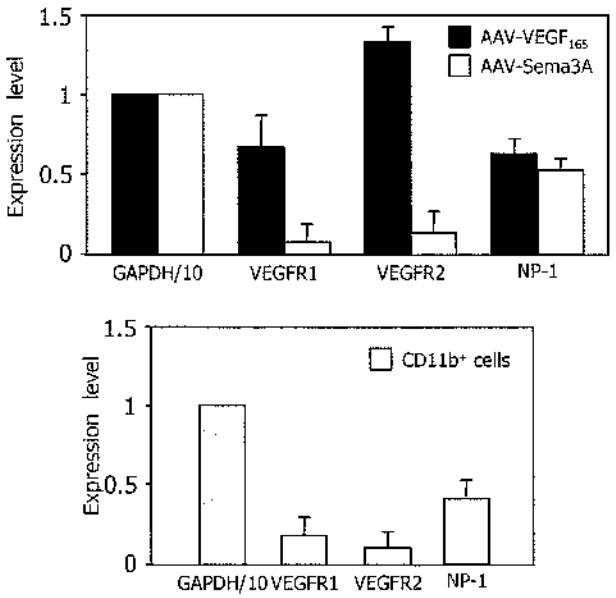


**Figure 3.31. Real-time quantification of VEGFR1, VEGFR2 and NP-1.** The cellular infiltrates from muscles treated with either AAV-VEGF165 or AAV-Sema3A were isolated by laser microdissection to determine the level of expression of the three receptors VEGFR1, VEGFR2 and NP-1. A similar expression level of NP-1 was detected in both cases, while a specific induction of VEGFR1 and VEGFR2 could be appreciated only in tissues expressing VEGF165. The same quantification was also performed on purified CD11b+ cells and the results are reported in the lower histogram, whose pattern strictly resembles the one observed in the cells recruited by Sema3A (white bars in the upper panel). All data are normalized taking the GAPDH housekeeping gene as a reference.

## NP-1 is required for the recruitment of CD11b+ cells by VEGF165 and Sema3A

In order to definitely prove the essential role of NP-1 in CD11b+ cell recruitment, we designed and in vitro transcribed three short interfering RNA (siRNA) molecules to specifically silence NP-1 expression. The specific sequences of the three siRNA and the relative position of their target sequence on NP-1 mRNA is schematically represented in Figure 3.32.

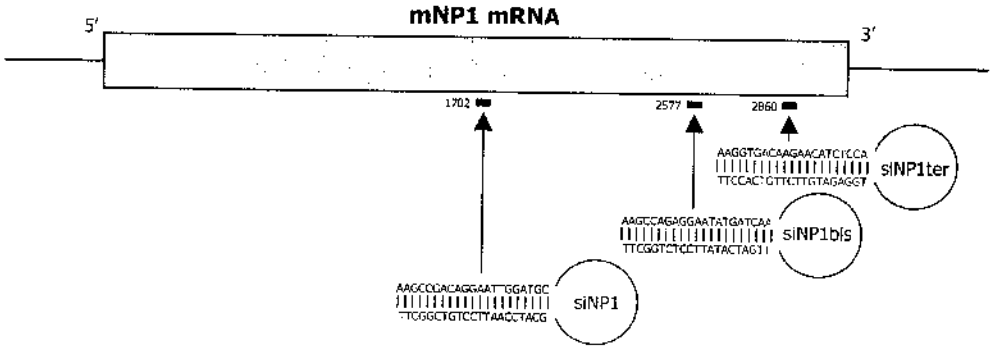


**Figure 3.32. Schematic representation of siRNA-mediated targeting of NP-1 mRNA.** Three siRNAs were designed to target NP-1 mRNA and silence its expression. Shown is the sequence of each siRNA and the position of the relative target sequence on NP-1 mRNA.

As a first experiment to select the most effective siRNA, we take advantage of an artificial construct in which the coding sequence for NP-1 was cloned in frame with the one of EGFP (Enhanced Green Fluorescent Protein). In this experimental system, the co-transfection of such a plasmid with a siRNA specific for NP-1 mRNA allowed the assessment of the silencing activity as a decrease in cell fluorescence. As evident from the FACS profiles collected in Figure 3.33, the co-transfection of HEK-293 cells with the pEGFP-NP1 fusion construct with a control siRNA directed against the bacterial LacZ coding sequence (siLacZ) produced >65% of fluorescent cells. In contrast, the co-transfection of the same plasmid with the three different siRNAs targeted to NP-1 mRNA produced a significant drop in the number of EGFP-expressing cells, with the third oligo (siNP1ter) being the most efficient (5.4% of fluorescent cells). This result, obtained in conditions of NP-1 overexpression, provides a strong indication of a high silencing activity of the siNP1ter oligo.

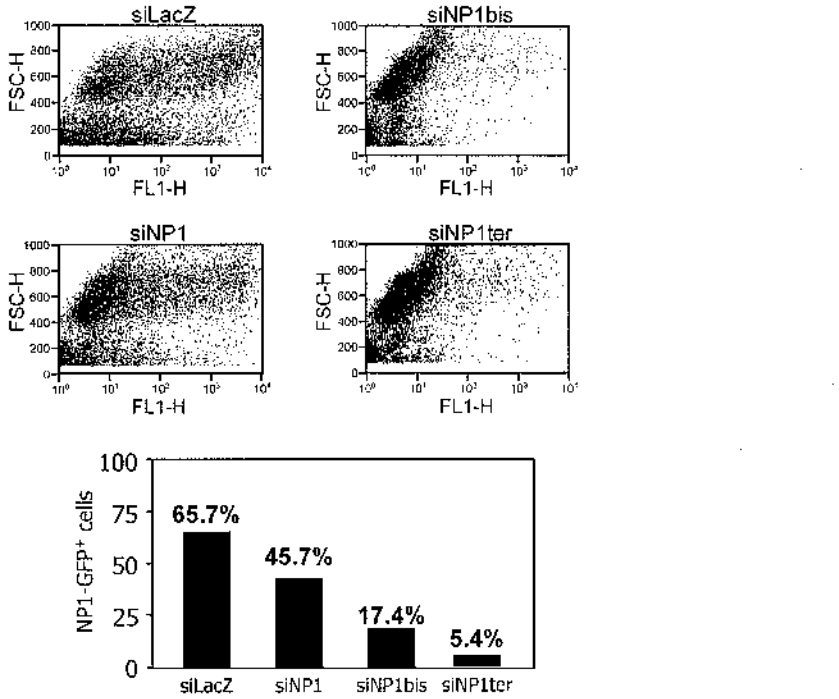


**Figure 3.33. Silencing of NP-1 by siRNA.** The three siRNAs were tested for their silencing activity by a co-transfection with a plasmid coding for the fusion protein EGFP-NP1. In this experimental system, the silencing activity through the targeted degradation of NP-1 mRNA could be read as a drop in the number of EGFP+ cells. As evident from the FACS plots and the histogram on the bottom, the most effective siRNA was siNP1ter, which resulted in a huge decrease in the fusion protein expression (from 65% to 6% of fluorescent cells).

We then looked at the ability of these siRNAs to silence the NP-1 gene on primary CD11b+ mononuclear cells. For this purpose, CD11b+ were purified from the bone marrow and transfected with a control siRNA or the three different siRNA designed to target NP-1 mRNA. The expression levels of the three receptors VEGFR-1, VEGFR-2 and NP-1 were determined by Real-Time PCR. As shown in the histogram on the bottom of Figure 3.34, a potent silencing activity on endogenous NP-1 expression was again exhibited by siNP1ter, while neither additive nor synergistic effect could be obtained by the co-transfection of siNP1ter with siNP1bis, probably indicating the saturation of the siRNA processing machinery. In addition, the specificity of siNP1ter was revealed by the lack of silencing on the other two receptors tested (VEGFR-1 and VEGFR-2). Untreated cells, cells transfected only with Lipofectamine 2000 or with siLacZ were used as controls. Data are obtained by normalizing the expression level of each receptor with the one of the housekeeping gene GAPDH.

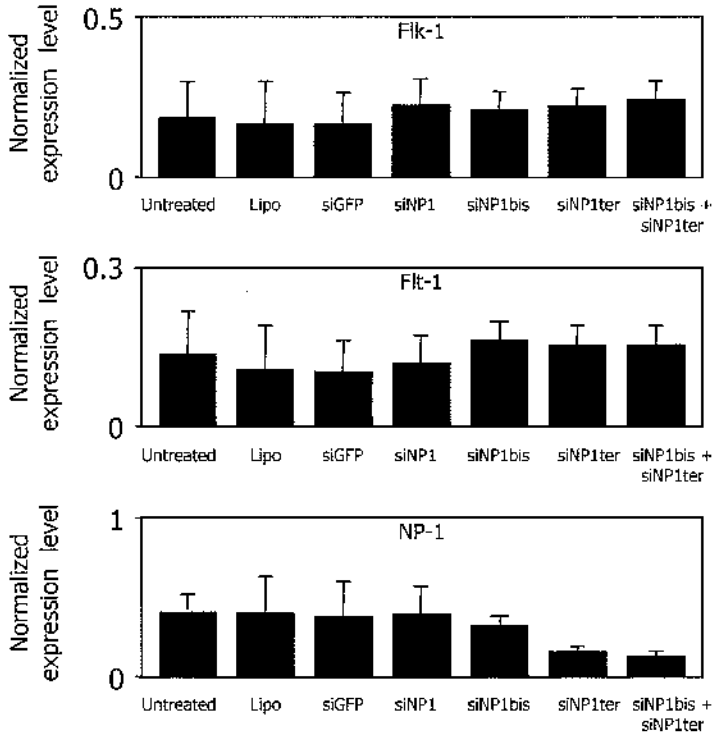


**Figure 3.34. NP-1-specific silencing on primary CD11b+ cells.** Purified CD11b+ were transfected with a control siRNA or with the three siRNAs directed against NP-1. The expression of the three receptors VEGFR-1, VEGFR-2 and NP-1, was then analyzed by Real-Time PCR. In accordance with the results of the previous Figure, the most effective oligo was siNP1ter, which also resulted to be specific, since no silencing activity could be detected on the other two receptors. No additive effect was observed when siNP1ter and siNP1bis were transfected together in CD11b+ cells.

After having obtained convincing evidence of the efficiency of the siNP1ter oligo in silencing endogenous NP-1 in primary CD11b+ cells, these transfected cells were used in a new migration assay, to assess whether the absence of NP-1 might affect their migratory ability in response to VEGF165 or Sema3A.

In agreement with our hypothesis, the silencing of NP-1 potently impaired the migration of CD11b+ cells in response to both chemoattractants. The most effective doses of VEGF165 (50 ng/ml) and Sema3A (700 ng/ml) were used in this experiment. The quantification of the migrated cells in the absence of treatment or after the transfection with siLacZ or siNP1ter is reported in Figure 3.35.

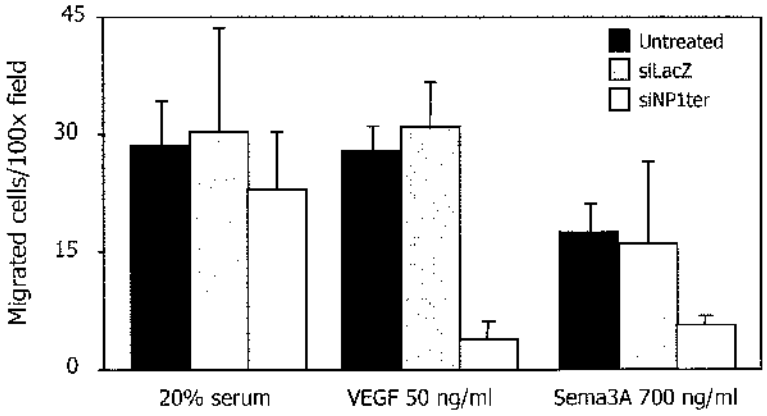


**Figure 3.35. Requirement of NP-1 for CD11b+ cell migration in response to VEGF165 and Sema3A.** Purified CD11b+ cells were treated with siLacZ or siNP1ter, and then tested for their ability to migrate in response to 50 ng/ml of VEGF165 or 700 ng/ml of Sema3A. As indicated by the white bars in the histogram, the silencing of NP-1 by a specific siRNA markedly affected the ability of these cells to respond to both chemoattractive stimuli.

### A key role of CD11b+ cells in promoting arteriogenesis

The results obtained so far clearly indicated that NP-1 expression is required for the migration of CD11b+ cells in response to VEGF165 and Sema3A in vitro, and likely also for their recruitment in vivo. As far as the possible function of these cells is concerned, the intriguing observation that VEGF121, which is not able to recruit CD11b+ cells, does not form arteries in vivo, suggested an important role of these cells for vessel maturation and for the acquisition of an arterial phenotype.

As a first step to verify this hypothesis, we performed another migration assay, in which total bone marrow was fractionated according to CD11b expression with the use of magnetic beads. The positive and the negative fractions were then separately tested for their ability to attract primary smooth muscle cells (SMCs). As shown in Figure 3.36, only the CD11b+ cells acted as chemoattractants for SMCs in a dose-dependent manner, while the negative population did not exert any significant effect.

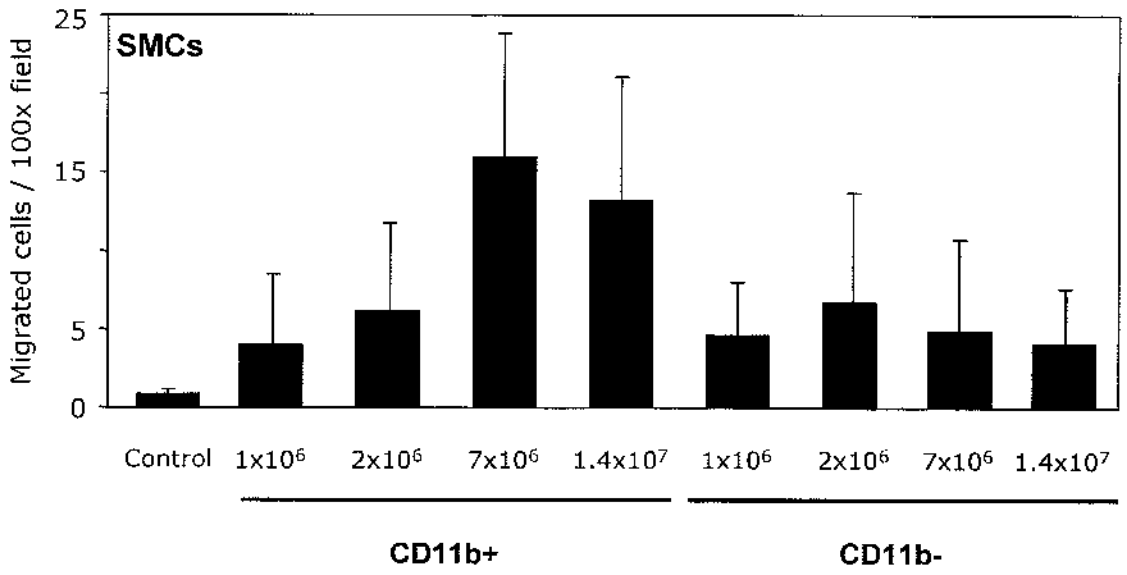


**Figure 3.36. Smooth muscle cell recruitment by CD11b+ cells.** After bone marrow fractionation according to CD11b expression, an increasing number of cells from the two fractions was used as chemoattractant for primary smooth muscle cells. Only CD11b+ cells were found to be able to attract SMCs in a dose-dependent manner.

Taken together, these results led to the outline of an experimental model that might provide a possible explanation of a role of bone marrow cells recruited to the sites of neo-angiogenesis in promoting arterial formation (Figure 3.37). According to this model, both VEGF165 and Sema3A, by binding to NP-1, are able to recruit bone marrow-derived mononuclear cells, which in turn promote smooth muscle cell enrollment around the growing vessels. However, only VEGF165 was indeed able to form arteries, by activating endothelial cell proliferation and migration through VEGFR-2, while Sema3A did not induce any angiogenic response, probably because of its inhibitory effect on endothelial cells. Concordantly, VEGF121 induced massive capillary sprouting through the direct activation of VEGFR-2 on endothelial cells, but did not recruit mononuclear cells from the bone marrow because of the lack of the NP-1-binding domain, and thus was not able to form arteries.

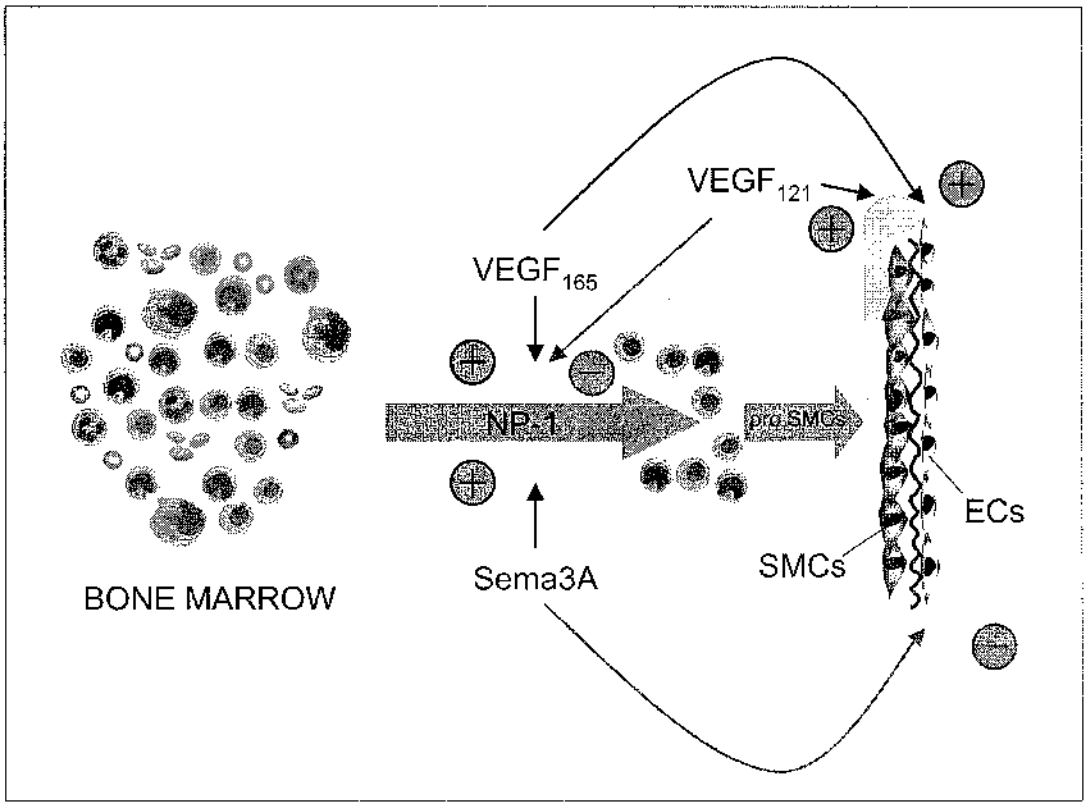


**Figure 3.37. A model to explain the possible role of bone marrow cells in arteriogenesis.** Positive stimulatory signals are shown in black, while negative inhibitory signals are shown in red.

In accordance with this model, the combination of the stimulatory effect of VEGF121 on endothelial cell proliferation, with the ability of bone marrow-derived CD11b+ mononuclear cells to recruit SMCs, should be sufficient to induce arterial formation. Therefore, we performed an additional in vivo experiment, in which the tibialis anterior muscle of mice was injected with AAV-VEGF121, alone or in combination with bone marrow CD11b+ cells purified from syngenic animals. As expected, VEGF121 overxpression determined a marked endothelial cell proliferation with capillary sprouting (upper panel of Figure 3.38). Interestingly, in the muscles co-injected with the same vector and with purified CD11+ cells, several arteries could be observed, in close proximity to the cellular infiltrates (lower panels of Figure 3.38).

This observation was in perfect agreement with our model as well as with our previous findings, providing a strong indication of an important functional role of myeloid cells in promoting the recruitment of SMCs around the growing vasculature, thus providing the acquisition of a tunica media proper of arterial vessels. The appearance of a SMCs layer has been extensively proposed to constitute a functional maturation step in the formation of new blood vessels.

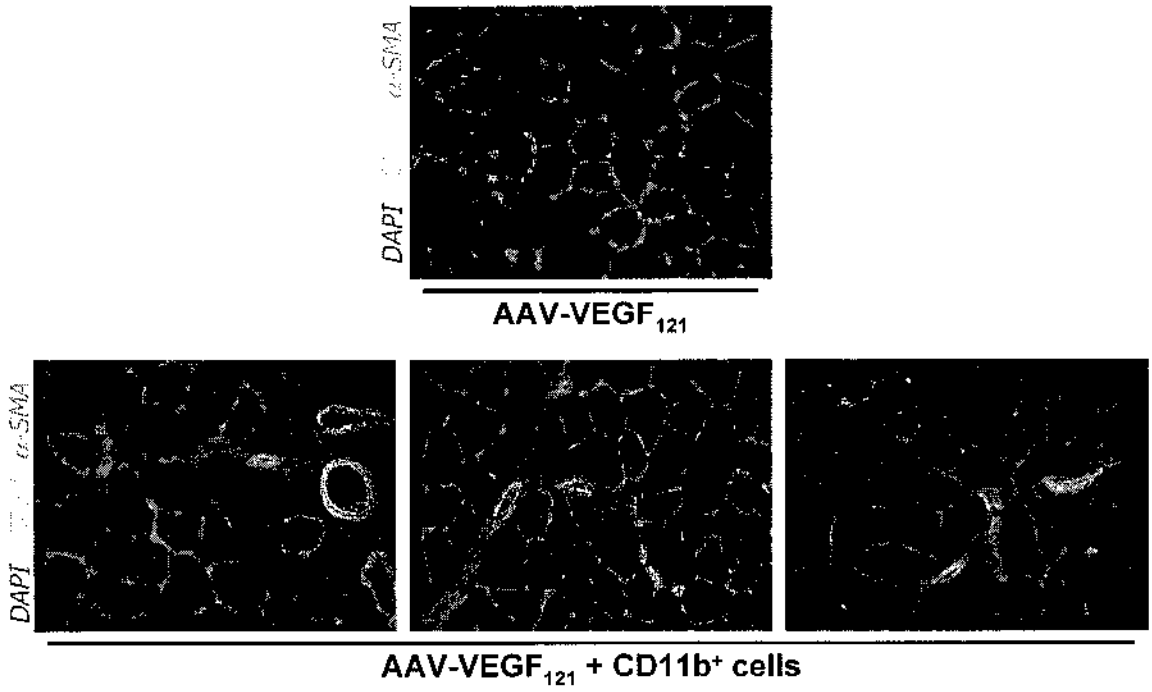


**Figure 3.38. In vivo arterial formation by the co-injection of AAV-VEGF121 and CD11b+ cells.** While the injection of AAV-VEGF121 resulted in the well known massive capillary sprouting, the simultaneous administration of purified CD11b+ cells determined the formation of several arteries in close proximity of the cellular infiltrates, suggesting an important role of the injected cells in the acquisition of an arterial phenotype in vivo.

We therefore injected a new set of animals (n=6 per group) to see whether the simultaneous injection of AAV-VEGF121 together with purified CD11b+ cells, beside the clear histological signs of arteriogenesis, also provided functional improvement relative to AAV-VEGF121 alone. The results of the Miles' test comparing the vascular leakiness of muscles treated with AAV-VEGF121 alone or together with CD11b+ cells are presented in Figure 3.39. As expected, AAV-VEGF121 exhibited a potent permeabilizing activity, while the co-injection of CD11b+ cells significantly reduced this effect, although did not allow a complete normalization of the permeability. The injection of CD11b+ cells alone had no effect on vascular leakiness.

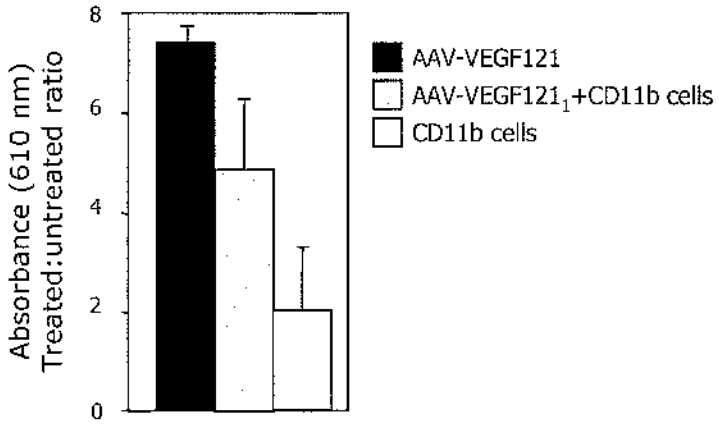


**Figure 3.39. Effect of CD11b+ cells on VEGF121-induced vascular leakiness.** The Miles' test provided a quantitative measure of the leakiness of muscles injected with AAV-VEGF121 alone or in combination with purified CD11b+ cells. Data are presented as a ratio of the absorbance measured from the treated and from the controlateral untreated tibialis anterior muscle. A clear reduction in vascular leakiness is evident when CD11b+ where co-injected with AAV-VEGF121, as compared to vector injection alone.

# 4. MATERIALS AND METHODS

### Recombinant AAV vector preparation and animal treatment

The rAAV vectors used in this study were produced by the AAV Vector Unit at ICGEB Trieste (http://www.icgeb.org/RESEARCH/TS/COREFACILITIES/AVU.htm), according to the protocol extensively described in the introduction.

Animals were injected in the tibialis anterior (50 µl of vector preparation for mice, 150 µl for rats), except than for PET imaging, in which a larger area was transduced, as described below. All the viral stocks used in this study had a titer ≥ $1x10^{12}$ viral genome particles/ml.

Animal care and treatment were conducted in conformity with institutional guidelines in compliance with national and international laws and policies (EEC Council Directive 86/ 609, OJL 358, December 12th 1987). Balb/c mice were purchased from Charles River Laboratories Italia Srl, while Wistar rats were obtained from Harlan and maintained under controlled environmental conditions.

### Real-Time PCR

Total RNA from purified CD11b+ cells or microdissected tissue samples was extracted using TRIzol reagent (Invitrogen) according to manufacturer instructions, and reverse transcribed using hexameric random primers. The cDNA was then used as a template for real-time PCR amplification to detect the expression levels the three murine VEGF receptors (VEGFR-1, VEGFR-2 and NP-1); the housekeeping gene GAPDH was also amplified and used to normalize the results. All the amplifications were performed on a 7000 ABI Prism Instrument (Applied Biosystems), using pre-developed assays (Applied Biosystems).

### Bone marrow transplantation studies

Six-weeks-old male Balb/c mice were killed by cervical dislocation and tibiae and femurs were flushed with RPMI 1640 to collect bone marrow cell suspensions. Recipient, age-matched syngenic female mice were lethally irradiated with a total dose of 8.5 Gy; $2x10^6$ cells, resuspended in 0.2 ml medium, were transplanted via tail vein injection. After 4 weeks, blood counts and hematocrit values confirmed the full hematopoietic recovery.

Successful engraftment of the transplanted cells was further confirmed by the quantification of a specific mouse Y chromosome sequences in DNA samples extracted from PBMC or bone marrow cells at 1, 2 and 6 months after transplantation, using primers Y-F (5'CATGCAAAATACAGAGATCA3') and Y-R (5'TAAAATGCCACTCCTCTGTG3'), to produce a genomic segment of 181 bp. As a cellular reference gene, mouse β-globin was amplified by primers BG-F (5'CAGCCTCAAGGGCACCTTTG3') and BG-R (5'AGCAGCAATTCTGAATAGAG3') to generate a 238 bp fragment. Exact quantification was obtained using an established competitive PCR procedure that uses a synthetic DNA competitor for the quantification of both targets (Todorovic, 2005).

**In vivo perfusion with fluorescent microspheres**

To quantify the vascular volume of treated and untreated muscles, 300 μl of orange fluorescent microspheres (FluoSpheres, Molecular Probe) were injected i.v. into living mice. After one minute (to ensure a proper distribution of the microspheres throughout the body), animals were sacrified and both tibialis anterior muscles immediately harvested. Recovery of microspheres and extraction of fluorescent dye was performed according to manufacturer's instruction. Briefly, weighted muscles were digested in 2M ethanolic KOH, 0.5% Tween 80 (v/v) (Sigma) at 60°C with periodic shaking. Homogenates were centrifuged in a swinging rotor and the pellet resuspended in 0.25% Tween 80. After an additional centrifugation and washing, microspheres were dissolved in 2-etoxyethyl acetate (Sigma). Debris were removed by centrifugation and fluorescence in the supernatant was measured with the VersaFluor Fluorometer System (BioRad). Values were normalized and expressed as ratios between fluorescence of treated and untreated controlateral muscle for each animal (n=6 per group).

To obtain a 3-D reconstruction of the vascular network, mice were subjected to in vivo perfusion with a 1:6 dilution of the same fluorescent microsphere solution (FluoSpheres, Molecular Probe). Afetr anesthesia, the chest was opened and the vasculature perfused with PBS for 3 minutes, followed by 20 ml of FluoSpheres (1:6 dilution of the stock), via a blunt 13 G needle inserted through the left ventricle into the ascending aorta. The treated muscles were removed and immediately frozen for cryosectioning. Thick (50-100 μm) sections were analyzed by confocal microscopy to obtain a Z-stack for the 3-D reconstruction of the vascular network.

**Primary cell cultures**

CD11b+ cells were isolated from total bone marrow (extracted by tibiae and femurs of Balb/c mice) using CD11b magnetic cell separation system beads (Miltenyi Biotec, Germany), and cultured in RPMI 1640 supplemented with 10% high quality fetal bovine serum (GIBCO). Transfection experiments with different siRNAs were performed using Lipofectamine 2000, according to manufacturer's instructions. Coronary artery smooth muscle cells were purchased from Clonetics and cultured in their own medium, also provided by the manufacturer.

**Migration assay**

Migration assays were performed with the use of 5-μm (for CD11b+ cells) or 8-μm (for SMCs) pore size transwell permeable supports with a polycarbonate membrane (Costar, Corning Incorporated). $1 \times 10^5$ cells were seeded in serum-free medium in the upper chamber, while chemoattractants were placed in the lower chamber. After 16 hours incubation, migrated cells on the lower surface of the membrane were fixed in methanol and stained with Giemsa. Each assay was carried out in triplicate, by counting 8 fields per membrane at 400x magnification. Results are expressed as the mean number of migrated cells ± standard deviation.

**Vessel wall permeability assay**

Analysis of vessel permeability was performed by an adaptation of the Miles assay (Miles, 1952) to rodent muscles. Mice or rats (n=6 per group) were injected in the jugular vein with 250 μl or 2.5 ml of 0.5% Evans blue (Sigma), respectively, and sacrificed after 30 minutes. The tibialis anterior muscles were removed and weighted. The dye was extracted by incubation in 2% formamide at 55°C and quantified spectrophotometrically at 610 nm. Absorbance values were converted, according to a standard curve, in Evans blue content and expressed as a ration between treated and control muscles from the same animal.

**PET and SPECT imaging**

All the PET and SPECT experiments were performed at Institute of Clinical Physiology, CNR, Pisa (Italy), in collaboration with G. Sambuceti.

After mild general anesthesia, the animals were injected with 400 μl of AAV vector (containing $4x10^{11}$ particles of each vector) in their right leg and with a similar volume of PBS in their left leg. Different muscles were transduced, defining 8 injection sites per leg: 2x50 μl into the tibialis anterior, 3x50 μl into the gastrocnemius, 3x50 μl into the rectus femoris. All the injections were performed transcutaneously, using a syringe with a 29 G needle. The animals were divided into 4 experimental groups according to the treatment they received: AAV-LacZ, AAV-VEGF, AAV-Ang1, or AAV-VEGF + AAV-Ang1 (n=21 for each group).

A clinical PET scanner was used to detect an index of muscle blood flow, by injecting the rats i.v. with 3.7 Mbq of $^{13}$N-ammonia (n=21 per group). All the animals were tested both under resting conditions and after 15 minutes of muscle activity induced by electrical stimulation at 180 spikes/min.

For the quantitative evaluation of intravascular volume and permeability of the differently treated muscles, $^{99}$Tc-diethylenetriaminepenta acetic acid (DTPA) was systemically injected into the jugular vein, and data elaborated according to a published protocol (Peters, 1987).

**Assessment of artero-venous shunting**

To evaluate the presence and quantify the entity of artero-venous shunts in the differently treated animals, a bolus of $^{99}$Tc macroaggregate, which do not normally transverse the capillary bed, was injected into the abdominal aorta. The detection of radioactive counts in the lungs provided an accurate quantification of the fraction of the abdominal aortic blood flow shunted to the venous circulation.

**Histology**

For histological evaluation, tissue samples were either snap frozen or fixed in 2% formaldehyde and embedded in paraffin.

Immunohistochemistry was performed on paraffin-embedded sections, with the use of the following antibodies: mouse monoclonal against α-SMA (clone 1A4, Sigma); goat polyclonal against CD31 (Santa-Cruz Biotechnology). Protocols were according to the Vectastain Elite ABC kit (universal or goat) from Vector Laboratories. After treatment, slides were rinsed in PBS and signals were developed using 3,3'-diaminobenzidine as a substrate for the peroxidase chromogenic reaction (Lab Vision Corporation).

For immunofluorescence, frozen sections (5-μm thick) were fixed in cold acetone (20°C) and blocked for 30 min with 5% goat or 5% horse serum in PBS, depending on the secondary antibody. The following primary antibodies were used diluted 1:200 in blocking buffer: anti CD11b (clone M1/70), anti CD31 (clone 390), anti Sca1 (clone E13-161.7), anti CD34 (RAM 34), anti c-Kit (2B8), (all from Pharmingen BD), mouse monoclonal anti Flk-1 (Santa Cruz), anti F4/80 (clone A3-1)(Serotec), Cy3-coniugated anti-α-SMA (clone 1A4) (Sigma), anti-cleaved Caspase 3 (Cell Signaling). Relative areas occupied by differently stained cells were quantified by the use of ImageJ software.

For the detection of the β-galactosidase activity, 2-4 mm fresh tissue biopsies were fixed in 4% paraformaldehyde (or 0.5 glutheraldeyde in case of carotid arteries) and then stained in X-gal solution (1mg/ml X-gal, 5mM K3Fe(CN)6, 5mM $K_4Fe(CN)_6$, 2mM $MgCl_2$). Samples were then rinsed in water and counterstained with nuclear fast red.

For the staining of whole animal vasculature with fluoresceinated lectin, 100 μl of Lycopersicum Esculentum lectin (Vector Laboratories) were injected into living mice through the jugular vein to ensure its systemic distribution. After 15 minutes, mice were anesthetized and in vivo perfused with 1% paraformaldheyde, via a blunt 13 G needle inserted through the left ventricle into the ascending aorta. The treated muscles were removed and immediately frozen for cryosectioning. 100 μm-thick sections were analyzed by confocal microscopy to obtain a Z-stack for the 3-D reconstruction of the vascular network.

**Immunofluorescence in situ hybridization (Immuno-FISH)**

Following immunofluorescent detection of CD31 or α-SMA antigens, tissue sections were postfixed by protein crosslinking using EGS (Sigma) at 50 mM in PBS for 30 min at 37°C (Brown, 2002). The EGS stock solution was made in DMSO and the final dilution in PBS was prepared just before use. After washing, DNA was denatured in 70% formamide by placing slides at 72°C for 10 min; alcohol-dehydrated samples were than hybridized over night at 42°C with a probe specific for mouse Y chromosome, labeled with FITC (Cambio). After low temperature washes, the tissue sections were mounted in an antifade medium containing DAPI as DNA counterstaining. Images were acquired using a Leica DMLB upright microscope connected to a Coolsnap CF CCD camera and processed by the MetaView 4.6 software.

**siRNA design and in vitro transcription**

Three possible siRNAs were designed according to the guidelines recommended by Elbashir et al. (Elbashir, 2002), looking for AA(GN)20 target sequences unique within the genome, located within ORF 100nt downstream of start codon, with a GC content ranging between 40 and 70% and not containing highly GC rich stretches which can alter the double stranded conformation of siRNAs. siRNA molecules were in vitro transcribed from a DNA template by using the AmpliScribe Transcription Kit (Epicentre) following the included protocol.

**Laser microdissection**

For microdissection, cryo-sections (10 µm) from muscles treated either with AAV-VEGF165 or AAV-Sema3A were mounted on glass slides. After hematoxylin staining for 45 seconds, the sections were subsequently immersed in 70% and 96% ethanol and stored in 100% ethanol until use. No more than 10 sections were prepared

at once to reduce the storage time. Cellular infiltrates having a diameter of 100-500 µm were selected and microdissected under optical control using the Laser Microbeam System (P.A.L.M., Bernried, Germany). Afterwards, tissue crumbs were collected in TRIzol (Invitrogen) for RNA extraction, according to manufacturer's instructions.

**Statistical analysis**

One-way ANOVA and Benferroni/Dunn's post-hoc test was used to compare multiple groups. Pair-wise comparison between groups was performed using the Student's t test. $P<0.05$ was considered statistically significant.

# 5. DISCUSSION

### AAV vectors for cardiovascular gene therapy

The experiments described in this thesis provide compelling evidence of the several advantages of AAV vectors as a unique tool for gene transfer in the cardiovascular field. The natural tropism of AAV vectors for quiescent cells, such as all kinds of muscle cells, and their ability to sustain persistent transgene expression up to several years after transduction is extremely appealing for therapeutic purposes. In fact, AAV is now established as a powerful gene delivery vehicle for human gene therapy, and has been used in more than 20 clinical trials (http://www.wiley.co.uk/genmed/clinical). In addition, the peculiar properties of AAV vectors render them an ideal investigational system to dissect the role of single genes, or their combination, in the pathogenesis of several diseases.

In this work we exploited a series of AAV vectors to express different molecules involved in blood vessel formation. By taking advantage of the long-term persistence of AAV in muscle cells, we could followed the effect of VEGF165 overexpression over time, and to disclose quite impressive side effects, such as the formation of abnormal vascular lacunae and artero-venous shunts with subsequent worsening in muscle perfusion, which would have never came to light by using transient gene delivery systems such as Adenoviral vectors. Moreover, the fact that AAV particles enter the target cells at high multiplicity of infection, offers the unique possibility to combine different AAV preparations for the simultaneous delivery of more than one factor. Here we made use of this approach to investigate the ability of Ang-1 to promote vessel maturation. In fact, we showed that functional muscle perfusion markedly improved, both at rest and after exercise, when AAV-VEGF165 was co-injected together with AAV-Ang1, thus providing factors involved in different phases of the angiogenic process. In a similar manner, we also demonstrated a potent anti-angiogenic activity of Sema3A in vivo, by showing that the combined delivery of AAV-VEGF165 and Sema3A almost completely abolished VEGF165-induced angiogenesis.

An additional remark has to be made about the safe profile of AAV vectors, which do not elicit any immune nor inflammatory response in the host. Beside the obvious importance of this issue for therapeutic purposes, it is worth noticing that in our work the complete absence of inflammation turned out to be an essential requirement to finely determine the role of bone-marrow derived myeloid cells in

promoting arteriogenesis. Again, these observations could not have been possible by the use of Adenoviral vectors, which are highly immunogenic and induce massive recruitment of inflammatory cells by themselves.

Although these appealing properties have been mainly highlighted by using AAV-2, the recent discovery of different naturally existing serotypes has additionally broaden the potential applications of this class of vectors. To date, at least seven alternate AAV serotypes to AAV-2 have been identified, showing great potential for gene delivery to certain tissue types. For example, AAV-6-based vectors have a high efficiency for airway epithelia (Halbert, 2001) and skeletal muscle, while those based on AAV-8 appear to be particularly prone to cross the endothelial barrier and transduce cardiac cells (Wang, Zhu, 2005). In the study of Rabinowitz et al. AAV-1 resulted to be the most efficient in transducing skeletal muscle cells, followed by serotypes 5, 6 and 7 (Rabinowitz, 2002). Whilst the primary receptors required for transduction for some of the AAV serotypes have been identified (such as heparan-sulfate proteoglycans for AAV-2, or sialic acid for AAV-4 and AAV-5), and can thus be associated to the transduction pattern for the relevant AAV, many of the serotypes bind through as yet uncharacterized mechanisms, and therefore their tropism cannot be predicted accurately. Since there is as yet little published work documenting the transduction capability of alternate serotypes on different cell types, a great challenge for the next future will be to see whether serotypes different from AAV-2 may offer enhanced gene delivery to cardiovascular cells and tissues in vivo.

**Functional consequences of prolonged VEGF165 overexpression**

Overall, the data presented in this work substantially demonstrate that proper neo-vascularization is not achievable by the constitutive overexpression of a single potent angiogenic factor, such as VEGF, and that a fine tuning of VEGF activity is probably required in order to obtain functional new blood vessel formation.

Of note, we showed that the angiogenic response elicited by VEGF165 in the normoperfused skeletal muscle does not account for an improved perfusion of the treated tissue, and even impairs the physiological increase of muscle blood flow during muscle exercise. This unexpected poor functional outcome is in complete disagreement with the clear histological evidence of massive arterial formation in response to VEGF165 and with the results of other experiments, including ours, aimed at determining muscle perfusion with the use of fluorescent microspheres (Springer, 2000; Arsic, Zentilin, 2003). Moreover, these observations constitute a big

challenge for the increasing number of clinical trials of therapeutic angiogenesis that have been approved to date, which are mostly based on VEGF single gene transfer. In this work, we provide at least two results that might help to conceal the apparent contradiction between the appearance of new arteries and the drop in muscle perfusion after VEGF165 gene transfer. The first one refers to the well known permeabilizing activity of VEGF, 50,000-fold greater than histamine (Senger, 1983). Accordingly, by both the Miles test and SPECT imaging, a marked increase in vascular permeability was observed in muscles treated with VEGF165. This permeabilizing effect of VEGF seems to be mainly due to the induction of endothelial fenestrations, and the dose at which it appears is probably lower than the one that sustains neo-angiogenesis (Eriksson, 2003). The fact that the occurrence of edema or of other side effects related to increased vascular leakiness has never emerged in recent clinical trials strongly suggests that probably an effective dose of VEGF has never been reached in these studies, thus explaining their negative outcome. This is likely due to the gene delivery systems used in clinical studies so far, namely plasmid DNA or adenoviral vectors, which display the major drawbacks of very low gene transfer efficiency and short transgene expression (no longer than 2-3 weeks in most mammalian organisms), respectively. Indeed, several experimental evidences indicate that the duration of gene expression following delivery by adenoviral vectors, such as in the RAVE trial (Rajagopalan, 2003; Rajagopalan, 2003), is probably too short to produce stable blood vessels, and that the early gain in vascularization rapidly regresses to control levels when VEGF production ceases (Gounis, 2005). This finding is in perfect line with previous results on a transgenic mice system for the conditional switching of VEGF expression, which showed that a relatively long presence (> 2 weeks) of VEGF is required to produce durable vessels (Dor, 2002). In contrast, it is likely that the growth of stable vessels and their arterialization require longer transgene expression, from several weeks up to months. This can be achieved using episomal vectors, such as those based on AAV, which have lower transduction efficiency than adenovirus but have natural tropism for muscle tissue and maintain transgene expression up to years after gene transfer (Monahan, 2000).

In addition to abnormal vascular leakiness, we also provide an alternative explanation for the worsening in muscle perfusion upon sustained VEGF165 expression, namely the formation of artero-venous shunts, which are probably formed by numerous wide "vascular lacunae" that appear to be specifically induced

by VEGF165 in the normoperfused skeletal muscle. The fact that these structures are actually filled of erythrocytes is in perfect agreement with the marked increase of the blood pool in the treated muscle, as measured by both in vivo perfusion with fluorescent microspheres and SPECT imaging after Tc-DTPA injection, as well as with the worsening in muscle fiber perfusion detected by PET. In accordance, different authors have raised important concerns about the possibility that a VEGF-based gene therapy approach may lead to excessive vessel growth, hemangiomas and glomeruloid body formation (Lee, 2000; Schwarz, 2000; Springer, 2003). In particular, an alternative approach, which also sustained a long-term stable production of VEGF, was obtained by myoblast-mediated gene transfer, by transplanting primary myoblasts previously transduced with a retroviral vector carrying the VEGF cDNA. Unexpectedly, but in agreement with our results, this strategy resulted in hemangiomas containing a localized network of vascular channels, supporting the notion that uncontrolled VEGF expression can have deleterious effects (Springer, Chen, 1998).

In contrast, a combination approach, in which both VEGF165 and Ang1 were simultaneously delivered to the skeletal muscle, resulted to be markedly effective in improving muscle perfusion, both at rest and after exercise. This result is particularly important for any future clinical application of therapeutic angiogenesis, probably suggesting that more than one factor is required for proper new blood vessels formation and maturation. Similar to the drug combination approach often proposed for non-responders in conventional therapeutics, the simultaneous delivery of two or more factors involved in different steps of the angiogenic process, might thus represent a possible improvement over the administration of single agents. As stated above, AAV vectors, by entering the target cells at high multiplicity of infection, appear particularly suitable for this purpose.

Our PET results also suggest that VEGF expression has to be strictly regulated to drive a physiological angiogenic stimulus. In fact, it might also turn out possible that a timely controlled expression of VEGF, sufficient to form numerous and stable new blood vessels, but short enough to avoid the appearance of abnormal vascular structures and to allow proper vessel maturation, could result in the formation of a functional and beneficial vascular network. To assess this hypothesis, we are developing new vectors for the controllable expression of the transgenes, by the use of hypoxia-sensitive or drug-inducible promoters.

**Modulation of VEGF activity by Angiopoietin-1**

The PET and SPECT experiments presented here clearly underscore a key role Ang-1 in stimulating proper maturation of the VEGF-induced vasculature. Indeed, in contrast with the deleterious effects observed after AAV-VEGF165 gene transfer, the co-expression of VEGF165 and Ang-1 resulted in a marked improvement in muscle blood flow, with an almost complete normalization of leakiness and a significant reduction of the vascular volume. These results are perfectly in line with a wealth of literature data supporting a specific ability of Ang-1 in promoting vessel maturation. In fact, Ang-1 null embryos die because remodeling and stabilization of the vessels are severely perturbed, while Ang-1 overexpression results in increased vascular branching and resistance to leakage induced by inflammatory agents (Suri, 1998; Thurston, 1999).

However, in sharp contrast to the findings from the transgenic studies showing that Ang1 is an essential promoter of new blood vessel formation during embryonic development, Ang-1 has never shown a mitogenic activity on endothelial cells (Davis, 1996). Moreover, the observation that Ang-1 is widely expressed in normal adult tissues (Wong, 1997) suggested that Ang1 might act on the stabilization of existing vessels, probably modulating the interactions between the endothelial and the surrounding mural cells. Results from several xenograft models also demonstrated that ectopic expression of Ang-1 results in decreased tumor growth and angiogenesis (Hayes, 2000; Ahmad, 2001), concomitant with an increased association of pericytes with vessels.

What is the mechanism by which Ang-1 can help vessel maturation? First of all, the potent effect in inhibiting vascular permeability, that we observed by the Miles test and SPECT, is though to be due to the stabilization of interendothelial junctional gaps specifically induced by VEGF (Bates, 2001), as well as to the recruitment of mural cells, which both express the Tie-2 receptor (Asahara, 1998; Gamble, 2000). In fact, while early studies pointed toward an indirect role of Ang-1 in the recruitment of pericytes, through the stimulation of endothelial cells to secrete a cocktail of chemoattractants, the finding that Tie-2 is actually expressed on the membrane of smooth muscle cells suggested a possible direct role of Ang-1 in the activation of mural cells (Tian, 2002). Even more interestingly, Ang-1, in concert with VEGF, turned out to be able to directly stimulate the migration of mural cells, as well

as of their mesenchymal precursors (Metheny-Barlow, Tian, 2004). It is also interesting to note that the absence of pericytes was shown to lead to major defects in endothelial junction formations (Hellstrom, 2001). Secondly, the presence of mural cells is postulated to be inhibitory for endothelial cell proliferation. Indeed, several studies have shown that actively proliferating endothelium lacks coverage by mural cells and that the loss of pericyte recruitment observed in PDGF-B/bR knock-out mice is concomitant with endothelial hyperplasia (Feldman, 1978; Hellstrom, Gerhardt, 2001). In addition, during wound healing, the arrival of mural cells coincides with the cessation of vessel growth, suggesting that contact with pericytes might lead to quiescence of endothelial cells (Crocker, 1970). Subsequent studies on co-cultures of endothelial and smooth muscle cells using a variety of models further substantiated the decreased growth of endothelial cells under these conditions, in a fashion that requires cell-cell contact (Orlidge, 1987; Antonelli-Orlidge, 1989). This idea is perfectly consistent with our in vivo data, obtained by the infusion of $^{99}$Tc-DTPA, which showed a clear effect of Ang-1 in reducing the overall vascular permeability of the treated leg, with a concomitant decrease in the intravascular volume. This latter effect might be reasonably due to a specific inhibition of Ang-1 on endothelial cell proliferation, likely mediated by the reinforcement of the contact between endothelial cells and pericytes, and the subsequent prevention of vessel overgrowth.

The clear reduction in the vascular volume observed by SPECT after AAV-VEGF165 and AAV-Ang-1 delivery, as compared to AAV-VEGF165 alone, is in apparent contradiction with the increase in muscle blood flow detected by PET and previously measured ex vivo by the use of microspheres (Arsic, Zentilin, 2003). This paradox can be explained by bearing in mind the large vascular lacunae formed by VEGF165, which evidently give reasons for a significant increase in blood volume and in the meantime can justify a reduced functional perfusion. The ability of Ang-1 to efficiently counteract the formation of these abnormal vascular structures is therefore consistent with a reduction in the vascular volume and with a simultaneous increase in functional perfusion. This concept also implies that a functional neovascularization does not necessarily requires the development of a great number of new vessels and that functional tests are absolutely required in order to demonstrate the effectiveness of a novel angiogenic strategy. Starting from these considerations, the next section includes a critical overview of the advantages of in vivo molecular imaging over conventional histological analysis to visualize and quantify the angiogenic process.

**Looking at angiogenesis: from histology to in vivo molecular imaging**

Conventional methods to visualize angiogenesis rely on microscopic analysis of histological tissue sections, by staining endothelial or mural cell-specific markers (such as CD31, CD34, von Willebrand factor or lectin for endothelial cells and α-SMA, PDGFR, desmin, nestin, high molecular weight melanoma-associated antigen (NG2) for pericytes). In this work, we also made use of some of these markers to highlight the presence of new blood vessels in the differently treated muscles, and showed that VEGF165 overexpression accounted for a 2-fold and 6-fold increase in the number of capillaries and arteriolae, respectively.

However, the results of our PET and SPECT experiments clearly demonstrate that these vessels are not functional at all and even impair muscle perfusion. From a clinical perspective, these results challenge the concept that an increase in vessel density necessarily means an improved tissue perfusion, and indicate that a morphological evidence of angiogenesis is not sufficient to speculate about the therapeutic value of a novel pro-angiogenic approach. Therefore, there is an absolute need for functional and non-invasive tests to accurately study the potential benefits as well as all the possible side effects that might rise as a consequence of transgene overexpression. So far, side effects of the different angiogenic growth factors in animal models and humans are poorly documented, as invasive approaches or toxic gene delivery systems in animals have masked negative aspects specific for the different angiogenic molecules. Also, the follow-up times of these studies have been quite short, mainly because of the short time of transgene expression after trunsduction with adenoviral vectors, or of the use of invasive and post-mortem procedures. Moreover, it is still unclear what should be the ideal mode of neovascularization (angiogenic sprouting or arteriogenesis?) and whether it should occur in the ischemic or in the more proximal healthy tissues. Since the aim of therapeutic neovascularization is to enhance perfusion and function of end-organ tissue, some authors have argued that large collaterals can contribute more to blood flow in end organs than small angiogenic network (Schaper, 2000) and therefore the goal should be to enhance arteriogenesis rather than angiogenesis or vasculogenesis.

In this context, molecular imaging techniques offer enormous potential to observe complex system functions, such as the angiogenic process, in vivo. In particular,

nuclear medicine-based techniques, such as PET, SPECT and planar scintigraphy, can efficiently detect radioactive probe distribution in vivo and provide accurate quantitative information. The high sensitivity of both PET and SPECT render them particularly suitable for monitoring of several biological processes. In particular, a major advantage of SPECT relates to the availability of numerous tracers and the potential for the simultaneous imaging of different isotopes (Brinkmann, 1999). On the other hand, because of the generally short half-lives of PET tracers (in our case ~ 10 minutes for $^{13}$N-ammonia), repetitive imaging of tracer retention by target tissues at short interval times is feasible. This allowed us to easily determine muscle blood flow in resting conditions and after 20 minutes of pacing-induced muscle contraction, on the same animal and at almost the same time, thus dramatically reducing experimental variability and increasing the reliability of the obtained results.

We also take advantage of the sensitivity of scintigraphic techniques to assess the presence of artero-venous shunts in the lower legs, by injecting $^{99}$Tc-macroaggregate in the distal abdominal aorta and looking for the appearance of the radioactive tracer in the lungs. A similar approach has been extensively used in clinics to detect and characterize the presence of congenital cardiac and pulmonary shunts (Komatsu, 1998), or of tumor-associated shunts (Ho, 1997; Inoue, 1997). To our knowledge, our results provide the first evidence of substantial artero-venous shunt formation as a consequence of long-term VEGF overexpression. Therefore, this approach could result to be of great value in assessing the efficiency of any strategy (administration of a cocktail of factors, use of controllable promoters, etc.) aimed at enhancing the maturation of the VEGF-induced vessels.

One major drawback of our study stems from the use of clinical PET and SPECT scanners, which do not have enough resolution to discriminate the rat hindlimb anatomical structures and thus are not able to recognize the transduced muscles. For this reason, all the differences we observed probably represent an underestimate of the real values, since they are calculated on the signal coming from the entire leg. To solve this limitation, additional experiments with the use of microPET and microSPECT dedicated to small animals will be highly desirable in the next future. An additional solution could come from the simultaneous delivery of a reporter gene to monitor the magnitude, location and duration of transgene expression will be needed in the next future. This approach has been already turned out to be feasible by Wu and coworkers (Wu, 2004), which in agreement with our results showed that despite

a documented angiogenic response induced by VEGF gene transfer in the myocardium, this did not translate into significant changes in myocardial contractility and perfusion.

**The role of bone marrow cells in vessel formation and maturation**

Another major finding of this work stems from the observation that VEGF165 induced a specific recruitment of bone marrow cells to the sites of neo-angiogenesis. This led us to investigate a possible direct contribution of these cells to new blood vessel formation, through transdifferentiation. The results obtained, however, clearly ruled out this hypothesis.

The possible incorporation of bone marrow-derived cells into the VEGF165-induced neovasculature was tested by transplanting male bone marrow into female mice, followed by the detection of donor cells in the VEGF-induced vessels by looking at the presence of the Y chromosome. Occasional donor cells of male origin (Y+) positive for the CD31 endothelial marker were indeed present in some of the mononuclear infiltrates; however we could not even clearly establish whether these sporadic cells were adjacent or truly incorporated into small capillaries.

These observations clearly indicate that the contribution of bone-marrow precursor cells to the process of neovascularization induced by VEGF165 does not mainly occur through the direct incorporation of these cells into the newly formed vasculature. Thus, the VEGF-driven neovascularization appears to essentially depend on classic angiogenic sprouting of locally resident endothelial cells. Although this conclusion has been obtained in a particular experimental setting, in which AAV vectors sustained prolonged expression of moderate levels of VEGF165, it is worth mentioning that others have also challenged the notion that bone marrow-derived precursors can effectively be incorporated into the new vessels, using different experimental models (De Palma, 2003; Balsam, Wagers, 2004; Rajantie, 2004; Ziegelhoeffer, 2004).

Despite the lack of incorporation into the newly formed vasculature, our results clearly indicate that mononuclear cells are massively recruited to the sites of VEGF165-induced angiogenesis. In agreement with the notion that VEGF165 is a potent chemotactic for monocytes and macrophages through the activation of the Flt-1 receptor (Barleon, Sozzani, 1996), the cells infiltrating the sites of VEGF165 neoangiogenesis display broad myeloid markers such as CD11b and CD45. Moreover, macrophages are also known to be attracted by VEGF (Shen, 1993), producing

angiogenic factors themselves that might play a synergistic role (Moore, 1985). While the phenotype of the recruited bone-marrow mononuclear cells still has to be exactly defined, we obtained interesting insights in their possible functional role during neo-vascularization, by comparing the angiogenic effect driven by the two main VEGF isoforms, composed of 121 and 165 aminoacids respectively, and differing for their ability to bind the co-receptor NP-1. We showed that, while VEGF165 induces massive formation of arterial vessels surrounded by mononuclear CD11b+ cells of bone marrow origin, VEGF121 is not able to recruit bone marrow cells and, most interestingly, does not seem able to form arteries. These findings are in perfect agreement with those of Stalmans and coworkers (Stalmans, 2002), who studied the role of the different VEGF isoforms in normal retinal angiogenesis in genetically engineered mice. These authors found a normal arterial development in $VEGF^{164/164}$ mice (the murine counterpart of VEGF165), while few arteriolae and impaired pericyte recruitment were evident in $VEGF^{121/121}$ mice. Moreover, hearts from $VEGF^{121/121}$ mice displayed impaired myocardial angiogenesis, with fewer coronary vessels (surrounded by $\alpha$-SMA+ cells), leading to ischemic cardiomyopathy (Carmeliet, 1999).

The notion that the main structural difference between VEGF121 and VEGF165 resides in a domain that confers NP-1 binding ability suggests an important role of this receptor in mediating the VEGF165-specific effect, bone marrow cell recruitment and arterial formation.

As far as bone marrow cell recruitment is concerned, we also provide additional evidence of the primary role of NP-1, by showing that the AAV-mediated overexpression of Sema3A, which also binds NP-1 with high affinity, is equally able to stimulate the homing of CD11b+ cell from the bone marrow. We also demonstrated here that the recruitment of these cells strictly depends on the expression of NP-1, since the silencing of this receptor severely affected their migration in response to both VEGF165 and Sema3A. However, these cells do not seem able to stimulate the formation of new vessels per se, since Sema3A did not exhibit any angiogenic effect. Moreover, when co-injected together with VEGF165, Sema3A exerted a potent inhibitory effect on VEGF-induced angiogenesis and leakiness. To our knowledge this is the first demonstration that Sema3A displays an anti-angiogenic activity in vivo, although the exact mechanism of this inhibition still remains to be elucidated. Indeed, it might simply depend on a competition between

VEGF165 and Sema3A for binding to VEGFR-2 on endothelial cells, or it might reflect a specific signaling activity of Sema3A on growing vessels. Of note, despite a pro-apoptotic activity of Sema3A on endothelial cells could never be demonstrated in cell culture, we observed massive apoptosis, only in muscles treated with AAV-VEGF165 and AAV-Sema3A. A representative immunostaining against caspase-3 to detect the presence of apoptotic cells is shown in Figure 5.1.

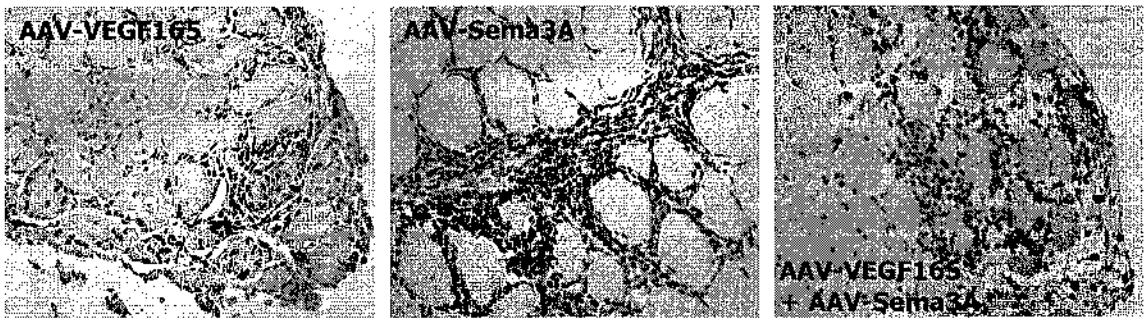


**Figure 5.1. In vivo apoptosis by AAV-VEGF165 and AAV-Sema3A co-injection.** The presence of apoptotic cells in differently treated muscle was highlighted by immunohistochemistry, using an antibody against the cleaved form of caspase-3. No apoptosis could be detected in muscles injected with either AAV-VEGF165 or AAV-Sema3A. In contrast, the combination of the two vectors induced the appearance of several cells with picnotic nuclei and a strong reactivity to caspase-3, two markers of active apoptosis.

As noted above, the other VEGF165-specific activity, which is likely mediated by NP-1, consists in the formation of arterial vessels. This concept perfectly matches a couple of recent studies supporting of a role for VEGF in promoting arterial differentiation in vivo. In zebrafish, VEGF was found to be essential for the proper formation of the dorsal aorta (Lawson, 2002). In mice, transgenic overexpression of VEGF in the heart promoted an increased number of cardiac arterial vessels (Visconti, 2002). Most interestingly, Mukouyama used a series of nerve-specific Cre lines to demonstrate that nerve-derived VEGF165 is required for arteriogenesis, which seems to be promoted by a NP-1-dependent positive feedback loop (Mukouyama, 2005).

In this work we suggest and substantiate a main role of bone marrow CD11b+ cells, recruited through NP-1 to the sites of neo-angiogenesis, in mediating the migration of smooth muscle cells and their enrollment in the vessel wall to form arteries in vivo. Indeed, the simultaneous injection of AAV-VEGF121, which only induces capillary sprouting, with purified CD11b+ cells, was sufficient to drive the formation

of arterial vessels in close proximity to the mononuclear cells. Actually, despite an increasing appreciation of the role of mural cells in maturation, remodeling and maintenance of the vascular system, little is known regarding the process of their recruitment. In particular, the exact nature of the cell-cell interactions that occur during vessel formation and their mediators are difficult to discern in vivo. Studies on embryonic vascular development revealed that cells of the vessel wall are added at later stages of vessel assembly (Nakamura, 1988; Hungerford, Owens, 1996). Many authors have suggested that concomitant with sprouting, endothelial cell direct the differentiation of mural cell precursors from the adjacent tissue by the secretion of soluble factors, such as PDGF-B (Beck, 1997; Hirschi, Rohovsky, 1998). Here we propose a similar role for bone marrow cells that are specifically homed to the sites of VEGF165-induced angiogenesis. Alternatively, the recruited mononuclear cells might secrete some factors able to stimulate the proliferation of the pericytes already associated to a pre-existing vessel, as well as their migration along the newly made vascular sprouts (Nicosia, 1995; Benjamin, 1998). Obviously, these results open the fundamental question of which are the molecules that mediate pericyte engagement in vivo. At the moment, plausible candidates that are likely to play a major role in this process essentially derive from gene knock-out studies, which imply the involvement of the Ang-1/Tie-2 system and of the PDGF-B/PDGF-β system in mesenchymal cell recruitment and differentiation, vessel maturation and maintenance of vascular integrity (Leveen, 1994; Suri, Jones, 1996; Lindahl, Johansson, 1997). Of particular interest is the observation of Carmeliet et al., that hearts of $VEGF^{121/121}$ mice expressed reduced levels of PDGF-B and its receptor typeβ as compared to $VEGF^{+/+}$ hearts, whereas levels of Ang1 were similar (Carmeliet, Ng, 1999).

However, in light of the complexity of the process, it seems likely that no one single factor is sufficient to do the entire job, and that a co-operation between different synergistic pathways might be required to achieve functional arteriogenesis.

Whatever the mechanisms of pericyte recruitment, these observations collectively indicate that bone marrow cells, although not directly incorporated into the newly formed vessels, might act in a paracrine manner, by secreting some factors important for pericyte activation and recruitment, thus promoting arteriogenesis. This notion is consistent with compelling evidence of beneficial effect exerted by the infusion of bone marrow-derived cells in various animal models of ischemia

(Pittenger, 2004) as well as in clinical settings (Mathur, 2004; Wollert, 2004), even in the absence of transdifferentiation.

As a final note, an important cause-effect relationship between the presence of bone marrow-derived CD11b+ cells and a proper vessel maturation was underscored by the significant drop in VEGF121-induced leakiness upon cell injection. Interestingly, the collection and analysis of all the data obtained by the Miles test in different experiments and in both rats and mice, revealed a significantly higher permeabilizing effect of VEGF121 relative to VEGF165 at 1 month after treatment, which is in perfect agreement with a putative role of the recruited cell in increasing arteriogenesis and promoting vessel maturation (Figure 5.2).

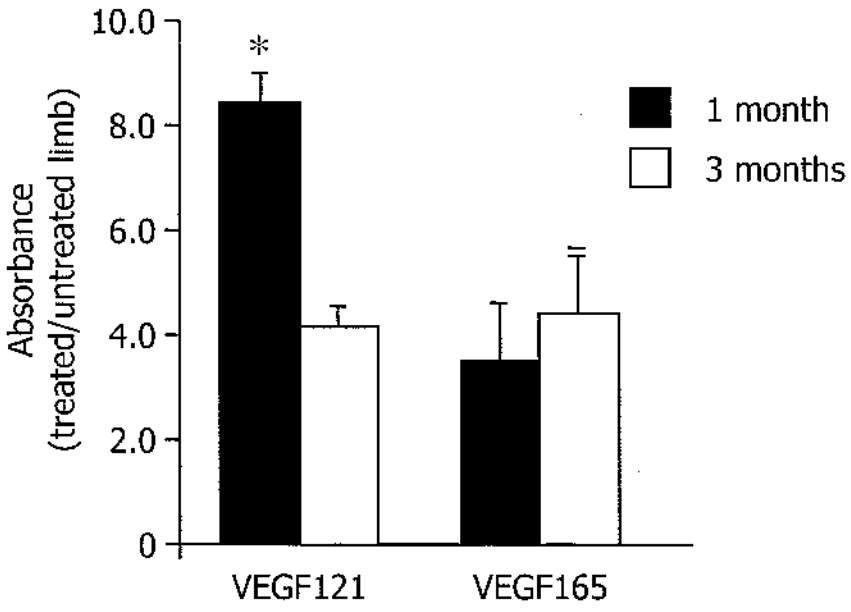


**Figure 5.2. Comparison between VEGF121- and VEGF165-induced vascular leakiness.** By collecting all the data obtained by the Miles test in both mice and rats, we observed that the permeabilizing effect of VEGF121 (n=12) was clearly higher than the one of VEGF165 (n=18) at 1 month after transduction. No such a difference was detected at 3 months. Asterisk denotes statistical significance between the two groups.

In light of these data, the fact that the same population of bone marrow mononuclear cells is similarly recruited by both VEGF165 and Sema3A, suggests an additional possible mechanism by in which Sema3A could inhibit angiogenesis. Indeed, the finding that these cells are associated to arterial development suggest their ability to secrete factors able to reinforce the intercellular junctions between endothelial and mural cells, thus leading to vessel stabilization and quiescence of

endothelial cells. Therefore, the ability of Sema3A to recruit cells that in turn activate smooth muscle cells, can at least partially explain its inhibitory effect on endothelial cell proliferation.

From a clinical perspective, the huge increase in permeability induced by VEGF121, together with the observation that this VEGF isoform seems only able to induce capillary sprouting with poor formation of arterial vessels, challenge the usefulness of VEGF121 as therapeutic gene for the induction of functional angiogenesis. Indeed, both REVASC and RAVE clinical trials did not provide the expected results and gave quite contradictory results: as a secondary endpoint, adenoviral delivery of VEGF121 into the myocardium during thoracotomy improved time to 1 mm ST segment depression during ETT (exercise tolerance test) at the 26-week time point (Rasmussen, 2002), whereas the same VEGF121 adenovirus was inefficient in the treatment of peripheral vascular disease (Rajagopalan, Mohler, 2003). Of note, the potent immunogenic effect of adenoviral vectors likely accounted for the recruitment of a number of inflammatory cells at the site of VEGF121 overexpression. These cells in turn might have promoted vessel maturation, thus explaining the partial clinical benefit observed in the REVASC trial.

As a final remark, it is worth noticing that the urgent need of for therapeutic solutions in no-option patients caused a too rapid transition of therapeutic angiogenesis from laboratory bench to the bedside. However, concerns generated during early clinical experience should be carefully considered. In particular, as the number of agents capable to stimulate vascular growth is soaring, a deeper understanding of their mechanisms of action is probably required in order to drive efficient neovascularization into the ischemic tissues. In this context, gene transfer techniques, and in particular AAV vectors, offer the unique possibility to investigate the functional role of single molecules, or of their combination, in vivo in adult organisms.

# 6. REFERENCES


(1999). "Unified nomenclature for the semaphorins/collapsins. Semaphorin Nomenclature Committee." Cell **97**(5): 551-2.

Ahmad, S. A., W. Liu, Y. D. Jung, F. Fan, M. Wilson, N. Reinmuth, R. M. Shaheen, C. D. Bucana and L. M. Ellis (2001). "The effects of angiopoietin-1 and -2 on tumor growth and angiogenesis in human colon cancer." Cancer Res **61**(4): 1255-9.

Alvarez-Dolado, M., R. Pardal, J. M. Garcia-Verdugo, J. R. Fike, H. O. Lee, K. Pfeffer, C. Lois, S. J. Morrison and A. Alvarez-Buylla (2003). "Fusion of bone-marrow-derived cells with Purkinje neurons, cardiomyocytes and hepatocytes." Nature **425**(6961): 968-73.

Antonelli-Orlidge, A., K. B. Saunders, S. R. Smith and P. A. D'Amore (1989). "An activated form of transforming growth factor beta is produced by cocultures of endothelial cells and pericytes." Proc Natl Acad Sci U S A **86**(12): 4544-8.

Arras, M., W. D. Ito, D. Scholz, B. Winkler, J. Schaper and W. Schaper (1998). "Monocyte activation in angiogenesis and collateral growth in the rabbit hindlimb." J Clin Invest **101**(1): 40-50.

Arsic, N., S. Zacchigna, L. Zentilin, G. Ramirez-Correa, L. Pattarini, A. Salvi, G. Sinagra and M. Giacca (2004). "Vascular endothelial growth factor stimulates skeletal muscle regeneration in vivo." Mol Ther **10**(5): 844-54.

Arsic, N., L. Zentilin, S. Zacchigna, D. Santoro, G. Stanta, A. Salvi, G. Sinagra and M. Giacca (2003). "Induction of functional neovascularization by combined VEGF and angiopoietin-1 gene transfer using AAV vectors." Mol Ther **7**(4): 450-9.

Asahara, T., D. Chen, T. Takahashi, K. Fujikawa, M. Kearney, M. Magner, G. D. Yancopoulos and J. M. Isner (1998). "Tie2 receptor ligands, angiopoietin-1 and angiopoietin-2, modulate VEGF-induced postnatal neovascularization." Circ Res **83**(3): 233-40.

Asahara, T. and A. Kawamoto (2004). "Endothelial progenitor cells for postnatal vasculogenesis." Am J Physiol Cell Physiol **287**(3): C572-9.

Asahara, T., H. Masuda, T. Takahashi, C. Kalka, C. Pastore, M. Silver, M. Kearne, M. Magner and J. M. Isner (1999). "Bone marrow origin of endothelial progenitor cells responsible for postnatal vasculogenesis in physiological and pathological neovascularization." Circ Res **85**(3): 221-8.

Asahara, T., T. Murohara, A. Sullivan, M. Silver, R. van der Zee, T. Li, B. Witzenbichler, G. Schatteman and J. M. Isner (1997). "Isolation of putative progenitor endothelial cells for angiogenesis." Science **275**(5302): 964-7.

Asahara, T., T. Takahashi, H. Masuda, C. Kalka, D. Chen, H. Iwaguro, Y. Inai, M. Silver and J. M. Isner (1999). "VEGF contributes to postnatal neovascularization by mobilizing bone marrow-derived endothelial progenitor cells." Embo J **18**(14): 3964-72.

Athanasopoulos, T., S. Fabb and G. Dickson (2000). "Gene therapy vectors based on adeno-associated virus: characteristics and applications to acquired and inherited diseases (review)." Int J Mol Med **6**(4): 363-75.

Autiero, M., F. De Smet, F. Claes and P. Carmeliet (2005). "Role of neural guidance signals in blood vessel navigation." Cardiovasc Res **65**(3): 629-38.

Autiero, M., J. Waltenberger, D. Communi, A. Kranz, L. Moons, D. Lambrechts, J. Kroll, S. Plaisance, M. De Mol, F. Bono, S. Kliche, G. Fellbrich, K. Ballmer-Hofer, D. Maglione, U. Mayr-Beyrle, M. Dewerchin, S. Dombrowski, D. Stanimirovic, P. Van Hummelen, C. Dehio, D. J. Hicklin, G. Persico, J. M. Herbert, M. Shibuya, D. Collen, E. M. Conway and P. Carmeliet (2003). "Role

of PlGF in the intra- and intermolecular cross talk between the VEGF receptors Flt1 and Flk1." Nat Med **9**(7): 936-43.
Azzouz, M., G. S. Ralph, E. Storkebaum, L. E. Walmsley, K. A. Mitrophanous, S. M. Kingsman, P. Carmeliet and N. D. Mazarakis (2004). "VEGF delivery with retrogradely transported lentivector prolongs survival in a mouse ALS model." Nature **429**(6990): 413-7.
Bachelder, R. E., A. Crago, J. Chung, M. A. Wendt, L. M. Shaw, G. Robinson and A. M. Mercurio (2001). "Vascular endothelial growth factor is an autocrine survival factor for neuropilin-expressing breast carcinoma cells." Cancer Res **61**(15): 5736-40.
Bachelder, R. E., E. A. Lipscomb, X. Lin, M. A. Wendt, N. H. Chadborn, B. J. Eickholt and A. M. Mercurio (2003). "Competing autocrine pathways involving alternative neuropilin-1 ligands regulate chemotaxis of carcinoma cells." Cancer Res **63**(17): 5230-3.
Bagnard, D., C. Vaillant, S. T. Khuth, N. Dufay, M. Lohrum, A. W. Puschel, M. F. Belin, J. Bolz and N. Thomasset (2001). "Semaphorin 3A-vascular endothelial growth factor-165 balance mediates migration and apoptosis of neural progenitor cells by the recruitment of shared receptor." J Neurosci **21**(10): 3332-41.
Balsam, L. B., A. J. Wagers, J. L. Christensen, T. Kofidis, I. L. Weissman and R. C. Robbins (2004). "Haematopoietic stem cells adopt mature haematopoietic fates in ischaemic myocardium." Nature **428**(6983): 668-73.
Barleon, B., S. Sozzani, D. Zhou, H. A. Weich, A. Mantovani and D. Marme (1996). "Migration of human monocytes in response to vascular endothelial growth factor (VEGF) is mediated via the VEGF receptor flt-1." Blood **87**(8): 3336-43.
Bartlett, J. S., R. Wilcher and R. J. Samulski (2000). "Infectious entry pathway of adeno-associated virus and adeno-associated virus vectors." J Virol **74**(6): 2777-85.
Basile, J. R., A. Barac, T. Zhu, K. L. Guan and J. S. Gutkind (2004). "Class IV semaphorins promote angiogenesis by stimulating Rho-initiated pathways through plexin-B." Cancer Res **64**(15): 5212-24.
Bates, D., G. I. Taylor, J. Minichiello, P. Farlie, A. Cichowitz, N. Watson, M. Klagsbrun, R. Mamluk and D. F. Newgreen (2003). "Neurovascular congruence results from a shared patterning mechanism that utilizes Semaphorin3A and Neuropilin-1." Dev Biol **255**(1): 77-98.
Bates, D. O., R. I. Heald, F. E. Curry and B. Williams (2001). "Vascular endothelial growth factor increases Rana vascular permeability and compliance by different signalling pathways." J Physiol **533**(Pt 1): 263-72.
Baumgartner, I., A. Pieczek, O. Manor, R. Blair, M. Kearney, K. Walsh and J. M. Isner (1998). "Constitutive expression of phVEGF165 after intramuscular gene transfer promotes collateral vessel development in patients with critical limb ischemia." Circulation **97**(12): 1114-23.
Baumgartner, I., G. Rauh, A. Pieczek, D. Wuensch, M. Magner, M. Kearney, R. Schainfeld and J. M. Isner (2000). "Lower-extremity edema associated with gene transfer of naked DNA encoding vascular endothelial growth factor." Ann Intern Med **132**(11): 880-4.
Beck, L., Jr. and P. A. D'Amore (1997). "Vascular development: cellular and molecular regulation." Faseb J **11**(5): 365-73.
Behar, O., J. A. Golden, H. Mashimo, F. J. Schoen and M. C. Fishman (1996). "Semaphorin III is needed for normal patterning and growth of nerves, bones and heart." Nature **383**(6600): 525-8.

Benjamin, L. E., I. Hemo and E. Keshet (1998). "A plasticity window for blood vessel remodelling is defined by pericyte coverage of the preformed endothelial network and is regulated by PDGF-B and VEGF." Development **125**(9): 1591-8.

Berns, K. I. and R. M. Linden (1995). "The cryptic life style of adeno-associated virus." Bioessays **17**(3): 237-45.

Bittner, R. E., C. Schofer, K. Weipoltshammer, S. Ivanova, B. Streubel, E. Hauser, M. Freilinger, H. Hoger, A. Elbe-Burger and F. Wachtler (1999). "Recruitment of bone-marrow-derived cells by skeletal and cardiac muscle in adult dystrophic mdx mice." Anat Embryol (Berl) **199**(5): 391-6.

Brazelton, T. R., F. M. Rossi, G. I. Keshet and H. M. Blau (2000). "From marrow to brain: expression of neuronal phenotypes in adult mice." Science **290**(5497): 1775-9.

Brinkmann, B. H., M. K. O'Connor, T. J. O'Brien, B. P. Mullan, E. L. So and R. A. Robb (1999). "Dual-isotope SPECT using simultaneous acquisition of 99mTc and 123I radioisotopes: a double-injection technique for peri-ictal functional neuroimaging." J Nucl Med **40**(4): 677-84.

Britten, M. B., N. D. Abolmaali, B. Assmus, R. Lehmann, J. Honold, J. Schmitt, T. J. Vogl, H. Martin, V. Schachinger, S. Dimmeler and A. M. Zeiher (2003). "Infarct remodeling after intracoronary progenitor cell treatment in patients with acute myocardial infarction (TOPCARE-AMI): mechanistic insights from serial contrast-enhanced magnetic resonance imaging." Circulation **108**(18): 2212-8.

Brogi, E., G. Schatteman, T. Wu, E. A. Kim, L. Varticovski, B. Keyt and J. M. Isner (1996). "Hypoxia-induced paracrine regulation of vascular endothelial growth factor receptor expression." J Clin Invest **97**(2): 469-76.

Brown, K. (2002). "Visualizing nuclear proteins together with transcribed and inactive genes in structurally preserved cells." Methods **26**(1): 10-8.

Brusselmans, K., F. Bono, D. Collen, J. M. Herbert, P. Carmeliet and M. Dewerchin (2005). "A novel role for vascular endothelial growth factor as an autocrine survival factor for embryonic stem cells during hypoxia." J Biol Chem **280**(5): 3493-9.

Cao, Y., A. Hong, H. Schulten and M. J. Post (2005). "Update on therapeutic neovascularization." Cardiovasc Res **65**(3): 639-48.

Carmeliet, P. (2003). "Blood vessels and nerves: common signals, pathways and diseases." Nat Rev Genet **4**(9): 710-20.

Carmeliet, P. and D. Collen (1999). "Role of vascular endothelial growth factor and vascular endothelial growth factor receptors in vascular development." Curr Top Microbiol Immunol **237**: 133-58.

Carmeliet, P., V. Ferreira, G. Breier, S. Pollefeyt, L. Kieckens, M. Gertsenstein, M. Fahrig, A. Vandenhoeck, K. Harpal, C. Eberhardt, C. Declercq, J. Pawling, L. Moons, D. Collen, W. Risau and A. Nagy (1996). "Abnormal blood vessel development and lethality in embryos lacking a single VEGF allele." Nature **380**(6573): 435-9.

Carmeliet, P., L. Moons, A. Luttun, V. Vincenti, V. Compernolle, M. De Mol, Y. Wu, F. Bono, L. Devy, H. Beck, D. Scholz, T. Acker, T. DiPalma, M. Dewerchin, A. Noel, I. Stalmans, A. Barra, S. Blacher, T. Vandendriessche, A. Ponten, U. Eriksson, K. H. Plate, J. M. Foidart, W. Schaper, D. S. Charnock-Jones, D. J. Hicklin, J. M. Herbert, D. Collen and M. G. Persico (2001). "Synergism between vascular endothelial growth factor and placental growth factor contributes to angiogenesis and plasma extravasation in pathological conditions." Nat Med **7**(5): 575-83.

Carmeliet, P., Y. S. Ng, D. Nuyens, G. Theilmeier, K. Brusselmans, I. Cornelissen, E. Ehler, V. V. Kakkar, I. Stalmans, V. Mattot, J. C. Perriard, M. Dewerchin, W. Flameng, A. Nagy, F. Lupu, L. Moons, D. Collen, P. A. D'Amore and D. T. Shima (1999). "Impaired myocardial angiogenesis and ischemic cardiomyopathy in mice lacking the vascular endothelial growth factor isoforms VEGF164 and VEGF188." Nat Med **5**(5): 495-502.

Carmeliet, P. and E. Storkebaum (2002). "Vascular and neuronal effects of VEGF in the nervous system: implications for neurological disorders." Semin Cell Dev Biol **13**(1): 39-53.

Castro-Rivera, E., S. Ran, P. Thorpe and J. D. Minna (2004). "Semaphorin 3B (SEMA3B) induces apoptosis in lung and breast cancer, whereas VEGF165 antagonizes this effect." Proc Natl Acad Sci U S A **101**(31): 11432-7.

Chen, H., A. Bagri, J. A. Zupicich, Y. Zou, E. Stoeckli, S. J. Pleasure, D. H. Lowenstein, W. C. Skarnes, A. Chedotal and M. Tessier-Lavigne (2000). "Neuropilin-2 regulates the development of selective cranial and sensory nerves and hippocampal mossy fiber projections." Neuron **25**(1): 43-56.

Chen, H., A. Chedotal, Z. He, C. S. Goodman and M. Tessier-Lavigne (1997). "Neuropilin-2, a novel member of the neuropilin family, is a high affinity receptor for the semaphorins Sema E and Sema IV but not Sema III." Neuron **19**(3): 547-59.

Chen, H., Z. He, A. Bagri and M. Tessier-Lavigne (1998). "Semaphorin-neuropilin interactions underlying sympathetic axon responses to class III semaphorins." Neuron **21**(6): 1283-90.

Clauss, M., H. Weich, G. Breier, U. Knies, W. Rockl, J. Waltenberger and W. Risau (1996). "The vascular endothelial growth factor receptor Flt-1 mediates biological activities. Implications for a functional role of placenta growth factor in monocyte activation and chemotaxis." J Biol Chem **271**(30): 17629-34.

Coffin, J. D., J. Harrison, S. Schwartz and R. Heimark (1991). "Angioblast differentiation and morphogenesis of the vascular endothelium in the mouse embryo." Dev Biol **148**(1): 51-62.

Conrotto, P., D. Valdembri, S. Corso, G. Serini, L. Tamagnone, P. M. Comoglio, F. Bussolino and S. Giordano (2005). "Sema4D induces angiogenesis through Met recruitment by Plexin B1." Blood **105**(11): 4321-9.

Couffinhal, T., M. Silver, M. Kearney, A. Sullivan, B. Witzenbichler, M. Magner, B. Annex, K. Peters and J. M. Isner (1999). "Impaired collateral vessel development associated with reduced expression of vascular endothelial growth factor in ApoE-/- mice." Circulation **99**(24): 3188-98.

Crisa, L., V. Cirulli, K. A. Smith, M. H. Ellisman, B. E. Torbett and D. R. Salomon (1999). "Human cord blood progenitors sustain thymic T-cell development and a novel form of angiogenesis." Blood **94**(11): 3928-40.

Crocker, D. J., T. M. Murad and J. C. Geer (1970). "Role of the pericyte in wound healing. An ultrastructural study." Exp Mol Pathol **13**(1): 51-65.

Davis, S., T. H. Aldrich, P. F. Jones, A. Acheson, D. L. Compton, V. Jain, T. E. Ryan, J. Bruno, C. Radziejewski, P. C. Maisonpierre and G. D. Yancopoulos (1996). "Isolation of angiopoietin-1, a ligand for the TIE2 receptor, by secretion-trap expression cloning." Cell **87**(7): 1161-9.

De Palma, M., M. A. Venneri, C. Roca and L. Naldini (2003). "Targeting exogenous genes to tumor angiogenesis by transplantation of genetically modified hematopoietic stem cells." Nat Med **9**(6): 789-95.

DiSalvo, J., M. L. Bayne, G. Conn, P. W. Kwok, P. G. Trivedi, D. D. Soderman, T. M. Palisi, K. A. Sullivan and K. A. Thomas (1995). "Purification and

characterization of a naturally occurring vascular endothelial growth factor.placenta growth factor heterodimer." J Biol Chem **270**(13): 7717-23.
Dong, G., Z. Chen, Z. Y. Li, N. T. Yeh, C. C. Bancroft and C. Van Waes (2001). "Hepatocyte growth factor/scatter factor-induced activation of MEK and PI3K signal pathways contributes to expression of proangiogenic cytokines interleukin-8 and vascular endothelial growth factor in head and neck squamous cell carcinoma." Cancer Res **61**(15): 5911-8.
Dor, Y., V. Djonov, R. Abramovitch, A. Itin, G. I. Fishman, P. Carmeliet, G. Goelman and E. Keshet (2002). "Conditional switching of VEGF provides new insights into adult neovascularization and pro-angiogenic therapy." Embo J **21**(8): 1939-47.
Druker, B. J. (2002). "STI571 (Gleevec) as a paradigm for cancer therapy." Trends Mol Med **8**(4 Suppl): S14-8.
Dumont, D. J., G. Gradwohl, G. H. Fong, M. C. Puri, M. Gertsenstein, A. Auerbach and M. L. Breitman (1994). "Dominant-negative and targeted null mutations in the endothelial receptor tyrosine kinase, tek, reveal a critical role in vasculogenesis of the embryo." Genes Dev **8**(16): 1897-909.
Dutheil, N., F. Shi, T. Dupressoir and R. M. Linden (2000). "Adeno-associated virus site-specifically integrates into a muscle-specific DNA region." Proc Natl Acad Sci U S A **97**(9): 4862-6.
Eriksson, A., R. Cao, J. Roy, K. Tritsaris, C. Wahlestedt, S. Dissing, J. Thyberg and Y. Cao (2003). "Small GTP-binding protein Rac is an essential mediator of vascular endothelial growth factor-induced endothelial fenestrations and vascular permeability." Circulation **107**(11): 1532-8.
Favre, D., N. Provost, V. Blouin, G. Blancho, Y. Cherel, A. Salvetti and P. Moullier (2001). "Immediate and long-term safety of recombinant adeno-associated virus injection into the nonhuman primate muscle." Mol Ther **4**(6): 559-66.
Feldman, P. S., D. Shneidman and C. Kaplan (1978). "Ultrastructure of infantile hemangioendothelioma of the liver." Cancer **42**(2): 521-7.
Ferrara, N. and K. Alitalo (1999). "Clinical applications of angiogenic growth factors and their inhibitors." Nat Med **5**(12): 1359-64.
Ferrara, N., K. Carver-Moore, H. Chen, M. Dowd, L. Lu, K. S. O'Shea, L. Powell-Braxton, K. J. Hillan and M. W. Moore (1996). "Heterozygous embryonic lethality induced by targeted inactivation of the VEGF gene." Nature **380**(6573): 439-42.
Ferrara, N., H. P. Gerber and J. LeCouter (2003). "The biology of VEGF and its receptors." Nat Med **9**(6): 669-76.
Ferrari, F. K., T. Samulski, T. Shenk and R. J. Samulski (1996). "Second-strand synthesis is a rate-limiting step for efficient transduction by recombinant adeno-associated virus vectors." J Virol **70**(5): 3227-34.
Ferrari, G., G. Cusella-De Angelis, M. Coletta, E. Paolucci, A. Stornaiuolo, G. Cossu and F. Mavilio (1998). "Muscle regeneration by bone marrow-derived myogenic progenitors." Science **279**(5356): 1528-30.
Fisher, K. J., K. Jooss, J. Alston, Y. Yang, S. E. Haecker, K. High, R. Pathak, S. E. Raper and J. M. Wilson (1997). "Recombinant adeno-associated virus for muscle directed gene therapy." Nat Med **3**(3): 306-12.
Folkman, J. (1971). "Tumor angiogenesis: therapeutic implications." N Engl J Med **285**(21): 1182-6.
Fong, G. H., J. Rossant, M. Gertsenstein and M. L. Breitman (1995). "Role of the Flt-1 receptor tyrosine kinase in regulating the assembly of vascular endothelium." Nature **376**(6535): 66-70.

Fuh, G., K. C. Garcia and A. M. de Vos (2000). "The interaction of neuropilin-1 with vascular endothelial growth factor and its receptor flt-1." J Biol Chem **275**(35): 26690-5.
Gagliardini, V. and C. Fankhauser (1999). "Semaphorin III can induce death in sensory neurons." Mol Cell Neurosci **14**(4-5): 301-16.
Gamble, J. R., J. Drew, L. Trezise, A. Underwood, M. Parsons, L. Kasminkas, J. Rudge, G. Yancopoulos and M. A. Vadas (2000). "Angiopoietin-1 is an antipermeability and anti-inflammatory agent in vitro and targets cell junctions." Circ Res **87**(7): 603-7.
Gerber, H. P., F. Condorelli, J. Park and N. Ferrara (1997). "Differential transcriptional regulation of the two vascular endothelial growth factor receptor genes. Flt-1, but not Flk-1/KDR, is up-regulated by hypoxia." J Biol Chem **272**(38): 23659-67.
Gerber, H. P., A. K. Malik, G. P. Solar, D. Sherman, X. H. Liang, G. Meng, K. Hong, J. C. Marsters and N. Ferrara (2002). "VEGF regulates haematopoietic stem cell survival by an internal autocrine loop mechanism." Nature **417**(6892): 954-8.
Gerety, S. S., H. U. Wang, Z. F. Chen and D. J. Anderson (1999). "Symmetrical mutant phenotypes of the receptor EphB4 and its specific transmembrane ligand ephrin-B2 in cardiovascular development." Mol Cell **4**(3): 403-14.
Germani, A., A. Di Carlo, A. Mangoni, S. Straino, C. Giacinti, P. Turrini, P. Biglioli and M. C. Capogrossi (2003). "Vascular endothelial growth factor modulates skeletal myoblast function." Am J Pathol **163**(4): 1417-28.
Giger, R. J., J. F. Cloutier, A. Sahay, R. K. Prinjha, D. V. Levengood, S. E. Moore, S. Pickering, D. Simmons, S. Rastan, F. S. Walsh, A. L. Kolodkin, D. D. Ginty and M. Geppert (2000). "Neuropilin-2 is required in vivo for selective axon guidance responses to secreted semaphorins." Neuron **25**(1): 29-41.
Giger, R. J., E. R. Urquhart, S. K. Gillespie, D. V. Levengood, D. D. Ginty and A. L. Kolodkin (1998). "Neuropilin-2 is a receptor for semaphorin IV: insight into the structural basis of receptor function and specificity." Neuron **21**(5): 1079-92.
Giordano, S., S. Corso, P. Conrotto, S. Artigiani, G. Gilestro, D. Barberis, L. Tamagnone and P. M. Comoglio (2002). "The semaphorin 4D receptor controls invasive growth by coupling with Met." Nat Cell Biol **4**(9): 720-4.
Gluzman-Poltorak, Z., T. Cohen, Y. Herzog and G. Neufeld (2000). "Neuropilin-2 is a receptor for the vascular endothelial growth factor (VEGF) forms VEGF-145 and VEGF-165." J Biol Chem **275**(38): 29922.
Gluzman-Poltorak, Z., T. Cohen, M. Shibuya and G. Neufeld (2001). "Vascular endothelial growth factor receptor-1 and neuropilin-2 form complexes." J Biol Chem **276**(22): 18688-94.
Goshima, Y., F. Nakamura, P. Strittmatter and S. M. Strittmatter (1995). "Collapsin-induced growth cone collapse mediated by an intracellular protein related to UNC-33." Nature **376**(6540): 509-14.
Gounis, M. J., M. G. Spiga, R. M. Graham, A. Wilson, S. Haliko, B. B. Lieber, A. K. Wakhloo and K. A. Webster (2005). "Angiogenesis is confined to the transient period of VEGF expression that follows adenoviral gene delivery to ischemic muscle." Gene Ther **12**(9): 762-71.
Grimm, D., A. Kern, K. Rittner and J. A. Kleinschmidt (1998). "Novel tools for production and purification of recombinant adenoassociated virus vectors." Hum Gene Ther **9**(18): 2745-60.
Gu, C., B. J. Limberg, G. B. Whitaker, B. Perman, D. J. Leahy, J. S. Rosenbaum, D. D. Ginty and A. L. Kolodkin (2002). "Characterization of neuropilin-1

structural features that confer binding to semaphorin 3A and vascular endothelial growth factor 165." J Biol Chem **277**(20): 18069-76.

Gu, C., E. R. Rodriguez, D. V. Reimert, T. Shu, B. Fritzsch, L. J. Richards, A. L. Kolodkin and D. D. Ginty (2003). "Neuropilin-1 conveys semaphorin and VEGF signaling during neural and cardiovascular development." Dev Cell **5**(1): 45-57.

Gu, C., Y. Yoshida, J. Livet, D. V. Reimert, F. Mann, J. Merte, C. E. Henderson, T. M. Jessell, A. L. Kolodkin and D. D. Ginty (2005). "Semaphorin 3E and plexin-D1 control vascular pattern independently of neuropilins." Science **307**(5707): 265-8.

Guzman, R. J., P. Lemarchand, R. G. Crystal, S. E. Epstein and T. Finkel (1993). "Efficient gene transfer into myocardium by direct injection of adenovirus vectors." Circ Res **73**(6): 1202-7.

Halbert, C. L., J. M. Allen and A. D. Miller (2001). "Adeno-associated virus type 6 (AAV6) vectors mediate efficient transduction of airway epithelial cells in mouse lungs compared to that of AAV2 vectors." J Virol **75**(14): 6615-24.

Hall, K. T., L. Boumsell, J. L. Schultze, V. A. Boussiotis, D. M. Dorfman, A. A. Cardoso, A. Bensussan, L. M. Nadler and G. J. Freeman (1996). "Human CD100, a novel leukocyte semaphorin that promotes B-cell aggregation and differentiation." Proc Natl Acad Sci U S A **93**(21): 11780-5.

Hariawala, M. D., J. R. Horowitz, D. Esakof, D. D. Sheriff, D. H. Walter, B. Keyt, J. M. Isner and J. F. Symes (1996). "VEGF improves myocardial blood flow but produces EDRF-mediated hypotension in porcine hearts." J Surg Res **63**(1): 77-82.

Hayes, A. J., W. Q. Huang, J. Yu, P. C. Maisonpierre, A. Liu, F. G. Kern, M. E. Lippman, S. W. McLeskey and L. Y. Li (2000). "Expression and function of angiopoietin-1 in breast cancer." Br J Cancer **83**(9): 1154-60.

He, Z. and M. Tessier-Lavigne (1997). "Neuropilin is a receptor for the axonal chemorepellent Semaphorin III." Cell **90**(4): 739-51.

Heil, M., T. Ziegelhoeffer, F. Pipp, S. Kostin, S. Martin, M. Clauss and W. Schaper (2002). "Blood monocyte concentration is critical for enhancement of collateral artery growth." Am J Physiol Heart Circ Physiol **283**(6): H2411-9.

Heil, M., T. Ziegelhoeffer, S. Wagner, B. Fernandez, A. Helisch, S. Martin, S. Tribulova, W. A. Kuziel, G. Bachmann and W. Schaper (2004). "Collateral artery growth (arteriogenesis) after experimental arterial occlusion is impaired in mice lacking CC-chemokine receptor-2." Circ Res **94**(5): 671-7.

Hellstrom, M., H. Gerhardt, M. Kalen, X. Li, U. Eriksson, H. Wolburg and C. Betsholtz (2001). "Lack of pericytes leads to endothelial hyperplasia and abnormal vascular morphogenesis." J Cell Biol **153**(3): 543-53.

Hendel, R. C., T. D. Henry, K. Rocha-Singh, J. M. Isner, D. J. Kereiakes, F. J. Giordano, M. Simons and R. O. Bonow (2000). "Effect of intracoronary recombinant human vascular endothelial growth factor on myocardial perfusion: evidence for a dose-dependent effect." Circulation **101**(2): 118-21.

Henry, T. D., B. H. Annex, G. R. McKendall, M. A. Azrin, J. J. Lopez, F. J. Giordano, P. K. Shah, J. T. Willerson, R. L. Benza, D. S. Berman, C. M. Gibson, A. Bajamonde, A. C. Rundle, J. Fine and E. R. McCluskey (2003). "The VIVA trial: Vascular endothelial growth factor in Ischemia for Vascular Angiogenesis." Circulation **107**(10): 1359-65.

Henry, T. D., K. Rocha-Singh, J. M. Isner, D. J. Kereiakes, F. J. Giordano, M. Simons, D. W. Losordo, R. C. Hendel, R. O. Bonow, S. M. Eppler, T. F. Zioncheck, E. B. Holmgren and E. R. McCluskey (2001). "Intracoronary administration of

recombinant human vascular endothelial growth factor to patients with coronary artery disease." Am Heart J **142**(5): 872-80.
Herzog, S., H. Sager, E. Khmelevski, A. Deylig and W. D. Ito (2002). "Collateral arteries grow from preexisting anastomoses in the rat hindlimb." Am J Physiol Heart Circ Physiol **283**(5): H2012-20.
Herzog, Y., C. Kalcheim, N. Kahane, R. Reshef and G. Neufeld (2001). "Differential expression of neuropilin-1 and neuropilin-2 in arteries and veins." Mech Dev **109**(1): 115-9.
Hiratsuka, S., O. Minowa, J. Kuno, T. Noda and M. Shibuya (1998). "Flt-1 lacking the tyrosine kinase domain is sufficient for normal development and angiogenesis in mice." Proc Natl Acad Sci U S A **95**(16): 9349-54.
Hirschi, K. K., S. A. Rohovsky and P. A. D'Amore (1998). "PDGF, TGF-beta, and heterotypic cell-cell interactions mediate endothelial cell-induced recruitment of 10T1/2 cells and their differentiation to a smooth muscle fate." J Cell Biol **141**(3): 805-14.
Ho, S., W. Y. Lau, W. T. Leung, M. Chan, K. W. Chan, P. J. Johnson and A. K. Li (1997). "Arteriovenous shunts in patients with hepatic tumors." J Nucl Med **38**(8): 1201-5.
Holder, N. and R. Klein (1999). "Eph receptors and ephrins: effectors of morphogenesis." Development **126**(10): 2033-44.
Horowitz, J. R., A. Rivard, R. van der Zee, M. Hariawala, D. D. Sheriff, D. D. Esakof, G. M. Chaudhry, J. F. Symes and J. M. Isner (1997). "Vascular endothelial growth factor/vascular permeability factor produces nitric oxide-dependent hypotension. Evidence for a maintenance role in quiescent adult endothelium." Arterioscler Thromb Vasc Biol **17**(11): 2793-800.
Horwitz, E. M., D. J. Prockop, L. A. Fitzpatrick, W. W. Koo, P. L. Gordon, M. Neel, M. Sussman, P. Orchard, J. C. Marx, R. E. Pyeritz and M. K. Brenner (1999). "Transplantability and therapeutic effects of bone marrow-derived mesenchymal cells in children with osteogenesis imperfecta." Nat Med **5**(3): 309-13.
Hungerford, J. E., G. K. Owens, W. S. Argraves and C. D. Little (1996). "Development of the aortic vessel wall as defined by vascular smooth muscle and extracellular matrix markers." Dev Biol **178**(2): 375-92.
Ikeda, E., M. G. Achen, G. Breier and W. Risau (1995). "Hypoxia-induced transcriptional activation and increased mRNA stability of vascular endothelial growth factor in C6 glioma cells." J Biol Chem **270**(34): 19761-6.
Inoue, Y., K. Machida, N. Honda, S. Takagi, T. Ohtake, J. Nishikawa and Y. Sasaki (1997). "Effect of angiotensin II on arteriovenous shunting assessed by hepatic arterial perfusion scintigraphy." Am J Clin Oncol **20**(3): 237-41.
Isner, J. M. and T. Asahara (1999). "Angiogenesis and vasculogenesis as therapeutic strategies for postnatal neovascularization." J Clin Invest **103**(9): 1231-6.
Isner, J. M., A. Pieczek, R. Schainfeld, R. Blair, L. Haley, T. Asahara, K. Rosenfield, S. Razvi, K. Walsh and J. F. Symes (1996). "Clinical evidence of angiogenesis after arterial gene transfer of phVEGF165 in patient with ischaemic limb." Lancet **348**(9024): 370-4.
Iwaguro, H., J. Yamaguchi, C. Kalka, S. Murasawa, H. Masuda, S. Hayashi, M. Silver, T. Li, J. M. Isner and T. Asahara (2002). "Endothelial progenitor cell vascular endothelial growth factor gene transfer for vascular regeneration." Circulation **105**(6): 732-8.
Jackson, K. A., S. M. Majka, H. Wang, J. Pocius, C. J. Hartley, M. W. Majesky, M. L. Entman, L. H. Michael, K. K. Hirschi and M. A. Goodell (2001). "Regeneration

of ischemic cardiac muscle and vascular endothelium by adult stem cells." J Clin Invest **107**(11): 1395-402.

Jiang, B. H., E. Rue, G. L. Wang, R. Roe and G. L. Semenza (1996). "Dimerization, DNA binding, and transactivation properties of hypoxia-inducible factor 1." J Biol Chem **271**(30): 17771-8.

Jin, Z. and S. M. Strittmatter (1997). "Rac1 mediates collapsin-1-induced growth cone collapse." J Neurosci **17**(16): 6256-63.

Kalka, C., H. Masuda, T. Takahashi, W. M. Kalka-Moll, M. Silver, M. Kearney, T. Li, J. M. Isner and T. Asahara (2000). "Transplantation of ex vivo expanded endothelial progenitor cells for therapeutic neovascularization." Proc Natl Acad Sci U S A **97**(7): 3422-7.

Kawakami, A., T. Kitsukawa, S. Takagi and H. Fujisawa (1996). "Developmentally regulated expression of a cell surface protein, neuropilin, in the mouse nervous system." J Neurobiol **29**(1): 1-17.

Kawasaki, T., T. Kitsukawa, Y. Bekku, Y. Matsuda, M. Sanbo, T. Yagi and H. Fujisawa (1999). "A requirement for neuropilin-1 in embryonic vessel formation." Development **126**(21): 4895-902.

Keck, P. J., S. D. Hauser, G. Krivi, K. Sanzo, T. Warren, J. Feder and D. T. Connolly (1989). "Vascular permeability factor, an endothelial cell mitogen related to PDGF." Science **246**(4935): 1309-12.

Kitsukawa, T., M. Shimizu, M. Sanbo, T. Hirata, M. Taniguchi, Y. Bekku, T. Yagi and H. Fujisawa (1997). "Neuropilin-semaphorin III/D-mediated chemorepulsive signals play a crucial role in peripheral nerve projection in mice." Neuron **19**(5): 995-1005.

Kitsukawa, T., A. Shimono, A. Kawakami, H. Kondoh and H. Fujisawa (1995). "Overexpression of a membrane protein, neuropilin, in chimeric mice causes anomalies in the cardiovascular system, nervous system and limbs." Development **121**(12): 4309-18.

Kocher, A. A., M. D. Schuster, M. J. Szabolcs, S. Takuma, D. Burkhoff, J. Wang, S. Homma, N. M. Edwards and S. Itescu (2001). "Neovascularization of ischemic myocardium by human bone-marrow-derived angioblasts prevents cardiomyocyte apoptosis, reduces remodeling and improves cardiac function." Nat Med **7**(4): 430-6.

Kolodkin, A. L., D. V. Levengood, E. G. Rowe, Y. T. Tai, R. J. Giger and D. D. Ginty (1997). "Neuropilin is a semaphorin III receptor." Cell **90**(4): 753-62.

Kolodkin, A. L., D. J. Matthes and C. S. Goodman (1993). "The semaphorin genes encode a family of transmembrane and secreted growth cone guidance molecules." Cell **75**(7): 1389-99.

Komatsu, S., Y. Sakata, Y. Ueda, Y. Higuchi, F. Ishikura, A. Hirayama, M. Mishima, H. Kusuoka, M. Hasegawa and K. Kodama (1998). "Estimation of shunt flow in coronary-pulmonary fistula by lung perfusion scintigraphy with technetium-99m macroaggregated albumin." Am J Cardiol **82**(9): 1158-61, A11.

Laitinen, M., K. Makinen, H. Manninen, P. Matsi, M. Kossila, R. S. Agrawal, T. Pakkanen, J. S. Luoma, H. Viita, J. Hartikainen, E. Alhava, M. Laakso and S. Yla-Herttuala (1998). "Adenovirus-mediated gene transfer to lower limb artery of patients with chronic critical leg ischemia." Hum Gene Ther **9**(10): 1481-6.

Lambrechts, D., E. Storkebaum, M. Morimoto, J. Del-Favero, F. Desmet, S. L. Marklund, S. Wyns, V. Thijs, J. Andersson, I. van Marion, A. Al-Chalabi, S. Bornes, R. Musson, V. Hansen, L. Beckman, R. Adolfsson, H. S. Pall, H. Prats, S. Vermeire, P. Rutgeerts, S. Katayama, T. Awata, N. Leigh, L. Lang-Lazdunski, M. Dewerchin, C. Shaw, L. Moons, R. Vlietinck, K. E. Morrison, W.

Robberecht, C. Van Broeckhoven, D. Collen, P. M. Andersen and P. Carmeliet (2003). "VEGF is a modifier of amyotrophic lateral sclerosis in mice and humans and protects motoneurons against ischemic death." Nat Genet **34**(4): 383-94.

Lawson, N. D., A. M. Vogel and B. M. Weinstein (2002). "sonic hedgehog and vascular endothelial growth factor act upstream of the Notch pathway during arterial endothelial differentiation." Dev Cell **3**(1): 127-36.

Lee, R. J., M. L. Springer, W. E. Blanco-Bose, R. Shaw, P. C. Ursell and H. M. Blau (2000). "VEGF gene delivery to myocardium: deleterious effects of unregulated expression." Circulation **102**(8): 898-901.

Lehrman, S. (1999). "Virus treatment questioned after gene therapy death." Nature **401**(6753): 517-8.

Lerman, M. I. and J. D. Minna (2000). "The 630-kb lung cancer homozygous deletion region on human chromosome 3p21.3: identification and evaluation of the resident candidate tumor suppressor genes. The International Lung Cancer Chromosome 3p21.3 Tumor Suppressor Gene Consortium." Cancer Res **60**(21): 6116-33.

Leung, D. W., G. Cachianes, W. J. Kuang, D. V. Goeddel and N. Ferrara (1989). "Vascular endothelial growth factor is a secreted angiogenic mitogen." Science **246**(4935): 1306-9.

Leveen, P., M. Pekny, S. Gebre-Medhin, B. Swolin, E. Larsson and C. Betsholtz (1994). "Mice deficient for PDGF B show renal, cardiovascular, and hematological abnormalities." Genes Dev **8**(16): 1875-87.

Li, J., L. F. Brown, M. G. Hibberd, J. D. Grossman, J. P. Morgan and M. Simons (1996). "VEGF, flk-1, and flt-1 expression in a rat myocardial infarction model of angiogenesis." Am J Physiol **270**(5 Pt 2): H1803-11.

Lindahl, P., B. R. Johansson, P. Leveen and C. Betsholtz (1997). "Pericyte loss and microaneurysm formation in PDGF-B-deficient mice." Science **277**(5323): 242-5.

Lobb, R. R., M. E. Key, E. M. Alderman and J. W. Fett (1985). "Partial purification and characterization of a vascular permeability factor secreted by a human colon adenocarcinoma cell line." Int J Cancer **36**(4): 473-8.

Losordo, D. W., P. R. Vale, J. F. Symes, C. H. Dunnington, D. D. Esakof, M. Maysky, A. B. Ashare, K. Lathi and J. M. Isner (1998). "Gene therapy for myocardial angiogenesis: initial clinical results with direct myocardial injection of phVEGF165 as sole therapy for myocardial ischemia." Circulation **98**(25): 2800-4.

Luo, Y., D. Raible and J. A. Raper (1993). "Collapsin: a protein in brain that induces the collapse and paralysis of neuronal growth cones." Cell **75**(2): 217-27.

Lyden, D., K. Hattori, S. Dias, C. Costa, P. Blaikie, L. Butros, A. Chadburn, B. Heissig, W. Marks, L. Witte, Y. Wu, D. Hicklin, Z. Zhu, N. R. Hackett, R. G. Crystal, M. A. Moore, K. A. Hajjar, K. Manova, R. Benezra and S. Rafii (2001). "Impaired recruitment of bone-marrow-derived endothelial and hematopoietic precursor cells blocks tumor angiogenesis and growth." Nat Med **7**(11): 1194-201.

Mack, C. A., S. R. Patel, E. A. Schwarz, P. Zanzonico, R. T. Hahn, A. Ilercil, R. B. Devereux, S. J. Goldsmith, T. F. Christian, T. A. Sanborn, I. Kovesdi, N. Hackett, O. W. Isom, R. G. Crystal and T. K. Rosengart (1998). "Biologic bypass with the use of adenovirus-mediated gene transfer of the complementary deoxyribonucleic acid for vascular endothelial growth factor 121 improves myocardial perfusion and function in the ischemic porcine heart." J Thorac Cardiovasc Surg **115**(1): 168-76; discussion 176-7.

Maestrini, E., L. Tamagnone, P. Longati, O. Cremona, M. Gulisano, S. Bione, F. Tamanini, B. G. Neel, D. Toniolo and P. M. Comoglio (1996). "A family of transmembrane proteins with homology to the MET-hepatocyte growth factor receptor." Proc Natl Acad Sci U S A **93**(2): 674-8.

Maglione, D., V. Guerriero, G. Viglietto, M. G. Ferraro, O. Aprelikova, K. Alitalo, S. Del Vecchio, K. J. Lei, J. Y. Chou and M. G. Persico (1993). "Two alternative mRNAs coding for the angiogenic factor, placenta growth factor (PlGF), are transcribed from a single gene of chromosome 14." Oncogene **8**(4): 925-31.

Magovern, C. J., C. A. Mack, J. Zhang, T. K. Rosengart, O. W. Isom and R. G. Crystal (1997). "Regional angiogenesis induced in nonischemic tissue by an adenoviral vector expressing vascular endothelial growth factor." Hum Gene Ther **8**(2): 215-27.

Makinen, T., B. Olofsson, T. Karpanen, U. Hellman, S. Soker, M. Klagsbrun, U. Eriksson and K. Alitalo (1999). "Differential binding of vascular endothelial growth factor B splice and proteolytic isoforms to neuropilin-1." J Biol Chem **274**(30): 21217-22.

Mallat, Z., J. S. Silvestre, S. Le Ricousse-Roussanne, L. Lecomte-Raclet, A. Corbaz, M. Clergue, M. Duriez, V. Barateau, S. Akira, A. Tedgui, G. Tobelem, Y. Chvatchko and B. I. Levy (2002). "Interleukin-18/interleukin-18 binding protein signaling modulates ischemia-induced neovascularization in mice hindlimb." Circ Res **91**(5): 441-8.

Marcello, A., P. Massimi, L. Banks and M. Giacca (2000). "Adeno-associated virus type 2 rep protein inhibits human papillomavirus type 16 E2 recruitment of the transcriptional coactivator p300." J Virol **74**(19): 9090-8.

Marchetti, S., C. Gimond, K. Iljin, C. Bourcier, K. Alitalo, J. Pouyssegur and G. Pages (2002). "Endothelial cells genetically selected from differentiating mouse embryonic stem cells incorporate at sites of neovascularization in vivo." J Cell Sci **115**(Pt 10): 2075-85.

Mathur, A. and J. F. Martin (2004). "Stem cells and repair of the heart." Lancet **364**(9429): 183-92.

Mesri, E. A., H. J. Federoff and M. Brownlee (1995). "Expression of vascular endothelial growth factor from a defective herpes simplex virus type 1 amplicon vector induces angiogenesis in mice." Circ Res **76**(2): 161-7.

Metheny-Barlow, L. J., S. Tian, A. J. Hayes and L. Y. Li (2004). "Direct chemotactic action of angiopoietin-1 on mesenchymal cells in the presence of VEGF." Microvasc Res **68**(3): 221-30.

Miao, H. Q., P. Lee, H. Lin, S. Soker and M. Klagsbrun (2000). "Neuropilin-1 expression by tumor cells promotes tumor angiogenesis and progression." Faseb J **14**(15): 2532-9.

Miao, H. Q., S. Soker, L. Feiner, J. L. Alonso, J. A. Raper and M. Klagsbrun (1999). "Neuropilin-1 mediates collapsin-1/semaphorin III inhibition of endothelial cell motility: functional competition of collapsin-1 and vascular endothelial growth factor-165." J Cell Biol **146**(1): 233-42.

Migdal, M., B. Huppertz, S. Tessler, A. Comforti, M. Shibuya, R. Reich, H. Baumann and G. Neufeld (1998). "Neuropilin-1 is a placenta growth factor-2 receptor." J Biol Chem **273**(35): 22272-8.

Miles, A. A. and E. M. Miles (1952). "Vascular reactions to histamine, histamine-liberator and leukotaxine in the skin of guinea-pigs." J Physiol **118**(2): 228-57.

Millauer, B., L. K. Shawver, K. H. Plate, W. Risau and A. Ullrich (1994). "Glioblastoma growth inhibited in vivo by a dominant-negative Flk-1 mutant." Nature **367**(6463): 576-9.

Mitola, S., S. Sozzani, W. Luini, L. Primo, A. Borsatti, H. Weich and F. Bussolino (1997). "Tat-human immunodeficiency virus-1 induces human monocyte chemotaxis by activation of vascular endothelial growth factor receptor-1." Blood **90**(4): 1365-72.

Monahan, P. E. and R. J. Samulski (2000). "AAV vectors: is clinical success on the horizon?" Gene Ther **7**(1): 24-30.

Moore, J. W., 3rd and M. M. Sholley (1985). "Comparison of the neovascular effects of stimulated macrophages and neutrophils in autologous rabbit corneas." Am J Pathol **120**(1): 87-98.

Moyon, D., L. Pardanaud, L. Yuan, C. Breant and A. Eichmann (2001). "Plasticity of endothelial cells during arterial-venous differentiation in the avian embryo." Development **128**(17): 3359-70.

Muhlhauser, J., M. J. Merrill, R. Pili, H. Maeda, M. Bacic, B. Bewig, A. Passaniti, N. A. Edwards, R. G. Crystal and M. C. Capogrossi (1995). "VEGF165 expressed by a replication-deficient recombinant adenovirus vector induces angiogenesis in vivo." Circ Res **77**(6): 1077-86.

Mukouyama, Y. S., H. P. Gerber, N. Ferrara, C. Gu and D. J. Anderson (2005). "Peripheral nerve-derived VEGF promotes arterial differentiation via neuropilin 1-mediated positive feedback." Development **132**(5): 941-952.

Murga, M., O. Fernandez-Capetillo and G. Tosato (2005). "Neuropilin-1 regulates attachment in human endothelial cells independently of vascular endothelial growth factor receptor-2." Blood **105**(5): 1992-9.

Murry, C. E., M. H. Soonpaa, H. Reinecke, H. Nakajima, H. O. Nakajima, M. Rubart, K. B. Pasumarthi, J. I. Virag, S. H. Bartelmez, V. Poppa, G. Bradford, J. D. Dowell, D. A. Williams and L. J. Field (2004). "Haematopoietic stem cells do not transdifferentiate into cardiac myocytes in myocardial infarcts." Nature **428**(6983): 664-8.

Nakamura, F., M. Tanaka, T. Takahashi, R. G. Kalb and S. M. Strittmatter (1998). "Neuropilin-1 extracellular domains mediate semaphorin D/III-induced growth cone collapse." Neuron **21**(5): 1093-100.

Nakamura, H. (1988). "Electron microscopic study of the prenatal development of the thoracic aorta in the rat." Am J Anat **181**(4): 406-18.

Nasarre, P., B. Constantin, L. Rouhaud, T. Harnois, G. Raymond, H. A. Drabkin, N. Bourmeyster and J. Roche (2003). "Semaphorin SEMA3F and VEGF have opposing effects on cell attachment and spreading." Neoplasia **5**(1): 83-92.

Nicosia, R. F. and S. Villaschi (1995). "Rat aortic smooth muscle cells become pericytes during angiogenesis in vitro." Lab Invest **73**(5): 658-66.

Nygren, J. M., S. Jovinge, M. Breitbach, P. Sawen, W. Roll, J. Hescheler, J. Taneera, B. K. Fleischmann and S. E. Jacobsen (2004). "Bone marrow-derived hematopoietic cells generate cardiomyocytes at a low frequency through cell fusion, but not transdifferentiation." Nat Med **10**(5): 494-501.

Oinuma, I., Y. Ishikawa, H. Katoh and M. Negishi (2004). "The Semaphorin 4D receptor Plexin-B1 is a GTPase activating protein for R-Ras." Science **305**(5685): 862-5.

Oosthuyse, B., L. Moons, E. Storkebaum, H. Beck, D. Nuyens, K. Brusselmans, J. Van Dorpe, P. Hellings, M. Gorselink, S. Heymans, G. Theilmeier, M. Dewerchin, V. Laudenbach, P. Vermylen, H. Raat, T. Acker, V. Vleminckx, L. Van Den Bosch, N. Cashman, H. Fujisawa, M. R. Drost, R. Sciot, F. Bruyninckx, D. J. Hicklin, C. Ince, P. Gressens, F. Lupu, K. H. Plate, W. Robberecht, J. M. Herbert, D. Collen and P. Carmeliet (2001). "Deletion of the hypoxia-response element in the vascular endothelial growth factor promoter causes motor neuron degeneration." Nat Genet **28**(2): 131-8.

Orlidge, A. and P. A. D'Amore (1987). "Inhibition of capillary endothelial cell growth by pericytes and smooth muscle cells." J Cell Biol **105**(3): 1455-62.
Peters, A. M., J. Brown, G. G. Hartnell, M. J. Myers, C. Haskell and J. P. Lavender (1987). "Non-invasive measurement of renal blood flow with 99mTc DTPA: comparison with radiolabelled microspheres." Cardiovasc Res **21**(11): 830-4.
Petersen, B. E., W. C. Bowen, K. D. Patrene, W. M. Mars, A. K. Sullivan, N. Murase, S. S. Boggs, J. S. Greenberger and J. P. Goff (1999). "Bone marrow as a potential source of hepatic oval cells." Science **284**(5417): 1168-70.
Pipp, F., M. Heil, K. Issbrucker, T. Ziegelhoeffer, S. Martin, J. van den Heuvel, H. Weich, B. Fernandez, G. Golomb, P. Carmeliet, W. Schaper and M. Clauss (2003). "VEGFR-1-selective VEGF homologue PlGF is arteriogenic: evidence for a monocyte-mediated mechanism." Circ Res **92**(4): 378-85.
Pittenger, M. F. and B. J. Martin (2004). "Mesenchymal stem cells and their potential as cardiac therapeutics." Circ Res **95**(1): 9-20.
Post, M. and J. Waltenberger (2005). "Modulation of growth factor action in the cardiovascular system." Cardiovasc Res **65**(3): 547-9.
Post, M. J., R. Laham, F. W. Sellke and M. Simons (2001). "Therapeutic angiogenesis in cardiology using protein formulations." Cardiovasc Res **49**(3): 522-31.
Rabbany, S. Y., B. Heissig, K. Hattori and S. Rafii (2003). "Molecular pathways regulating mobilization of marrow-derived stem cells for tissue revascularization." Trends Mol Med **9**(3): 109-17.
Rabinowitz, J. E., F. Rolling, C. Li, H. Conrath, W. Xiao, X. Xiao and R. J. Samulski (2002). "Cross-packaging of a single adeno-associated virus (AAV) type 2 vector genome into multiple AAV serotypes enables transduction with broad specificity." J Virol **76**(2): 791-801.
Rajagopalan, S., E. Mohler, 3rd, R. J. Lederman, J. Saucedo, F. O. Mendelsohn, J. Olin, J. Blebea, C. Goldman, J. D. Trachtenberg, M. Pressler, H. Rasmussen, B. H. Annex and A. T. Hirsch (2003). "Regional Angiogenesis with Vascular Endothelial Growth Factor (VEGF) in peripheral arterial disease: Design of the RAVE trial." Am Heart J **145**(6): 1114-8.
Rajagopalan, S., E. R. Mohler, 3rd, R. J. Lederman, F. O. Mendelsohn, J. F. Saucedo, C. K. Goldman, J. Blebea, J. Macko, P. D. Kessler, H. S. Rasmussen and B. H. Annex (2003). "Regional angiogenesis with vascular endothelial growth factor in peripheral arterial disease: a phase II randomized, double-blind, controlled study of adenoviral delivery of vascular endothelial growth factor 121 in patients with disabling intermittent claudication." Circulation **108**(16): 1933-8.
Rajantie, I., M. Ilmonen, A. Alminaite, U. Ozerdem, K. Alitalo and P. Salven (2004). "Adult bone marrow-derived cells recruited during angiogenesis comprise precursors for periendothelial vascular mural cells." Blood **104**(7): 2084-6.
Ramirez Correa, G. A., S. Zacchigna, N. Arsic, L. Zentilin, A. Salvi, G. Sinagra and M. Giacca (2004). "Potent inhibition of arterial intimal hyperplasia by TIMP1 gene transfer using AAV vectors." Mol Ther **9**(6): 876-84.
Raper, J. A. (2000). "Semaphorins and their receptors in vertebrates and invertebrates." Curr Opin Neurobiol **10**(1): 88-94.
Rasmussen, H. S., C. S. Rasmussen and J. Macko (2002). "VEGF gene therapy for coronary artery disease and peripheral vascular disease." Cardiovasc Radiat Med **3**(2): 114-7.
Sato, K., R. J. Laham, J. D. Pearlman, D. Novicki, F. W. Sellke, M. Simons and M. J. Post (2000). "Efficacy of intracoronary versus intravenous FGF-2 in a pig model of chronic myocardial ischemia." Ann Thorac Surg **70**(6): 2113-8.

Schachinger, V., B. Assmus, M. B. Britten, J. Honold, R. Lehmann, C. Teupe, N. D. Abolmaali, T. J. Vogl, W. K. Hofmann, H. Martin, S. Dimmeler and A. M. Zeiher (2004). "Transplantation of progenitor cells and regeneration enhancement in acute myocardial infarction: final one-year results of the TOPCARE-AMI Trial." J Am Coll Cardiol **44**(8): 1690-9.

Schaper, W. (2000). "Quo vadis collateral blood flow? A commentary on a highly cited paper." Cardiovasc Res **45**(1): 220-3.

Schuch, G., J. V. Heymach, M. Nomi, M. Machluf, J. Force, A. Atala, J. P. Eder, Jr., J. Folkman and S. Soker (2003). "Endostatin inhibits the vascular endothelial growth factor-induced mobilization of endothelial progenitor cells." Cancer Res **63**(23): 8345-50.

Schwarz, E. R., M. T. Speakman, M. Patterson, S. S. Hale, J. M. Isner, L. H. Kedes and R. A. Kloner (2000). "Evaluation of the effects of intramyocardial injection of DNA expressing vascular endothelial growth factor (VEGF) in a myocardial infarction model in the rat--angiogenesis and angioma formation." J Am Coll Cardiol **35**(5): 1323-30.

Seetharam, L., N. Gotoh, Y. Maru, G. Neufeld, S. Yamaguchi and M. Shibuya (1995). "A unique signal transduction from FLT tyrosine kinase, a receptor for vascular endothelial growth factor VEGF." Oncogene **10**(1): 135-47.

Sekido, Y., S. Bader, F. Latif, J. Y. Chen, F. M. Duh, M. H. Wei, J. P. Albanesi, C. C. Lee, M. I. Lerman and J. D. Minna (1996). "Human semaphorins A(V) and IV reside in the 3p21.3 small cell lung cancer deletion region and demonstrate distinct expression patterns." Proc Natl Acad Sci U S A **93**(9): 4120-5.

Senger, D. R., S. J. Galli, A. M. Dvorak, C. A. Perruzzi, V. S. Harvey and H. F. Dvorak (1983). "Tumor cells secrete a vascular permeability factor that promotes accumulation of ascites fluid." Science **219**(4587): 983-5.

Serini, G., D. Valdembri, S. Zanivan, G. Morterra, C. Burkhardt, F. Caccavari, L. Zammataro, L. Primo, L. Tamagnone, M. Logan, M. Tessier-Lavigne, M. Taniguchi, A. W. Puschel and F. Bussolino (2003). "Class 3 semaphorins control vascular morphogenesis by inhibiting integrin function." Nature **424**(6947): 391-7.

Shalaby, F., J. Rossant, T. P. Yamaguchi, M. Gertsenstein, X. F. Wu, M. L. Breitman and A. C. Schuh (1995). "Failure of blood-island formation and vasculogenesis in Flk-1-deficient mice." Nature **376**(6535): 62-6.

Shen, H., M. Clauss, J. Ryan, A. M. Schmidt, P. Tijburg, L. Borden, D. Connolly, D. Stern and J. Kao (1993). "Characterization of vascular permeability factor/vascular endothelial growth factor receptors on mononuclear phagocytes." Blood **81**(10): 2767-73.

Shi, Q., S. Rafii, M. H. Wu, E. S. Wijelath, C. Yu, A. Ishida, Y. Fujita, S. Kothari, R. Mohle, L. R. Sauvage, M. A. Moore, R. F. Storb and W. P. Hammond (1998). "Evidence for circulating bone marrow-derived endothelial cells." Blood **92**(2): 362-7.

Shima, D. T. and C. Mailhos (2000). "Vascular developmental biology: getting nervous." Curr Opin Genet Dev **10**(5): 536-42.

Shoji, W., S. Isogai, M. Sato-Maeda, M. Obinata and J. Y. Kuwada (2003). "Semaphorin3a1 regulates angioblast migration and vascular development in zebrafish embryos." Development **130**(14): 3227-36.

Silvestre, J. S., Z. Mallat, R. Tamarat, M. Duriez, A. Tedgui and B. I. Levy (2001). "Regulation of matrix metalloproteinase activity in ischemic tissue by interleukin-10: role in ischemia-induced angiogenesis." Circ Res **89**(3): 259-64.

Simons, M., B. H. Annex, R. J. Laham, N. Kleiman, T. Henry, H. Dauerman, J. E. Udelson, E. V. Gervino, M. Pike, M. J. Whitehouse, T. Moon and N. A. Chronos (2002). "Pharmacological treatment of coronary artery disease with recombinant fibroblast growth factor-2: double-blind, randomized, controlled clinical trial." Circulation **105**(7): 788-93.

Soker, S., H. Fidder, G. Neufeld and M. Klagsbrun (1996). "Characterization of novel vascular endothelial growth factor (VEGF) receptors on tumor cells that bind VEGF165 via its exon 7-encoded domain." J Biol Chem **271**(10): 5761-7.

Soker, S., S. Takashima, H. Q. Miao, G. Neufeld and M. Klagsbrun (1998). "Neuropilin-1 is expressed by endothelial and tumor cells as an isoform-specific receptor for vascular endothelial growth factor." Cell **92**(6): 735-45.

Song, H., G. Ming, Z. He, M. Lehmann, L. McKerracher, M. Tessier-Lavigne and M. Poo (1998). "Conversion of neuronal growth cone responses from repulsion to attraction by cyclic nucleotides." Science **281**(5382): 1515-8.

Springer, M. L., A. S. Chen, P. E. Kraft, M. Bednarski and H. M. Blau (1998). "VEGF gene delivery to muscle: potential role for vasculogenesis in adults." Mol Cell **2**(5): 549-58.

Springer, M. L., T. K. Ip and H. M. Blau (2000). "Angiogenesis monitored by perfusion with a space-filling microbead suspension." Mol Ther **1**(1): 82-7.

Springer, M. L., C. R. Ozawa, A. Banfi, P. E. Kraft, T. K. Ip, T. R. Brazelton and H. M. Blau (2003). "Localized arteriole formation directly adjacent to the site of VEGF-induced angiogenesis in muscle." Mol Ther **7**(4): 441-9.

Stabile, E., M. S. Burnett, C. Watkins, T. Kinnaird, A. Bachis, A. la Sala, J. M. Miller, M. Shou, S. E. Epstein and S. Fuchs (2003). "Impaired arteriogenic response to acute hindlimb ischemia in CD4-knockout mice." Circulation **108**(2): 205-10.

Stalmans, I., Y. S. Ng, R. Rohan, M. Fruttiger, A. Bouche, A. Yuce, H. Fujisawa, B. Hermans, M. Shani, S. Jansen, D. Hicklin, D. J. Anderson, T. Gardiner, H. P. Hammes, L. Moons, M. Dewerchin, D. Collen, P. Carmeliet and P. A. D'Amore (2002). "Arteriolar and venular patterning in retinas of mice selectively expressing VEGF isoforms." J Clin Invest **109**(3): 327-36.

Storkebaum, E. and P. Carmeliet (2004). "VEGF: a critical player in neurodegeneration." J Clin Invest **113**(1): 14-8.

Street, J., M. Bao, L. deGuzman, S. Bunting, F. V. Peale, Jr., N. Ferrara, H. Steinmetz, J. Hoeffel, J. L. Cleland, A. Daugherty, N. van Bruggen, H. P. Redmond, R. A. Carano and E. H. Filvaroff (2002). "Vascular endothelial growth factor stimulates bone repair by promoting angiogenesis and bone turnover." Proc Natl Acad Sci U S A **99**(15): 9656-61.

Sunderkotter, C., M. Goebeler, K. Schulze-Osthoff, R. Bhardwaj and C. Sorg (1991). "Macrophage-derived angiogenesis factors." Pharmacol Ther **51**(2): 195-216.

Suri, C., P. F. Jones, S. Patan, S. Bartunkova, P. C. Maisonpierre, S. Davis, T. N. Sato and G. D. Yancopoulos (1996). "Requisite role of angiopoietin-1, a ligand for the TIE2 receptor, during embryonic angiogenesis." Cell **87**(7): 1171-80.

Suri, C., J. McClain, G. Thurston, D. M. McDonald, H. Zhou, E. H. Oldmixon, T. N. Sato and G. D. Yancopoulos (1998). "Increased vascularization in mice overexpressing angiopoietin-1." Science **282**(5388): 468-71.

Takahashi, T., A. Fournier, F. Nakamura, L. H. Wang, Y. Murakami, R. G. Kalb, H. Fujisawa and S. M. Strittmatter (1999). "Plexin-neuropilin-1 complexes form functional semaphorin-3A receptors." Cell **99**(1): 59-69.

Takahashi, T., F. Nakamura, Z. Jin, R. G. Kalb and S. M. Strittmatter (1998). "Semaphorins A and E act as antagonists of neuropilin-1 and agonists of neuropilin-2 receptors." Nat Neurosci **1**(6): 487-93.

Takeshita, S., L. Q. Pu, L. A. Stein, A. D. Sniderman, S. Bunting, N. Ferrara, J. M. Isner and J. F. Symes (1994). "Intramuscular administration of vascular endothelial growth factor induces dose-dependent collateral artery augmentation in a rabbit model of chronic limb ischemia." Circulation **90**(5 Pt 2): II228-34.

Takeshita, S., L. P. Zheng, E. Brogi, M. Kearney, L. Q. Pu, S. Bunting, N. Ferrara, J. F. Symes and J. M. Isner (1994). "Therapeutic angiogenesis. A single intraarterial bolus of vascular endothelial growth factor augments revascularization in a rabbit ischemic hind limb model." J Clin Invest **93**(2): 662-70.

Tamagnone, L., S. Artigiani, H. Chen, Z. He, G. I. Ming, H. Song, A. Chedotal, M. L. Winberg, C. S. Goodman, M. Poo, M. Tessier-Lavigne and P. M. Comoglio (1999). "Plexins are a large family of receptors for transmembrane, secreted, and GPI-anchored semaphorins in vertebrates." Cell **99**(1): 71-80.

Taniguchi, M., S. Yuasa, H. Fujisawa, I. Naruse, S. Saga, M. Mishina and T. Yagi (1997). "Disruption of semaphorin III/D gene causes severe abnormality in peripheral nerve projection." Neuron **19**(3): 519-30.

Tessier-Lavigne, M. and C. S. Goodman (1996). "The molecular biology of axon guidance." Science **274**(5290): 1123-33.

Thurston, G., C. Suri, K. Smith, J. McClain, T. N. Sato, G. D. Yancopoulos and D. M. McDonald (1999). "Leakage-resistant blood vessels in mice transgenically overexpressing angiopoietin-1." Science **286**(5449): 2511-4.

Tian, S., A. J. Hayes, L. J. Metheny-Barlow and L. Y. Li (2002). "Stabilization of breast cancer xenograft tumour neovasculature by angiopoietin-1." Br J Cancer **86**(4): 645-51.

Todorovic, V., S. Giadrossi, C. Pelizon, R. Mendoza-Maldonado, H. Masai and M. Giacca (2005). "Human origins of DNA replication selected from a library of nascent DNA." Mol Cell **19**(4): 567-75.

Tomizawa, Y., Y. Sekido, M. Kondo, B. Gao, J. Yokota, J. Roche, H. Drabkin, M. I. Lerman, A. F. Gazdar and J. D. Minna (2001). "Inhibition of lung cancer cell growth and induction of apoptosis after reexpression of 3p21.3 candidate tumor suppressor gene SEMA3B." Proc Natl Acad Sci U S A **98**(24): 13954-9.

Tuder, R. M., B. E. Flook and N. F. Voelkel (1995). "Increased gene expression for VEGF and the VEGF receptors KDR/Flk and Flt in lungs exposed to acute or to chronic hypoxia. Modulation of gene expression by nitric oxide." J Clin Invest **95**(4): 1798-807.

Visconti, R. P., C. D. Richardson and T. N. Sato (2002). "Orchestration of angiogenesis and arteriovenous contribution by angiopoietins and vascular endothelial growth factor (VEGF)." Proc Natl Acad Sci U S A **99**(12): 8219-24.

Waeckel, L., Z. Mallat, S. Potteaux, C. Combadiere, M. Clergue, M. Duriez, L. Bao, C. Gerard, B. J. Rollins, A. Tedgui, B. I. Levy and J. S. Silvestre (2005). "Impairment in postischemic neovascularization in mice lacking the CXC chemokine receptor 3." Circ Res **96**(5): 576-82.

Waltenberger, J., L. Claesson-Welsh, A. Siegbahn, M. Shibuya and C. H. Heldin (1994). "Different signal transduction properties of KDR and Flt1, two receptors for vascular endothelial growth factor." J Biol Chem **269**(43): 26988-95.

Wang, C., C. Jiao, H. D. Hanlon, W. Zheng, R. J. Tomanek and G. C. Schatteman (2004). "Mechanical, cellular, and molecular factors interact to modulate circulating endothelial cell progenitors." Am J Physiol Heart Circ Physiol **286**(5): H1985-93.

Wang, H. and J. A. Keiser (1998). "Vascular endothelial growth factor upregulates the expression of matrix metalloproteinases in vascular smooth muscle cells: role of flt-1." Circ Res **83**(8): 832-40.

Wang, H. U., Z. F. Chen and D. J. Anderson (1998). "Molecular distinction and angiogenic interaction between embryonic arteries and veins revealed by ephrin-B2 and its receptor Eph-B4." Cell **93**(5): 741-53.

Wang, Z., T. Zhu, C. Qiao, L. Zhou, B. Wang, J. Zhang, C. Chen, J. Li and X. Xiao (2005). "Adeno-associated virus serotype 8 efficiently delivers genes to muscle and heart." Nat Biotechnol **23**(3): 321-8.

Willett, C. G., Y. Boucher, E. di Tomaso, D. G. Duda, L. L. Munn, R. T. Tong, D. C. Chung, D. V. Sahani, S. P. Kalva, S. V. Kozin, M. Mino, K. S. Cohen, D. T. Scadden, A. C. Hartford, A. J. Fischman, J. W. Clark, D. P. Ryan, A. X. Zhu, L. S. Blaszkowsky, H. X. Chen, P. C. Shellito, G. Y. Lauwers and R. K. Jain (2004). "Direct evidence that the VEGF-specific antibody bevacizumab has antivascular effects in human rectal cancer." Nat Med **10**(2): 145-7.

Winberg, M. L., J. N. Noordermeer, L. Tamagnone, P. M. Comoglio, M. K. Spriggs, M. Tessier-Lavigne and C. S. Goodman (1998). "Plexin A is a neuronal semaphorin receptor that controls axon guidance." Cell **95**(7): 903-16.

Wollert, K. C., G. P. Meyer, J. Lotz, S. Ringes-Lichtenberg, P. Lippolt, C. Breidenbach, S. Fichtner, T. Korte, B. Hornig, D. Messinger, L. Arseniev, B. Hertenstein, A. Ganser and H. Drexler (2004). "Intracoronary autologous bone-marrow cell transfer after myocardial infarction: the BOOST randomised controlled clinical trial." Lancet **364**(9429): 141-8.

Wong, A. L., Z. A. Haroon, S. Werner, M. W. Dewhirst, C. S. Greenberg and K. G. Peters (1997). "Tie2 expression and phosphorylation in angiogenic and quiescent adult tissues." Circ Res **81**(4): 567-74.

Wu, J. C., I. Y. Chen, Y. Wang, J. R. Tseng, A. Chhabra, M. Salek, J. J. Min, M. C. Fishbein, R. Crystal and S. S. Gambhir (2004). "Molecular imaging of the kinetics of vascular endothelial growth factor gene expression in ischemic myocardium." Circulation **110**(6): 685-91.

Xiao, X., J. Li and R. J. Samulski (1996). "Efficient long-term gene transfer into muscle tissue of immunocompetent mice by adeno-associated virus vector." J Virol **70**(11): 8098-108.

Yamada, T., R. Endo, M. Gotoh and S. Hirohashi (1997). "Identification of semaphorin E as a non-MDR drug resistance gene of human cancers." Proc Natl Acad Sci U S A **94**(26): 14713-8.

Yamada, Y., N. Takakura, H. Yasue, H. Ogawa, H. Fujisawa and T. Suda (2001). "Exogenous clustered neuropilin 1 enhances vasculogenesis and angiogenesis." Blood **97**(6): 1671-8.

Yang, Y., S. E. Haecker, Q. Su and J. M. Wilson (1996). "Immunology of gene therapy with adenoviral vectors in mouse skeletal muscle." Hum Mol Genet **5**(11): 1703-12.

Zentilin, L., A. Marcello and M. Giacca (2001). "Involvement of cellular double-stranded DNA break binding proteins in processing of the recombinant adeno-associated virus genome." J Virol **75**(24): 12279-87.

Zhang, Y. W. and G. F. Vande Woude (2003). "HGF/SF-met signaling in the control of branching morphogenesis and invasion." J Cell Biochem **88**(2): 408-17.

Ziegelhoeffer, T., B. Fernandez, S. Kostin, M. Heil, R. Voswinckel, A. Helisch and W. Schaper (2004). "Bone marrow-derived cells do not incorporate into the adult growing vasculature." Circ Res **94**(2): 230-8.

# 7. APPENDIX

In this last section, I have collected all the studies, already published or currently submitted for publication, in which I have been personally involved during my PhD course. Overall, they are mainly focused on gene therapy approaches using AAV vectors, thus providing evidence of the different possible applications of this class of vectors in the cardiovascular field, but also in the study of tumor-associated angiogenesis.

The first two papers represent the starting point for all the subsequent work described in this thesis (Arsic, Zentilin et al. 2003); (Zentilin et al., submitted for publication). An additional application of AAV-mediated therapeutic angiogenesis has been developed in the plastic surgery field, with the particular aim of improving skin flap survival (Zacchigna, Papa et al. 2005).

The fourth and fifth papers address the direct role of VEGF165 on muscle cells, either skeletal muscle fibers or cardiomyocytes, suggesting a key role of this factors in protecting the muscle from apoptosis, and in promoting its regeneration after different kinds of damage (Arsic, Zacchigna et al. 2004); (Ferrarini et al., submitted for publication).

Two additional papers are focused on the use of AAV vectors in a rat model of carotid restenosis. In particular, they assess the therapeutic value of two molecules, the tissue inhibitor of metalloproteinases-1 (Timp-1) and Pentraxin 3, a specific inhibitor of FGF-2 (Ramirez Correa, Zacchigna et al. 2004; Camozzi, Zacchigna et al. 2005).

Finally, the last two studies investigate some aspects of the tumor-associated angiogenesis (Secchiero, Gonelli et al. 2004; Zacchigna, Zentilin et al. 2004).

**References:**


Arsic, N., S. Zacchigna, L. Zentilin, G. Ramirez-Correa, L. Pattarini, A. Salvi, G. Sinagra and M. Giacca (2004). "Vascular endothelial growth factor stimulates skeletal muscle regeneration in vivo." Mol Ther 10(5): 844-54.

Arsic, N., L. Zentilin, S. Zacchigna, D. Santoro, G. Stanta, A. Salvi, G. Sinagra and M. Giacca (2003). "Induction of functional neovascularization by combined VEGF and angiopoietin-1 gene transfer using AAV vectors." Mol Ther 7(4): 450-9.

Camozzi, M., S. Zacchigna, M. Rusnati, D. Coltrini, G. Ramirez-Correa, B. Bottazzi, A. Mantovani, M. Giacca and M. Presta (2005). "Pentraxin 3 inhibits fibroblast growth factor 2-dependent activation of smooth muscle cells in vitro and neointima formation in vivo." Arterioscler Thromb Vasc Biol 25(9): 1837-42.

Ramirez Correa, G. A., S. Zacchigna, N. Arsic, L. Zentilin, A. Salvi, G. Sinagra and M. Giacca (2004). "Potent inhibition of arterial intimal hyperplasia by TIMP1 gene transfer using AAV vectors." Mol Ther 9(6): 876-84.

Secchiero, P., A. Gonelli, E. Carnevale, F. Corallini, C. Rizzardi, S. Zacchigna, M. Melato and G. Zauli (2004). "Evidence for a proangiogenic activity of TNF-related apoptosis-inducing ligand." Neoplasia 6(4): 364-73.

Zacchigna, S., G. Papa, A. Antonini, F. Novati, S. Moimas, A. Carrer, N. Arsic, L. Zentilin, V. Visintini, M. Pascone and M. Giacca (2005). "Improved survival of ischemic cutaneous and musculocutaneous flaps after vascular endothelial growth factor gene transfer using adeno-associated virus vectors." Am J Pathol 167(4): 981-91.

Zacchigna, S., L. Zentilin, M. Morini, R. Dell'Eva, D. M. Noonan, A. Albini and M. Giacca (2004). "AAV-mediated gene transfer of tissue inhibitor of metalloproteinases-1 inhibits vascular tumor growth and angiogenesis in vivo." Cancer Gene Ther 11(1): 73-80.

doi:10.1016/S1525-0016(03)00034-0

# Induction of Functional Neovascularization by Combined VEGF and Angiopoietin-1 Gene Transfer Using AAV Vectors

Nikola Arsic,[1] Lorena Zentilin,[1] Serena Zacchigna,[1] Daniela Santoro,[1] Giorgio Stanta,[2] Alessandro Salvi,[3] Gianfranco Sinagra,[3] and Mauro Giacca[1,4,*]

[1]*Molecular Medicine Laboratory, International Centre for Genetic Engineering and Biotechnology (ICGEB), Trieste, Italy*
[2]*Istituto di Anatomia Patologica, University of Trieste, Italy*
[3]*Unita' di Cardiologia, Ospedale Maggiore, Trieste, Italy*
[4]*Scuola Normale Superiore and NEST/INFM, Pisa, Italy*

**To whom correspondence and reprint requests should be addressed. Head, Molecular Medicine Laboratory, ICGEB, Padriciano, 99, 34012 Trieste, Italy. Tel.: +39-040-3757.324. Fax: +39-040-226555. E-mail: giacca@icgeb.org.*

**Vectors based on the adeno-associated virus (AAV) deliver therapeutic genes to muscle and heart at high efficiency and maintain transgene expression for long periods of time. Here we report about the synergistic effect on blood vessel formation of AAV vectors expressing the 165 aa isoform of vascular endothelial growth factor (VEGF165), a powerful activator of endothelial cells, and of angiopoietin-1 (Ang-1), which is required for vessel maturation. High titer AAV-VEGF165 and AAV-Ang-1 vector preparations were injected either alone or in combination in the normoperfused tibialis anterior muscle of rats. Long term expression of VEGF165 determined massive cellular infiltration of the muscle tissues over time, with the formation of a large set of new vessels. Strikingly, some of the cells infiltrating the treated muscles were found positive for markers of activated endothelial precursors (VEGFR-2/KDR and Tie-2) and for c-kit, an antigen expressed by pluripotent bone marrow stem cells. Expression of VEGF165 eventually resulted in the formation of structured vessels surrounded by a layer of smooth muscle cells. Presence of these arteriolae correlated with significantly increased blood perfusion in the injected areas. Co-expression of VEGF165 with angiopoietin-1-which did not display angiogenic effect per se-remarkably reduced leakage of vessels produced by VEGF165 alone.**

**Key Words: adeno-associated vectors, angiogenesis, angiopoietin-1, gene therapy, muscle, stem cells, vascular endothelial growth factor**

## Introduction

Formation of new blood vessels in the adult (angiogenesis) occurs by sprouting from existing vessels, a process that requires proliferation, activation and migration of endothelial cells and remodeling of extracellular matrix. Subsequent maturation consists in structural organization of unstable vessels with the formation of a layer of smooth muscle cells surrounding the proliferated endothelium [1,2]. Members of the vascular endothelial growth factor (VEGF) family are powerful inducers of angiogenesis [3]. Transient VEGF-A expression in vivo results in potent angiogenic sprouting with the formation of immature and leaky vessels, associated with tissue swelling due to markedly increased vascular permeability [4,5]. One class of molecules required for later stages of angiogenesis, involving vessel remodeling, maturation and stabilization, consists of the angiopoietins and their receptors [6,7]. Studies in transgenic mice have indicated that overexpression of angiopoietin-1 mitigates leakiness of skin microvasculature resulting from VEGF expression [8]. Consistently, an adenoviral vector expressing angiopoietin-1 was shown to protect adult vasculature from leakiness, counteracting the permeabilization activity of VEGF and of inflammatory agents [9]. A distinct mechanism of blood vessel formation occurring during early embryonic development is vasculogenesis, a process involving the differentiation of angioblasts into blood islands that fuse to form the primitive vascular network [2]. Increasing evidence suggests that angioblast-like cell precursors derived from the bone marrow circulate in the adult vasculature and contribute to physiological and pathological neovascularization in the adult [10,11].



Molecular Therapy Vol. 7, No. 4, April 2003

1525-0016/03 $30.00

These circulating stem cell precursors are able to invade tissues and differentiate into several cell types after ischemic damage of the heart or of the skeletal muscle [12], and might constitute a reservoir for tissue and vessel regeneration of important therapeutic value. Very little is currently known about the actual molecules triggering recruitment, activation and differentiation of these cells. Induction of new blood vessel formation by gene transfer remains a very attractive clinical possibility for the treatment of ischemia in tissues not susceptible to conventional revascularization procedures. However, significant technical barriers remain in terms of safe and effective local gene delivery to the ischemic muscle and heart. In this context, viral vectors based on the adeno-associated virus (AAV) offer the unique possibility of obtaining high level and persistent gene expression of the encoded factors in skeletal muscle and heart, in the absence of immune or inflammatory reaction [13–15]. In addition, since cell transduction with AAV vectors occurs at high multiplicity of infection [16,17], this vector system also allows simultaneous expression of different factors in the same cell or tissue in vivo. Given the patent biological complexity of the process of new blood vessel formation, combined growth factor administration appears to be an important requisite in therapeutic terms.

In this work we exploit the potential of AAV gene transfer to the skeletal muscle to understand the long term biological effect of VEGF-A and angiopoietin-1 expression.

## Results

### Transduction of Rat Muscle using AAV-VEGF and AAV-Ang1

We constructed two AAV vectors expressing the coding regions of the 165 aa isoform of human VEGF-A (AAV-VEGF165) and of human angiopoietin-1 (AAV-Ang1) under the control of the constitutive cytomegalovirus (CMV) promoter (Figure 1A). Efficiency of transduction and expression of the transgenes using these vectors was initially demonstrated by infection of hamster CHO cells followed by immunocytochemistry using antibodies reacting with human VEGF-A and angiopoietin-1 (Figure 1B).

High titer AAV vector preparations were injected into the muscle tibialis anterior of the right leg of normoperfused Wistar rats. Each animal was also injected in the muscle tibialis anterior of its left leg with either AAV-LacZ or PBS.

Long-term expression of VEGF165 and angiopoietin-1 in muscle fibers was assessed by immunohistochemistry at 3 months after treatment. In both cases, muscle areas injected with these vectors showed a large number of fibers positive for expression of the respective factors (shown in Figure 1C for an animal injected with both vectors).

To quantitatively assess the extent of transduction of injected muscles, as well as the dissemination of AAV vectors to other body districts, a quantitative competitive PCR procedure was developed measuring the AAV-VEGF165 DNA copy number in comparison with an endogenous rat gene. Primer pairs were selected in the human VEGF165 cDNA and in the rat GAPDH gene (Figure 1D). For both targets, DNA competitors were obtained that were recognized by the same primer pairs and differed from the respective targets by a 20 bp deletion (for VEGF165) or a 20 bp insertion (for GAPDH; Figure 1E). Genomic DNA extracted from injected and mock-injected muscles, heart, lung and liver from two animals treated with AAV-VEGF165 were mixed with scalar amounts of competitors and submitted to competitive PCR amplification (an example of which is shown in Figure 1F). The results of quantification are shown in Figure 1G and are expressed as a ratio between VEGF165 and GAPDH copy numbers. In injected muscle areas, one AAV DNA molecule was found every 200 rat genomic DNA molecules. In mock-injected muscle, as well as in heart and lung, AAV DNA copy number was at least five orders of magnitude lower than that found in the injected muscle. In one animal, we found one AAV DNA molecule every $1 \times 10^6$ rat genomes in liver, while in the other one this amount was 10 times lower (Figure 1G). From these data, we conclude that AAV preparations locally injected in the skeletal muscle persist for long times in the sites of inoculation and have a minimal capacity to spread to other body districts.

### Biological Effects of Long Term VEGF165 and Angiopoietin-1 Expression

When histological sections were examined, striking findings were noticed in AAV-injected animals. Muscles that received VEGF165 either alone or in combination with angiopoietin-1 showed remarkably increased cellularity as compared to mock or LacZ-injected controls (Figure 2A). By immunohistochemistry, most of the infiltrating cells scored positive for expression of the proliferating cell nuclear antigen (PCNA), a marker associated with cellular proliferation (Figure 6).

To quantify the number of these cells, three independent investigators blinded for experimental procedures observed 50 different sections from 4 animals per group; the results are expressed in Figure 2B as number of cells per muscle fiber. As compared to LacZ-injected muscles, cellularity was increased of over 5 times in animals treated with VEGF165, either alone or in combination with angiopoietin-1. In contrast, treatment with angiopoietin-1 alone only had a modest apparent effect.

To understand whether increased cellularity of injected muscles was paralleled by neoangiogenesis, we performed immunohistochemistry with an antibody against CD31, a marker of endothelial cells. The number of CD31-positive cells was greatly increased in muscles transduced with AAV-VEGF165 (Figure 2C). We also quantified the

doi:10.1016/S1525-0016(03)00034-0

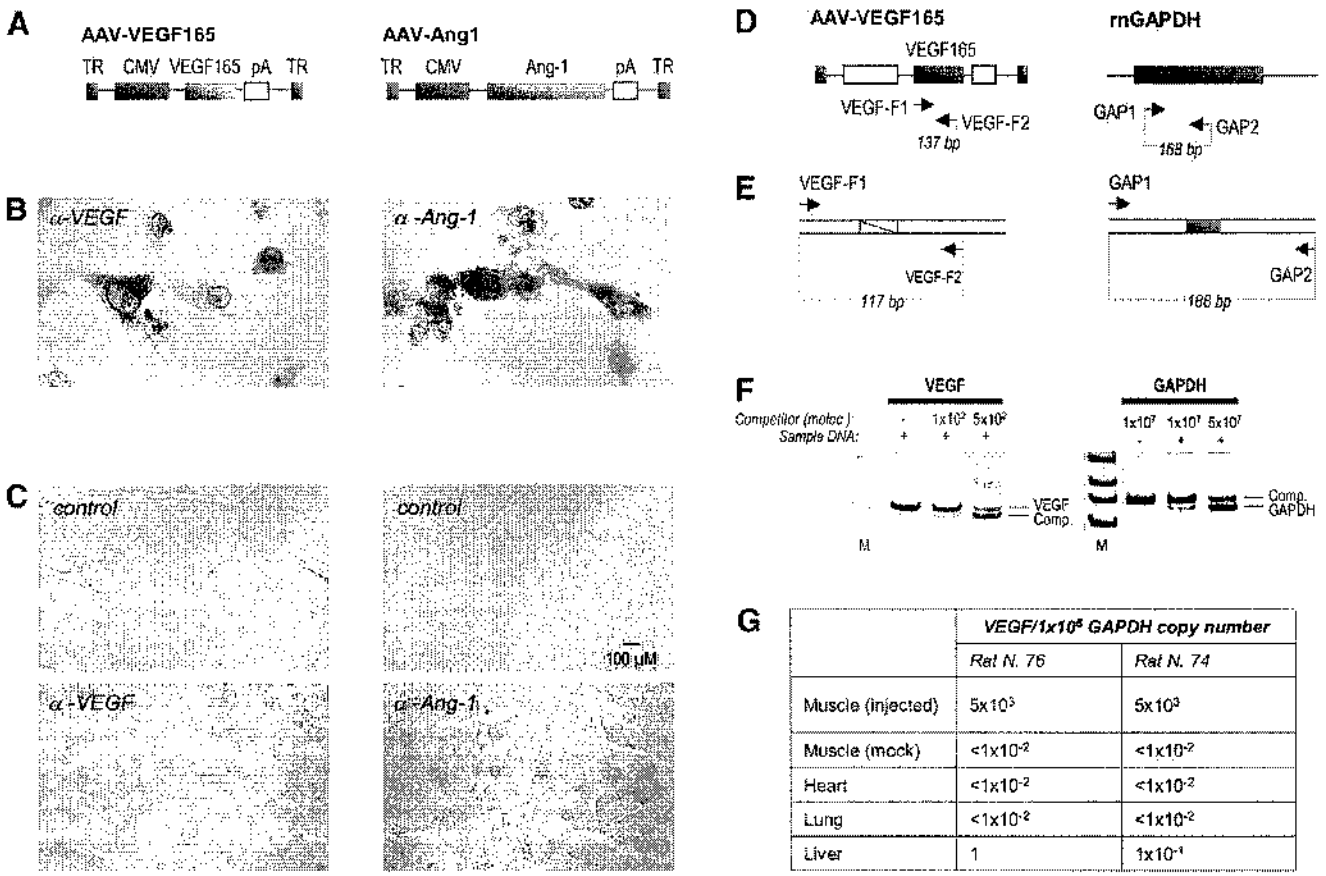


| | VEGF/1x10⁶ GAPDH copy number | |
|---|---|---|
| | *Rat N. 76* | *Rat N. 74* |
| Muscle (injected) | $5x10^{3}$ | $5x10^{3}$ |
| Muscle (mock) | $<1x10^{-2}$ | $<1x10^{-2}$ |
| Heart | $<1x10^{-2}$ | $<1x10^{-2}$ |
| Lung | $<1x10^{-2}$ | $<1x10^{-2}$ |
| Liver | 1 | $1x10^{-1}$ |

FIG. 1. Delivery of VEGF165 and angiopoietin-1 cDNAs to rat skeletal muscle using AAV vectors. A. Schematic representation of the AAV vectors used in this study. TR: terminal repeat sequences; CMV: cytomegalovirus immediate early promoter; pA: polyadenylation site B. Immunocytochemistry of CHO cells transduced with AAV-VEGF165 (left panel) and AAV-Ang1 (right panel). C. Immunostaining of muscle sections of mock treated rats (upper panels) and of rats treated with AAV-VEGF165 plus AAV-Ang1 at 3 months after injection (lower panels) using antibodies against VEGF-A (panels on the left side) and angiopoietin-1 (panels on the right side). Several muscle fibers in the injected areas show reactivity to the respective antibodies only in treated muscles. D. Primers for PCR amplification. Two primer pairs were selected in the AAV-VEGF165 construct (VEGF-F1 and VEGF-F2) and in the rat GAPDH gene (GAP1 and GAP2) amplifying 137 bp and 168 bp DNA fragments respectively. E. Schematic representation of DNA competitors for competitive PCR amplification of AAV-VEGF165 and rat genomic GAPDH DNAs. F. Example of competitive PCR amplification. Fixed amounts of sample DNA from different organs were mixed with scalar amounts of competitor DNA and PCR-amplified with the two primer pairs. After amplification, gels were stained with ethidium bromide and the competitor (Comp.), VEGF or GAPDH DNA bands were quantified. According to the principles of competitive PCR, the ratio between the amplification products in each reaction is linearly correlated with the input DNA amounts for the two species. M: molecular weight markers, molec.: DNA molecules. G. Results of VEGF165 DNA quantification in different organs. Two rats injected with AAV-VEGF165 were sacrificed 3 months after treatment and DNA extracted from the indicated organs. Results are expressed as ratios between VEGF165 and GAPDH DNA copy number.

number of capillaries in these sections-defined as small (5–10 μm diameter) vessels surrounded only by CD31-positive cells (shown by arrows in Figure 2C). The number of capillaries per muscle fiber was increased ~2 fold in samples treated with VEGF165 compared to controls and to muscles injected with angiopoietin-1 alone. No difference in the number of capillaries was observed in animals sacrificed at one month as compared to those sacrificed at three months post injection. However, an enlargement of the muscle area in which neovascularization was observed was clearly detectable in the latter group (not shown).

Increased formation of capillaries is an expected outcome of short term VEGF overexpression, given the very well known stimulating properties of VEGF on endothelial cell proliferation and migration [18]. In contrast, largely unexpected was the remarkable increase in larger and more mature vessels, surrounded by a thick layer of cells expressing smooth muscle α-actin (α-SMA), a marker of smooth muscle cells. These arteriolae with a diameter in the 20–120 μm range were ~8-fold more represented in AAV-VEGF expressing muscles, either alone or in combination with angiopoietin-1, as compared to AAV-LacZ or mock injected controls (Figure 3).

In our experiments we never observed formation of

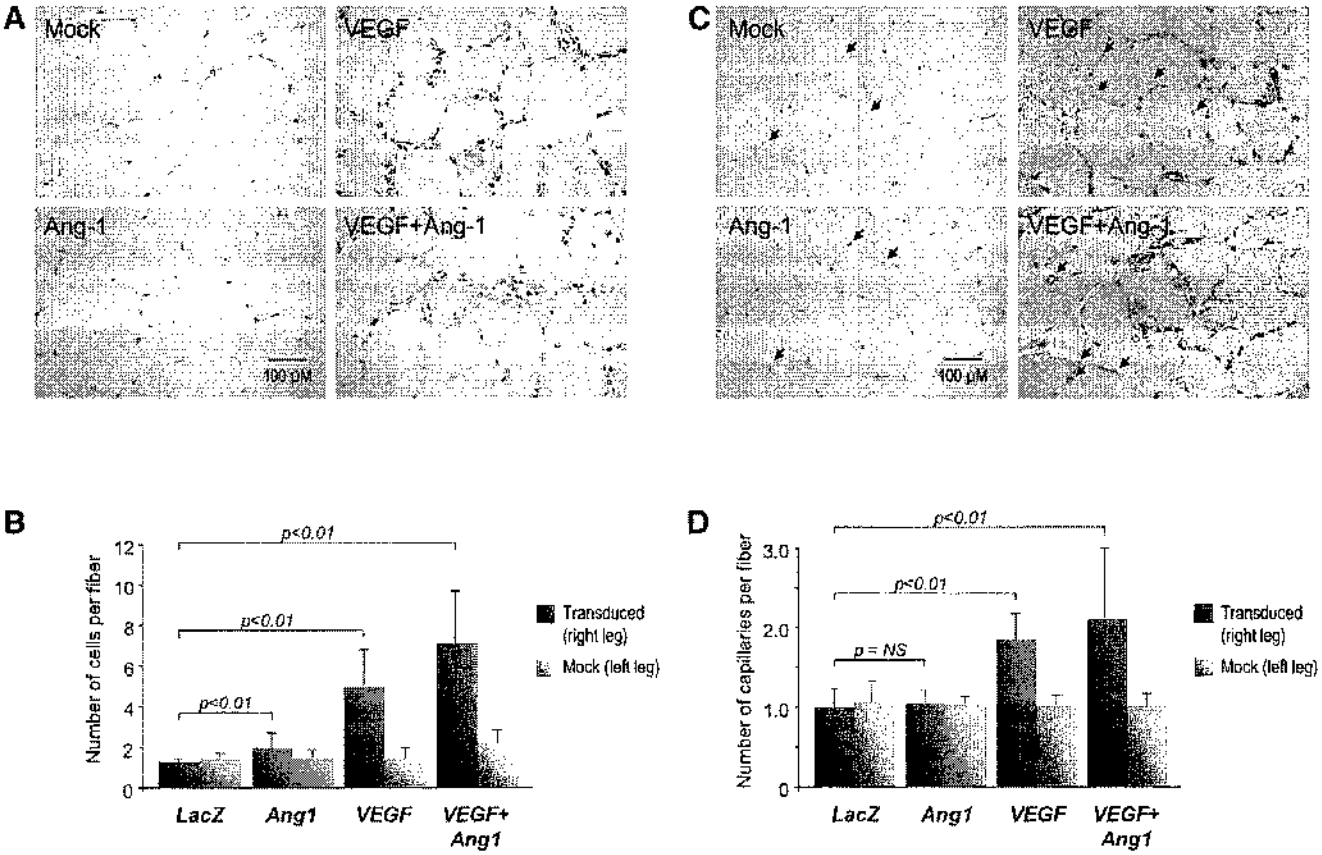


FIG. 2. Quantification of proliferating cells and capillaries in transduced muscles. A. Muscle sections injected with AAV-VEGF165, AAV-Ang1 or both at 3 months after treatment, stained with hematoxylin. B. Quantification of cells in treated muscles. For each animal, counts were obtained from both the leg injected with the angiogenic vector and the controlateral leg. Shown are means and standard deviations of counts, expressed as number of nuclei per muscle fiber. Values were analyzed using a two-tailed t test, considering unequal variance in groups and assuming statistical significance at $p < 0.01$. Large cellular infiltrations in the interstitial space (such as those shown in Figure 6) were not included in the counts. C. Immunostaining of muscle sections of animals treated with the different vector combinations, as indicated, at three months after injection using an antibody against the endothelial cell marker CD31. An increase in the number of cells positive to this antibody is visible in samples of animals injected with AAV-VEGF165. Arrows indicate capillaries, defined as 5–10 μm diameter vessels surrounded only by CD31-positive cells. D. Number of capillaries in injected muscles. Counts were obtained from both the leg injected with the angiogenic vector and the controlateral leg. Presentation of data and statistics are as in Panel 2B. NS: not significant.

hemangioma-like structures even after prolonged expression of VEGF165. However, in several histological sections of muscles expressing this factor we observed that PCNA-positive proliferating cells, several of which showed reactivity to α-SMA antibody, accumulated at the periphery of muscle fibers, with a tendency to invaginate into and invade them (Figure 4E and 4F). In addition, we also noticed a peculiar effect by which some muscle fibers were substituted by vascular lacunae filled of red blood cells (Figure 4A–D), as demonstrated by staining samples with 3,3′-diaminobenzidine (DAB), a chemical compound reacting with oxidized hemoglobin (Figure 4D).

### Functional Analysis of Vasculature in Transduced Muscles

To investigate whether the observed histological effects were paralleled by increased blood flow in the injected areas, muscle perfusion was analyzed by using fluorescent microspheres. The results obtained, which are expressed in Figure 5A as a ratio between treated and control muscles, indicate that perfusion of muscles expressing VEGF165 was significantly increased both in the presence or absence of angiopoietin-1. In contrast, transduction of angiopoietin-1 had no effect on perfusion.

The results so far described in terms of cell proliferation, increase in the number of CD31- and α-SMA-positive cells, formation of new blood vessels and perfusion indicate that overexpression of angiopoietin-1 had no apparent role in promoting and sustaining these processes. However, it is still debated whether VEGF alone might be sufficient to determine the development of a mature and functional vascular network, one of the major concerns being the well documented permeabilization

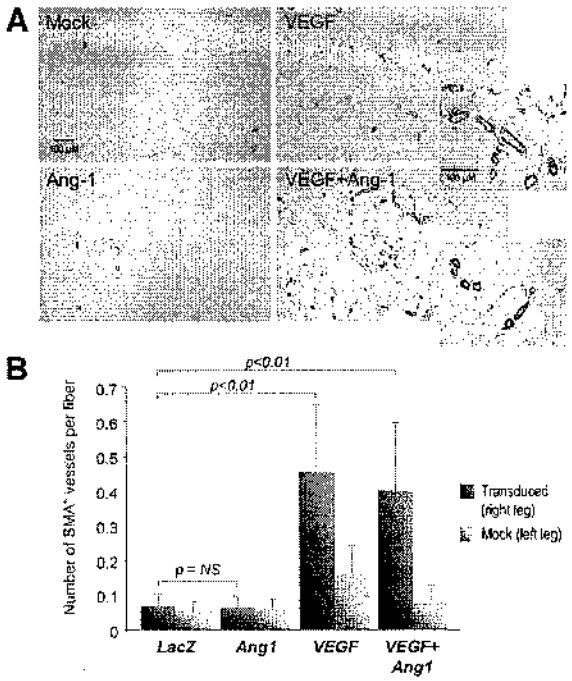


FIG. 3. Immunohistochemistry using an antibody against smooth muscle α-actin (α-SMA). A. Sections of muscles treated with AAV vectors expressing the factors indicated in the different panels were reacted to an antibody against smooth muscle α-actin, a marker of smooth muscle cells. Muscles treated with AAV-VEGF165 show a large number of newly formed vessels (enlarged in the insets) with the characteristics of arteriolae in the 20–120 μm diameter range. Shown are immunostainings from animals sacrificed at 3 months post vector injection. B. Quantification of α-SMA positive vessels. Presentation of data and statistics are as in Panel 2B.

effect exerted by this factor on the vascular wall [4]. In facts, when we analyzed vascular leakiness by injection of Evans blue in the femoral arteries supplying both control and transduced muscles (an adaptation of the Miles test), we found that vessels in muscles expressing VEGF alone were remarkably (~6 times) more leaky than controlateral controls (visually shown in Figure 5B and quantified by spectrophometric analysis of dye in Figure 5C). By contrast, leakiness of vessels produced by co-expression of VEGF with angiopoietin-1 was remarkably reduced and more similar to that of the normal muscle vasculature.

### Characterization of Cells Infiltrating Muscles Treated with VEGF165

As described above, a peculiar feature of muscle areas expressing VEGF165 was the presence of a large number of PCNA-positive, proliferating cells. In several instances, the presence of these cells was massive, especially in the interstitial area surrounding large vessels (Figure 6A).

To start understanding the source of these cells, we attempted their phenotypic characterization using immunohistochemistry with different antibodies. As already discussed above, several of the infiltrating cells were found positive for the endothelial-specific CD31 and the smooth muscle cell-specific α-SMA markers. Relatively few cells were found reactive to an antibody against the pan-leukocyte CD45 marker, thus also ruling out a major role of inflammation as a process of cellular recruitment. Interestingly, some infiltrating cells expressed two markers of the activated and proliferating endothelium, namely Tie-2, the receptor for angiopoietin-1 the expression of which is restricted to the vascular endothelial lineage, and VEGFR-2/KDR, the major receptor for VEGF-A. These antigens start to be expressed by a bone marrow derived cell population comprising the early hematopoietic/endothelial cell precursors [19]. Consistent with a possible derivation of these cells from a stem cell precursor is the observation that several of them were found positive for the c-kit/CD117 marker, an antigen that commonly defines pluripotent bone marrow stem cells [19].

## Discussion

Prolonged expression of the 165 aa form of VEGF-A in the normoperfused skeletal muscle had several important bi-

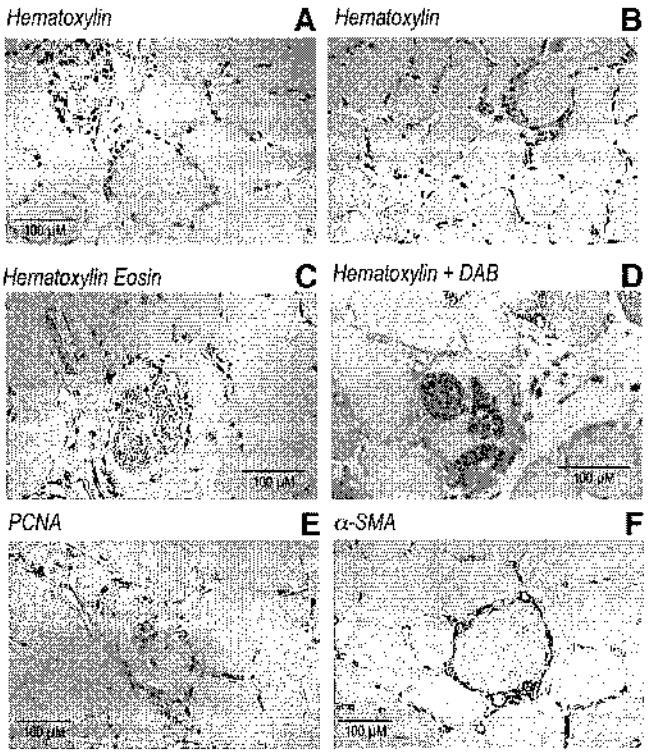


FIG. 4. Substitution of muscle fibers by vascular lacunae in muscles treated with AAV-VEGF165. A to F. Sections from treated muscles showing muscle fibers substituted with vascular lacunae at 3 months post vector injection. Sections were stained with hematoxylin (A and B), hematoxylin and eosin (C), hematoxylyin + 3,3′-diaminobenzidine (DAB) to reveal red blood cells (D), or immunostained with antibodies against PCNA (E) or α-SMA (F).

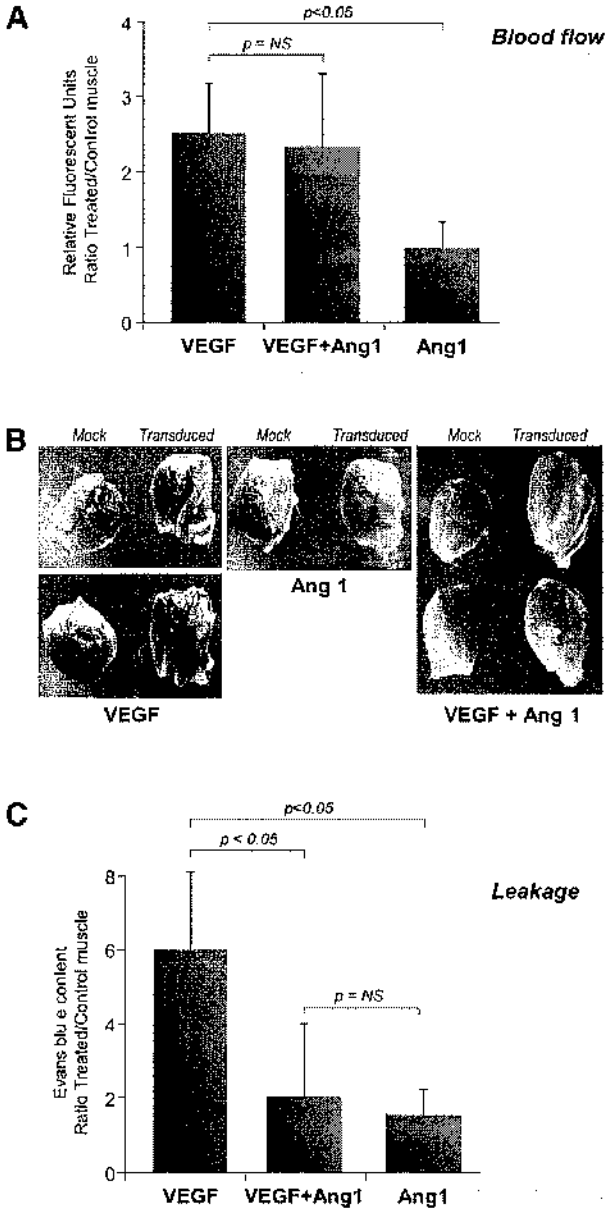


FIG. 5. Functional analysis of vasculature in treated and control muscles. A. Analysis of blood flow. Fluorescent microspheres injected in the abdominal aorta were recovered from isolated muscle tibialis anterior from both the right (treated) and left (mock) legs of each animal and quantified. Shown are mean and standard deviation of the ratios between the two measurements. Values were analyzed using a two-tailed t test, considering unequal variance in groups and assuming statistical significance at $p < 0.05$. Experiments were performed at 3 months after injection of AAV-VEGF165, AAV-Ang1 or both vectors as indicated. B and C. Miles assay for vascular leakage performed at 3 months after vector injection. Evans blue was injected in the femoral artery, and animals were sacrificed 30 minutes later. The muscle tibialis anterior was isolated from both the right (treated) and left (mock) legs of each animal. Panel B shows massive dye infiltration in muscles treated with AAV-VEGF165 alone. Panel C reports spectrophotometric quantification of the dye in muscle samples, expressed as a ratio between treated and mock-treated legs. Evans blue diffusion in muscles treated with VEGF165 is markedly reduced by co-expression of angiopoietin-1. Shown are means and standard deviations of 4 measurements. Statistical evaluation was performed as in Figure 5A.

ological consequences. The most striking phenotypic change we observed was the increase in the number of blood vessels present in the injected areas. This event was somehow expected as far as capillaries are concerned, given the very well known properties of VEGF on endothelial cell proliferation and migration [18] and according to studies that analyzed capillary formation after intramuscular injection of adenoviral vectors expressing VEGF [20,21] or of skeletal myoblasts engineered to secrete the factor [22,23]. In contrast, largely unexpected was the increase in larger vessels, surrounded by a layer of cells expressing α-smooth muscle actin, a marker of smooth muscle cells. The distribution of these arteriolae was irregular and massive close to the injection site and progressively more regular moving to the periphery of the injected area, suggesting a gradient effect correlated to VEGF dosage. The presence of these vessels demonstrates that prolonged angiogenic stimulation by VEGF not only determines activation, proliferation and migration of endothelial cells, but eventually turns out to trigger formation of larger blood vessels coated with α-SMA-positive cells. Besides the direct effect of VEGF itself on smooth muscle cells, vessel maturation is also most likely the consequence of the release of other cytokines from activated endothelial cells [2]. Experiments recently performed by implantation of myoblasts constitutively expressing VEGF-A also revealed formation of smooth muscle-coated vessels similar to arterioles directly adjacent to the implantation site, in perfect agreement with our results [24]. Finally, analogous findings have also been recently reported by studying the effect of long term VEGF overexpression in a transgenic mouse model [25].

While the size of the arteriolae formed after VEGF overexpression is too small to permit angiographic detection of the newly formed vascular network (not shown), they still determined an important increase in blood perfusion of the injected muscles, as detected by perfusion studies using fluorescent microspheres. In this respect, it is worth noticing that these studies most likely understimate the actual perfusion rate of the VEGF-expressing areas, since they were performed on the whole tibialis anterior muscle, in which injected areas represent less than 20% of the total muscle volume. Injection of skeletal myoblasts engineered to deliver VEGF to the skeletal muscle [23] and to the myocardium [26] promotes a potent angiogenic response but also leads to the formation of vascular tumors resembling hemangiomas. In over 100 animals (including rats, some of which shown in this study, and mice) injected with AAV-VEGF165 we never observed the formation of such tumors. These differences are most likely related to AAV gene transfer biology, in which the onset of growth factor expression is progressive [13] and the peak levels of produced factor are lower than with other vector systems, while expression persists for much longer periods of time. In contrast, we observed a previously unnoticed event consisting of the substitution

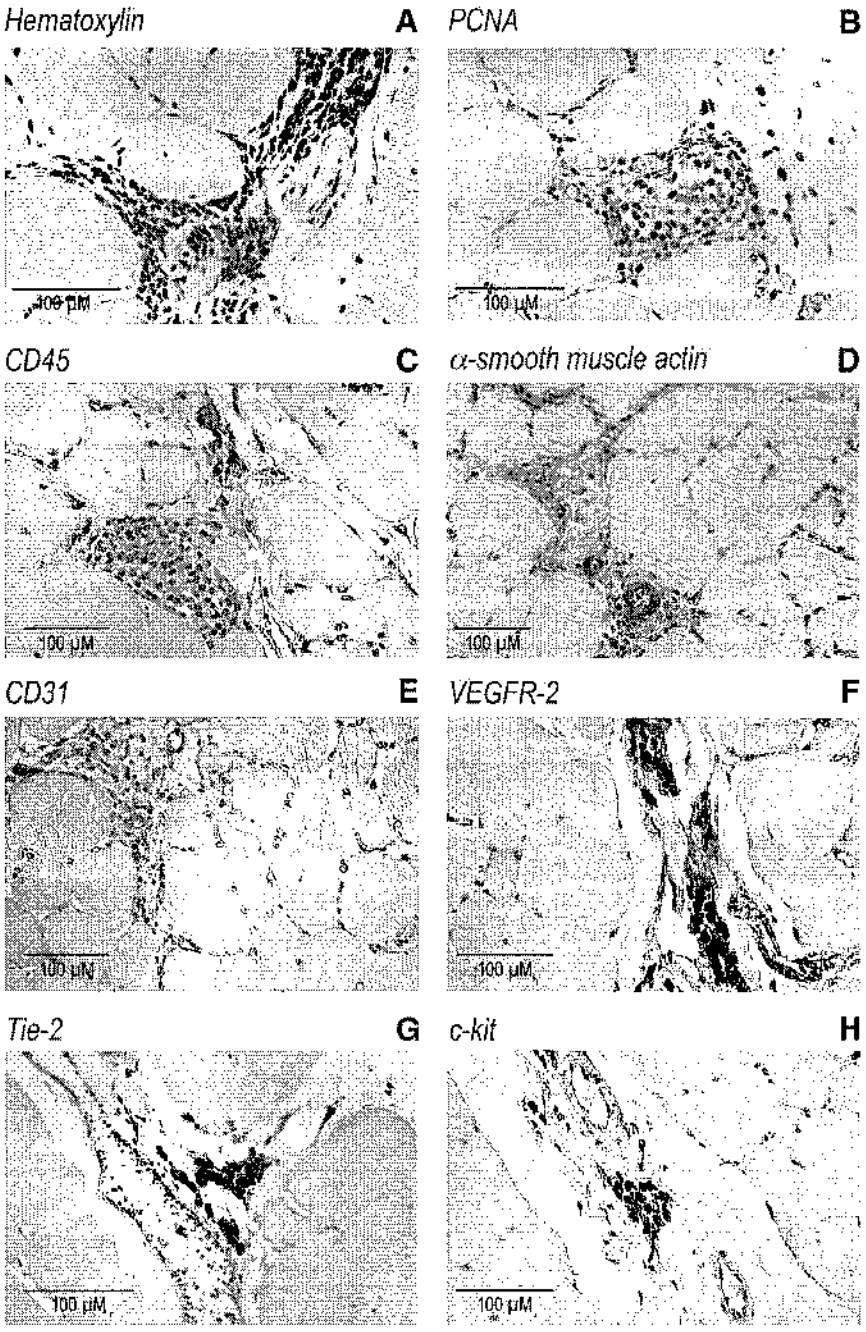


FIG. 6. Characterization of cells infiltrating muscles expressing VEGF165. A to F. Histological sections of muscles that were injected with AAV-VEGF165, analyzed at 3 months after treatment. Massive infiltrates of cells were found in the interstitial space surrounding large arteries (panel A). Most of these cells were expressing PCNA, indicating their active proliferation (B). Panels C to H show characterization of these cellular infiltrates by different antigenic markers, as indicated on top of each panel.

of several muscle fibers (1–5% of fibers in the injected areas) with vascular structures filled of red blood cells and thus connected to the general circulation. Staining of these areas with an anti-CD31 antibody reveled that, with few exceptions, these structures were lacking evident endothelial wall. These vascular structures might be cautiously interpreted as the effect of invagination of muscle cell membrane and its fusion to the membrane of endothelial cells, thus forming a vascular lacunae which is connected to the circulation. Alternatively, they might result from the invasion of muscular cells by locally proliferating cells eventually regressing and differentiating to form a vascular lacuna in which a thin endothelial layer remains undetected by immunohistochemistry. In contrast to the potent stimulatory effect of VEGF on endothelial cell proliferation and migration, and to its powerful vascular permeabilization activity [27], angiopoietin-1 has been shown to be essential for maturation of blood

vessels during embryonic development [28] and for the mitigation of vasal leakiness promoted by inflammation in the adult vasculature [9]. Consistent with these observations, in our experiments overexpression of VEGF alone determined highly increased vascular permeability. In contrast, leakiness of vessels produced by co-expression of VEGF with angiopoietin-1 was remarkably more similar to that of the normal muscle vasculature. This result underlines the notion that new blood vessel formation is a multistep process sustained by the sequential and coordinated activity of several factors, and that therapeutic angiogenesis will require not only increase in vessel number in the ischemic area but also their proper functional maturation. It is very likely that these and other functional and structural requirements will be met only by delivering a proper cocktail of regulated growth factor genes to the ischemic area, a demand that appear feasible using AAV vectors.

An interesting finding of our study was the observation that some of the proliferating cells found in muscles expressing VEGF were positive for markers of hematopoietic/endothelial cell precursors. Different investigators have recently reported that lineage negative, c-kit positive bone marrow cells are capable of infiltrating the infarcted myocardium (in which expression of VEGF is probably high) where they undergo alternate differentiation routes, including cardiomiocytes, endothelial and smooth muscle cells [12,29,30]. In addition, circulating endothelial progenitor cells of bone marrow origin have been isolated that are incorporated in sites of myocardial neovascularization [31]. Altogether these observations suggest that circulating stem cells might sense ischemic or damaged tissues and migrate to these areas, where they promote tissue formation by a mechanism that is probably different from angiogenic sprouting and might resemble embryonic vasculogenesis. Our results suggest that prolonged expression of VEGF, either directly or through the induction of other cytokines, might be one of the local triggers for progenitor cell accumulation and proliferation. Consistent with this conclusion are the results obtained by intravenous administration of an adenoviral vector expressing VEGF165, which determined rapid mobilization of hematopoietic stem cells and marked increase in circulating endothelial precursors [32]. Alternative to their bone marrow origin, the source of cells infiltrating VEGF-expressing tissues might be from a pool of resident progenitor cells, which are found in the heart and in the muscle [33–35] and might be triggered to proliferate in response to growth factor overexpression. Preliminary experiments performed by bone marrow transplantation from mouse male donors to lethally irradiated female recipients indicate that a large number of these infiltrating cells derive from the transplant (data not shown).

In conclusion, the results obtained by this study indicate that functional angiogenesis can be obtained by simultaneous expression of different cytokines for prolonged periods of time. While long-term expression of angiogenic growth factors is not required for the induction of angiogenesis in experimental models of acute or subacute ischemia, it may still turn out to be essential to attain therapeutic benefit for the treatment of human myocardial or limb chronic ischemia, in which new blood vessels formation is likely to require prolonged stimulation over time to promote maturation of larger collaterals. Furthermore, stable persistence of AAV vector genomes would permit the implementation of molecular systems for regulated control over transgene expression. This would have the additional advantage to overcome the concerns raised by the possibility that disregulated expression of angiogenic genes might favor the risk of pathological neovascularization at distant sites. Finally, the possibility of triggering progenitor cells accumulation and proliferation at specific sites by overexpressing VEGF-A has obvious important clinical implications, since it might permit tissue and blood vessel reconstitution through gene transfer to ischemic or damaged areas as a possible alternative to cellular transplantation.

## Materials and Methods

***Production, purification and characterization of rAAV vectors.*** The rAAV vectors used in this study are based on the pTR-UF5 construct, kindly provided by N. Muzyczka (University of Florida, Gainesville, FL). The coding sequences of the VEGF165 and angiopoietin-1 cDNAs were obtained by RT-PCR amplification from HL60 and 293 cell RNA respectively and cloned in the vector under the control of the CMV promoter to substitute the GFP gene. Cloning and propagation of AAV plasmids was carried in the JC 8111 E. coli strain. Infectious AAV2 vector particles were generated in 293 cells, cultured in 150-mm-diameter Petri dishes, by co-transfecting each plate with 15 μg of each vector plasmid together with 45 μg of the packaging/helper plasmid, pDG (kindly provided by J.A. Kleinschmidt, Heidelberg, Germany), expressing AAV and adenovirus helper functions. Viral stocks were obtained by CsCl gradient centrifugation as already described [16,36]. rAAV titers were determined by measuring the copy number of viral genomes in pooled, dialyzed gradient fractions using a competitive PCR procedure with primers and competitors mapping in the CMV promoter region common to all vectors [16]. Viral preparations used in this work for animal transduction had titers between $1 \times 10^{13}$ and $1 \times 10^{14}$ viral genome particles per ml.

***Competitive PCR quantification of vector and GAPDH genomic DNAs.*** Primers for PCR amplification of VEGF165 cDNA were VEGF-F1 (5′-GAGGGCAGAATCATCACGAAGT-3′) and VEGF-R1 (5′-TCCTATGTGCTGGCCTTGGTGA-3′). Primers for rat GAPDH gene amplification were GAP1 (5′-GACCTCAACTACATGGTCRA-3′) and GAP2 (5′-ATACTCAGCACCAGCATCAC-3′). Localization of these primers is schematically shown in Figure 1D. Competitors for both target DNAs were constructed by an established recombinant PCR procedure [16].

***Animals and experimental protocols.*** Animal care and treatment were conducted in conformity with institutional guidelines in compliance with national and international laws and policies (EEC Council Directive 86/609, OJL 358, December 12th 1987). Adult male Wistar rats weighting 250-300 grams were housed one per cage and maintained under controlled environmental conditions. After general anesthesia, rats were injected through a small skin incision in the tibialis anterior muscle using a 0.5 ml tuberculin syringe with a 27.5 G needle. Each muscle received 3–5 injections for a total of 200 μl volume of purified AAV vector preparations or

PBS (mock controls). A total of 48 rats were injected for this study. Each animal received in the tibialis anterior muscle of the right leg AAV-VEGF, AAV-Ang1, or the combination of both vectors (16 animals per group). In animals treated with both AAV-VEGF and AAV-Ang1, injection of the latter vector was performed 7 days after the first treatment. All animals received in their left legs mock injections of either AAV-LacZ or PBS. Animals were sacrificed after one (4 animals per group) and three months (12 animals per group) from AAV vector injection. Rats sacrificed one month post-injection were used only for histological characterization. Out of the three-month groups, 4 animals were used for blood flow tests, other 4 animals for the permeability tests and the last 4 animals for histological examination.

***Histological evaluation and immunohistochemistry.*** For histological evaluation, muscle samples were fixed in 2% formaldehyde and embedded in paraffin. Three μm sections were stained with haematoxylin and eosin or haematoxylin only. Immunohistochemical detection of specific antigens was performed with the following antibodies: rabbit polyclonal against VEGF (sc-152, Santa Cruz Biotechnology, Santa Cruz, CA); goat polyclonal against angiopoietin-1 (sc-6320, Santa Cruz Biotechnology); mouse monoclonal against CD45 (OX30, Abcam Ltd, Cambridge, UK); mouse monoclonal against α-smooth muscle actin (clone 1A4, Sigma); rabbit polyclonal against Tie2 (sc-9026, Santa Cruz Biotechnology); goat polyclonal against PECAM1 (sc-1506, Santa Cruz Biotechnology, Inc), mouse monoclonal against Flk-1 (sc-6251, Santa Cruz Biotechnology); rabbit polyclonal against c-kit (sc-168, Santa Cruz Biotechnology); mouse monoclonal against PCNA (sc-56, Santa Cruz Biotechnology). Protocols for immunohistochemistry were according to the Vectastain Elite ABC Kit (universal or goat) from Vector Laboratories. After treatment, slides were rinsed in PBS and signals were developed using 3,3'-diaminobenzidine as substrate for the peroxidase chromogenic reaction (Lab Vision Corporation, Fremont, CA).

***Blood flow assay.*** Blood flow was determined by injections of $2 \times 10^5$ 15 μm yellow-green fluorescent microspheres (Molecular Probes Inc, Eugene, OR) in the abdominal aorta of animals, as described [37]. Recovery of microspheres from tissue and extraction of fluorescent dye was performed according to the manufacturer's instruction. Briefly, weighted muscles were digested in 10 ml of 2 M ethanolic KOH, 0.5% tween 80 (v/v) (Sigma) overnight at 60°C with periodic shaking. Homogenates were centrifuged at $2000 \times g$ for 20 min in a swinging rotor. The supernatant, with the exception of 1 ml, was removed and the pellet was resuspended in 9 ml 0.25% Tween 80 in water. After an additional centrifugation and washing in deionised water, microspheres were dissolved in 3 ml 2-etoxyethyl acetate (Sigma-Aldrich) for 4 hours at room temperature. Debris was removed by centrifugation and fluorescence was measured in the supernatant by the VersaFluor Fluorometer System (BioRad, Richmond, CA) using EX 490/10 and EM 510/10 (BioRad) as excitation and emission filters respectively. Values were normalised and results are expressed as ratios between fluorescence of treated and control muscles.

***Vessel wall permeability assay.*** Analysis of vessel permeability was performed by an adaptation of the Miles assay [38] to rat muscle. Animals were injected in the femoral artery with 300 μl of 0.5% (w/v) Evans blue (Sigma) in PBS and sacrificed after 30 min. The muscle tibialis anterior was removed and weighted, and the dye was extracted by overnight incubation in 2 ml formamide at 55°C and quantified spectrophotometrically at 610 nm. Values of absorbance were converted, according to a standard curve, in Evans blue content. The results are shown in Figure 5C expressed as a ratio between treated and control muscles from the same animal, in order to reduce inter-animal variations.

## Acknowledgments

*This work was supported by grants from Progetto Finalizzato "Genetica Molecolare" of CNR Italy, from Fondo Trieste, Italy, and from Fondazione CR Trieste, Italy. We are grateful to Barbara Boziglav and Maria Elena Lopez for excellent technical support.*

RECEIVED FOR PUBLICATION SEPTEMBER 3, 2002; ACCEPTED JANUARY 27, 2003.

## References

1. Risau, W. (1997). Mechanisms of angiogenesis. *Nature* **386:** 671–674.
2. Yancopoulos, G. D., Davis, S., Gale, N. W., Rudge, J. S., Wiegand, S. J., and Holash, J. (2000). Vascular-specific growth factors and blood vessel formation. *Nature* **407:** 242–248.
3. Ferrara, N. (1999). Vascular endothelial growth factor: molecular and biological aspects. *Curr. Top. Microbiol. Immunol.* **237:** 1–30.
4. Dvorak, H. F., Nagy, J. A., Feng, D., Brown, L. F., and Dvorak, A. M. (1999). Vascular permeability factor/vascular endothelial growth factor and the significance of microvascular hyperpermeability in angiogenesis. *Curr. Top. Microbiol. Immunol.* **237:** 97–132.
5. Carmeliet, P., and Collen, D. (1999). Role of vascular endothelial growth factor and vascular endothelial growth factor receptors in vascular development. *Curr. Top. Microbiol. Immunol.* **237:** 133–158.
6. Davis, S., and Yancopoulos, G. D. (1999). The angiopoietins: Yin and Yang in angiogenesis. *Curr. Top. Microbiol. Immunol.* **237:** 173–185.
7. Asahara, T., *et al.* (1998). Tie2 receptor ligands, angiopoietin-1 and angiopoietin-2, modulate VEGF-induced postnatal neovascularization. *Circ. Res.* **83:** 233–240.
8. Thurston, G., *et al.* (1999). Leakage-resistant blood vessels in mice transgenically overexpressing angiopoietin-1. *Science* **286:** 2511–2514.
9. Thurston, G., *et al.* (2000). Angiopoietin-1 protects the adult vasculature against plasma leakage. *Nat. Med.* **6:** 460–463.
10. Rafii, S. (2000). Circulating endothelial precursors: mystery, reality, and promise. *J. Clin. Invest.* **105:** 17–19.
11. Isner, J. M., and Asahara, T. (1999). Angiogenesis and vasculogenesis as therapeutic strategies for postnatal neovascularization. *J. Clin. Invest.* **103:** 1231–1236.
12. Orlic, D., *et al.* (2001). Bone marrow cells regenerate infarcted myocardium. *Nature* **410:** 701–705.
13. Fisher, K. J., *et al.* (1997). Recombinant adeno-associated virus for muscle directed gene therapy. *Nat. Med.* **3:** 306–312.
14. Svensson, E. C., *et al.* (1999). Efficient and stable transduction of cardiomyocytes after intramyocardial injection or intracoronary perfusion with recombinant adeno-associated virus vectors. *Circulation* **99:** 201–205.
15. Snyder, R. O., *et al.* (1997). Efficient and stable adeno-associated virus-mediated transduction in the skeletal muscle of adult immunocompetent mice. *Hum. Gene Ther.* **8:** 1891–1900.
16. Zentilin, L., Marcello, A., and Giacca, M. (2001). Involvement of cellular double-strand DNA break-binding proteins in processing of recombinant adeno-associated virus (AAV) genome. *J. Virol.* **75:** 12279–12287.
17. Duan, D., Yue, Y., and Engelhardt, J. F. (2001). Expanding AAV packaging capacity with trans-splicing or overlapping vectors: a quantitative comparison. *Mol. Ther.* **4:** 383–391.
18. Neufeld, G., Cohen, T., Gengrinovitch, S., and Poltorak, Z. (1999). Vascular endothelial growth factor (VEGF) and its receptors. *Faseb J.* **13:** 9–22.
19. Goodell, M. A., Brose, K., Paradis, G., Conner, A. S., and Mulligan, R. C. (1996). Isolation and functional properties of murine hematopoietic stem cells that are replicating in vivo. *J. Exp. Med.* **183:** 1797–1806.
20. Gowdak, L. H., *et al.* (2000). Adenovirus-mediated VEGF(121) gene transfer stimulates angiogenesis in normoperfused skeletal muscle and preserves tissue perfusion after induction of ischemia. *Circulation* **102:** 565–571.
21. Vajanto, I., *et al.* (2002). Evaluation of angiogenesis and side effects in ischemic rabbit hindlimbs after intramuscular injection of adenoviral vectors encoding VEGF and LacZ. *J. Gene Med.* **4:** 371–380.
22. Lu, Y., Shansky, J., Del Tatto, M., Feriand, P., Wang, X., and Vandenburgh, H. (2001). Recombinant vascular endothelial growth factor secreted from tissue-engineered bioartificial muscles promotes localized angiogenesis. *Circulation* **104:** 594–599.
23. Springer, M. L., Chen, A. S., Kraft, P. E., Bednarski, M., and Blau, H. M. (1998). VEGF gene delivery to muscle: potential role for vasculogenesis in adults. *Mol. Cell* **2:** 549–558.
24. Springer, M. L., et al.2002. Localized arteriolae formation directly adjacent to the site of VEGF delivery in muscle. Molecular Therapy ACCOMPANYING PAPER: EDITOR PLEASE FILL IN.
25. Dor, Y., *et al.* (2002). Conditional switching of VEGF provides new insights into adult neovascularization and pro-angiogenic therapy. *Embo J.* **21:** 1939–1947.
26. Lee, R. J., Springer, M. L., Blanco-Bose, W. E., Shaw, R., Ursell, P. C., and Blau, H. M. (2000). VEGF gene delivery to myocardium: deleterious effects of unregulated expression. *Circulation* **102:** 898–901.
27. Senger, D. R., Galli, S. J., Dvorak, A. M., Perruzzi, C. A., Harvey, V. S., and Dvorak, H. F. (1983). Tumor cells secrete a vascular permeability factor that promotes accumulation of ascites fluid. *Science* **219:** 983–985.
28. Suri, C., *et al.* (1996). Requisite role of angiopoietin-1, a ligand for the TIE2 receptor, during embryonic angiogenesis. *Cell* **87:** 1171–1180.
29. Jackson, K. A., *et al.* (2001). Regeneration of ischemic cardiac muscle and vascular endothelium by adult stem cells. *J. Clin. Invest.* **107:** 1395–1402.
30. Kocher, A. A., *et al.* (2001). Neovascularization of ischemic myocardium by human bone-marrow-derived angioblasts prevents cardiomyocyte apoptosis, reduces remodeling and improves cardiac function. *Nat. Med.* **7:** 430–436.

31. Asahara, T., *et al.* (1999). Bone marrow origin of endothelial progenitor cells responsible for postnatal vasculogenesis in physiological and pathological neovascularization. *Circ. Res.* **85:** 221–228.
32. Hattori, K., *et al.* (2001). Vascular endothelial growth factor and angiopoietin-1 stimulate postnatal hematopoiesis by recruitment of vasculogenic and hematopoietic stem cells. *J. Exp. Med.* **193:** 1005–1014.
33. Gussoni, E., *et al.* (1999). Dystrophin expression in the mdx mouse restored by stem cell transplantation. *Nature* **401:** 390–394.
34. Jackson, K. A., Mi, T., and Goodell, M. A. (1999). Hematopoietic potential of stem cells isolated from murine skeletal muscle. *Proc. Natl. Acad. Sci. USA* **96:** 14482–14486.
35. Seale, P., Sabourin, L. A., Girgis-Gabardo, A., Mansouri, A., Gruss, P., and Rudnicki, M. A. (2000). Pax7 is required for the specification of myogenic satellite cells. *Cell* **102:** 777–786.
36. Deodato, B., *et al.* (2002). Recombinant AAV vector encoding human VEGF165 enhances wound healing. *Gene Therapy* **9:** 777–785.
37. Byun, J., *et al.* (2001). Efficient expression of the vascular endothelial growth factor gene in vitro and in vivo, using an adeno-associated virus vector. *J. Mol. Cell. Cardiol.* **33:** 295–305.
38. Miles, A. A., and Miles, E. M. (1952). Vascular reaction to histamine, histamine-liberator, and leukotaxine in the skin of guinea pigs. *J. Physiol.* **118:** 228–257.

# BONE MARROW MONONUCLEAR CELLS ARE RECRUITED TO THE SITES OF VEGF-INDUCED NEOVASCULARIZATION BUT ARE NOT INCORPORATED INTO THE NEWLY FORMED VESSELS

Lorena Zentilin[1], Sabrina Tafuro[1], Serena Zacchigna[1], Nikola Arsic[1,*], Milena Sinigaglia[1], and Mauro Giacca[1,2]

[1]Molecular Medicine Laboratory, International Centre for Genetic Engineering and Biotechnology (ICGEB), Trieste, Italy
[2]University of Trieste, Faculty of Medicine, Trieste, Italy

Short title: Bone marrow cells in VEGF-induced neovascularization

[*]Current address: Institute of Human Genetics, CNRS UPR 1142, Montpellier, France

Grant support: This work was supported by grants from the Progetto Finalizzato "Genetica Molecolare" of the "Consiglio Nazionale delle Ricerche", Italy; from the FIRB program of the "Ministero dell'Istruzione, Universita' e Ricerca", Italy; from the "Fondazione Cassa di Risparmio" of Trieste, Italy and from the "Fondo Trieste", Italy.

Address for correspondence:
Mauro Giacca, MD. Ph.D.
Director, ICGEB Trieste
Padriciano, 99
34012 Trieste (Italy)
tel.: +39-040-3757.324
fax: +39-040-226555
e-mail: giacca@icgeb.org

**ABSTRACT**

Vascular endothelial growth factor (VEGF) is a key regulator of blood vessel formation during both vasculogenesis and angiogenesis. The prolonged expression of VEGF in the normoperfused skeletal muscles of adult rodents after gene transfer using AAV vectors induces the formation of a large set of new capillaries and small arteries. Notably, this process is accompanied by the massive infiltration by mononuclear cells. This observation raises the possibility that these cells might represent circulating progenitors that are eventually incorporated in the newly formed vessels. Here we explore this possibility by exploiting four different experimental models, based on: a) the transplantation of male bone marrow into female recipients; b) the transplantation of Tie2-GFP transgenic bone marrow; c) the transplantation of bone marrow in the presence of erythropoietin (EPO), a mobilizer of endothelial progenitor cells (EPCs); d) the re-implantation of ex vivo expanded EPCs. In all four models, VEGF acted as a powerful attractor of bone marrow-derived mononuclear cells, bearing different myeloid and endothelial markers proper of the EPCs, to the sites of neovascularization. In no case, however, the attracted cells were incorporated in the newly formed vasculature. These observations indicate that new blood vessel formation induced by VEGF occurs through bona fide sprouting angiogenesis; the contribution of the infiltrating bone marrow-derived cells to this process still remains enigmatic.

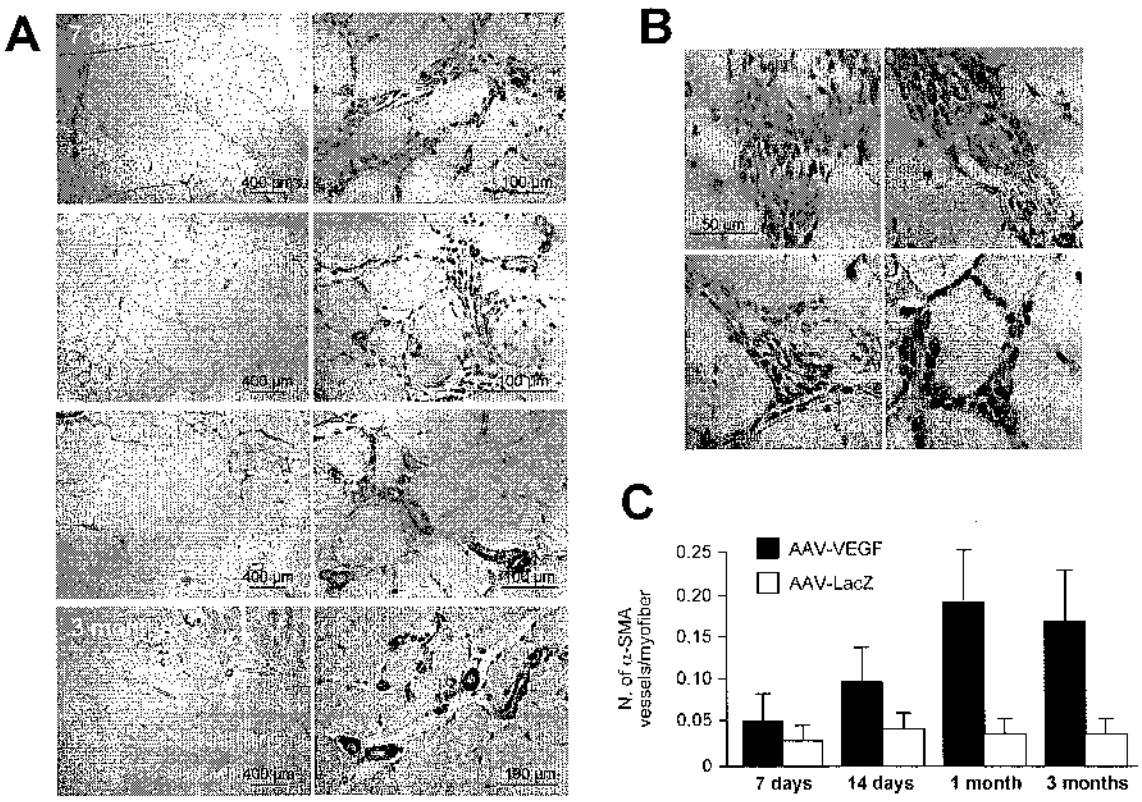


**Figure 1. Mononuclear cells infiltrate the foci of VEGF-induced neovascularization.**

**A.** Immunohistochemical time course analysis of the angiogenic response induced by AAV-mediated VEGF expression in normal skeletal muscle at different times after vector injection, by the visualization of small arteries using an antibody against smooth muscle actin (α-SMA). Abundant mononuclear cell infiltrates are detectable in the perivascular spaces of the injected muscles at 7 and 15 days (enlargements in panel **B**) after transduction and persist, although at lower levels, after 1 and 3 months of continuous VEGF expression.

**C.** Quantification of the number of α-SMA-positive vessels, which progressively increased up to 1 month and remained stable thereafter.

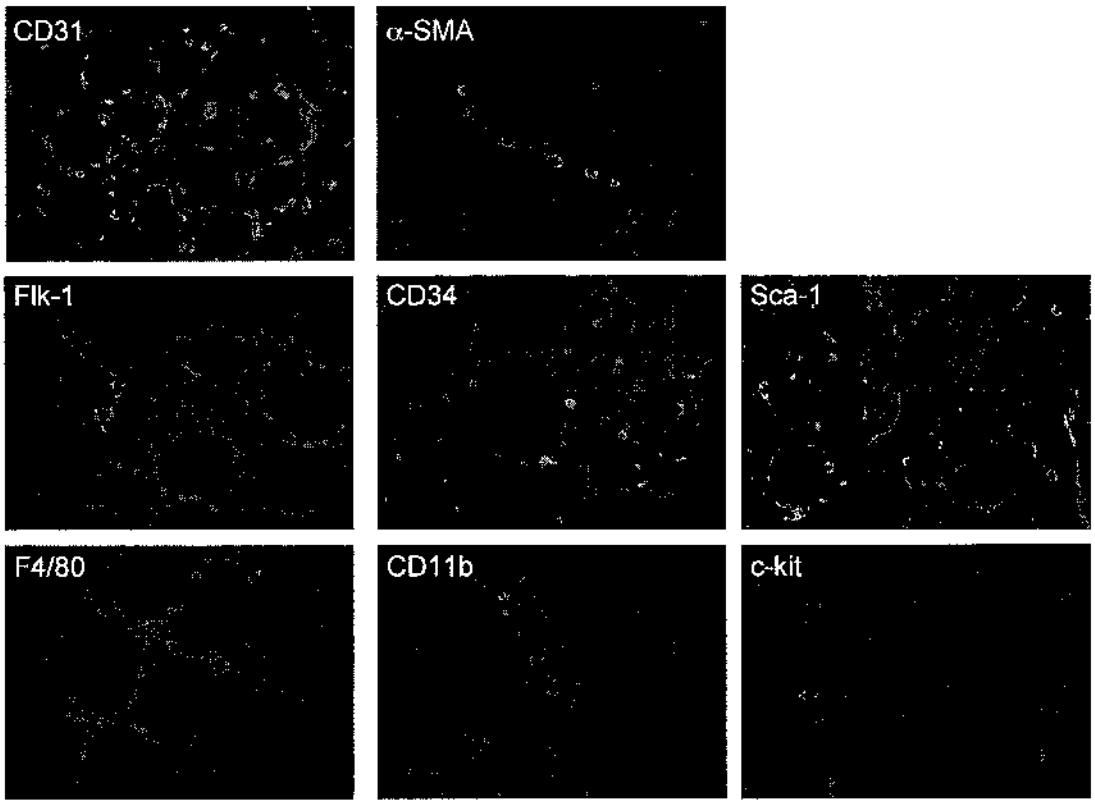


**Figure 2. Immunological characterization of the mononuclear cells infiltrating the foci of VEGF-induced neovascularization.**

Immunofluorescence staining was performed using CD31, α-SMA, Flk-1, CD34, Sca-1, F4/80, CD11b and c-kit specific antibodies, on histological sections of mouse tibialis anterior muscles injected with AAV-VEGF at 2 weeks after transduction. Positive cells are stained in red. Blue: nuclei stained with DAPI.

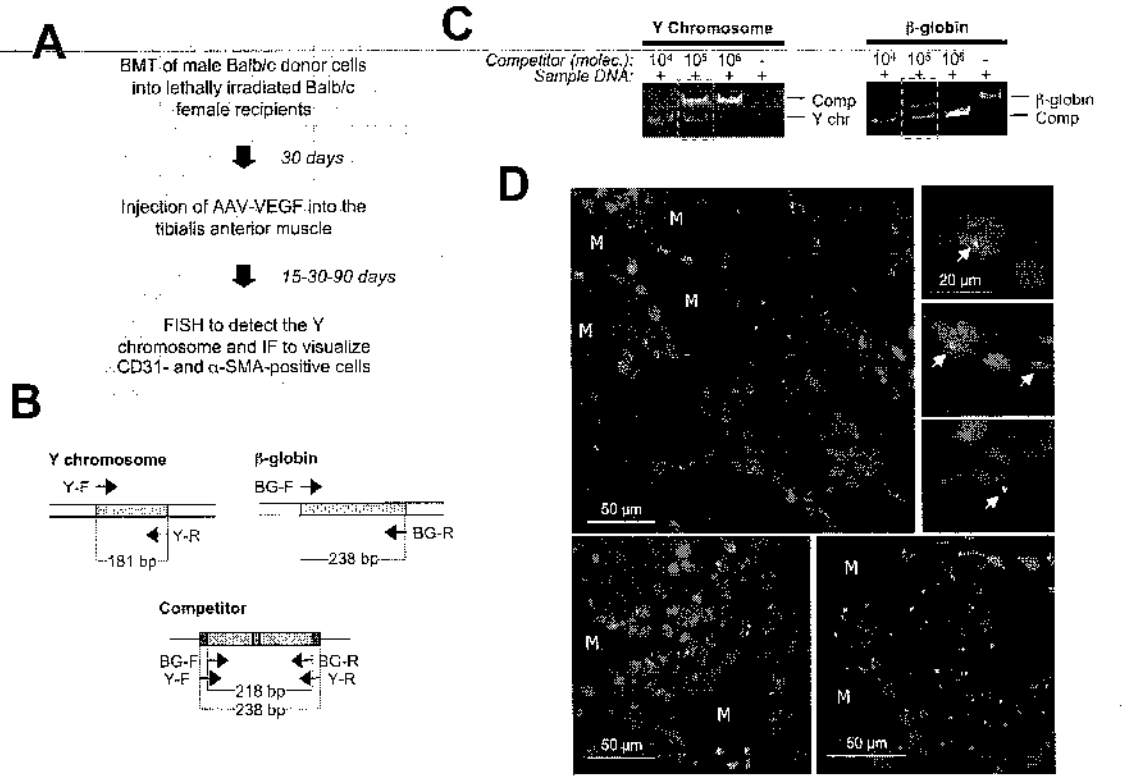


**Figure 3. Sex-mismatch bone marrow transplantation model.**

**A.** Flow chart of the experimental procedure. Unfractionated BM cells from male Balb/c donor mice were transplanted into lethally irradiated syngenic female recipients. After hematopoietic recovery, the efficiency of engraftment was evaluated by quantifying the copies of donor-specific Y chromosome sequences in the bone marrow of the transplanted animals by competitive PCR, using β-globin as reference gene.

**B.** Schematic representation of the templates for quantitative PCR. Amplification of the Y chromosome sequence and of the β-globin gene were obtained with primer pairs Y-F/Y-R and BG-F/BG-R respectively. The multicompetitor used for competitive PCR contains a core sequence of 218 bp, corresponding to a 20 bp-deleted version of the mouse β-globin amplification fragment, flanked by Y-F and Y-R primer sequences.

**C.** Example of competitive PCR amplification. Fixed amounts of sample DNA from peripheral blood mononuclear cells were mixed with scalar amounts of the multicompetitor DNA and PCR-amplified with the two primer pairs. After amplification, the gels were stained with ethidium bromide and the competitor (Comp.), Y chromosome (Y-chr) or β-globin DNA bands were quantified. According to the principles of competitive PCR, the ratio between the amplification products in each reaction is linearly correlated with the input DNA amounts for the two DNA species.

**D.** Examples of FISH analysis on muscle sections from transplanted mice at 30 days after injection of AAV-VEGF, using a mouse-specific Y chromosome probe labeled with FITC. The green dots, indicated by arrows in the enlargements, correspond to Y chromosome specific signals. Red, nuclei stained by propidium iodide, M, muscle fibers.

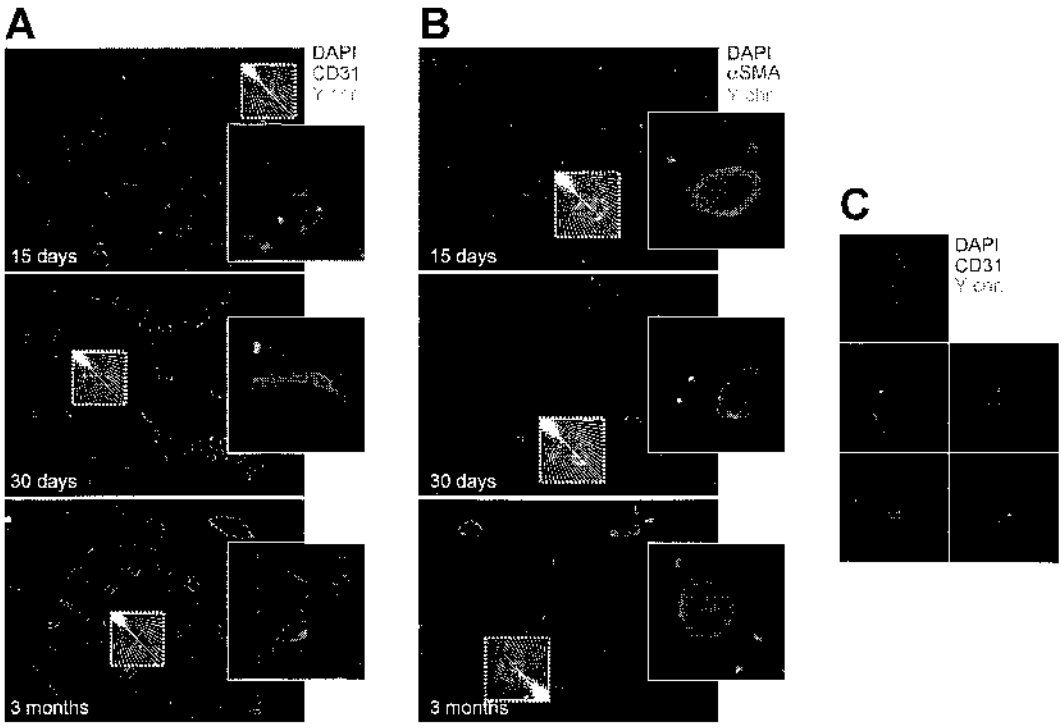


**Figure 4. ImmunoFISH analysis of VEGF-treated muscles of transplanted mice at 15, 30 days and 3 months after vector injection.**

Immunofluorescence staining for endothelial (CD31, **A**) and smooth muscle (α-SMA, **B**) antigens was combined with Y chromosome fluorescent in situ hybridization. The vast majority of cells expressing either of the two markers were not found to contain a Y chromosome (enlargements in A and B). Very rare cells (<1% of total Y chromosome-positive nuclei) were positive for CD31 and Y chromosome markers (shown in the enlargements in **C**); cells of donor origin and positive for the α-SMA antigen were never found in the tunica media of vessels.

Blu, nuclei stained with DAPI, Red, CD31 (A) and α-SMA (B) positive cells, Yellow, Y chromosome.

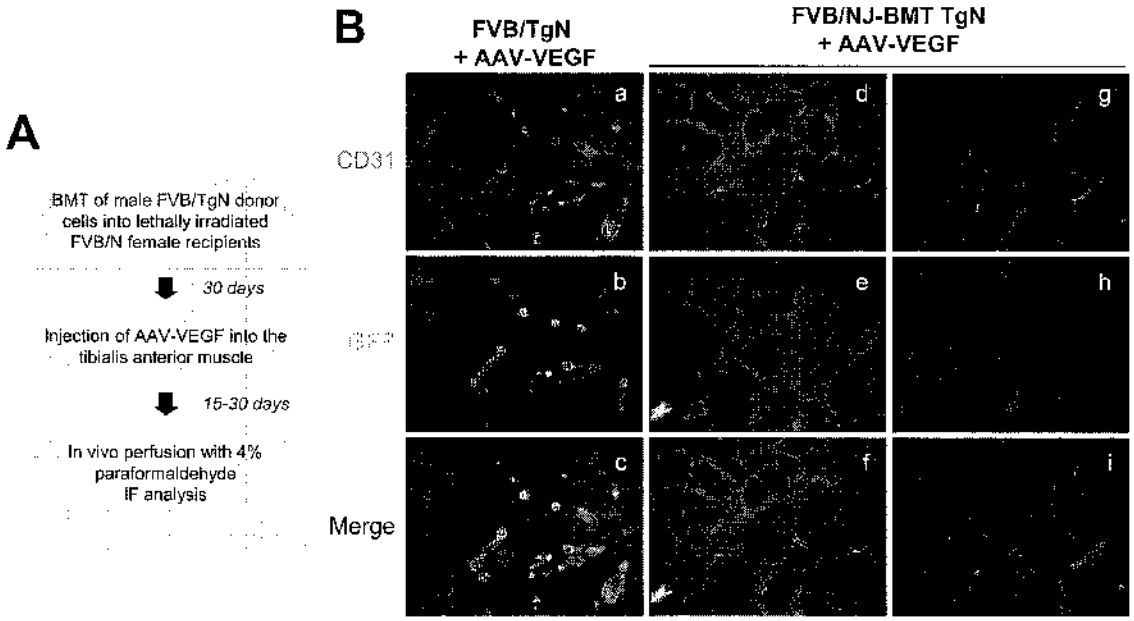


**Figure 5. FVB/TgN transgenic mouse bone marrow transplantation model.**

**A.** Flow chart of the experimental procedure. BM from FVB/TgN transgenic mice, expressing GFP under the transcriptional control of the endothelial specific Tie-2 promoter, was transplanted into lethally irradiated FVB/N wild type recipients 30 days before treatment with AAV-VEGF.

**B.** Immunostaining for the endothelial-specific CD31 and GFP markers in muscle sections of VEGF-treated mice at 1 month after vector injection. In the FVB/TgN transgenic control mouse, most of the endothelial cells also stained positive for GFP (a to c). In contrast, no Tie2-GFP-positive cells were found within the cellular infiltrates or incorporated into the wall of the newly formed vessels in the FVB/NJ-BMT TgN chimeric mice (d to i).

Red, CD31 positive cells; Green, GFP; Blue, nuclei stained with DAPI.

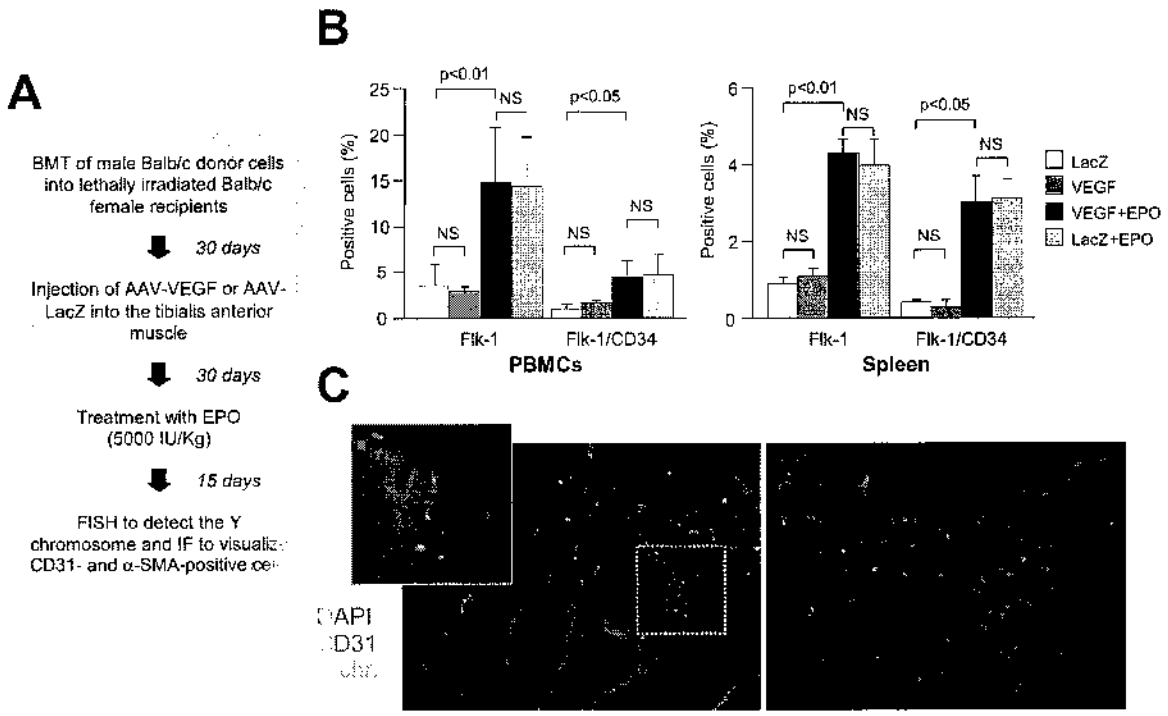


**Figure 6. Erythropoietin (EPO) mobilizes bone marrow cells with an EPC phenotype that are recruited to the sites of neovascularization but are not incorporated in the neovessels.**

**A.** Flow chart of the experimental procedure. Sex-mismatched transplanted, AAV-VEGF-treated mice were treated with EPO in order to mobilize endothelial progenitor cells from the bone marrow.

**B.** Flow cytometry analysis of mononuclear cells from peripheral blood and spleen. Animals treated with EPO (but not those injected with AAV-VEGF or AAV-LacZ) showed a significant increase of Flk-1 and Flk-1/CD34 positive cell populations, indicative of the mobilization of endothelial progenitors.

**C.** ImmunoFISH analysis of VEGF-treated muscle sections of animals treated with EPO. Despite the mobilization of EPCs, there was no increase in the number of Y-chromosome positive cells expressing the CD31 endothelial markers at the sites of VEGF-induced neovascularization.

Red, CD31-positive cells; Green, Y chromosome; Blue, nuclei stained with DAPI.

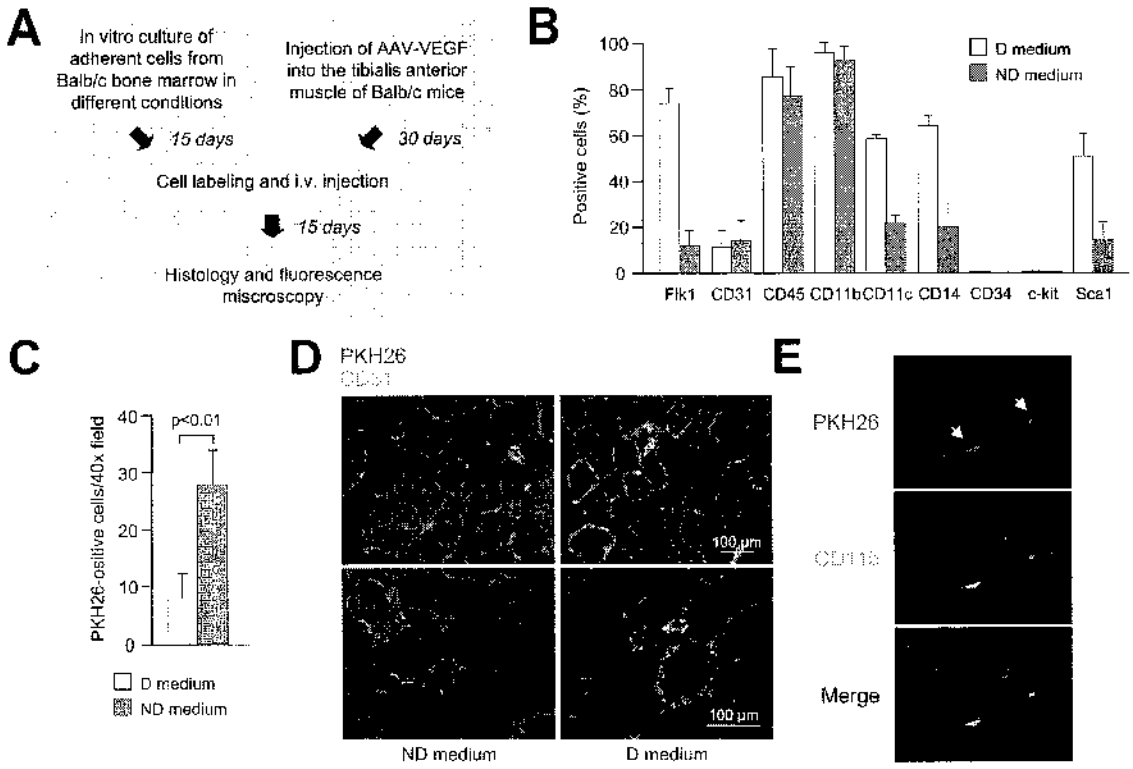


**Figure 7. In vitro cultured bone marrow cells with EPC phenotype home at sites of VEGF-induced angiogenesis but are not incorporated into the vessel wall.**

**A.** Experimental design. Balb/c mice adherent bone marrow cells were cultured in vitro for 15 days in Differentiating (D) and Non Differentiating medium (ND; see text) in order to enrich for endothelial progenitor cells. After 15 days, the EPCs were labeled with the PKH26 red fluorescent die and administered i.v. to syngenic recipient mice previously injected with AAV-VEGF in the right tibialis anterior muscle.

**B.** Flow cytometry phenotypic profile of the cell populations before injection into the animals (mean ± SEM of three different experiments).

**C.** Number of PKH16-positive cells infiltrating the sites of VEGF-induced neovascularization at day 15 after cell injection. The cells expanded ex vivo using the ND medium were recruited ~4 times more efficiently than those cultivated in differentiating medium (mean ± SEM of three different experiments).

**D.** Immunofluorescence analysis for the visualization of CD31 (green) and PKH26 (red). Co-localization of the two markers in the same cells was highly infrequent.

**E.** Immunofluorescence analysis for the visualization of CD11b (green) and PKH26 (red). Most of the recruited cells were positive for the myelo/monocytic marker CD11b.

American Journal of Pathology, Vol. 167, No. 4, October 2005


# Improved Survival of Ischemic Cutaneous and Musculocutaneous Flaps after Vascular Endothelial Growth Factor Gene Transfer Using Adeno-Associated Virus Vectors

Serena Zacchigna,* Giovanni Papa,† Andrea Antonini,† Federico Novati,† Silvia Moimas,* Alessandro Carrer,* Nikola Arsic,* Lorena Zentilin,* Valentina Visintini,† Michele Pascone,† and Mauro Giacca*

*From the Molecular Medicine Laboratory,* International Centre for Genetic Engineering and Biotechnology, Trieste, and the Plastic Surgery Unit,† Faculty of Medicine, University of Trieste, Trieste, Italy*

**A major challenge in reconstructive surgery is flap ischemia, which might benefit from induction of therapeutic angiogenesis. Here we demonstrate the effect of an adeno-associated virus (AAV) vector delivering vascular endothelial growth factor (VEGF)165 in two widely recognized *in vivo* flap models. For the epigastric flap model, animals were injected subcutaneously with $1.5 \times 10^{11}$ particles of AAV-VEGF at day 0, 7, or 14 before flap dissection. In the transverse rectus abdominis musculocutaneous flap model, AAV-VEGF was injected intramuscularly. The delivery of AAV-VEGF significantly improved flap survival in both models, reducing necrosis in all treatment groups compared to controls. The most notable results were obtained by administering the vector 14 days before flap dissection. In the transverse rectus abdominis musculocutaneous flap model, AAV-VEGF reduced the necrotic area by >50% at 1 week after surgery, with a highly significant improvement in the healing process throughout the following 2 weeks. The therapeutic effect of AAV-VEGF on flap survival was confirmed by histological evidence of neoangiogenesis in the formation of large numbers of CD31-positive capillaries and α-smooth muscle actin-positive arteriolae, particularly evident at the border between viable and necrotic tissue. These results underscore the efficacy of VEGF-induced neovascularization for the prevention of tissue ischemia and the improvement of flap survival in reconstructive surgery. *(Am J Pathol 2005, 167:000–000)***

Partial necrosis of skin flaps represents a major clinical problem in patients undergoing reconstructive procedures, with significant morbidity and no effective therapy available. The lack of oxygen and nutrients in the distal part of the flap strongly compromises skin viability, resulting in flap necrosis, which often requires secondary reconstructive interventions.[1] The recent concept of therapeutic angiogenesis by local administration of angiogenic growth factors has emerged as an attractive approach to enhance blood supply and perfusion in compromised tissues, thus improving flap survival. Fn1

The angiogenic response to tissue ischemia is a complex process involving the coordinated interplay of a variety of soluble factors, controlling new blood vessel formation. One of the fundamental molecules that are required in the angiogenic process is the vascular endothelial growth factor (VEGF). Four different isoforms of VEGF have been described, with 121, 165, 189, and 206 amino acids arising by differential splicing of the primary VEGF gene transcript. VEGF165 is the predominant form in all cells and tissues and its expression is promptly induced by tissue hypoxia. The main activity of VEGF is to stimulate the proliferation and migration of endothelial cells, with the constitution of a primitive capillary network, which subsequently matures to form larger vessels.

Research on therapeutic angiogenesis relating to plastic and reconstructive surgery is in its early stages. Several laboratories have explored the possibility of promoting skin flap neovascularization by using recombinant VEGF proteins. In most of these studies, with some exceptions,[2] recombinant VEGF provided a beneficial effect on the flap survival,[3–9] although the exact mechanisms have not always been specifically addressed. Despite these encouraging findings, the use of recombi-

Supported by grants from the Progetto Finalizzato "Genetica Molecolare" of the "Consiglio Nazionale delle Ricerche," Italy; the FIRB program of the "Ministero dell'Istruzione, Universita' e Ricerca," Italy; the "Fondazione Cassa di Risparmio" of Trieste, Italy; and the "Fondo Trieste," Italy. AQ: C

S.Z. and G.P. contributed equally to this work.

Accepted for publication June 19, 2005.

Address reprint requests to Mauro Giacca, M.D. Ph.D., Director, ICGEB Trieste, Padriciano, 99, 34012 Trieste, Italy. E-mail: giacca@icgeb.org.

balt2/zjh-jpath/zjh-jpath/zjh01005/zjh6633-05a | hurtr | S=8 | 8/11/05 | 7:13 | 4/Color Figure(s): 1,2,4-6 | Art: AJP05-0091 | Input-krb



nant proteins in a clinical setting is hampered by several factors, such as their short half-lives, poor bioavailability, and consequent need for frequent administrations to sustain long-lasting effects. Delivery of therapeutic genes to induce neo-angiogenesis represents an appealing alternative strategy that might overcome most of these problems. Moreover, the easy accessibility of the flaps makes them an ideal target for an *in vivo* gene transfer approach.

A variety of techniques allow for a coding DNA to be taken up by host cells, which then express the respective protein. Many of them have been used for gene delivery to the muscle and skin, including the use of naked plasmid DNA and viral vectors.[10–18] The use of viral vectors presents a notable advantage over nonviral systems, by providing a higher rate of transduction and expression. Among the novel approaches that hold promise to become a relevant therapeutic modality in humans is the use of vectors based on the adeno-associated virus (AAV), a nonpathogenic and widespread parvovirus, incapable of autonomous replication. Vectors based on AAV are able to transduce both dividing and nondividing cells and show a specific tropism for poststitotic cells, including skeletal and cardiac muscle,[16,19] neurons,[20] and liver.[21,22] Because these vectors do not contain any viral genes—which are transiently transfected in trans for the packaging process—they elicit virtually no inflammatory or immune response.[23,24] As a consequence, transgene expression from these vectors persists for several months in a variety of animal tissues *in vivo*.[25]

Besides being able to transduce human keratinocytes *in vitro*,[26] we and others have observed that the subcutaneous delivery of AAV vectors results in the efficient transduction of hair follicles, sweat gland ducts,[27] and the panniculus carnosus (the skeletal muscle layer within the dermal sheet in rodents).[28,29] To our knowledge, the data reported in this study are the first demonstration that AAV can be successfully used in the plastic surgery field to deliver the VEGF165 gene as a tool to promote therapeutic angiogenesis and skin flap survival in two different *in vivo* flap models.

## Materials and Methods

### Recombinant AAV Vector Preparation and Characterization

Two recombinant AAV vectors were obtained in this study, expressing the LacZ reporter gene and the cDNA for the 165 amino acid isoform of VEGF (VEGF165) under the control of the constitutive cytomegalovirus immediate early promoter. Infectious vector stocks were generated in 293 cells and titrated by a competitive polymerase chain reaction procedure, as already described.[30]

### Animals and Experimental Protocols

Animal care and treatment were conducted in conformity with institutional guidelines in compliance with national and international laws and policies (EEC Council Directive 86/609, OJL 358, December 12th, 1987). A total of 88 adult male Wistar rats weighting 250 to 300 g were used for this study and housed under controlled environmental conditions. After general anesthesia with Avertin 2% (10 ml/kg), abdominal hair was removed and skin washed with sterile water. A flap measuring 5 × 8 cm was outlined on the skin, extending cranially from the xiphoid process and bilaterally from the midline (Figure 2).

In the first model, the skin flap was raised from the fascia on the inferior epigastric artery, by cutting all of the vessels from the left side of the abdomen, all of the perforators, and the right lateral thoracic artery. At the end of the procedure, the skin was immediately resutured in place. In this model, 150 μl of either AAV-VEGF or placebo were injected at 10 equally spaced subcutaneous sites along the midline of the flap.

For the TRAM model, the entire left part of the flap was raised on a plane between the panniculus carnosus and the abdominal fascia, but on the right side the medial portion of the flap was left attached to the anterior rectus sheet. In this way, the rectus abdominis represents the muscular component of the flap, providing the blood supply to the cutaneous component through the perforator arteries. This time, AAV-VEGF or placebo was injected intramuscularly in the same region where each perforator artery arises from the rectus abdominis.

Each of the 12 experimental groups described in Figure 3 was initially composed of four rats (an overview of the experimental groups is provided in Table 1). Rats in groups 1, 2, 3, 7, 8, and 9 received AAV-VEGF at 0, 7, and 14 days before surgery, respectively, whereas groups 4, 5, 6, 10, 11, and 12 were control groups, in which the same volume of AAV-LacZ or saline was administered at the same time points (in every control group, two animals received AAV-LacZ and the other two received saline). Based on the results of this first set of experiments, 40 additional rats were treated with the TRAM flap and injected with AAV-VEGF or AAV-LacZ ($n = 20$ per group) vectors 14 days before surgery. Flap survival was first assessed at day 7 after surgery by taking digital images of the flaps using a Nikon E995 camera followed by the measurement of the necrotic area using the UTHSCSA Image Tool software. At the same time point, 12 animals per group were sacrificed for

**Table 1.** Experimental Groups

| Treatment | Time of vector delivery | Group no. |
|---|---|---|
| Epigastric flap ($n = 24$) | | |
| AAV-VEGF | During surgery | 1 |
| | 7 days before surgery | 2 |
| | 14 days before surgery | 3 |
| AAV-LacZ | During surgery | 4 |
| | 7 days before surgery | 5 |
| | 14 days before surgery | 6 |
| TRAM flap ($n = 24$) | | |
| AAV-VEGF | During surgery | 7 |
| | 7 days before surgery | 8 |
| | 14 days before surgery | 9 |
| AAV-LacZ | During surgery | 10 |
| | 7 days before surgery | 11 |
| | 14 days before surgery | 12 |

AQ: A

AQ: B

balt2/zjh-jpath/zjh-jpath/zjh01005/zjh6633-05a | hurtr | S=8 | 8/11/05 | 7:13 | 4/Color Figure(s): 1,2,4-6 | Art: AJP05-0091 | Input-krb



histological assessment. Flaps were harvested after the scars, as described in Figure 6, and tissue biopsies were fixed overnight in 10% buffered formalin. The other rats ($n$ = 8 per group) were followed for an additional 2 weeks at 3-day intervals, by measuring the extent of the necrotic area to assess the efficacy of the healing process.

### *Histological and Immunohistochemical Evaluation*

Fixed samples were dehydrated with graded ethanol and embedded in paraffin. Five-$\mu$m sections were stained with hematoxylin for morphological analysis of tissues. For the histological score assignment, six slides of each biopsy were independently examined by three researchers without knowledge of the previous treatment; biopsies were harvested from at least six different animals per experimental group. The inflammatory and adipose areas were calculated by digital planimetry of tissue sections.

To visualize blood vessels by immunohistochemistry, rehydrated serial paraffin sections were subjected to antigen retrieval procedures. After inactivation of endogenous peroxidase with 3% hydrogen peroxide, samples were rinsed in phosphate-buffered saline (PBS) and blocked with nonimmune horse serum followed by incubation with an anti-CD31 antibody (Santa Cruz) or an anti-$\alpha$-smooth muscle actin ($\alpha$-SMA) antibody (Sigma). Slides were rinsed in PBS and then incubated with biotinylated horse secondary antibody (Vector). After an additional washing in PBS, slides were incubated in the presence of an avidin-biotin complex and developed with 3,3′-diaminobenzidine (Lab Vision).

### *Statistical Analysis*

The comparison of the efficacy of AAV vector delivery at different time points with respect to flap surgery was performed by two-way factorial analysis of variance, followed by appropriate one-way analysis of variance and posthocs. Posthoc analysis was performed with Bonferroni/Dunn. Pair-wise comparison between groups was performed using the Student's $t$-test.

## *Results*

### *Efficacy of AAV-VEGF Gene Transfer in Two Skin Flap Models in the Rat*

This study is based on the use of two AAV vectors (AAV2 serotype), delivering either the LacZ reporter gene (AAV-LacZ) as a control, or the 165 amino acid isoform of human VEGF (AAV-VEGF) under the control of the constitutive human cytomegalovirus immediate early promoter. Both vectors were obtained by standard co-transfection procedures at a titer of $1 \times 10^{12}$ viral genome particles/ml in the International Centre for Genetic Engineering and Biotechnology AAV Vector Unit facility. We have already described the angiogenic effect of the AAV-VEGF vector *in vivo* after intramuscular injection in the rat skeletal muscle, in conditions of both normal perfusion[30] or after ischemia,[31] as well as in a rat skin wound model.[29]

Considering the strong angiogenic effect exerted throughout time by the AAV-VEGF vector, we wanted to assess its therapeutic potential to improve skin flap survival. Two different *in vivo* flap models in the rat were developed, the first one involving only the epidermis and dermis (cutaneous), while the second one also included a muscular layer (musculocutaneous). A total number of 48 animals were involved in a first set of experiments, aimed at exploring the optimal timing of AAV vector delivery: half of the animals were treated with the cutaneous flap and half with the musculocutaneous flap. In both cases, a rectangular skin paddle was raised on the epigastrium, an area having a predictable axial vascular system consisting of the lateral thoracic artery (bilaterally), of the inferior superficial epigastric artery (bilaterally), and of four musculocutaneous perforator branches, arising from the rectus abdominis on both sides (Figure 1A). F1

In the animals treated with the cutaneous flap ($n$ = 24), a skin flap was raised from the muscular fascia, on the inferior epigastric artery (epigastric flap); a solution containing the AAV vectors was injected at 10 equally spaced subcutaneous sites along the midline of the flap (Figure 1B). In the other group of animals ($n$ = 24) a musculocutaneous flap was obtained by raising the entire left part of the skin paddle on a plane between the panniculus carnosus (which is equivalent to the subcutaneous fat in humans) and the abdominal fascia, while on the right side the medial portion of the flap was left attached to the anterior rectus sheet (transverse rectus abdominis musculocutaneous, TRAM, flap). In this way, the rectus abdominis represented the muscular component of the flap, providing the blood supply to the cutaneous component through the perforator arteries. In the TRAM-treated animals, the viral vector preparations were injected intramuscularly in the same region where each perforator artery arises from the rectus abdominis (Figure 1C).

As described in Table 1, each group of animals was further divided into six subgroups (12 in total; $n$ = 4 per group), according to the vector they received (either AAV-LacZ or AAV-VEGF) and the time of vector administration (0, 7, or 14 day before surgery). The overall results of these experiments are presented in Figure 2, A and B, for the epigastric flap and Figure 2, C and D, for the TRAM flap; these figures show the extent of flap necrosis at day 7 after surgery. In both flap models, a notable beneficial effect of AAV-VEGF injection on flap survival was observed. The flaps treated with AAV-LacZ predictably underwent necrosis in their distal portion, similar to the untreated flaps, in which the extent of the necrotic area reached 37.4 ± 1.8% and 24.4 ± 2.3% of the total flap surface for the cutaneous and the TRAM flaps, respectively (data not shown). As shown in Figure 2B, the treatment with AAV-VEGF significantly reduced epigastric flap necrosis in all of the three paired experimental groups ($P < 0.01$ by two-way analysis of variance). The reduction in the necrotic area was 23.0% F2

balt2/zjh-jpath/zjh-jpath/zjh01005/zjh6633-05a | hurtr | S=8 | 8/11/05 | 7:13 | 4/Color Figure(s): 1,2,4-6 | Art: AJP05-0091 | Input-krb



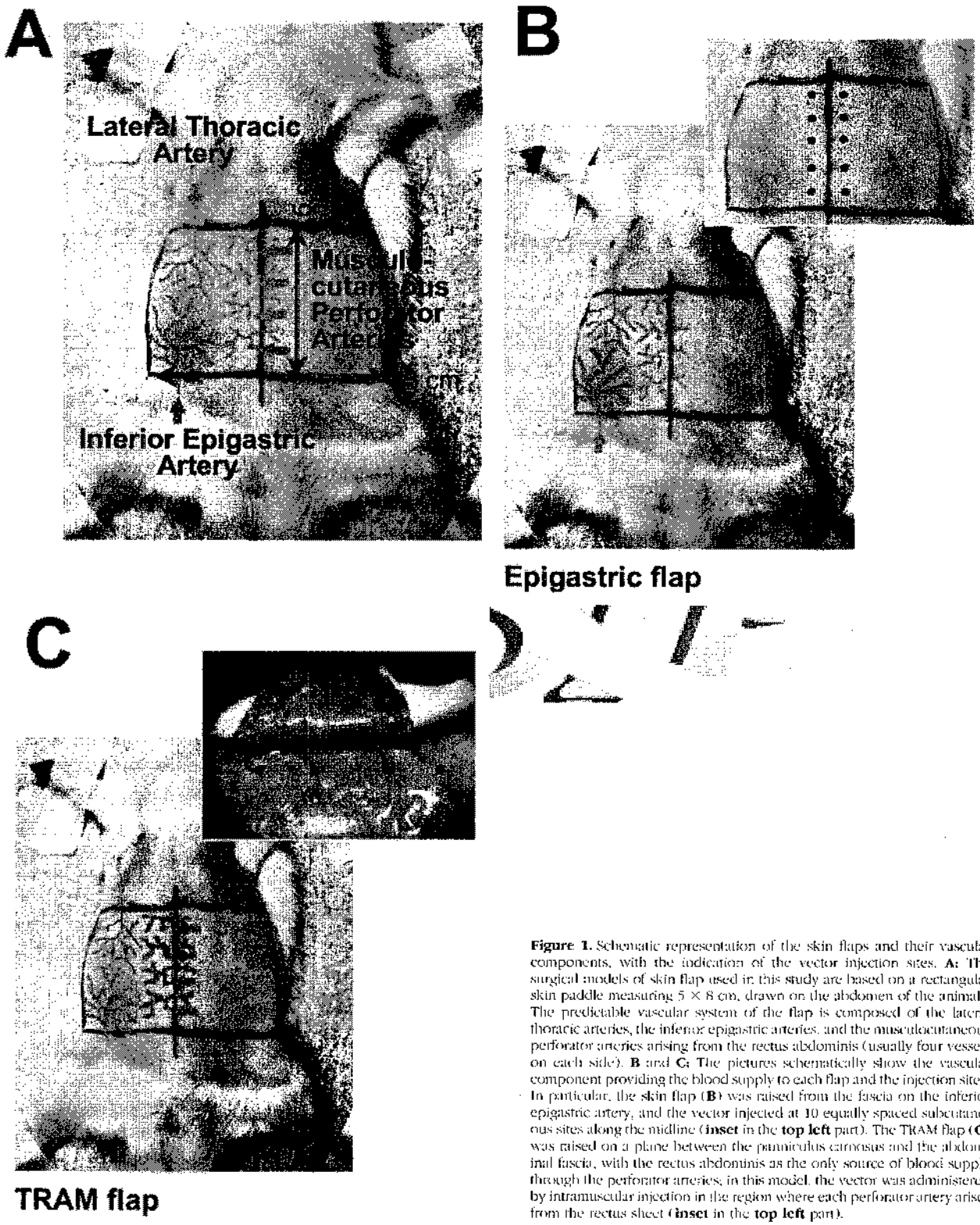


**Figure 1.** Schematic representation of the skin flaps and their vascular components, with the indication of the vector injection sites. **A:** The surgical models of skin flap used in this study are based on a rectangular skin paddle measuring 5 × 8 cm, drawn on the abdomen of the animals. The predictable vascular system of the flap is composed of the lateral thoracic arteries, the inferior epigastric arteries, and the musculocutaneous perforator arteries arising from the rectus abdominis (usually four vessels on each side). **B** and **C:** The pictures schematically show the vascular component providing the blood supply to each flap and the injection sites. In particular, the skin flap (**B**) was raised from the fascia on the inferior epigastric artery, and the vector injected at 10 equally spaced subcutaneous sites along the midline (**inset** in the **top left** part). The TRAM flap (**C**) was raised on a plane between the panniculus carnosus and the abdominal fascia, with the rectus abdominis as the only source of blood supply through the perforator arteries; in this model, the vector was administered by intramuscular injection in the region where each perforator artery arises from the rectus sheet (**inset** in the **top left** part).

when the vector was injected during surgery, and 40.0% and 41.7% when injected 7 or 14 days before surgery, respectively. Similar results were also obtained for the TRAM model ($P < 0.01$), in which the reduction of flap necrosis in the VEGF-treated animals versus LacZ controls was not evident when the vector was injected during surgery, and it was 38.1% and 50.0% when AAV-VEGF was injected at 7 or 14 days before surgery, respectively (Figure 2D).

Taken together, these results indicate that the injection of AAV-VEGF significantly increases flap survival. In particular, posthoc statistical analysis in the TRAM flap

balt2/zjh-jpath/zjh-jpath/zjh01005/zjh6633-05a | hurtr | S=8 | 8/11/05 | 7:13 | 4/Color Figure(s): 1,2,4-6 | Art: AJP05-0091 | Input-krb



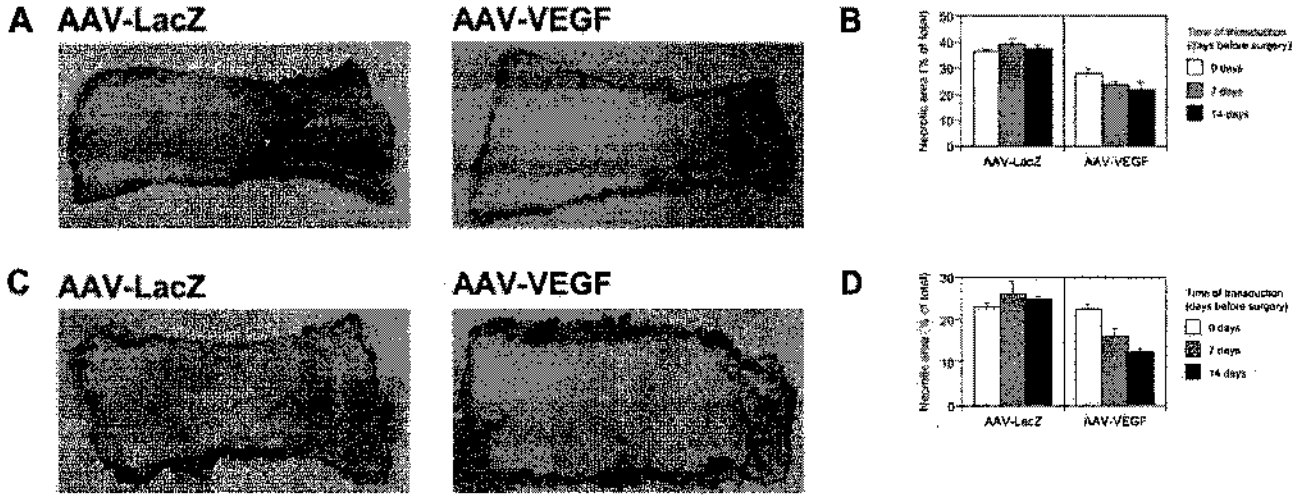


**Figure 2.** Effect of VEGF on skin flap survival at different times of administration. At postoperative day 7, the regions of survival and necrosis were clearly defined in all of the flaps: the surviving skin appeared pink and tender, whereas the distal necrotic portion was black and rigid. **A:** The pictures show two selected epigastric flaps, treated with AAV-LacZ (**left**) and AAV-VEGF (**right**), 14 days before flap elevation. The viability of the skin appears clearly improved after AAV-VEGF administration. **B:** The effect of AAV-VEGF on epigastric flap survival was assessed by injecting the vector at different time points before surgery (0, 7, 14 days). The histograms represent the mean values and SD of the necrotic area relative to the total flap area, as measured by digital planimetry, for each experimental group. **C:** The pictures show two selected TRAM flaps, treated with AAV-LacZ (**left**) and AAV-VEGF (**right**), 14 days before flap elevation. Also in this model, the treatment with AAV-VEGF resulted in a significant improvement in tissue viability. **D:** The effect of AAV-VEGF on TRAM flap survival was assessed by injecting the vector at different time points before surgery (0, 7, 14 days). The histograms represent the mean values and SD of the necrotic area relative to the total flap area, as measured by digital planimetry, for each experimental group.

model indicated that statistical significance was achieved when the vector was administered at 14 days before surgery ($P < 0.05$). Representative pictures of flaps treated with AAV-LacZ or AAV-VEGF 14 days before surgery are shown in Figure 2, A and C, for the epigastric and TRAM flap models, respectively.

### *AAV-VEGF Significantly Improves Flap Survival, Vascularization, and Healing in the TRAM Model*

According to the results obtained by this first set of *in vivo* experiments, a larger number or animals was used for a subsequent experiment in which the efficacy of AAV-VEGF delivery was assessed in the TRAM flap model, followed by histological and immunohistochemical evaluation of the injected tissues. Rats received either AAV-LacZ or AAV-VEGF ($n = 20$ per group) 14 days before surgery, followed by the measurement of the necrotic area at day 7 after surgery. The results of this experiment are shown in Figure 3A. The percentage of the necrotic area was 22.8 ± 2.7% and 8.9 ± 2.8% in the animals treated with AAV-LacZ and AAV-VEGF, respectively, resulting in almost 60% improvement in flap viability ($P < 0.01$).

Flap healing was further assessed for an additional 15 days by measuring the extension of the viable area of the flaps ($n = 8$ for each group). As shown in Figure 3B, treatment with AAV-VEGF determined a marked improvement in the healing process, resulting in >95% flap viability as early as 10 days after surgery and in the almost complete disappearance of the necrotic area at day 22. In contrast, healing was remarkably delayed in the rats

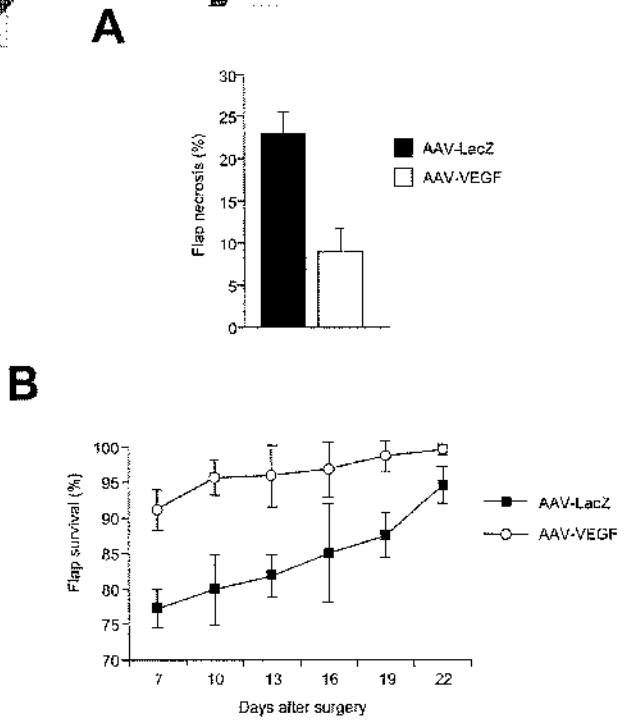


**Figure 3.** Pretreatment with AAV-VEGF significantly improves TRAM flap survival and healing. **A:** The histogram shows the mean and SD of percent flap necrosis measured in 40 rats (20 per group) that were treated with the TRAM flap and injected with either AAV-LacZ or AAV-VEGF at day 14 before flap elevation. Measurements were performed at day 7 after surgery. **B:** The healing process was monitored throughout time after surgery up to 22 days, by measuring the extent of flap survival in animals treated with AAV-LacZ or AAV-VEGF ($n = 8$ per group). The means and SD of survived flap areas are shown at each time point (expressed as a percentage of the total flap area).

balt2/zjh-jpath/zjh-jpath/zjh01005/zjh6633-05a | hurtr | S=8 | 8/11/05 | 7:13 | 4/Color Figure(s): 1,2,4-6 | Art: AJP05-0091 | Input-krb



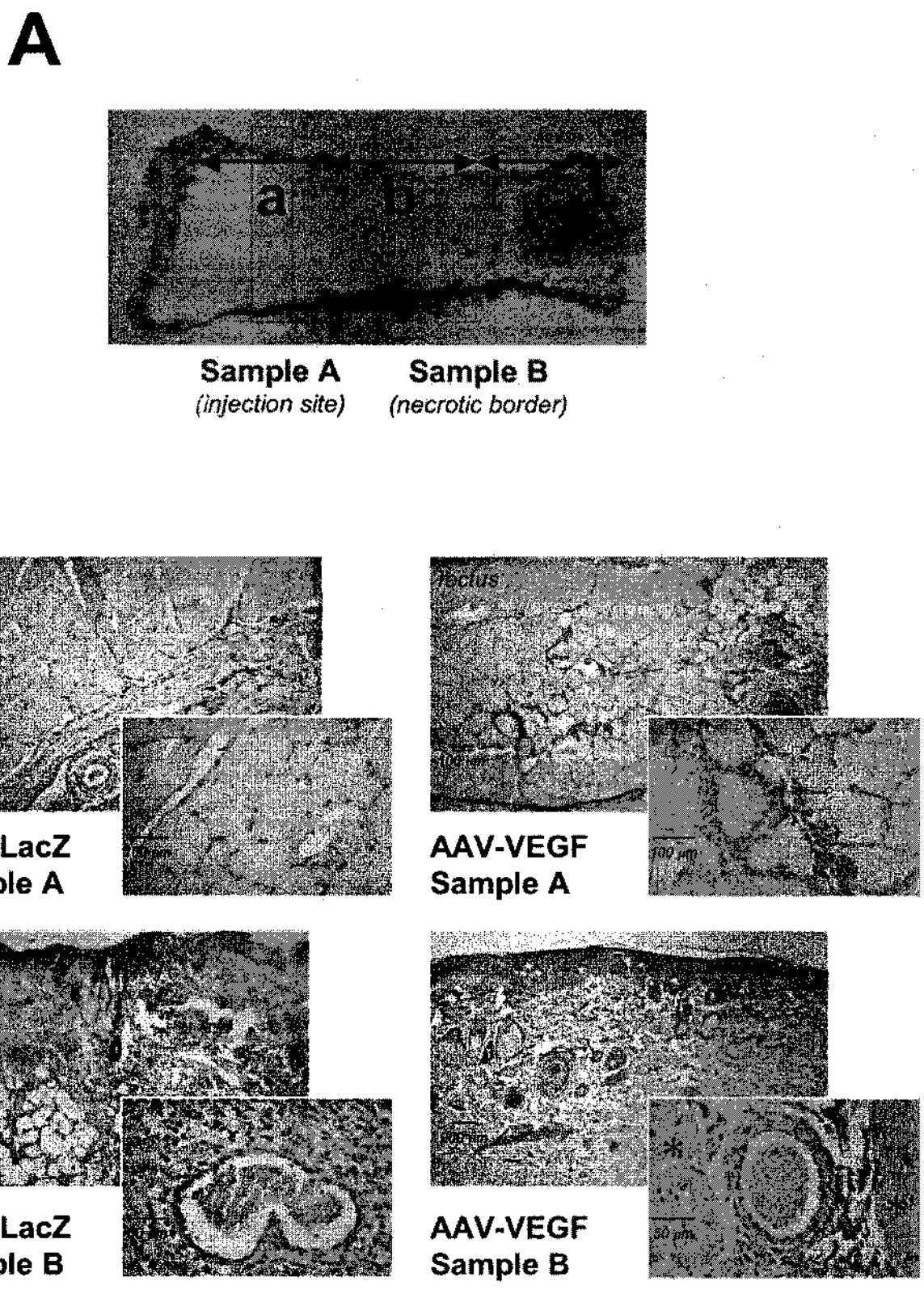


**Figure 4.** Histological sampling and assessment of TRAM flap viability. **A:** Each flap presented three distinguishable zones, according to their distance from the vascular pedicle: a survived zone (**a**), an intermediate zone (**b**), and a necrotic zone (**c**). To histologically examine flap viability, we harvested the skin and the muscular sheet from the injection site (sample A), as well as a more distal cutaneous sample (sample B, at ~3 cm from sample A) from the intermediate zone. **B:** Shown are representative sections of samples A and B from AAV-VEGF-treated (**right**) and control (**left**) animals. At the injection site (sample A), a massive cellular infiltration appeared as a consequence of AAV-VEGF treatment (**top**). More notably, sample B of VEGF-treated flaps showed an intact and viable epithelial layer with conserved tissue architecture, whereas, in control flaps, the epithelium was thin and discontinuous, with massive inflammation and adipose substitution. Myonecrosis was detected only in LacZ-treated flaps, as indicated by the disappearance of the panniculus carnosus (shown by **asterisks** in the VEGF sample). Note the presence of circulating inflammatory cells in the arterial lumen in the **insets**, more abundant in the LacZ-treated as compared to the VEGF-treated samples.

balt2/zjh-jpath/zjh-jpath/zjh01005/zjh6633-05a | hurtr | S=8 | 8/11/05 | 7:13 | 4/Color Figure(s): 1,2,4-6 | Art: AJP05-0091 | Input-krb



treated with AAV-LacZ ($P < 0.01$ by one-way analysis of variance).

To determine whether the improved tissue viability was actually due to a sustained angiogenic response induced by VEGF, representative sections from flap biopsies harvested at day 7 after surgery were examined by histology and immunohistochemistry. All flaps were designed to have three zones (indicated as a, b, and c in Figure 4A), according to their distance from the vascular pedicle: a survived zone (a), from which we took sample A, corresponding to the injection site; an intermediate zone (b), from which we took sample B at ~3 cm from sample A, a region corresponding to the border between viable and necrotic skin; and a necrotic zone (c). Marked differences were observed by histological analysis between AAV-VEGF- and AAV-LacZ-treated animals (Figure 4B). In sample A, the animals injected with AAV-VEGF showed massive cellular infiltration close to the injection site. This finding is consistent with our previous study, in which we injected the same AAV-VEGF vector in the normoperfused skeletal muscle, and observed the recruitment of a large number of proliferating cells in close proximity to the newly formed blood vessels, suggesting an important role of these cells in VEGF-induced neoangiogenesis.[22] In sample B, a remarkable difference was also observed in terms of tissue viability. In the control, AAV-LacZ-treated animals, the epithelial layer was thin and immature, with evidence of acute inflammation, adipose substitution, and myonecrosis (as shown by the almost complete disappearance of the panniculus carnosus); the infiltrating inflammatory cells, mostly monocytes and neutrophils, were dispersed throughout the skin layers, concomitant with a severe disruption of the tissue architecture. In contrast, the morphology was preserved in the AAV-VEGF-treated flaps, as revealed by the presence of an intact epithelial layer and of skin appendages, with only mild and focal inflammation, and poor accumulation of adipose tissue.

To quantify the main differences between the two experimental groups observed by histological examination, three independent researchers blindly assigned a quantitative score for several parameters, including epidermal integrity, inflammation, adipose substitution, and tissue architecture, according to the criteria reported in Table 2. The overall scores obtained from all of the analyzed parameters clearly indicated a better viability of AAV-VEGF-treated flaps, with preservation of tissue architecture very similar to that of the normal skin.

Finally, in the same groups of animals we also assessed the effect of vector transduction on the extent of new blood vessel formation. By using an antibody specific for the endothelial marker CD31, we could detect a massive formation of new capillaries (shown in Figure 5 at different magnifications for one selected animal), both in the proximity of the injection site (sample A) and in the skin of the more distal intermediate zone (sample B). This was most apparent deep to the panniculus carnosus layer, as shown by the insets, resulting in a more than twofold increase in the number of capillaries detectable in the dermal sheet ($P < 0.05$) (Figure 5B). F5

Even more evident were the results obtained by immunostaining the same samples with an antibody that specifically recognizes the smooth muscle-specific isoform of $\alpha$-actin ($\alpha$-SMA), and thus highlights the presence of arterial vessels. As shown in Figure 6A an increase in the number of arteriolae was detected at the level of the injection site (sample A) and, more evidently, in the dermis of the intermediate zone (sample B) in the AAV-VEGF-treated animals (more than threefold increase in the latter area; $P < 0.05$; quantified in the histogram shown in Figure 6B). Several of these arterial vessels, with a diameter in the 20- to 120-$\mu$m range, were filled with erythrocytes (not shown), indicating their functional connection to the systemic circulation. F6

## Discussion

The use of biological agents to promote new blood vessel formation represents an exciting field of research and has recently aroused considerable interest as an innovative approach to treat tissue ischemia in a wide variety of clinical settings. To date, most of the studies have concerned a possible application of therapeutic angiogenesis for the treatment of cardiovascular disorders, such as myocardial infarction and lower limb ischemia. Nevertheless, the same strategy might result of equal interest in many plastic surgery techniques, in which ischemia is often a contributing cause of surgical failure. Tissue necrosis at the distal part of the flaps is generally attributed

**Table 2.** Evaluation of Control Flaps and Flaps Treated with Either AAV-VEGF or AAV-LacZ Using a Quantitative Score Assessing the Indicated Histological Parameters

| Histological score (sample B) | Normal skin | AAV-LacZ | AAV-VEGF |
|---|---|---|---|
| Epidermal integrity (mean number of discontinuities per ×40 microscopic field) 3 = ≤1, 2 = 2 to 4, 1 = ≥5 | 3.0 | 1.2 | 2.9 |
| Skin appendages (mean number of hair follicles, sebaceous glands, and sweat glands per ×40 microscopic field) 3 = ≥15, 2 = 14 to 4, 1 = ≤5 | 2.8 | 1.1 | 1.9 |
| Inflammation (mean cross-sectional area infiltrated by leukocytes per ×40 microscopic field) 3 = ≤10%, 2 = 11 to 49%, 1 = ≥50% | 3.0 | 1.2 | 2.2 |
| Adipose substitution (mean cross-sectional area infiltrated by adipocytes per ×40 microscopic field) 3 = ≤10%, 2 = 11 to 49%, 1 = ≥50% | 3.0 | 1.8 | 2.8 |
| Tissue architecture 3 = preserved, 2 = moderate structural changes, 1 = grossly altered | 3.0 | 1.0 | 2.1 |
| Total score | 14.8 | 6.3 | 11.9 |

balt2/zjh-jpath/zjh-jpath/zjh01005/zjh6633-05a | hurtr | S=8 | 8/11/05 | 7:15 | 4/Color Figure(s): 1,2,4-6 | Art: AJP05-0091 | Input-krb



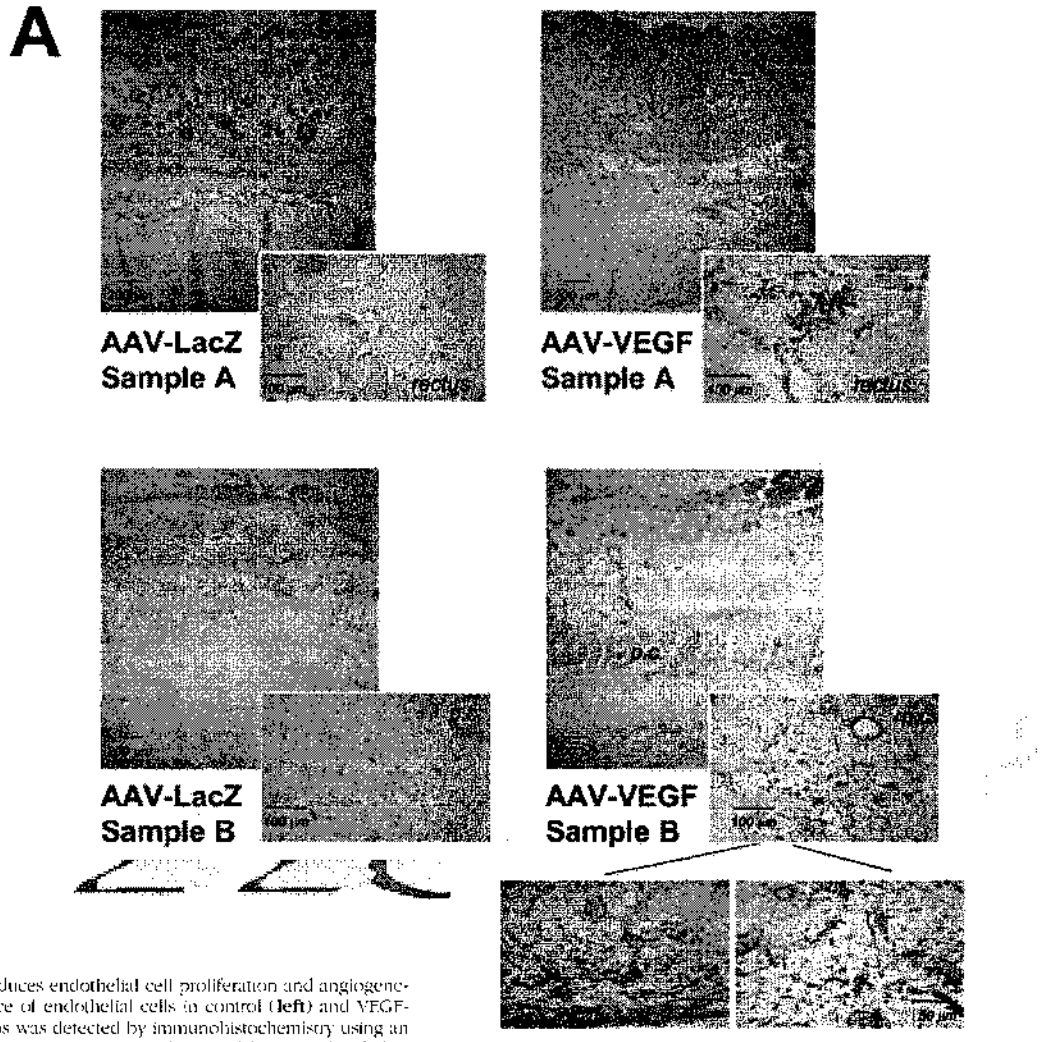


**Figure 5.** VEGF induces endothelial cell proliferation and angiogenesis. **A:** The presence of endothelial cells in control (**left**) and VEGF-treated (**right**) flaps was detected by immunohistochemistry using an anti-CD31 antibody. AAV-VEGF induced the proliferation of endothelial cells at the injection site (sample A), in which several CD31-positive cells infiltrated the interstitial spaces between the fibers of the rectus abdominis muscle (**inset** on the **right**), as well as in the more distal sample B. This endothelial cell proliferation was paralleled by the formation of a great number of new capillaries, most evident at the level of the panniculus carnosus (p.c.), as shown in the **bottom** panels at a higher magnification. **B:** Quantification of capillaries in treated flaps. Counts were obtained from samples B of both AAV-LacZ- and AAV-VEGF-treated flaps. Shown are the means and SD of the counts, expressed as number of capillaries per ×40 field, assuming statistical significance at $P < 0.05$ using a two-tailed *t*-test.

to deficient blood perfusion, and thus should benefit from the induction of therapeutic angiogenesis. Among the number of molecules involved in the angiogenic process, VEGF has been shown to play a central role during the early phases of angiogenesis, promoting endothelial cell migration and proliferation, and preventing their apoptosis.[32]

Several studies have already provided the proof of concept that the administration of exogenous recombinant VEGF enhances the survival of the distal portion of the flap to a certain extent.[3–9] These studies, however, also highlighted an important limitation of such an approach, mainly related to the short half-life of recombinant proteins *in vivo*. In contrast, gene transfer can maintain the production and secretion of the growth factors for prolonged periods, thus sustaining the proangiogenic stimulus throughout time.

Among the vectors currently considered for gene transfer in plastic surgery, those based on adenovirus can mediate high levels of protein expression, but are associated with the disadvantage of producing strong inflammatory and immune reactions, which, on one side, can further compromise tissue viability while, on the other side, lead to the early loss of transgene expression.[33] The drawbacks of adenoviral vectors have already emerged in a recent study, which evaluated the effect of VEGF gene transfer on the survival of epigastric skin flaps.[13]

balt2/zjh-jpath/zjh-jpath/zjh01005/zjh6633-05a | hurtr | S=8 | 8/11/05 | 7:15 | 4/Color Figure(s): 1,2,4-6 | Art: AJP05-0091 | Input-krb



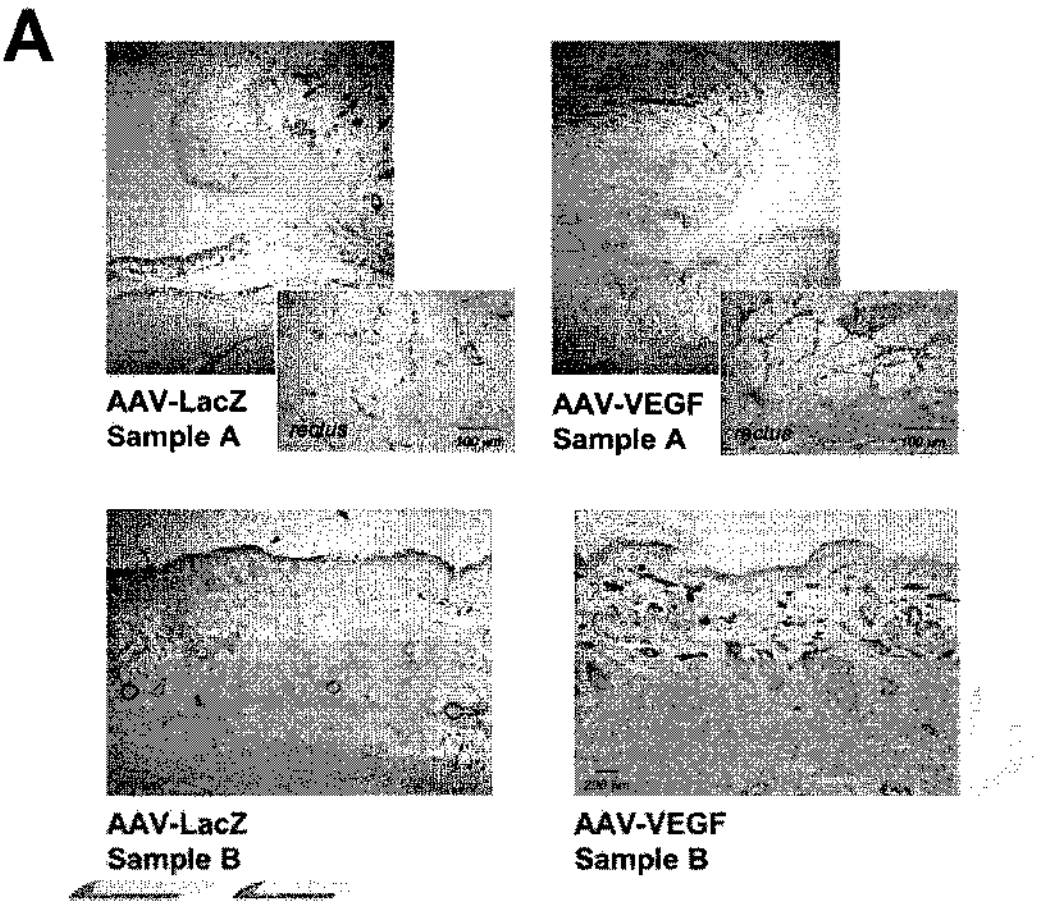


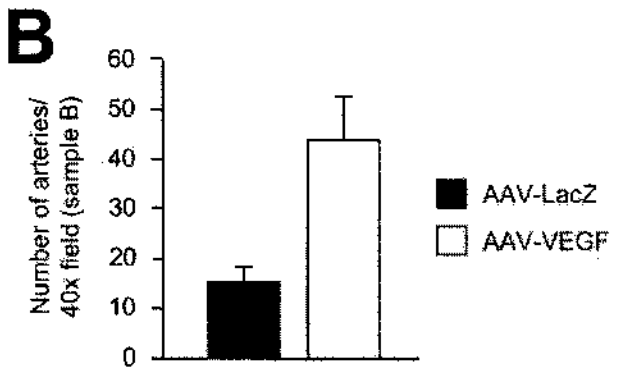


**Figure 6.** VEGF induces the formation of α-SMA-positive arteriolae. **A:** The property of VEGF to sustain the formation of arterial vessels was assessed by immunohistochemistry using an antibody against the α-actin isoform specific for the smooth muscle cells (α-SMA). A modest effect was detected in sample A, with a greater reactivity in the AAV-VEGF-injected muscle (**inset** on the **right**), whereas a remarkable increase in the number of arteriolae was observed after VEGF treatment in the more distal sample B (**bottom**), approximately corresponding to the border between viable and necrotic skin. **B:** Quantification of α-SMA-positive vessels in samples B. Presentation of the data and statistics are as in Figure 5B.

In contrast, a constantly increasing number of preclinical and clinical gene therapy studies exploit vectors based on AAV. We and others have previously demonstrated the exquisite and still unexplained tropism of AAV for muscle cells,[29–31] which suggested that AAV might be the ideal vector to target the muscular component of the musculocutaneous flaps. Starting from these considerations, our study was initially designed as a preliminary control trial to identify the optimal site and time for vector administration. Our results show that the greatest improvement in flap survival can be obtained after intramuscular injection of the vector 14 days before surgery, further strengthening the concept of AAV as an ideal vector to transduce muscle cells for long periods of time. Expression of VEGF significantly improved flap survival, with a macroscopically evident reduction of the necrotic portion, as well as with a significant improvement in tissue viability at histological examination. The beneficial effect of AAV-VEGF on flap survival well correlated with an impressive formation of new blood vessels—both capillaries and arteriolae. At least for the TRAM flap, the clear improvement in tissue viability might be ascribed to a better perfusion through the muscular layer due to a local angiogenic effect of VEGF. Alternatively, secreted VEGF might have diffused from the muscle to the skin layer of the more distal portion of the flap, thus promoting angiogenesis within the derma, in agreement with a series of recent reports showing that AAV vectors delivered to the skeletal muscle are able to

drive the expression and secretion of different molecules into the circulation.[24,28] The increase in the density of arteriolae in the skin distal to the injection site (sample B) in the TRAM model is strongly in favor of the second hypothesis, although we cannot exclude an indirect effect of VEGF through an enhancement of the blood supply.

In accordance with the marked improvement in flap viability after AAV-VEGF transduction, our time course experiment clearly indicates a persistent therapeutic effect of the vector up to 3 weeks after surgery. Although the extent of flap necrosis is usually assessed at no longer that 7 days after flap elevation, reflecting the timing by which the problem appears to be clinically relevant, an increased vascularization driven by VEGF might provide an additional benefit in the following healing process. Our results strongly support this hypothesis, and reinforce the notion that a delivery system able to sustain a prolonged expression of the therapeutic gene is extremely desirable for this kind of therapeutic application.

The observation that the administration of AAV-VEGF is particularly effective when performed preoperatively also supports the usefulness of AAV-mediated therapeutic angiogenesis in elective surgery conditions. Considering that the problem of flap breakdown is especially prevalent in patients who have diabetes, obesity, and peripheral vascular disease,[34] as well as in smokers,[35] it seems reasonable that AAV-VEGF administration during the preoperative phase might represent a useful therapeutic method to enhance blood flow in skin areas undergoing elevation and transposition in high-risk patients. In terms of clinical applications, the observation that the efficacy of AAV-mediated gene transfer is more evident in the TRAM model rather than in the epigastric flap model, renders AAV-VEGF gene transfer even more attractive. In fact, the results obtained from the epigastric flap model, in which the panniculus carnosus (present in rodents but not in humans) represents the major target of AAV vector transduction, cannot be directly extrapolated to the human skin. In contrast, the TRAM flap, including a muscular component in both species, is much more representative of the human condition.

Taken together, our results reinforce the notion that adequate blood supply is an essential requisite for flap survival, and indicate the feasibility of an angiogenic gene therapy approach in plastic and reconstructive surgery. In addition, considering the prolonged gene expression driven by AAV vectors, this delivery system might become a novel and powerful experimental tool to investigate the biological role of other relevant growth factors, as well as their combinations, to find new therapeutic approaches for the treatment of tissue ischemia in plastic surgery. Few recent studies have reported about the angiogenic potential of other factors, such as angiopoietin-1,[36–38] platelet-derived growth factor,[39] and fibroblast growth factor,[40–42] in different animal models of skin flaps. Because AAV vectors enter the cells at high multiplicity of infection, an attractive approach could be the simultaneous administration of different vector preparations, expressing different proteins involved in the angiogenic process.[30]

Although it is the myocardium and the muscles of the lower limb that have been the intended sites of angiogenesis in the majority of studies to date, there is optimism that plastic and reconstructive surgery and its patients could be major beneficiaries of the knowledge currently being accumulated. The various types of flaps, from local skin flaps to complex free flaps could be helped by reinforcement of the natural angiogenic process occurring in the microvasculature. One of the major potential applications of a therapeutic angiogenesis approach using gene therapy will be the design of larger flaps than would otherwise be possible, able to cover tissue defects previously considered too large or complex.

## Acknowledgments

We thank Marina Dapas and Maria Elena Lopez for excellent technical support in AAV vector production, Maria Cristina Prati and Matteo Dell'Omodarme for statistical consultancy, and Suzanne Pavcic for editorial assistance.

## References

1. Hallock GG: Physiological studies using laser Doppler flowmetry to compare blood flow to the zones of the free TRAM flap. Ann Plast Surg 2001, 47:229–233
2. Machens HG, Sallehi J, Weich H, Munch S, Siemers F, Krapohl BD, Herter KH, Kruger S, Reichert B, Berger A, Vogt P, Mailander P: Angiogenic effects of injected VEGF165 and sVEGFR-1 (sFLT-1) in a rat flap model. J Surg Res 2003, 111:136–142
3. Padubidri A, Browne Jr E: Effect of vascular endothelial growth factor (VEGF) on survival of random extension of axial pattern skin flaps in the rat. Ann Plast Surg 1996, 37:604–611
4. Li QF, Reis ED, Zhang WX, Silver L, Fallon JT, Weinberg H: Accelerated flap prefabrication with vascular endothelial growth factor. J Reconstr Microsurg 2000, 16:45–49
5. Kryger Z, Dogan T, Zhang F, Komorowska-Timek E, Shi DY, Cheng C, Lineaweaver WC, Buncke HJ: Effects of VEGF administration following ischemia on survival of the gracilis muscle flap in the rat. Ann Plast Surg 1999, 43:172–178
6. Kryger Z, Zhang F, Dogan T, Cheng C, Lineaweaver WC, Buncke HJ: The effects of VEGF on survival of a random flap in the rat: examination of various routes of administration. Br J Plast Surg 2000, 53:234–239
7. Banbury J, Siemionow M, Porvasnik S, Petras S, Browne E: Improved perfusion after subcritical ischemia in muscle flaps treated with vascular endothelial growth factor. Plast Reconstr Surg 2000, 106:1541–1546
8. Zhang F, Fischer K, Komorowska-Timek E, Guo M, Cui D, Dorsett-Martin W, Buncke HJ, Lineaweaver WC: Improvement of skin paddle survival by application of vascular endothelial growth factor in a rat TRAM flap model. Ann Plast Surg 2001, 46:314–319
9. Zhang F, Richards L, Angel MF, Zhang J, Liu H, Dorsett-Martin W, Lineaweaver WC: Accelerating flap maturation by vascular endothelium growth factor in a rat tube flap model. Br J Plast Surg 2002, 55:59–63
10. Snyder RO, Spratt SK, Lagarde C, Bohl D, Kaspar B, Sloan B, Cohen LK, Danos O: Efficient and stable adeno-associated virus-mediated transduction in the skeletal muscle of adult immunocompetent mice. Hum Gene Ther 1997, 8:1891–1900
11. Greenhalgh DA, Rothnagel JA, Roop DR: Epidermis: an attractive target tissue for gene therapy. J Invest Dermatol 1994, 103:63S–69S

12. Cui L, Li FC, Zhang Q, Qian YL, Guan WX: Effect of adenovirus-mediated gene transfection of vascular endothelial growth factor on survival of random flaps in rats. Chin J Traumatol 2003, 6:199–204
13. Gurunluoglu R, Ozer K, Skugor B, Lubiatowski P, Carnevale K, Siemionow M: Effect of transfection time on the survival of epigastric skin flaps pretreated with adenovirus encoding the VEGF gene. Ann Plast Surg 2002, 49:161–169
14. Ghazizadeh S, Taichman LB: Virus-mediated gene transfer for cutaneous gene therapy. Hum Gene Ther 2000, 11:2247–2251
15. O'Toole G, MacKenzie D, Lindeman R, Buckley MF, Marucci D, McCarthy N, Poole M: Vascular endothelial growth factor gene therapy in ischaemic rat skin flaps. Br J Plast Surg 2002, 55:55–58
16. Neumeister MW, Song YH, Mowlavi A, Suchy H, Mathur A: Effects of liposome-mediated gene transfer of VEGF in ischemic rat gracilis muscle. Microsurgery 2001, 21:58–62
17. Lubiatowski P, Goldman CK, Gurunluoglu R, Carnevale K, Siemionow M: Enhancement of epigastric skin flap survival by adenovirus-mediated VEGF gene therapy. Plast Reconstr Surg 2002, 109:1986–1993
18. Liu PY, Tong W, Liu K, Han SH, Wang XT, Badiavas E, Rieger-Christ K, Summerhayes I: Liposome-mediated transfer of vascular endothelial growth factor cDNA augments survival of random-pattern skin flaps in the rat. Wound Repair Regen 2004, 12:80–85
19. Su H, Lu R, Kan YW: Adeno-associated viral vector-mediated vascular endothelial growth factor gene transfer induces neovascular formation in ischemic heart. Proc Natl Acad Sci USA 2000, 97:13801–13806
20. Kaplitt MG, Leone P, Samulski RJ, Xiao X, Pfaff DW, O'Malley KL, During MJ: Long-term gene expression and phenotypic correction using adeno-associated virus vectors in the mammalian brain. Nat Genet 1994, 8:148–154
21. Nakai H, Herzog RW, Hagstrom JN, Walter J, Kung SH, Yang EY, Tai SJ, Iwaki Y, Kurtzman GJ, Fisher KJ, Colosi P, Couto B, High KA: Adeno-associated viral vector-mediated gene transfer of human blood coagulation factor IX into mouse liver. Blood 1998, 91:4600–4607
22. Xiao W, Berta SC, Lu MM, Moscioni AD, Tazelaar J, Wilson JM: Adeno-associated virus as a vector for liver-directed gene therapy. J Virol 1998, 72:10222–10226
23. Chirmule N, Propert K, Magosin S, Qian Y, Qian R, Wilson J: Immune responses to adenovirus and adeno-associated virus in humans. Gene Ther 1999, 6:1574–1583
24. Kay MA, Manno CS, Ragni MV, Larson PJ, Couto LB, McClelland A, Glader B, Chew AJ, Tai SJ, Herzog RW, Arruda V, Johnson F, Scallan C, Skarsgard E, Flake AW, High KA: Evidence for gene transfer and expression of factor IX in haemophilia B patients treated with an AAV vector. Nat Genet 2000, 24:257–261
25. Monahan PE, Samulski RJ: AAV vectors: is clinical success on the horizon? Gene Ther 2000, 7:24–30
26. Descamps V, Blumenfeld N, Beuzard Y, Perricaudet M: Keratinocytes as a target for gene therapy. Sustained production of erythropoietin in mice by human keratinocytes transduced with an adenoassociated virus vector. Arch Dermatol 1996, 132:1207–1211
27. Hengge UR, Mirmohammadsadegh A: Adeno-associated virus expresses transgenes in hair follicles and epidermis. Mol Ther 2000, 2:188–194
28. Donahue BA, McArthur JG, Spratt SK, Bohl D, Lagarde C, Sanchez L, Kaspar BA, Sloan BA, Lee YL, Danos O, Snyder RO: Selective uptake and sustained expression of AAV vectors following subcutaneous delivery. J Gene Med 1999, 1:31–42
29. Deodato B, Arsic N, Zentilin L, Galeano M, Santoro D, Torre V, Altavilla D, Valdembri D, Bussolino F, Squadrito F, Giacca M: Recombinant AAV vector encoding human VEGF165 enhances wound healing. Gene Ther 2002, 9:777–785
30. Arsic N, Zentilin L, Zacchigna S, Santoro D, Stanta G, Salvi A, Sinagra G, Giacca M: Induction of functional neovascularization by combined VEGF and angiopoietin-1 gene transfer using AAV vectors. Mol Ther 2003, 7:450–459
31. Arsic N, Zacchigna S, Zentilin L, Ramirez-Correa G, Pattarini L, Salvi A, Sinagra G, Giacca M: Vascular endothelial growth factor stimulates skeletal muscle regeneration in vivo. Mol Ther 2004, 10:844–854
32. Ferrara N, Alitalo K: Clinical applications of angiogenic growth factors and their inhibitors. Nat Med 1999, 5:1359–1364
33. Yang Y, Haecker SE, Su Q, Wilson JM: Immunology of gene therapy with adenoviral vectors in mouse skeletal muscle. Hum Mol Genet 1996, 5:1703–1712
34. Hultman CS, Daniza S: Skin-sparing mastectomy flap complications after breast reconstruction: review of incidence, management, and outcome. Ann Plast Surg 2003, 50:249–255
35. Craig S, Rees TD: The effects of smoking on experimental skin flaps in hamsters. Plast Reconstr Surg 1985, 75:842–846
36. Gurunluoglu R, Lubiatowski P, Goldman CK, Carnevale K, Siemionow M: Enhancement of muscle flap hemodynamics by angiopoietin-1. Ann Plast Surg 2002, 48:401–409
37. Lubiatowski P, Gurunluoglu R, Goldman CK, Skugor B, Carnevale K, Siemionow M: Gene therapy by adenovirus-mediated vascular endothelial growth factor and angiopoietin-1 promotes perfusion of muscle flaps. Plast Reconstr Surg 2002, 110:149–159
38. Jung H, Gurunluoglu R, Scharpf J, Siemionow M: Adenovirus-mediated angiopoietin-1 gene therapy enhances skin flap survival. Microsurgery 2003, 23:374–380
39. Carroll CM, Carroll SM, Schuschke DA, Barker JH: Augmentation of skeletal muscle flap survival using platelet derived growth factor. Plast Reconstr Surg 1998, 102:407–415
40. Rashid MA, Akita S, Rezzaque MS, Yoshimoto H, Ishihara H, Fujii T, Tanaka K, Taguchi T: Coadministration of basic fibroblast growth factor and sucrose octasulfate (sucralfate) facilitates the rat dorsal flap survival and viability. Plast Reconstr Surg 1999, 103:941–948
41. Khouri RK, Brown DM, Leal-Khouri SM, Tark KC, Shaw WW: The effect of basic fibroblast growth factor on the neovascularisation process: skin flap survival and staged flap transfers. Br J Plast Surg 1991, 44:585–588
42. Bayati S, Russell RC, Roth AC: Stimulation of angiogenesis to improve the viability of prefabricated flaps. Plast Reconstr Surg 1998, 101:1290–1295

ARTICLE doi:10.1016/j.ymthe.2004.08.007

# Vascular Endothelial Growth Factor Stimulates Skeletal Muscle Regeneration *in Vivo*

Nikola Arsic,[1] Serena Zacchigna,[1] Lorena Zentilin,[1] Genaro Ramirez-Correa,[1] Lucia Pattarini,[1] Alessandro Salvi,[2] Gianfranco Sinagra,[2] and Mauro Giacca[1,3,*]

[1]*Molecular Medicine Laboratory, International Center for Genetic Engineering and Biotechnology, Padriciano 99, 34012 Trieste, Italy*
[2]*Cardiology Unit, Ospedale di Cattinara, Trieste, Italy*
[3]*Scuola Normale Superiore and Istituto di Fisiologia Clinica of CNR, Area della Ricerca, Via Moruzzi 1, 56100 Pisa, Italy*

*To whom correspondence and reprint requests should be addressed at the Molecular Medicine Laboratory, ICGEB, Padriciano 99, 34012 Trieste, Italy. Fax: +39 040 226555. E-mail: giacca@icgeb.org.*

Available online 17 September 2004

**Vascular endothelial growth factor (VEGF) is a major regulator of blood vessel formation during development and in the adult organism. Recent evidence indicates that this factor also plays an important role in sustaining the proliferation and differentiation of different cell types, including progenitor cells of different tissues, including bone marrow, bone, and the central nervous system. Here we show that the delivery of the 165-aa isoform of VEGF-A cDNA using an adeno-associated virus (AAV) vector exerts a powerful effect on skeletal muscle regeneration *in vivo*. Following ischemia-, glycerol-, or cardiotoxin-induced damage in mouse skeletal muscle, the delivery of AAV-VEGF markedly improved muscle fiber reconstitution with a dose-dependent effect. The expression of both VEGF receptor-1 (VEGFR-1) and VEGFR-2 was upregulated both in the satellite cells of the damaged muscles and during myotube formation *in vitro;* the VEGF effect was mediated by the VEGFR-2, since the transfer of PlGF, a VEGF family member interacting with the VEGFR-1, was ineffective. These results are consistent with the observation that VEGF promotes the growth of myogenic fibers and protects the myogenic cells from apoptosis *in vitro* and prompt a therapeutic use for VEGF gene transfer in a variety of muscular disorders.**

**Key Words: muscle, gene therapy, adeno-associated virus, vascular endothelial growth factor, vascular endothelial growth factor receptor-2**

## Introduction

Vascular endothelial growth factor-A (VEGF-A) is a main regulator of blood vessel formation during embryogenesis and a potent inducer of neovascularization during adult life. The biological effects of the VEGF family members are transduced by three main receptors: VEGFR-1 (Flt-1), VEGFR-2 (KDR, Flk-1), and VEGFR-3 (Flt-4). The VEGFR-2 is the main receptor that mediates the angiogenic and permeabilizing effects of VEGF-A, through its powerful activity on endothelial cell proliferation and migration. The precise role of the other receptors in the angiogenic process still remains poorly understood; VEGFR-1 has been proposed as a decoy receptor, limiting the access of free VEGF to VEGFR-2, while VEGFR-3 seems to have a fundamental role on the lymphatic endothelium mainly through interaction with VEGF-C and VEGF-D (for reviews, see [1–3]).

Originally described as an endothelial-specific growth factor, recent evidence suggests that the effects of VEGF-A might extend to a variety of other cell types. In particular, the factor appears to have a direct neuroprotective potential, preventing neuronal cell death from ischemia and promoting neurogenesis *in vitro* and *in vivo* [4–6]. The demonstration that VEGF receptors are actually expressed by Schwann cells as well as by neurons is consistent with the direct trophic effect of VEGF-A on these cells [7]. Recently, the ability of VEGF-A to promote hepatocyte proliferation by the selective activation of VEGFR-1 has been exploited to reduce liver damage in mice exposed to a hepatotoxin [8]. Furthermore, VEGF-A and its receptors have been shown to play an important role during cartilage and bone formation, by promoting skeletogenesis; this effect might be secondary to the induction of neoangiogenesis into the perichondrium and the primary ossification center or might result from the direct promotion of osteoblast migration and differentiation [9–12]. Smooth muscle cells have also been shown to express both VEGFR-1 and VEGFR-2 and to respond to VEGF-A chemoattraction in culture [13,14].



1525-0016/$30.00

Finally, the effect of VEGF-A on hematopoietic cells has been described by several groups, showing that this factor is able to mediate monocyte chemotaxis [15], hematopoietic stem cell survival [16], and the recruitment of endothelial progenitor cells [17], through its interaction with VEGFR-1.

We have recently exploited the potential of vectors based on the adeno-associated virus (AAV)—which offer a unique opportunity to study the effects of gene expression for prolonged periods of time *in vivo*, in the absence of an inflammatory or immune response [18–20]—to assess the powerful angiogenic effect of the 165-aa isoform of VEGF-A (hereafter, VEGF) *in vivo* [21]. In the course of our studies, we unexpectedly observed that the expression of VEGF in the normal mouse skeletal muscle also resulted in the appearance of a notable subset of muscle fibers displaying a central nucleus, a widely recognized hallmark of muscle regeneration. This finding raises the important possibility that VEGF might also exert a direct effect on myogenesis *in vivo*, consistent with the observations that hypoxic muscle fibers express both VEGF and its receptors [22] and that the factor plays an important role in myoblast migration and survival [23].

Here we specifically demonstrate that AAV-VEGF administration exerts a powerful effect on muscle survival and regeneration following different types of muscle damage. This effect is mediated by its interaction with VEGFR-2 and involves the protection of myogenic cells from apoptosis and the stimulation of myogenic fiber growth. This observation prompts a therapeutic use of AAV-VEGF in a variety of muscular disorders.

## RESULTS

### Long-Term VEGF Expression in Skeletal Muscle Induces Muscle Fiber Regeneration

To investigate directly whether VEGF might affect the growth of skeletal muscle, we injected a purified AAV-VEGF preparation into the normoperfused right tibialis anterior muscles of six mice. Real-time PCR quantification of transgene expression in a parallel set of animals indicated that, under these conditions, the hVEGF mRNA is already detectable at 3 days after transduction and that its levels progressively increase over time (Supplementary Fig. 1), a kinetics that is consistent with previous observations [24]. One month after injection, a notable subset of muscle fibers (>5%) evidently displayed a central nucleus, a widely recognized hallmark of muscle regeneration (Fig. 1A). This effect was not evident after injection of an AAV vector expressing LacZ in a matched group of control animals (Fig. 1A) or of a variety of other AAV vectors used in the laboratory (not shown). In addition, this effect persisted for at least 3 months after transduction.

To quantify this effect better, we measured the areas of the muscle fiber cross sections in the AAV-VEGF- and AAV-LacZ-injected animals. The distribution of these values was relatively narrow and symmetric in the AAV-LacZ-injected muscles, with >75% of the fibers in the range $1–2 \times 10^3$ $\mu m^2$, and was indistinguishable from the uninjected normal muscle (not shown; Fig. 1B). In contrast, the fiber area distribution of the AAV-VEGF-expressing muscles skewed toward the left and included almost 20% of the fibers with a size of $<1 \times 10^3$ $\mu m^2$ (as opposed to 10.7% in the normal muscle). In addition, this distribution was also much broader toward the right side, with almost 20% of the fibers being hypertrophic, with an area of $>2.5 \times 10^3$ $\mu m^2$ (1% in the control muscle). The two distributions were different with a high statistical significance ($P < 1 \times 10^{-4}$).

Finally, we also observed that when AAV-VEGF was injected into the gastrocnemius or the tibialis anterior, prior to the induction of acute ischemia by the resection of the femoral artery, the tissue viability of the ischemic area was remarkably preserved at day 20 after surgery, with the damaged muscle showing large areas containing small regenerating fibers with a central nucleus (Fig. 1C). A more extensive survey of the protective and proregenerative effect of AAV-VEGF injection after acute ischemia is shown in Supplementary Fig. 2.

### VEGF Promotes the Growth of Myogenic Fibers and Protects Myogenic Cells from Apoptosis

The above-reported observations suggest that, in addition to its well-documented angiogenic properties, VEGF might also exert a direct effect on muscle fibers. We reasoned that these effects would imply that the muscle cells should express at least one of the VEGF receptors and therefore looked for the presence of VEGFR-1 and VEGFR-2 in C2C12 myogenic cells and in primary mouse myoblasts. We detected expression of these receptors in both cell types through RT-PCR amplification of the total RNAs from these cells and by Western blotting on total cell lysates (not shown). Of note, we found that the expression of both receptors was strikingly increased upon switching the cultures to a differentiation medium. As shown by immunocytochemistry, myotubes formed by the differentiation of C2C12 cells (Fig. 2A) expressed a myogenic differentiation marker—myosin heavy chain (MHC)—as well as high levels of VEGFR-1 and VEGFR-2. The expression of both receptors was already detectable as early as 2 days after switching the cultures to the differentiation medium and subsequently remained very high. The same effects were observed upon differentiation of the primary myoblasts from mouse skeletal muscle (Supplementary Fig. 3).

To assess the activity of VEGF along the differentiation process, we switched C2C12 cells at 85% confluence to a differentiating medium and either supplemented them or not with recombinant VEGF at a concentration of 100

doi:10.1016/j.ymthe.2004.08.007

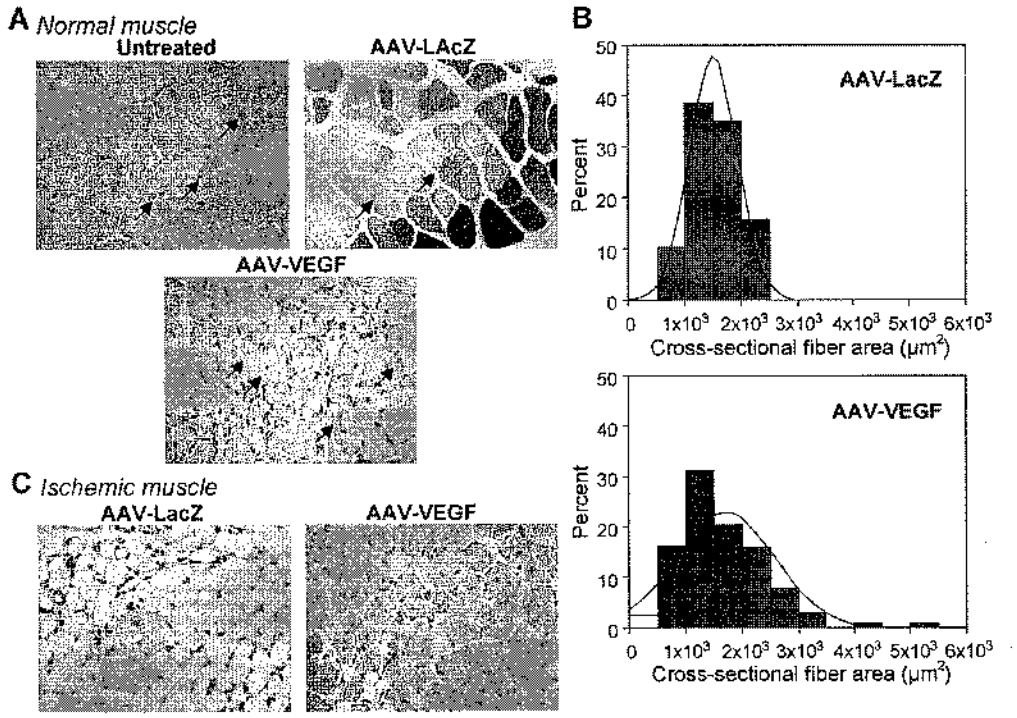


FIG. 1. Sustained expression of VEGF in normoperfused and ischemic skeletal muscle induces muscle fiber regeneration. (A) Hematoxylin-stained sections of normoperfused muscle tibialis anterior from untreated and AAV-LacZ- or AAV-VEGF-injected mice, at 1 month after transduction. Muscles injected with AAV-LacZ were also stained for β-galactosidase expression. Long-term expression of VEGF in normoperfused muscles induced the appearance of small fibers with a central nucleus (arrows), a hallmark of an ongoing regeneration process. (B) Fiber size analysis in normal muscles injected with AAV-LacZ or AAV-VEGF. The histograms show the distribution of the fiber cross-sectional areas ($\mu m^2$) with a normal distribution curve superimposed. Data were obtained from the analysis of 20 cross sections from six different animals per group. The fiber area distribution of the AAV-VEGF-expressing muscles skewed toward the left compared to the control and also included a significant number of fibers with large cross-sectional areas. (C) Hematoxylin and eosin-stained histological sections of AAV-LacZ- and AAV-VEGF-treated muscles at 20 days after induction of acute ischemia. A massive fiber loss with adipose substitution was evident in control ischemic muscles; in contrast, the VEGF-treated samples showed substantial recovery, with the presence of several regenerating fibers (×400 original magnification).

ng/ml. As shown in Fig. 2B, the number of myotubes expressing MHC, detected by immunofluorescence, at day 3 from induction was clearly increased in the cultures supplemented with VEGF. In particular, in the cultures without VEGF, >80% of MHC-positive cells were mononucleated (myocytes) and <2.5% of the multinucleated myofibers contained three or more nuclei. In contrast, the distribution of the number of nuclei was far more dispersed in the cultures treated with VEGF, with ~50% of the MHC-positive cells being mononucleated and >20% of the myofibers containing three or more nuclei per fiber ($P < 1 \times 10^{-4}$). Consistent with the profusogenic role of VEGF, the length of the mono- or polynucleated MHC-positive cells was significantly increased in the cultures exposed to VEGF ($P < 0.05$; Fig. 2C).

The increase in the number, length, and nuclear content of the differentiated C2C12 cells upon VEGF treatment clearly indicated that this growth factor has an important effect in promoting muscle fiber growth. This notion was further reinforced by the analysis of the rate of C2C12 cell proliferation after treatment with VEGF, as measured by the 1-(4,5-dimethylthiazol-2-yl)-3,5-diphenylformazan (MTT) assay scoring for cell metabolic activity. Under both proliferating and differentiating conditions, the addition of VEGF determined a decrease in the proliferation rate of the cells, with a dose-dependent response (Fig. 2D). The same effect was also observed by exposing primary mouse myoblasts to differentiating conditions in the presence of VEGF (Supplementary Fig. 4A).

We also explored the possibility that the increased differentiation promoted by VEGF might be paralleled by the protection of these cells from apoptotic cell death. To address this issue, we treated C2C12 cells with camptothecin (50 nM), a well-known apoptosis-triggering agent, for 5 h and analyzed the percentage of cells reactive to annexin V on the surface by flow cytometry (Fig. 2E). The percentage of cells expressing this marker—but still excluding propidium iodide, an indicator of necrosis—decreased from 29.0 to 7.5% after treatment with hrVEGF (50 ng/ml). In a consistent manner, the protective effect of VEGF was highly decreased (21.2% of annexin V-positive cells) when the cells were also treated with SU1498 (5 μM), an inhibitor of the VEGFR-2 tyrosine

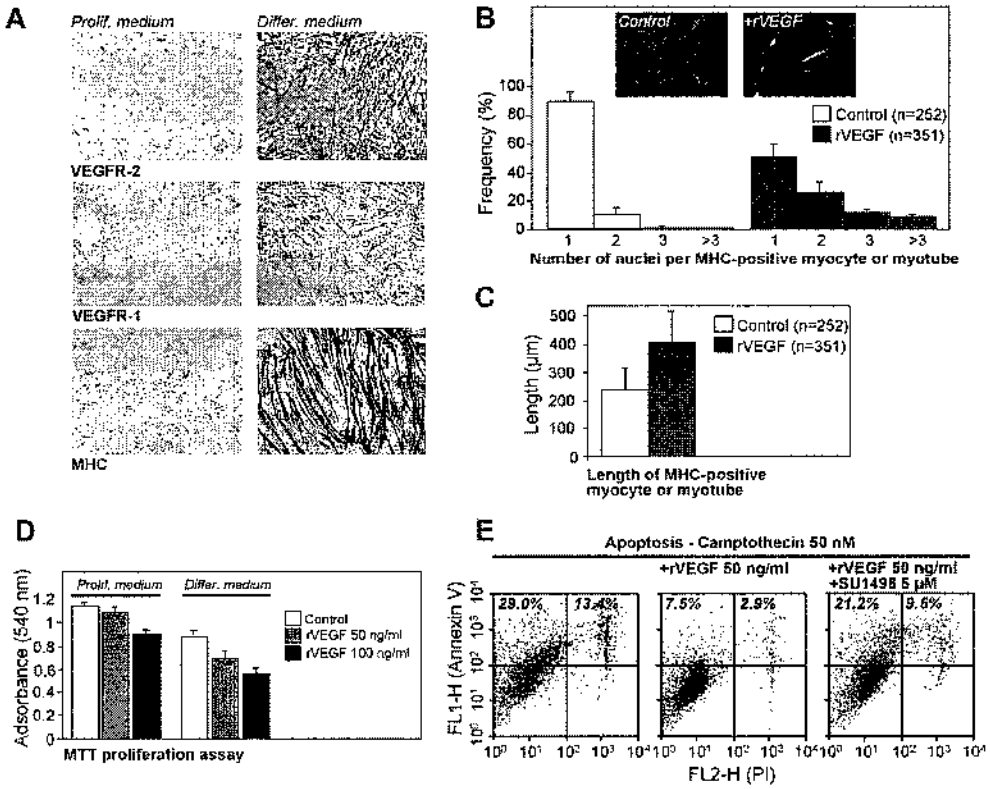


FIG. 2. Effects of VEGF on myogenic cells *in vitro*. (A) Immunocytochemistry performed on C2C12 cells using specific anti-mouse VEGFR-2, VEGFR-1, and slow myosin heavy chain (MHC) antibodies. Cells under proliferating conditions showed very low levels of positivity for all three antibodies (images on the left). In contrast, both VEGF receptors were markedly upregulated in cells cultured for 4 days in differentiation medium (images on the right), showing massive myotube formation and positive staining for the differentiation marker MHC. (B) Frequency distribution of the number of nuclei present in differentiated C2C12 cells with or without treatment with VEGF (100 ng/ml). Cells were cultured under differentiating conditions for 3 days followed by immunofluorescence with an antibody against MHC. The histograms show the frequency distribution of the number of nuclei present in the MHC-positive myocytes (one nucleus) and myofibers (two or more nuclei). After VEGF treatment, the total number of MHC-positive cells was significantly increased (351 vs 252 in 10 microscopic fields from four independent experiments; $P < 0.01$), with a higher content of multinucleated myofibers. Representative immunofluorescence images are shown at the top. (C) Length of MHC-positive myocytes and myotubes. The length of the MHC-positive, differentiating C2C12 cells of the experiment described in B was significantly increased after treatment with VEGF. (D) MTT proliferation assay. In C2C12 cells, the addition of VEGF decreased the cell proliferation rate, with a dose-dependent response, during proliferation as well as in the early phase of differentiation. (E) Flow cytometry analysis of C2C12 cells stained for annexin V reactivity and propidium iodide (PI) incorporation after treatment with camptothecin. The percentage of annexin-positive and PI-negative apoptotic cells (upper left quadrants) induced by the camptothecin treatment was significantly decreased in the presence of recombinant VEGF 50 ng/ml. The protective effect of VEGF was highly diminished when the cells were also treated with SU1498, an inhibitor of the VEGFR-2 tyrosine kinase activity.

kinase activity. This observation also suggests the specific involvement of the VEGFR-2 in mediating the antiapoptotic effect of VEGF. We noticed similar findings in primary myoblasts treated with camptothecin in the presence or absence of hrVEGF (Supplementary Fig. 4B).

### The Delivery of AAV-VEGF Promotes Dose-Dependent Recovery after Muscle Damage

To explore the therapeutic potential of AAV-VEGF administration after skeletal muscle damage independent of hypoxia, we studied the effects of AAV-VEGF transduction in CD1 mice after glycerol (50% v/v) injection into the tibialis anterior muscle. This treatment resulted in the destabilization of the cytoplasmic membrane followed by cell death. In the absence of treatment, muscle regeneration was brought to a complete recovery in ~35 days. We administered doses of $3 \times 10^8$ AAV-VEGF vector particles 5 days before glycerol injection, immediately after glycerol, or 5 days after glycerol, to assess the effects of timing of vector administration. We sacrificed the treated animals at day 20 after injury and three independent investigators who were blinded to the experimental procedures evaluated the extent of the damaged area in transverse muscle sections. At this time point, the control muscles still showed a large area of degeneration (>15% of the transversal muscle section area), with a massive substitution of muscle fibers with adipose tissue and only a few regenerating muscle fibers (Fig. 4A). In contrast, all the AAV-VEGF-treated muscles showed a remarkable reduction in the damaged area (Fig.

doi:10.1016/j.ymthe.2004.08.007

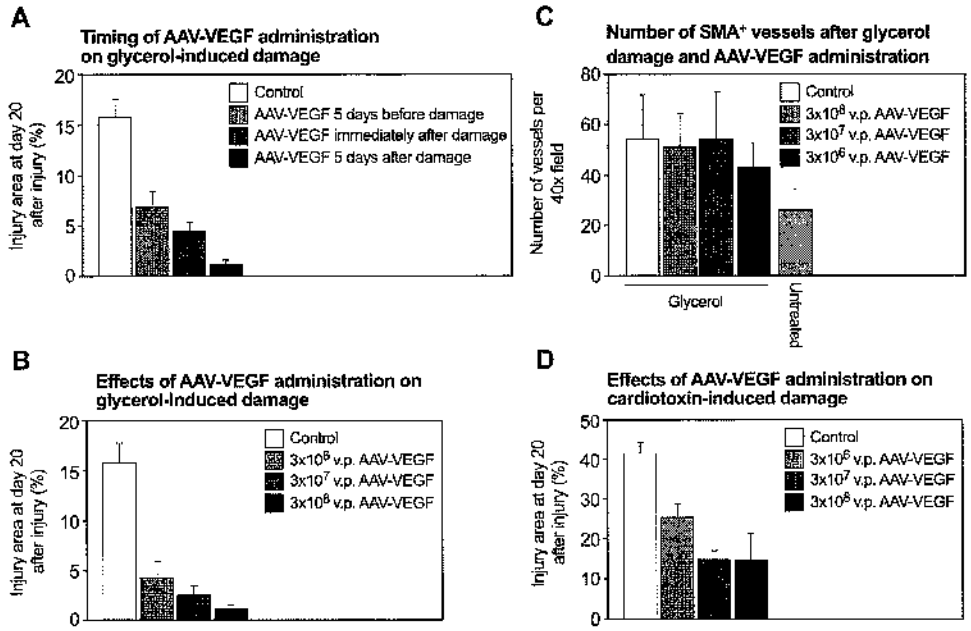


FIG. 3. Quantification of the VEGF protective effects on glycerol- and cardiotoxin-induced muscle damage. (A) Quantification of injured areas in digital images of muscle sections treated with AAV-VEGF at different time points after glycerol damage. Doses of $3 \times 10^8$ viral particles were administered 5 days before, immediately after, or 5 days after injury; analysis of the injured area was performed 20 days after injury. The results of these experiments clearly show that the maximum efficacy was obtained by injecting the vector 5 days after injury ($P < 0.01$ for the comparison between the most effective treatment with any of the other two). (B) Quantification of injured areas in regenerating muscles at 20 days after glycerol injury. The injection of increasing doses of AAV-VEGF at day 5 after injury (from $3 \times 10^6$ to $3 \times 10^8$ viral particles) dramatically improved the regeneration process in a dose–response manner ($P < 0.001$ for all doses). (C) Quantification of α-SMA-positive blood vessels in glycerol-injured muscles. Animals (5 per group) were injured with glycerol and 5 days later injected with PBS or AAV-LacZ (control groups) or with increasing doses of AAV-VEGF165. Animals were then sacrificed 20 days after muscle injury and muscle sections were immunostained for α-SMA. The histograms show the means and SD of the numbers of vessels per microscopic field. The column on the right (Untreated) shows the number of vessels in normal, untreated muscles for comparison. (D) Quantification of injured areas in control and AAV-VEGF-treated muscle sections at 20 days after cardiotoxin-induced damage, showing dose–response reduction of the damaged areas after injection of AAV-VEGF ($P < 0.001$ for all vector doses).

3A). Maximum efficacy was obtained by injecting the vector 5 days after injury (damage in <1% of the transversal muscle section area, compared with ~4 and ~7% for the simultaneous injection and the injection before injury, respectively ($P < 0.01$ for the comparison between the most effective treatment with any of the other two; Fig. 3A)). The observation that the highest efficacy of AAV-VEGF administration is obtained when the vector is injected after the damage is consistent with the notion that VEGF might affect myogenesis directly in addition to its well-established proangiogenic role.

We proceeded to investigate the effects on muscle regeneration of different doses of AAV-VEGF (from $3 \times 10^6$ to $3 \times 10^8$ viral particles) injected 5 days after glycerol-induced damage. A remarkable dose-dependent response was observed. The degenerated area was ~4% of the muscle section with the lowest AAV-VEGF amount, ~3% with the intermediate amount, and less than 1% with the highest amount ($P < 0.001$ for all doses; Fig. 3B shows quantification and Fig. 4 shows histology). In the last group of animals, the entire damaged region was replaced by regenerating muscle fibers showing a central nucleus (Fig. 4D). In the same group of animals, we also counted the number of blood vessels after immunostaining with an antibody against smooth muscle α-actin. We found that, in all the injured animals, the number of arteriolae was slightly increased (~2.5 times) compared to normal muscles, irrespective of the dose of injected vectors; this small increase is most likely due to the inflammatory response after muscle injury (Fig. 3C). This result is again consistent with the notion that the effect on VEGF on muscle regeneration is not mediated by its angiogenic activity.

Finally, we injected the same scalar doses of AAV-VEGF into the tibialis anterior muscles of mice that were treated, 5 days in advance, with 1 mM cardiotoxin, a powerful inducer of muscle fiber degeneration. The damage induced by this treatment is more severe than that obtained with glycerol, with broader fiber degeneration and extensive infiltration of inflammatory cells (shown at day 20 after damage in Fig. 5A); in the absence of treatment, muscle fiber recovery is complete after ~40

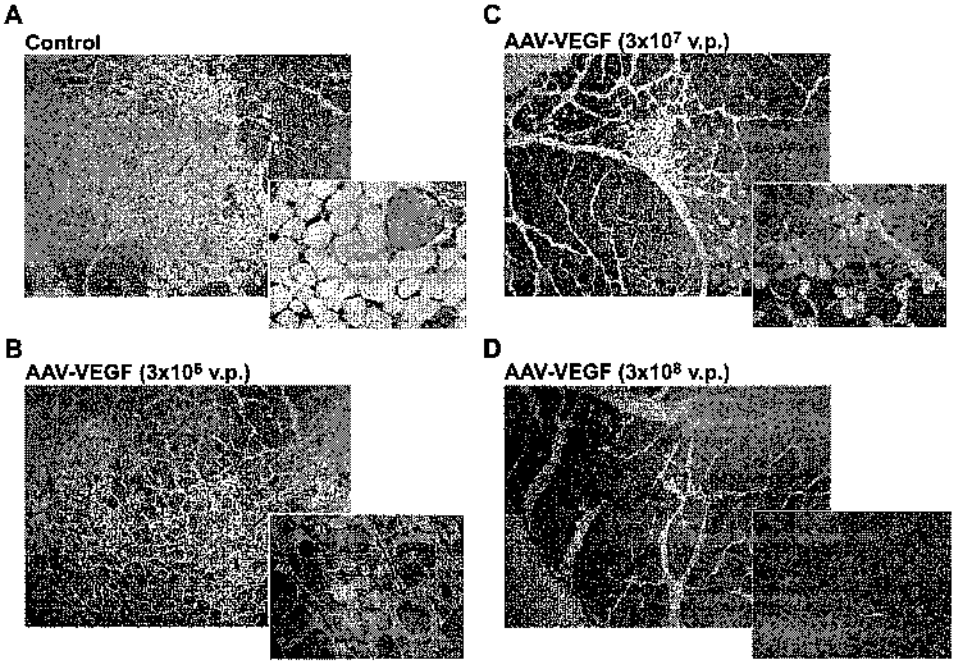


FIG. 4. Histological sections of glycerol-damaged muscles after AAV-VEGF treatment. (A) Hematoxylin and eosin-stained muscle section at day 20 after glycerol injury. The muscle was injected with PBS 5 days after damage. The inset shows a 400× original magnification of the injured area, showing massive fiber loss. (B–D) Glycerol-injured muscles were injected with different doses of AAV-VEGF (from $3 \times 10^6$ to $3 \times 10^8$ viral particles) at day 5 after injury; animals were sacrificed at day 20 after injury. The marked improvement in muscle regeneration correlates with the number of administered vector particles.

days (not shown). Treatment with AAV-VEGF resulted in a remarkable improvement in the regeneration process. At day 20 after injury, with the lowest dose ($3 \times 106$ viral particles), the damaged area encompassed ~25% of the transversal muscle section area, compared with >40% of the control ($P < 0.01$). The size of the injured area was lower still with the two higher AAV doses (~13% for both doses; Fig. 3D shows quantification and Figs. 5A–5D show histology). Recovery was almost complete at day 20 after injury with the use of even higher doses of AAV-VEGF ($9 \times 10^{11}$ viral particles; data not shown).

### The *in Vivo* Activity of VEGF on Muscle Fiber Regeneration is Mediated by VEGFR-2

The finding that VEGF exerts a powerful role on muscle fiber regeneration *in vivo* implies that the skeletal myoblasts and the regenerating fibers express one or more VEGF receptors, as observed on the differentiating

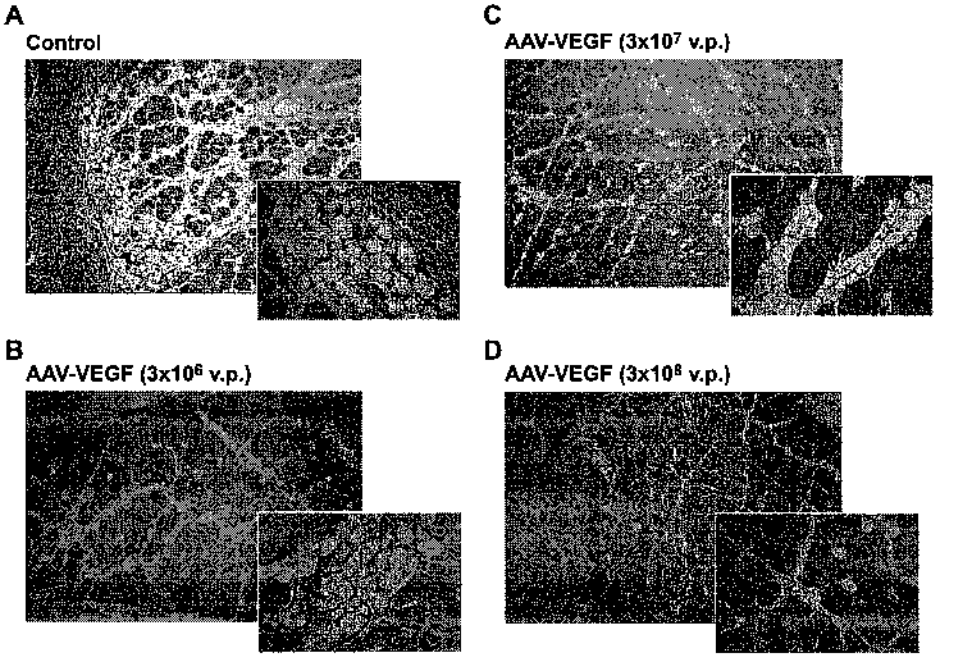


FIG. 5. AAV-VEGF promotes recovery of muscle injury after cardiotoxin injection. (A–D) The tibialis anterior muscles of mice were injected with 25 μl of 1 mM cardiotoxin. Escalating doses of AAV-VEGF ($3 \times 10^6$, $3 \times 10^7$, $3 \times 10^8$ viral particles) were injected into damaged muscles at 5 days after cardiotoxin injection. Hematoxylin and eosin-stained muscle sections were examined 20 days after injury. A remarkably faster, dose-dependent regeneration was observed in the AAV- VEGF-injected animals (B to D) compared to controls (A).

doi:10.1016/j.ymthe.2004.08.007

C2C12 and primary myoblast cultures *in vitro*. We therefore investigated the presence of VEGFR-1 and VEGFR-2 in normal mouse skeletal muscle as well as at different time points after glycerol-induced damage.

Normal muscle fibers did not express levels of VEGFR-1 or VEGFR-2 detectable by immunohistochemistry; in contrast, injury resulted in a marked increase in the presence of these receptors (Fig. 6). In particular, both receptors were highly expressed by elongated cells surrounding the newly formed fibers—identifiable by the presence of a central nucleus—with a half-moon appearance resembling that of activated satellite cells at the edge of the regenerating fibers. Expression was detectable early after injury and persisted until the late stages of the regenerative process. In addition, we also found highly expressed VEGFR-2 on the surface of mature muscle fibers at early time points after injury (shown at day 7 after injury in Fig. 6).

Which receptor mediates the muscle regenerative effect of VEGF? To address this question, we constructed an AAV vector expressing the mouse placental growth factor (PlGF), a member of the VEGF family that specifically targets VEGFR-1 [25,26]. We assessed expression of PlGF from this vector by Western blotting following the transduction of CHO cells in culture (not shown). We injected different doses of AAV-PlGF into the tibialis anterior muscles of mice 5 days after glycerol-induced damage, similar to the experiments performed with AAV-VEGF. However, in contrast with AAV-VEGF, we could detect no effect on the extent of the damaged area. Even one dose of $1.2 \times 10^{11}$ AAV-PlGF viral particles, which is 400 times higher than the dose of AAV-VEGF that reduced muscle damage to <1% (Fig. 3B), only marginally affected the area of muscle degeneration (Fig. 7). This result strongly suggests that the effect of VEGF on

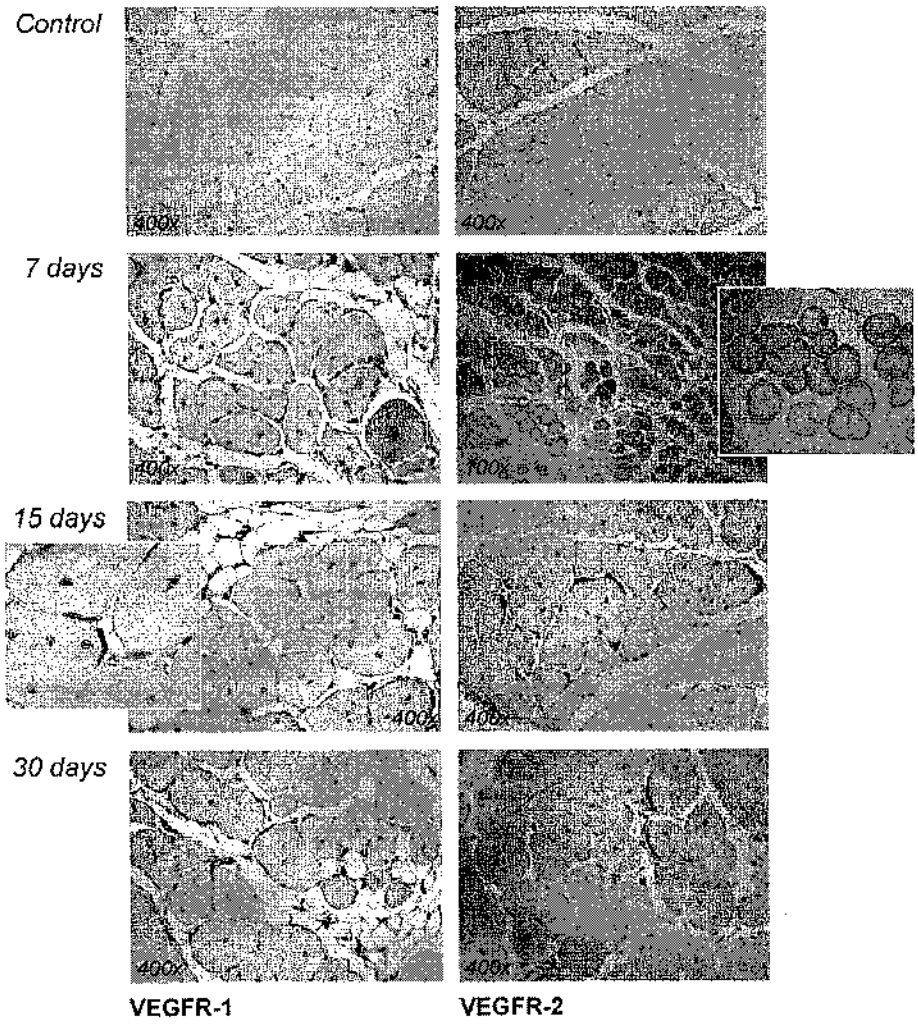


FIG. 6. VEGFR-1 and VEGFR-2 are expressed in regenerating muscles. Immunohistochemistry for VEGFR-1 and VEGFR-2 on untreated and glycerol-damaged muscle sections. Regenerating muscle showed robust expression of both receptors in elongated cells surrounding muscle fibers and resembling satellite cells. Expression of the receptors was detectable early after injury (7 days) and persisted until the late stages of the regenerative process (30 days). In addition, VEGFR-2 was also highly expressed on the surface of mature muscle fibers at the earlier days after injury (shown at day 7 after injury). In contrast, neither VEGFR-1 nor VEGFR-2 was detectable in normal muscle sections (control).

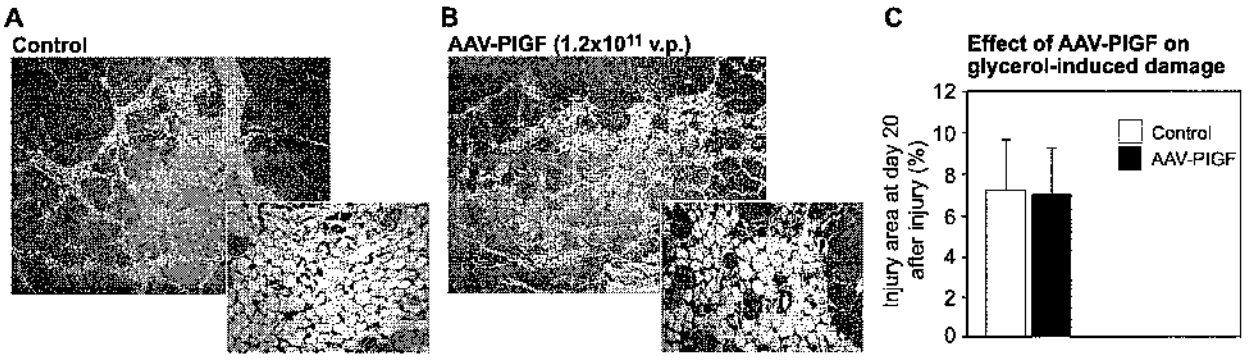


FIG. 7. Effects of AAV-PlGF on muscle regeneration after glycerol-induced damage. (A, B) Hematoxylin and eosin-stained histological sections of muscles injected with either PBS (control) or $1.2 \times 10^{11}$ AAV-PlGF particles 5 days after glycerol-induced muscle damage. Samples were harvested 20 days after injury. (C) Quantification of the injured muscle areas in digital images of muscle sections from control and AAV-PlGF-treated muscles. AAV-mediated overexpression of mouse PlGF, which interacts only with VEGFR-1, did not exert any protective or proregenerative effect on the damaged muscle tissue.

muscle regeneration is mediated by its interaction with VEGFR-2.

## Discussion

The results presented in this paper indicate that VEGF possesses a novel biological role in stimulating skeletal muscle fiber regeneration *in vivo*. The direct effect of VEGF on myogenic cells is supported by a number of observations. *In vitro*, hrVEGF promotes the fusion of myogenic cells to form myotubes and protects these cells from apoptotic cell death; differentiating myocytes and myotubes express high levels of both VEGFR-1 and VEGFR-2, as detected by both immunocytochemistry and immunofluorescence. *In vivo*, the long-term expression of VEGF using AAV vectors under normal conditions promotes the appearance of a regenerating muscle phenotype in the injected areas, with several muscle fibers containing a central nucleus and a much broader muscle fiber size distribution, including small (regenerating) and enlarged (hypertrophic) fibers. Under conditions of ischemic or chemical damage (the latter obtained by glycerol or cardiotoxin), the muscle satellite cells express high levels of both VEGFR-1 and VEGFR-2. Finally, and perhaps most strikingly, the delivery of VEGF determines a dramatic decrease in the size of the damaged area and in the time required for complete regeneration.

Other studies in the past have addressed the effects of VEGF overexpression in normoperfused skeletal muscle, merely indicating a strong angiogenic effect of the factor. In particular, the implantation of genetically modified myoblasts into nonischemic muscle caused an accumulation of endothelial cells and macrophages, followed by networks of vascular channels and hemangiomas [27,28]. The pattern of VEGF expression using AAV vectors is clearly different. The production of the factor progressively increases over time, while its expression persists for longer periods at levels that are probably lower than those obtained by genetically modified myoblasts. These properties might favor the direct effect of the factor on the muscle fibers.

The effects of VEGF on the promotion of muscle recovery after damage are likely to be exerted by different mechanisms. The factor has a very well known proangiogenic activity; in addition, our results show that it also prevents apoptosis and promotes muscle fiber growth. These three effects most likely cooperate in improving recovery after muscle damage. An additional possibility is that VEGF, by mobilizing bone marrow progenitor cells [29,30], might favor muscle regeneration through transdifferentiation or fusion of these cells [31,32], although recent evidence argues against this event [33,34].

Interestingly, the regenerative effects of AAV-VEGF injection are greater when the vector is injected 5 days after damage, an observation that indicates that the major therapeutic role of VEGF has to be attributed to its direct activity on the myofiber regeneration. This result is consistent with the high levels of expression of the VEGF receptors on muscle satellite cells and muscle fibers at this time point after damage ([22] and Fig. 5 in this work). In this respect, it is also worth noticing that the efficiency of AAV vector transduction is highly increased after muscle damage, with a decreased time lapse before the onset of transgene expression [35].

Muscle regeneration is a complex biological process. After damage, satellite cells, which are normally in the G0 phase of the cell cycle, reenter the cell cycle and proliferate, thus providing a sufficient number of cells necessary for repair. This proliferative phase ends with the appearance of the first small regenerating myotubes at approximately 3 days after injury [36,37]. At this time point, part of the proliferated cells become quiescent again, while the remaining ones start to fuse to form multinucleated myotubes (terminal differentiation), an event that is followed by the maturation of these myotubes into muscle fibers (biochemical differentiation) [38–40]. Concomitant with these events is the process of macrophage accumulation and the disman-

doi:10.1016/j.ymthe.2004.08.007

tling of the damaged fibers. The results obtained by studying the effects of hrVEGF on myotube formation *in vitro* indicate that this most likely stimulates the terminal differentiation phase, by increasing maturation of the multinucleated myofibers. This effect is most possibly achieved by promoting the fusion of the differentiated, MHC-positive myocytes to form myofibers that are longer and contain more nuclei.

To identify the receptor that mediates these effects of VEGF on myogenic cells one must consider that both VEGFR-1 and VEGFR-2 are upregulated in the differentiating myogenic cells, in myotubes *in vitro*, and in satellite cells *in vivo* after muscle damage. In cultured myoblasts and C2C12 cells, treatment with SU1498, an inhibitor of the VEGFR-2 protein kinase, abolishes the protective effect of VEGF on camptothecin-induced cell apoptosis, suggesting the participation of VEGFR-2 in mediating the VEGF signal. Most strikingly, *in vivo* overexpression of PlGF, an agonist of the VEGFR-1 but not of the VEGFR-2, was not able to promote muscle regeneration after damage, not even at very high doses of vector. These results clearly point to the VEGFR-2 as the main mediator of the effect of VEGF on myogenic cells. Elucidation of the biochemical pathway triggered after VEGFR-2 activation in these cells clearly requires further investigation. In this respect, however, it is worth noticing that at least two signaling pathways that are important for muscle survival and regeneration are known to be set in motion by the activation of the VEGFR-2 in endothelial cells, namely the PI3K/Akt and the MAP kinase pathways. The activation of Akt signaling in the muscle cells is important to inhibit apoptosis during differentiation [41,42] and to control the myofiber size [43,44]. In endothelial cells, Akt signaling after activation of the VEGFR-2 by VEGF is crucial for endothelial cell survival [16]. Intriguingly, insulin growth factor-1, a powerful promoter of muscle regeneration that stimulates muscle differentiation through Akt [45], also increases VEGF synthesis in C2C12 cells [46], indirectly suggesting the involvement of VEGF in the regeneration process. Accordingly, muscle fibers transduced by a constitutively active Akt formed *in vivo* also produce increased levels of VEGF and show signs of muscle hypertrophy [46]. Another important biochemical pathway in muscle cell differentiation involves MAP kinase signaling, which leads to the increased expression and activity of the MyoD protein [47]. The same pathway is also known to be activated in endothelial cells by the interaction of VEGF with VEGFR-2.

The observation that VEGF promotes muscle fiber regeneration when delivered a few days after muscle damage opens the way to possible, important therapeutic applications in the treatment of acute and chronic muscular diseases of different origins, including traumatic injury (in which the regenerative process might be accelerated) or inherited muscular dystrophies (in which a sustained stimulus for muscle regeneration might prove beneficial). In this respect, we wish to point out that the use of vectors based on AAV offers an important possibility to maintain sustained expression of the VEGF gene over prolonged periods of time in the absence of inflammation or vector-induced immune response, a property that might prove advantageous in several clinical applications.

On a final note, for a long time VEGF has been considered an endothelial-specific growth factor that promotes a powerful angiogenic response. The observation that VEGF also induces myofiber regeneration in the skeletal muscle now extends the recent evidence that challenges this notion. Beyond angiogenesis, the interaction of VEGF with its receptors is important in maintaining survival and promoting differentiation of cells with a progenitor phenotype in a broad array of different tissues, including bone marrow, bone, the central nervous system, and skeletal muscle. These observations pave the way to the possible exploitation of VEGF gene transfer under varying conditions of damage in adult tissues to provide cellular protection and tissue regeneration.

## Materials and Methods

### Cell Culture and Reagents

Primary myoblast cultures were prepared from newborn CD1 mice (2–7 days of age) according to [48]. Myoblasts were plated on gelatin-coated flasks and cultured in proliferation medium (DMEM, 10% fetal bovine serum, 10% horse serum, 0.5% chick embryo extract, 1% penicillin–streptomycin and 1‰ amphotericin B, 4.5 g glucose/liter). Differentiation was induced by switching the myoblast cultures to a low-serum differentiation medium (DMEM, 0.4% UltraserG (BioSepra Sa, France), 4.5 g glucose/liter).

C2C12 myogenic cells were maintained in high glucose DMEM plus 10% fetal bovine serum and induced to form myotubes by 3–4 days culture in differentiation medium. When indicated, hrVEGF165 (R&D Systems) was added twice a day to a final concentration of 100 ng/ml.

### Production, Purification, and Characterization of rAAV Vectors

The rAAV vectors used in this study were prepared as already described [21,49].

### Animals and Experimental Protocols

Animal care and treatments were conducted in conformity with institutional guidelines in compliance with national and international laws and policies (EEC Council Directive 86/609, OJL 358, December 12, 1987). All experiments were performed in male CD1 mice, 4–6 weeks of age.

***Animal model of hind-limb ischemia and muscle injury.*** Unilateral hind-limb ischemia was induced by resecting a 2.5-cm segment of the left femoral artery. The lower leg muscles were harvested 20 days after the induction of ischemia and their viability was tested by staining with tetrazolium red (2,3,5-triphenyltetrazolium chloride; Sigma), an indicator of enzymatic redox reactions. Injury in the tibialis anterior muscle was induced by injecting 25 μl of 1 mM cardiotoxin (Sigma) or 25 μl of 50% v/v glycerol in two injection sites.

***Intramuscular administration of rAAV vectors.*** In the hind-limb ischemia mouse model, the recombinant vector solution (100 μl; 3 × 1011 AAV-VEGF vector particles) was injected into the tibialis anterior,

adductor, and gastrocnemius muscles (one, two, and one injection per muscle, respectively).

The normoperfused muscles or the muscles treated with glycerol and cardiotoxin were injected with different doses of AAV-VEGF or AAV-PlGF in a total volume of 25 μl and in two distinct injection sites. Muscles were harvested 20 days after damage, fixed in 2% formaldehyde, and embedded in paraffin. Control animals were injected with either PBS or $3 \times 10^{11}$ AAV-LacZ. All the experiments were performed in groups including four to six animals.

### Immunostaining and Histological Evaluation

Staining of 2-μm muscle histological sections was performed as described [21]. Myogenic cells (C2C12, myoblasts) cultured on multichamber slides (Nalge Nunc International) were fixed in 2% paraformaldehyde followed by permeabilization in 0.1% Triton X-100 for immunofluorescence or fixed in cold (−20°C) methanol for immunocytochemistry. Monoclonal anti-mouse Flk-1 (Santa Cruz Biotechnology, sc-6251) and rabbit polyclonal anti-Flt-1 (Santa Cruz Biotechnology, sc-316) antibodies were used to detect VEGF receptors on cultured cells and muscle tissue samples. A monoclonal anti-mouse skeletal slow MHC antibody (Sigma, clone NOQ7.5.4D) was used to visualize differentiating myocytes and myofibers. A secondary antibody conjugated with a green fluorochrome (Alexa 449, Jackson ImmunoResearch Laboratories) was used for immunofluorescence. The procedures for immunohistochemistry were undertaken according to the Vectastain Universal ABC kit and MOM Kit (Vector Laboratories). Signals were developed using 3,3′-diaminobenzidine as the substrate for the peroxidase chromogenic reaction (Lab Vision Corp., Fremont, CA, USA).

### Apoptosis and MTT Assays

To study apoptosis, subconfluent myogenic cells were serum-starved and then exposed for 4 days at 12-h intervals to hrVEGF 165 (50 ng/ml). The VEGFR-2 inhibitor SU1498 (5 μM; Calbiochem) was added every 12 h from day 2 to day 4; camptothecin (50 nM for C2C12 cells and 50 μM for primary myoblasts; Calbiochem) was added on day 4, 5 h before the cells were harvested. Both reagents were diluted in DMSO. Detection of apoptotic cells was performed by detecting annexin V expression on a flow cytometer (FACSCalibur; BD) using the Annexin- V-FLUOS kit (Roche), using propidium iodide to distinguish apoptosis from necrosis.

The effect of VEGF on myogenic cell proliferation was assessed by plating cells in 96-well plates (5000 cells/well). After overnight incubation, the medium was replaced by fresh proliferation or differentiation medium containing different concentrations of hrVEGF. After 3 days incubation, proliferation was assessed using the MTT conversion kit (Boehringer) according to the manufacturer's instructions.

### Quantification of Myotube Length and Ploidy

Myotube differentiation was induced in C2C12 cells in the presence or absence of hrVEGF165. After staining of slow MHC by immunofluorescence, digital images of the cell cultures were acquired with an Axiovert 100M confocal laser-scanning microscope (Zeiss LSM 510). Ten fields from four independent experiments (10× objective) were randomly taken for each treatment. The length of all positive slow MHC fibers was analyzed using the measurement tools of the LSM510 2.02 software. The quantification of the number of nuclei per MHC-positive fiber was performed by three independent investigators blinded to experimental procedures.

### Quantification of Glycerol and Cardiotoxin Muscle Injury areas

To quantify glycerol-induced injury, microphotographs of histological samples of transversal sections of the tibialis anterior muscle were examined in a blinded fashion by three different examiners. Quantification was performed on histological sections from the upper, middle, and lower regions of the tibialis anterior muscle (three sections per region; $n$ = 4 animals per group). The areas of injury, identified by the absence of myofibers, were quantified using the ImageJ software (NIH Software) and expressed as the percentage ± SD of the total cross-sectional area of the tissue section.

### Real-Time PCR

The expression of hVEGF in the transduced muscles was assessed by real-time quantification using the TaqMan technology. Briefly, total RNA was extracted from the AAV-VEGF-injected tibialis anterior muscles of 16 animals at 3, 7, 14, and 28 days after injection (four animals per group). RNA (4 μg) was reverse-transcribed and subjected to quantification using an Applied Biosystems Assay-on-Demand for human VEGF. All values are expressed as number of molecules using an external calibration curve. The same procedure was also used for the quantification of hVEGF in the tibialis anterior of the uninjected, contralateral leg; in this case, the levels of hVEGF mRNA were below the levels of detection after at least 40 PCR cycles. Amplifications were carried out in an ABI Prism 7000 Sequence Detection System.

### Statistical Analysis

Statistical comparison between treated and control groups was performed by the two-tailed Student $t$ test on paired samples; the nonparametric Kolmogorov–Smirnov test was used to compare continuous distributions. All analyses were performed using the StatView 4.5 statistical software package for the Macintosh (Abacus Concepts, Berkeley, CA, USA).

## ACKNOWLEDGMENTS

*This work was supported by grants from the Progetto Finalizzato "Genetica Molecolare" of the Consiglio Nazionale delle Ricerche, Italy; from the FIRB program of the Ministero dell'Istruzione, Universita' e Ricerca, Italy; and from the Fondazione Cassa di Risparmio of Trieste, Italy. We are very grateful to Barbara Boziglav and Mauro Sturnega for excellent technical support and to Suzanne Kerbavcic for editorial assistance.*

RECEIVED FOR PUBLICATION MARCH 14, 2004; ACCEPTED AUGUST 9, 2004.

## APPENDIX A. SUPPLEMENTARY DATA

Supplementary data associated with this article can be found, in the online version, at doi:10.1016/j.ymthe.2004.08.007.

## REFERENCES

1. Yancopoulos, G. D., Davis, S., Gale, N. W., Rudge, J. S., Wiegand, S. J., and Holash, J. (2000). Vascular-specific growth factors and blood vessel formation. *Nature* **407:** 242–248.
2. Gale, N. W., and Yancopoulos, G. D. (1999). Growth factors acting via endothelial cell-specific receptor tyrosine kinases: VEGFs, angiopoietins, and ephrins in vascular development. *Genes Dev.* **13:** 1055–1066.
3. Ferrara, N., Gerber, H. P., and LeCouter, J. (2003). The biology of VEGF and its receptors. *Nat. Med.* **9:** 669–676.
4. Lambrechts, D., *et al.* (2003). VEGF is a modifier of amyotrophic lateral sclerosis in mice and humans and protects motoneurons against ischemic death. *Nat. Genet.* **34:** 383–394.
5. Jin, K., Zhu, Y., Sun, Y., Mao, X. O., Xie, L., and Greenberg, D. A. (2002). Vascular endothelial growth factor (VEGF) stimulates neurogenesis in vitro and in vivo. *Proc. Natl. Acad. Sci. USA* **99:** 11946–11950.
6. Jin, K. L., Mao, X. O., and Greenberg, D. A. (2000). Vascular endothelial growth factor: direct neuroprotective effect in in vitro ischemia. *Proc. Natl. Acad. Sci. USA* **97:** 10242–10247.
7. Schratzberger, P., *et al.* (2000). Favorable effect of VEGF gene transfer on ischemic peripheral neuropathy. *Nat. Med.* **6:** 405–413.
8. LeCouter, J., *et al.* (2003). Angiogenesis-independent endothelial protection of liver: role of VEGFR-1. *Science* **299:** 890–893.
9. Zelzer, E., *et al.* (2002). Skeletal defects in VEGF(120/120) mice reveal multiple roles for VEGF in skeletogenesis. *Development* **129:** 1893–1904.
10. Deckers, M. M., Karperien, M., van der Bent, C., Yamashita, T., Papapoulos, S. E., and Lowik, C. W. (2000). Expression of vascular endothelial growth factors and their receptors during osteoblast differentiation. *Endocrinology* **141:** 1667–1674.
11. Mayr-Wohlfart, U., *et al.* (2002). Vascular endothelial growth factor stimulates chemotactic migration of primary human osteoblasts. *Bone* **30:** 472–477.

doi:10.1016/j.ymthe.2004.08.007


12. Street, J., *et al.* (2002). Vascular endothelial growth factor stimulates bone repair by promoting angiogenesis and bone turnover. *Proc. Natl. Acad. Sci. USA* **99:** 9656–9661.
13. Ishida, A., *et al.* (2001). Expression of vascular endothelial growth factor receptors in smooth muscle cells. *J. Cell. Physiol.* **188:** 359–368.
14. Wang, Z., Castresana, M. R., and Newman, W. H. (2001). Reactive oxygen and NF-kappaB in VEGF-induced migration of human vascular smooth muscle cells. *Biochem Biophys. Res. Commun.* **285:** 669–674.
15. Barleon, B., Sozzani, S., Zhou, D., Weich, H. A., Mantovani, A., and Marme, D. (1996). Migration of human monocytes in response to vascular endothelial growth factor (VEGF) is mediated via the VEGF receptor flt-1. *Blood* **87:** 3336–33343.
16. Gerber, H. P., *et al.* (2002). VEGF regulates haematopoietic stem cell survival by an internal autocrine loop mechanism. *Nature* **417:** 954–958.
17. Lyden, D., *et al.* (2001). Impaired recruitment of bone-marrow-derived endothelial and hematopoietic precursor cells blocks tumor angiogenesis and growth. *Nat. Med.* **7:** 1194–1201.
18. Snyder, R. O., *et al.* (1997). Efficient and stable adeno-associated virus-mediated transduction in the skeletal muscle of adult immunocompetent mice. *Hum. Gene Ther.* **8:** 1891–1900.
19. Bouchard, S., *et al.* (2003). Long-term transgene expression in cardiac and skeletal muscle following fetal administration of adenoviral or adeno-associated viral vectors in mice. *J. Gene Med.* **5:** 941–950.
20. Chirmule, N., Propert, K., Magosin, S., Qian, Y., Qian, R., and Wilson, J. (1999). Immune responses to adenovirus and adeno-associated virus in humans. *Gene Ther.* **6:** 1574–1583.
21. Arsic, N., *et al.* (2003). Induction of functional neovascularization by combined VEGF and angiopoietin-1 gene transfer using AAV vectors. *Mol. Ther.* **7:** 450–459.
22. Rissanen, T. T., *et al.* (2002). Expression of vascular endothelial growth factor and vascular endothelial growth factor receptor-2 (KDR/Flk-1) in ischemic skeletal muscle and its regeneration. *Am. J. Pathol.* **160:** 1393–1403.
23. Germani, A., *et al.* (2003). Vascular endothelial growth factor modulates skeletal myoblast function. *Am. J. Pathol.* **163:** 1417–1428.
24. Fisher, K. J., *et al.* (1997). Recombinant adeno-associated virus for muscle directed gene therapy. *Nat. Med.* **3:** 306–312.
25. Autiero, M., *et al.* (2003). Role of PlGF in the intra- and intermolecular cross talk between the VEGF receptors Flt1 and Flk1. *Nat. Med.* **9:** 936–943.
26. Carmeliet, P., *et al.* (2001). Synergism between vascular endothelial growth factor and placental growth factor contributes to angiogenesis and plasma extravasation in pathological conditions. *Nat. Med.* **7:** 575–583.
27. Springer, M. L., *et al.* (2003). Localized arteriole formation directly adjacent to the site of VEGF-induced angiogenesis in muscle. *Mol. Ther.* **7:** 441–449.
28. Springer, M. L., Chen, A. S., Kraft, P. E., Bednarski, M., and Blau, H. M. (1998). VEGF gene delivery to muscle: potential role for vasculogenesis in adults. *Mol. Cell* **2:** 549–558.
29. Hattori, K., *et al.* (2001). Vascular endothelial growth factor and angiopoietin-1 stimulate postnatal hematopoiesis by recruitment of vasculogenic and hematopoietic stem cells. *J. Exp. Med.* **193:** 1005–1014.
30. Asahara, T., *et al.* (1999). VEGF contributes to postnatal neovascularization by mobilizing bone marrow-derived endothelial progenitor cells. *EMBO J.* **18:** 3964–3972.
31. Gussoni, E., *et al.* (1999). Dystrophin expression in the mdx mouse restored by stem cell transplantation. *Nature* **401:** 390–394.
32. LaBarge, M. A., and Blau, H. M. (2002). Biological progression from adult bone marrow to mononucleate muscle stem cell to multinucleate muscle fiber in response to injury. *Cell* **111:** 589–601.
33. Balsam, L. B., Wagers, A. J., Christensen, J. L., Kofidis, T., Weissman, I. L., and Robbins, R. C. (2004). Haematopoietic stem cells adopt mature haematopoietic fates in ischaemic myocardium. *Nature* **428:** 668–673.
34. Murry, C. E., *et al.* (2004). Haematopoietic stem cells do not transdifferentiate into cardiac myocytes in myocardial infarcts. *Nature* **428:** 664–668.
35. Abadie, J., Blouin, V., Guigand, L., Wyers, M., and Cherel, Y. (2002). Recombinant adeno-associated virus type 2 mediates highly efficient gene transfer in regenerating rat skeletal muscle. *Gene Ther.* **9:** 1037–1043.
36. Yan, Z., *et al.* (2003). Highly coordinated gene regulation in mouse skeletal muscle regeneration. *J. Biol. Chem.* **278:** 8826–8836.
37. Kawai, H., Nishino, H., Kusaka, K., Naruo, T., Tamaki, Y., and Iwasa, M. (1990). Experimental glycerol myopathy: a histological study. *Acta Neuropathol. (Berlin)* **80:** 192–197.
38. Nadal-Ginard, B. (1978). Commitment, fusion and biochemical differentiation of a myogenic cell line in the absence of DNA synthesis. *Cell* **15:** 855–864.
39. Endo, T., and Nadal-Ginard, B. (1987). Three types of muscle-specific gene expression in fusion-blocked rat skeletal muscle cells: translational control in EGTA-treated cells. *Cell* **49:** 515–526.
40. Stockdale, F. E. (1992). Eclipse of the identifiable myoblast. *Symp. Soc. Exp. Biol.* **46:** 1–7.
41. Fujio, Y., Guo, K., Mano, T., Mitsuuchi, Y., Testa, J. R., and Walsh, K. (1999). Cell cycle withdrawal promotes myogenic induction of Akt, a positive modulator of myocyte survival. *Mol. Cell Biol.* **19:** 5073–5082.
42. Alessi, D. R., *et al.* (1996). Mechanism of activation of protein kinase B by insulin and IGF-1. *EMBO J.* **15:** 6541–6551.
43. Bodine, S. C., *et al.* (2001). Akt/mTOR pathway is a crucial regulator of skeletal muscle hypertrophy and can prevent muscle atrophy in vivo. *Nat. Cell Biol.* **3:** 1014–1019.
44. Rommel, C., *et al.* (2001). Mediation of IGF-1-induced skeletal myotube hypertrophy by PI(3)K/Akt/mTOR and PI(3)K/Akt/GSK3 pathways. *Nat. Cell Biol.* **3:** 1009–1013.
45. Tureckova, J., Wilson, E. M., Cappalonga, J. L., and Rotwein, P. (2001). Insulin-like growth factor-mediated muscle differentiation: collaboration between phosphatidylinositol 3-kinase-Akt-signaling pathways and myogenin. *J. Biol. Chem.* **276:** 39264–39270.
46. Takahashi, A., *et al.* (2002). Myogenic Akt signaling regulates blood vessel recruitment during myofiber growth. *Mol. Cell Biol.* **22:** 4803–4814.
47. Gredinger, E., Gerber, A. N., Tamir, Y., Tapscott, S. J., and Bengal, E. (1998). Mitogen-activated protein kinase pathway is involved in the differentiation of muscle cells. *J. Biol. Chem.* **273:** 10436–11044.
48. Rando, T. A., and Blau, H. M. (1994). Primary mouse myoblast purification, characterization, and transplantation for cell-mediated gene therapy. *J. Cell Biol.* **125:** 1275–1287.
49. Deodato, B., *et al.* (2002). Recombinant AAV vector encoding human VEGF165 enhances wound healing. *Gene Ther.* **9:** 777–785.

**Adeno-Associated Virus-mediated transduction of VEGF165 after permanent LAD occlusion markedly improves cardiac functional recovery and tissue regeneration in conscious dogs**

Matteo Ferrarini[#], Nikola Arsic*[#], Fabio A Recchia, Lorena Zentilin*, Serena Zacchigna*, Xiaobin Xu, Axel Linke, Mauro Giacca*, Thomas H Hintze

Department Physiology, New York Medical College, Valhalla, NY and *Molecular Medicine Laboratory, International Centre for Genetic Engineering and Biotechnology (ICGEB), Trieste, Italy. [#] contributed equally to the project.

Key Words: contractile segment function, echocardiography, transthoracic injection, VEGF receptors, angiogenesis, myocardial infarction, cardiac stem cells, cardiac regeneration

Support: Supported by PO-1 HL43023, and RO-1 HL 50142 and HL61290 form the Heart Lung and Blood Institute and by grants RBNE0184PH and RBNE01SP72 of the FIRB program of the "Ministero dell'Istruzione, Universita' e Ricerca", Italy.

**Abstract**

We have previously found that the delivery of the VEGF165 cDNA into skeletal muscle using AAV vectors, not only stimulates angiogenesis and arteriogenesis, but also exerts a remarkable anti-apoptotic and pro-regenerative activity during severe ischemic injury. Based on these observations, the aim of the present study was to determine whether rAAV-VEGF delivery into cardiac tissue, during the acute phase of myocardial infarction, exerts a protective effect on the injured myocardium to promote long-term functional recovery. Acute infarction of the anterior LV wall was induced in twelve chronically instrumented anesthetized dogs by permanent occlusion of the LAD coronary artery. Four hours after occlusion, using an echo-guided needle, rAAV-VEGF or -LacZ (n= 6 each; $4x1x10^{12}$ viral particles per animal) was directly injected into the paradoxical segment. Hemodynamics, echocardiographic data and segmental shortening of the infarcted region were measured in awake dogs at baseline (pre-occlusion) and monitored each week for four weeks. LV and arterial systolic and mean pressure, LV $dP/dt_{max}$ and ejection fraction were not significantly different between the two groups over time. In contrast, the indices of contraction of the infarcted area displayed marked differences after the second week post-infarction: at four weeks, the fractional shortening was 75 ±18% and -3 ±15% of baseline and regional shortening work was 54 ±15% and 0.8 ±15% of baseline in VEGF165 vs. LacZ group, respectively ($P<0.05$). The histological analysis of the border regions between the infarcted and viable cardiac tissue showed a marked increase in the number of $\alpha$-SMA-positive arterioles (50-120 µm diameter; 68±2.8 vs. 100±3.8 vessels per 100x microscopic field in the LacZ and VEGF-treated animals respectively; $p<0.05$). In both groups of animals, the expression of the three main VEGF receptors (VEGFR-1, VEGFR-2 and NP-1) was clearly up-regulated in the border of the infarct; in particular, VEGFR-2 was found to be expressed diffusely on the surviving cardiomyocytes. Consistent with this finding, the histological analysis of transmural sections showed a significant improvement in myocardial viability in the VEGF group, with the presence of several troponin T-expressing cardiomyocytes displaying a clear nuclear positivity for the proliferation marker PCNA. Altogether, these observations are consistent with a direct role of VEGF on cardiomyocytes viability.

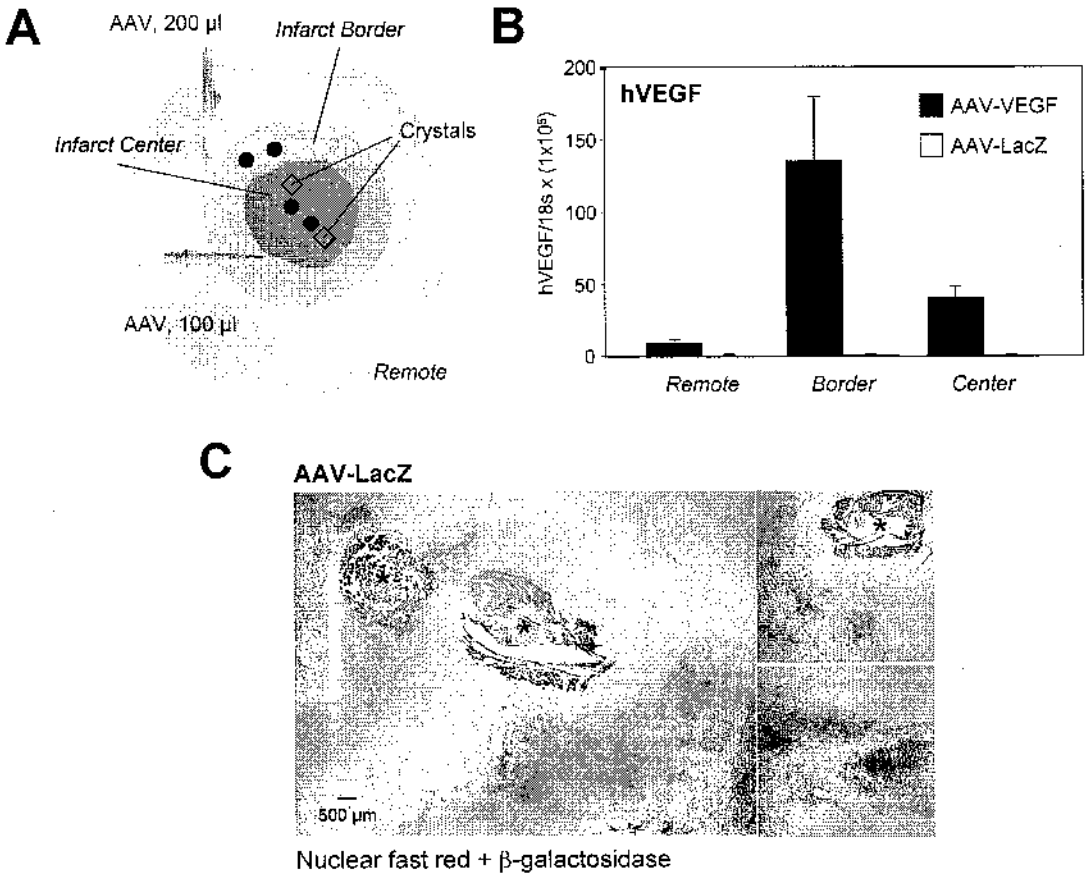


**Figure 1. AAV vectors efficiently transduce infarcted myocardial tissue.**

**A.** Experimental strategy. The acute occlusion of the LAD coronary artery defined three different myocardial zones (the infarct center, the infarct border and the remote zone), here represented by different gray shadings. Every heart received a total amount of 600 µl of the viral vector preparation (either AAV-VEGF or AAV-LacZ), with two injections of 200 µl within the border zone and two additional injections of 100 µl in the infarcted area center, in close proximity to the piezoelectric crystals. The black dots indicate the injection sites.

**B.** Quantification of hVEGF expression in transduced hearts. The quantification of the expression level of human VEGF (hVEGF) by Real-time PCR at 1 month showed that the transgene was highly expressed in the infarcted myocardium, particularly in the border zone that had been injected with the highest vector dose. No hVEGF expression was detected in LacZ-treated animals. The results are expressed relative to the levels of the housekeeping gene 18S (mean±SEM of three independent quantifications from three different dogs per group).

**C.** β-galactosidase expression in the hearts transduced with AAV-LacZ. The X-gal staining of frozen myocardial sections showed transgene expression throughout the infarct center (left and right upper panels) and border (right lower panel). The asterisks correspond to the wires left in place for the chronic heart instrumentation.

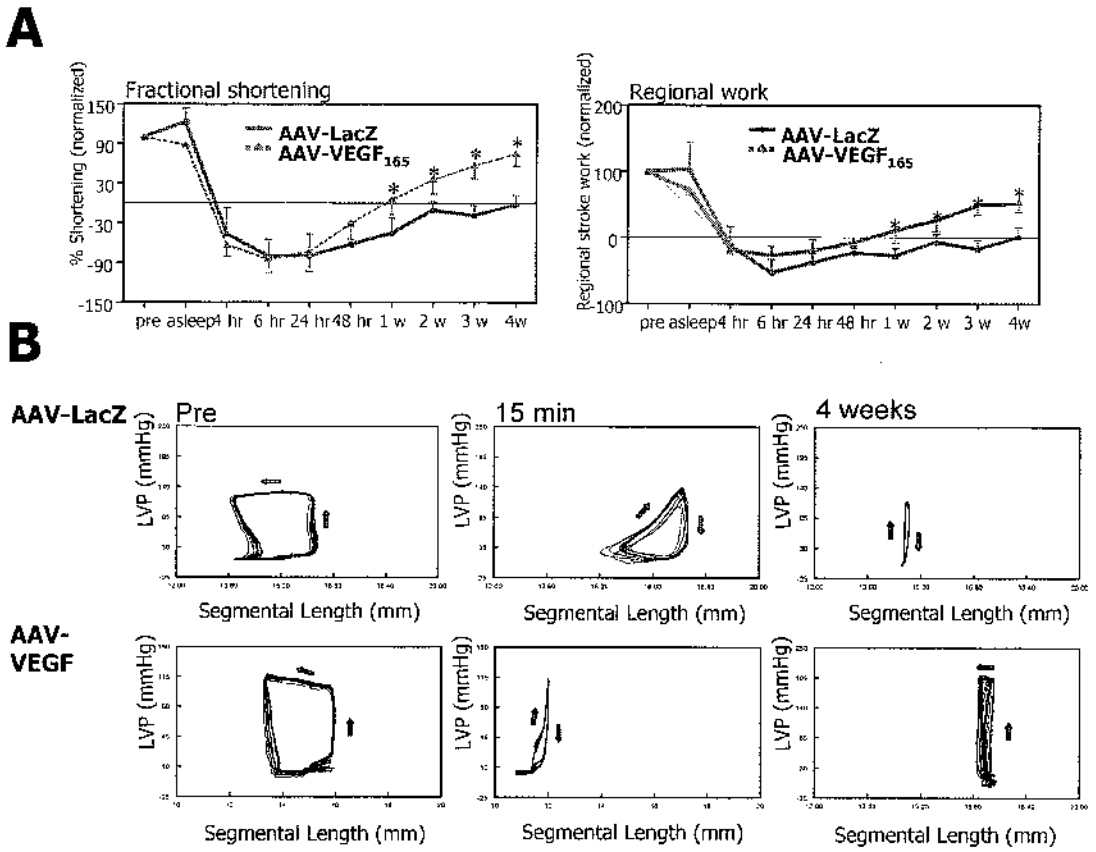


**Figure 2. Recovery of regional contractility in severely ischemic segments after AAV-VEGF transdcution.**

**A.** Assessment of regional contractility. In segments that were initially paradoxical at 48 hours after infarction, there was an almost complete normalization of segment function (graph on the left side) and a 50% recovery of the stroke work (graph on the right side), at 4 weeks after AAV-VEGF delivery. No return of function was observed in the hearts treated with AAV-LacZ. Values are mean±SD; * denotes statistical significance between the two experimental groups.

**B.** Effect of VEGF on regional work and paradoxical movement. The panels on the left side show normal basal pressure/shortening curves, in which the included area represents segment work. At 15 minutes after LAD occlusion, the reverse spin of the curve indicates a paradoxical motion (panels in the center) in both experimental groups. At 4 weeks (panels on the right side), segmental length shows almost complete absence of movement in the LacZ group, a typical akinetic long-term outcome of myocardial ischemia (upper panel). In contrast, in the animal treated with AAV-VEGF segmental bulging is vanished and cardiac work is partially restored (lower panel). A return to a physiological spin curve can be observed in these animals.

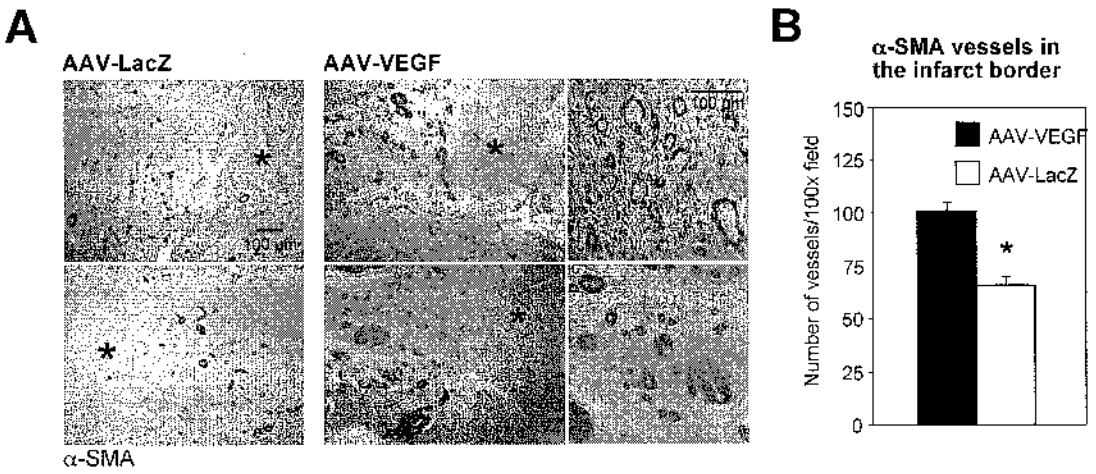


**Figure 3. Massive angiogenesis induced by AAV-VEGF after myocardial infarction**

**A.** Immunostaining of arterial vessels. The immunoistochemistry against the muscle-specific isoform of α-actin (α-SMA) showed massive formation of arterial vessels in the border zone of the infarct, in both the animals treated with AAV-LacZ (left panels) or in those treated with AAV-VEGF (right panels).

**B.** Quantification of α-SMA-positive vessels. The number of of α-SMA-positive arterioles (50-120 μm diameter) in the border zone of the infarct was significantly increased after the transduction with AAV-VEGF as compared to AAV-LacZ. The results are expressed as mean±SEM of at least 10 sections per animal (n=6 for each group); * denotes statistical significance between the two experimental groups.

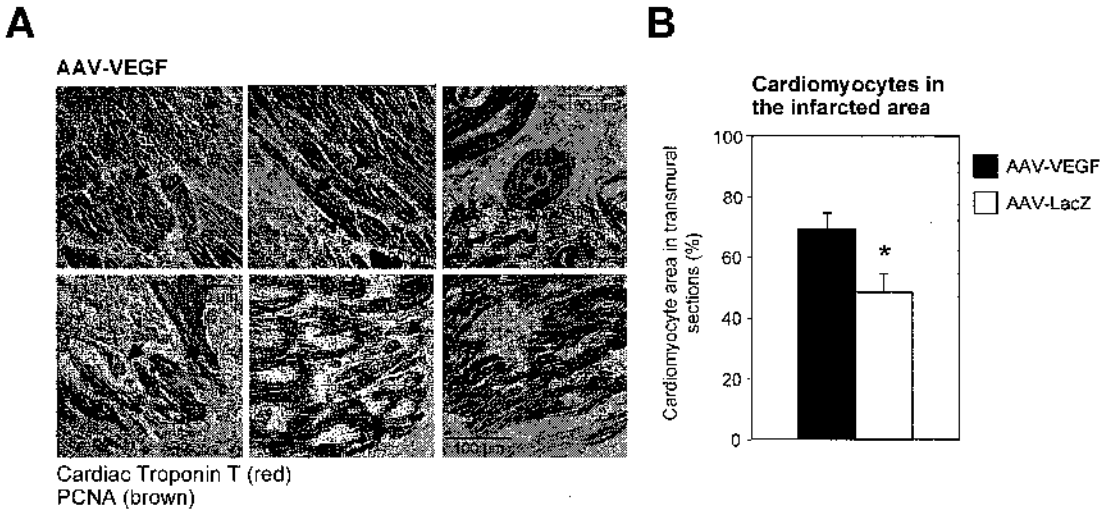


**Figure 4. Increased survival and proliferation of myocardial cells after AAV-VEGF transduction**

**A.** Simultaneous detection of cardiac Troponin T (red) and of the nuclear proliferation marker PCNA (brown) by double immunohistochemistry at day 30 after treatment. Double-positive cells are suggestive of a process of active cardiac reneration.

**B.** Quantification of viable myocardium at day 30 after treatment. Forty transmural sections of the infarct central zone were analyzed for each animal, by measuring the area occupied by troponin-T-positive cardiomyocytes and expressing it as a percentage relative to the area of the total section. Values are mean±SEM; * denotes statistical significance between the two experimental groups.

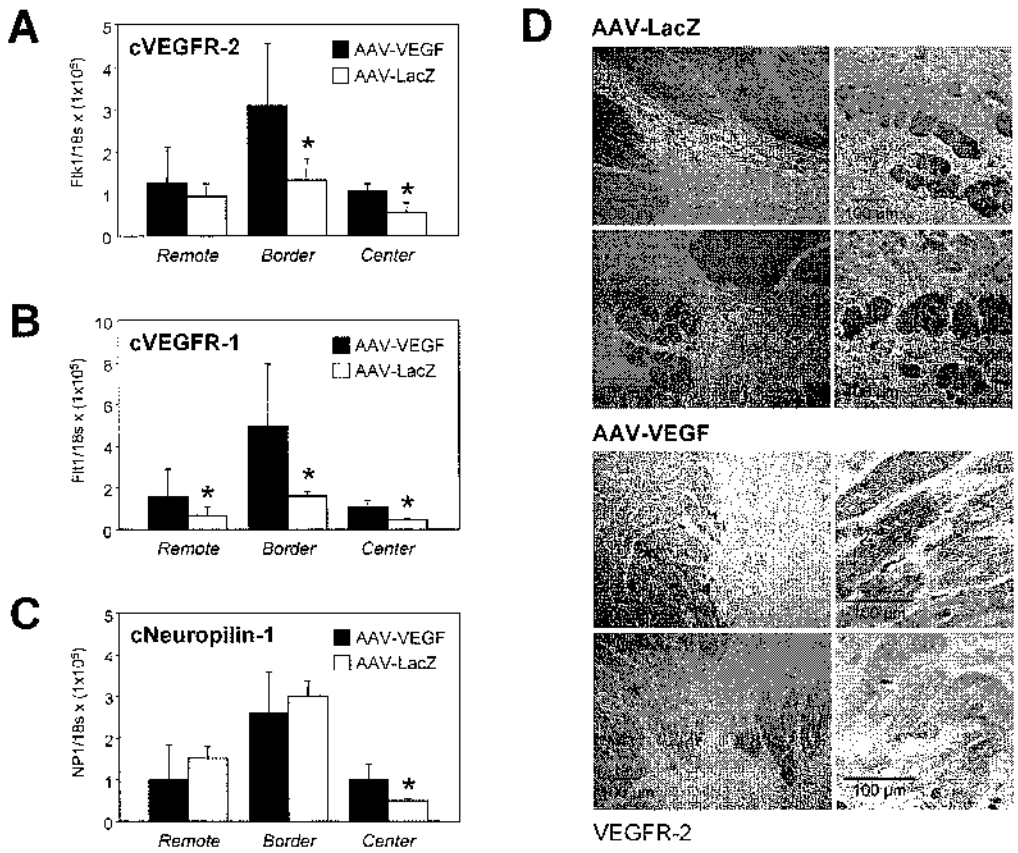


**Figure 5. Expression of the VEGF receptors by the infarcted myocardium**

**A-C.** Levels of VEGF receptor mRNAs. The graphs show the results of the quantification of the levels of the three main endogenous VEGF receptors (VEGFR-2, VEGFR-1, Neuropilin-1) by real-time PCR at 30 days after treatment. Values are mean±SEM; * denotes statistical significance between the two experimental groups.

**D.** Expression of VEGFR-2 by cardiomyocytes. As detected by immunohistochemical staining, the survived cardiomyocytes (indicated by asterisks) at the border of the infarct or interspersed within the connective tissue of the scar abundantly express VEGFR-2.

Table I
Hemodynamic evaluation (anesthetized animals)

| | **Baseline** | | **1 hour** | | **6 hours** | |
|---|---|---|---|---|---|---|
| | AAV-LacZ | AAV-VEGF | AAV-LacZ | AAV-VEGF | AAV-LacZ | AAV-VEGF |
| *LV SV (ml)* | 46±4.7 | 45±5.8 | 27±0.6 | 27±4.9 | 23±2.0 | 26±3.6 |
| *EF (%)* | 63±2 | 66±1 | 52±4 | 43±3 | 45±8 | 41±4 |

*LV SV*: left ventricle stroke volume; *EF*: ejection fraction

Table II
Global cardiac function assessment (awake animals)

| | **Baseline** | | **2 days** | | **4 weeks** | |
|---|---|---|---|---|---|---|
| | AAV-LacZ | AAV-VEGF | AAV-LacZ | AAV-VEGF | AAV-LacZ | AAV-VEGF |
| *MAP (mmHg)* | 107±3 | 110±3.1 | 97±14 | 95±7 | 99±4.7 | 97±3.8 |
| *HR (b/min)* | 79±5 | 83±4 | 127±15 | 127±9 | 95±13 | 76±5 |
| *LVSP (mmHg)* | 131±5 | 133±5 | 120±15 | 118±8 | 119±6 | 116±5 |
| *LVEDP (mmHg)* | 7±0.5 | 8±0.2 | 12±1 | 13±0.5 | 10±0.8 | 11±1.9 |

*MAP*: mean arterial pressure; *HR*: heart rate; *LVSP*: left ventricle systolic pressure; LVEDP: left ventricle end-dyastolic pressure

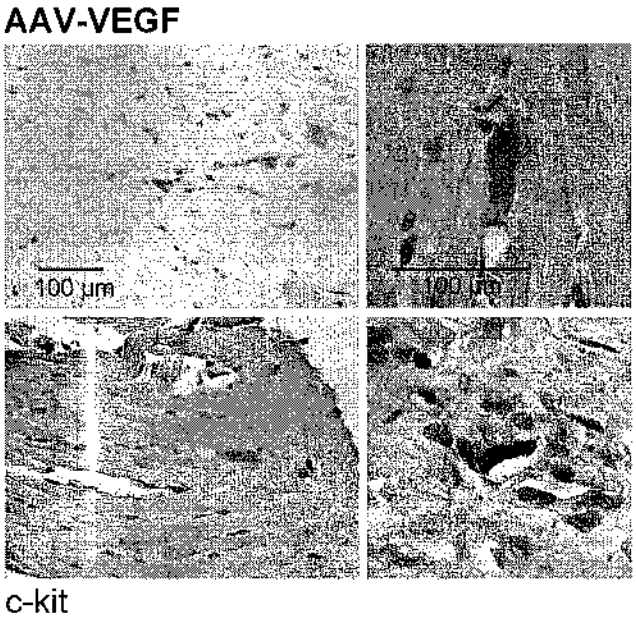


**Supplementary Figure 1. Presence of c-kit-positive cells in the infarcted myocardium**

In the border region of the infarct, a few c-kit-positive cells (1-3 per 40x field) were detected by immunohistochemistry, exclusively in the AAV-VEGF-treated group.

ARTICLE

doi:10.1016/j.ymthe.2004.02.020

# Potent Inhibition of Arterial Intimal Hyperplasia by *TIMP1* Gene Transfer Using AAV Vectors

Genaro A. Ramirez Correa,[1] Serena Zacchigna,[1] Nikola Arsic,[1] Lorena Zentilin,[1] Alessandro Salvi,[2] Gianfranco Sinagra,[2] and Mauro Giacca[1,3,*]

[1] *Molecular Medicine Laboratory, International Center for Genetic Engineering and Biotechnology, Padriciano 99, 34012 Trieste, Italy*
[2] *Cardiology Unit, Ospedale Maggiore, Trieste, Italy*
[3] *Scuola Normale Superiore and Istituto di Fisiologia Clinica, CNR, Pisa, Italy*

*To whom correspondence and reprint requests should be addressed. Fax: +39-040-226555. E-mail: giacca@icgeb.org.*

Available online 15 April 2004

**Seminal to the process of arterial restenosis after balloon angioplasty is extracellular matrix degradation by metalloproteinases (MMPs); activity of these proteins is strongly inhibited by the tissue inhibitors of MMPs (TIMPs). Here we exploit gene transfer using an adeno-associated virus (AAV) for *TIMP1* gene delivery in a rat model of intimal hyperplasia. High-titer AAV-Timp1 efficiently transduced human coronary artery smooth muscle cells (SMCs) *in vitro* and inhibited the capacity of these cells to migrate through a Matrigel barrier. In injured rat carotid arteries, AAV vectors were found to transduce SMCs efficiently and to maintain transgene expression for several weeks *in vivo*. In AAV-Timp1-transduced animals, the intima:media ratio of injured carotids was significantly reduced by 70.5% after 2 weeks, by 58.5% after 1 month, and by 52.4% after 2 months from treatment. The decrease in intimal hyperplasia was paralleled by a significant inhibition of collagen accumulation and by increased elastin deposition in the neointima, two findings that relate to the inhibition of MMP activity. These results indicate that AAV vectors are efficient tools for delivering genes to the arterial wall and emphasize the importance of MMPs for the generation of intimal hyperplasia. Local *TIMP1* gene transfer might thus represent an efficient strategy to prevent restenosis.**

## INTRODUCTION

Restenosis of the arterial lumen after percutaneous angioplasty still represents a major challenge in interventional cardiology [1]. Luminal loss is a complex biological process determined by remodeling of both the arterial wall and the intimal hyperplasia. In particular, intimal thickening relies on vascular smooth muscle cell (SMC) migration across the internal elastic lamina and subsequent proliferation within the neointima [2]. While stent placement has significantly decreased the restenosis rate, by blocking early elastic recoil and inward remodeling [3], in several cases lumen gain improvement is later relapsed by the exacerbation of intimal hyperplasia [4].

The remodeling of the extracellular matrix by metalloproteinases (MMP) is essential for neointima formation in postangioplasty restenosis and in aortocoronary vein graft vasculopathy [1,5]. MMPs are zinc- and calcium-dependent proteases that degrade collagen as well as other matrix proteins such as elastin and proteoglycans [6,7]. In particular, MMP-2 and MMP-9 are expressed early after endothelial injury and are required for local extracellular matrix breakdown and subsequent migration of vascular SMCs from the media to the intima [7–9]. In the later phase of the arterial response, SMCs stop their migration and proliferation and start accumulating extracellular matrix [10].

Tissue inhibitors of metalloproteinases (TIMPs) belong to a family of low-molecular-weight proteins that bind to MMPs at high affinity and that stoichiometrically inhibit their enzymatic activity. The expression of *TIMP1* has been shown to modulate a number of biological events that involve extracellular matrix remodeling, including intimal hyperplasia [11–14], intravascular thrombus formation [15], and atherosclerosis [16,17]. Thus, the transfer and expression of the *TIMP1* gene in the arterial wall, concomitant with balloon angioplasty or stent implantation, emerges as an appealing possibility for the prevention of restenosis [18].

*In vivo* gene transfer to the arterial wall is a powerful experimental approach in the investigation of the role of individual genes in the development of arterial disease, as



1525-0016/03 $30.00

well as in the interference with local molecular pathways for therapeutic purposes. During the past few years, vectors based on the adeno-associated virus (AAV) have continued to gain popularity in the gene therapy community, due to a number of appealing features. These vectors can be purified and produced at high titers, they are not immunogenic nor do they induce an inflammatory reaction, they can be safely injected *in vivo*, and they maintain transgene expression for very long periods of time [19,20].

Here we assess the potential of AAV vectors to transduce arterial smooth muscle cells both *in vitro* and *in vivo* and demonstrate the efficacy of single endovascular delivery of an AAV vector expressing human TIMP1 to prevent intimal hyperplasia in a rat model of postangioplasty restenosis.

## RESULTS

### Permissivity of Human Coronary Artery Smooth Muscle Cells to AAV Transduction and the Functional Effect of AAV-Timp1

We obtained a high titer preparation of an AAV vector expressing the green fluorescent protein (*GFP*) reporter gene (AAV-GFP) and used this vector to assess the *in vitro* permissivity of vascular SMCs. Fig. 1A shows the flow cytometry profile of primary SMCs from human coronary artery at day 5 after transduction with AAV-GFP, indicating transgene expression by ~20% of the cells.

Next, we obtained an AAV vector expressing the human TIMP1 cDNA (AAV-Timp1) under the control of the CMV promoter, as schematically shown in Fig. 1B. We evaluated the efficiency of the transduction with AAV-Timp1 in transduced SMCs. By Western blot analysis, we demonstrated TIMP1 secretion into the supernatant of these cells as a 28-kDa band, showing proper glycosylation (data not shown). We also assessed TIMP1 expression in the same cells by immunocytochemistry with an antibody against TIMP1, which showed intense cytoplasmic positivity (Fig. 1C).

We assessed the effects of TIMP1 expression in SMCs by a chemoinvasion assay, measuring the capacity of the cells to degrade a Matrigel membrane and migrate in response to chemoattraction. As shown in Fig. 1D, the transduction of SMCs with AAV-Timp1 significantly inhibited their ability to invade the Matrigel barrier, inducing a 46% reduction in the number of migrated cells (23.5 ± 2.55 vs 41 ± 4.24, $P < 0.001$, $n = 3$). The same vector also proved to inhibit efficiently angiogenesis in the chorioallantoic membrane of embryonated eggs induced by rhVEGF (data not shown).

Together, these results indicate that primary human vascular SMCs are permissive to AAV transduction *in vitro* and that the AAV-Timp1 vector is highly active in preventing cell migration and invasion.

### Efficiency of AAV Vector Transduction of Rat Carotid Arteries after Balloon Injury

We proceeded to assess the capacity of AAV vectors to transduce the damaged arterial wall *in vivo*. We injured rat carotid arteries with a Fogarty catheter and exposed them to either PBS or AAV-LacZ ($1 \times 10^{11}$ viral particles) for 40 min before restoring blood flow. We analyzed AAV-LacZ-transduced arteries for β-galactosidase (β-gal) expression by X-gal staining at 2 and 4 weeks after treatment. Marker gene expression was already high at 2 weeks after vector delivery and persisted afterward. β-Gal expression was distributed in all three layers of the vessel wall with a degree of preference for the cells of the neointima, followed by media and adventitia (shown at 2 weeks after transduction, in Fig. 2A, right). Cells that showed positive for β-gal in the neointima also reacted to an antibody against α-actin of SMCs, indicating their SMC phenotype (Fig. 2A, left).

In the injured carotid arteries, we observed a remarkable neointimal hyperplasia at 2, 4, and 8 weeks after damage. Morphometric examination of the arterial cross sections at 2 and 4 weeks revealed that the hyperplastic response was not statistically different in arteries treated with either PBS ($n = 6$) or AAV-LacZ ($n = 12$; data not shown), thus ruling out any nonspecific effect of AAV transduction per se on the hyperplastic process.

To ascertain the long-term expression of TIMP1 after AAV vector transduction *in vivo*, we exposed 12 rats to a high dose of AAV-Timp1 ($1 \times 10^{11}$ viral particles) immediately after balloon injury. We studied expression of TIMP1 in the treated animals by immunohistochemistry and by real-time RT-PCR quantification of human TIMP1 mRNA. Similar to AAV-LacZ transduction, cells that were positive for human *TIMP1* transgene expression were mostly found in the neointima and media layers (Fig. 2B). As shown in Fig. 2C, transgene expression was already detectable at 1 week after transduction and persisted at comparable levels for at least 8 weeks.

### Inhibition of Rat Arterial MMPs by TIMP1

To visualize the production of active MMPs by injured rat carotid arteries, we performed an *in vitro* zymography. Three days after balloon injury, we harvested a rat carotid artery and kept it in culture for 3 additional days. We resolved the concentrated conditioned medium by SDS–PAGE on a 0.1% gelatin gel and incubated it at 37°C in collagenase buffer for 16 h. Fig. 3A shows the appearance of two major areas of proteolysis, corresponding to the molecular weight of active MMP9 and MMP2, indicating the active secretion of these MMPs by the injured rat carotid artery.

To assess the effects of human TIMP1 on rat MMP2 and MMP9 activity, we performed a reverse zymography using the supernatants of balloon-injured rat ca-

doi:10.1016/j.ymthe.2004.02.020

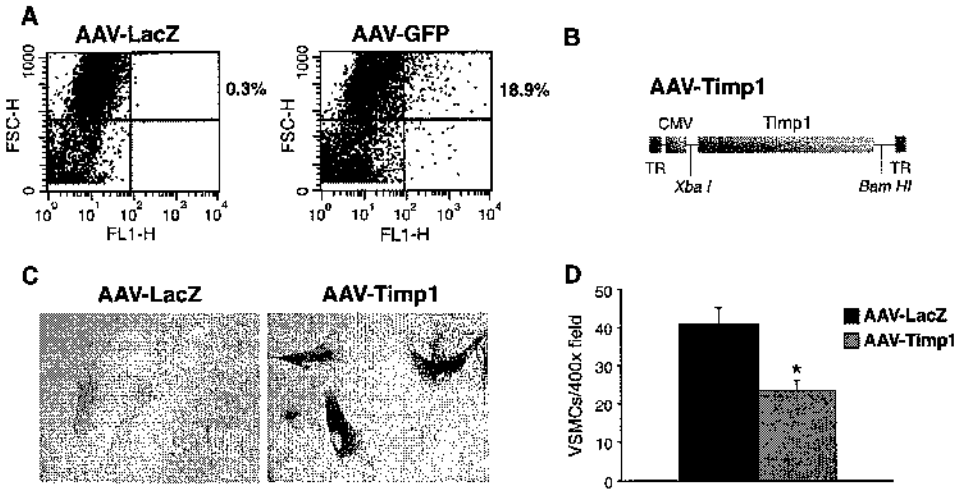


FIG. 1.

rotid arteries (obtained as above) as a source of MMPs. Serum-free media conditioned for 48 h were collected from *TIMP1*- and mock-transfected 293 cells, concentrated, resolved by 0.6% gelatin SDS–PAGE, and incubated in the presence of MMPs. A clear band at 28 kDa (Fig. 3B), absent in the control lane, indicated that the secreted human TIMP1 efficiently inhibited the gelatinolytic activity of the rat MMPs.

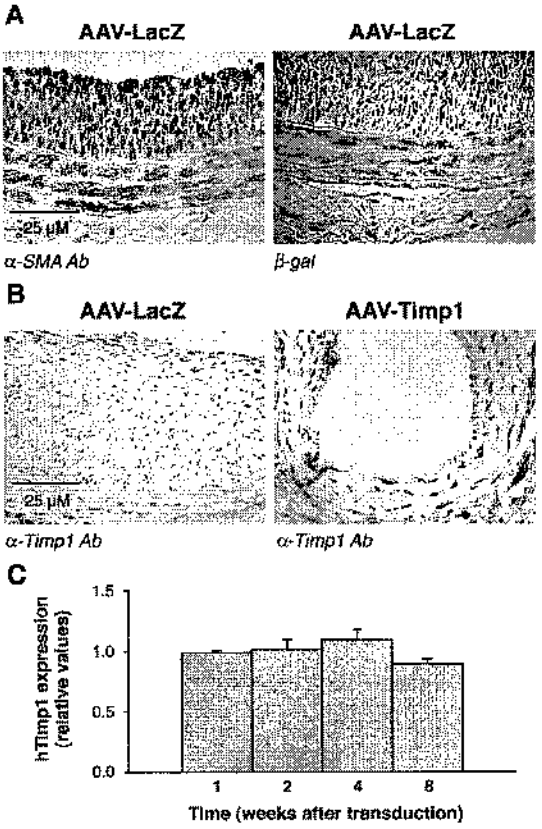


FIG. 2.

### Efficacy of AAV-Timp1 in the Reduction of Intimal Hyperplasia

Next we evaluated the efficacy of TIMP1 to prevent neointima formation. Immediately after balloon injury, we exposed the rat carotid arteries of 15 rats to $1 \times 10^{11}$ viral particles of AAV-Timp1 for 40 min. A matched group of controls received either AAV-LacZ or PBS. We quantitated the stenotic response after 2, 4, and 8 weeks by measuring the intima and media areas of at least four sections per animal. The thickness of the media of injured rat carotids was similar in the control and AAV-Timp1-treated groups (Fig. 4B), whereas the neointimal area of the treated group was reduced by 55.3, 51.9, and 55% at 2, 4, and 8 weeks, respectively ($0.132 \pm 0.01$ vs $0.059 \pm 0.006$ mm$^2$, $P < 0.0001$ at 2 weeks; $0.179 \pm 0.012$ vs $0.086 \pm 0.013$ mm$^2$, $P < 0.0001$ at 4 weeks; $0.198 \pm 0.03$ vs $0.089 \pm 0.04$ mm$^2$, $P < 0.05$ at 8 weeks; Fig. 4A). The intima-to-media ratio, which is a more sensitive parameter for assessing relative changes in intima and media thickness, is reported in Fig. 4C. This ratio was significantly lower in the TIMP1 group at 2 weeks ($0.46 \pm 0.16$ vs $1.56 \pm 0.22$; $P = 0.0001$), 4 weeks ($0.86 \pm 0.22$ vs $2.08 \pm 0.3$; $P = 0.003$), and 8 weeks ($2.0 \pm 0.33$ vs $0.91 \pm 0.49$, $P < 0.05$) after treatment. These values correspond to 70.5, 58.5, and 54.5% reduction in the intima-to-media ratio, respectively. The higher efficacy of treatment at the earlier time might be indicative of a specific effect of TIMP1 in the early phases of the stenotic process, when MMPs are overexpressed. Two representative cross sections of *LacZ*-

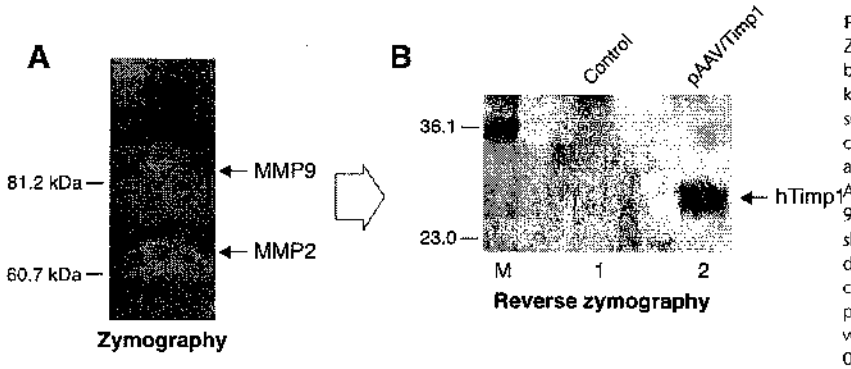


FIG. 3. Inhibition of rat MMPs by human TIMP1. (A) Zymography of a rat carotid artery. Three days after balloon injury, a rat carotid artery was harvested and kept in organ culture. After 3 days, the concentrated supernatant was loaded in a 10% SDS–PAGE gel containing 0.1% gelatin. Clear bands indicate MMP activity in a background of gelatin. MMP2, gelatinase A, 72-kDa type IV collagenase; MMP9, gelatinase B, 94-kDa type IV collagenase. (B) Reverse zymography showing human TIMP1-mediated inhibition of gelatin degradation by rat arterial MMPs. Concentrated cell culture supernatants from 293 cells transfected with pAAV-Timp1 (lane 2) or a control plasmid (lane 1) were resolved on an 11% SDS–PAGE gel containing 0.6% gelatin. The gel was then washed and incubated in collagenase buffer mixed 1:1 with the supernatants of balloon-injured rat carotid arteries—obtained as in (A)—as a source of rat gelatinases. After Coomassie staining, a dark band of ~28 kDa was evident in the supernatants of pAAV-Timp1-transfected cells, corresponding to the area in which gelatin degradation by rat arterial MMPs was prevented by secreted human TIMP1 (indicated by an arrow). M, molecular weight markers.

and *TIMP1*-transduced arteries at two weeks after transduction are shown in Fig. 4D.

### Extracellular Matrix Content after AAV-Timp1 Transduction

Given the reported effects of MMP blockage by nonspecific inhibitors on collagen synthesis and degradation [10] and the effects of TIMP1 overexpression on elastin metabolism [21], we set out to explore the extracellular matrix composition in the AAV-Timp1-treated and control animals. For this purpose, we analyzed cross sections of rat carotid arteries at 2 and 4 weeks after injury by staining with the Azan–Mallory and Weigert–Van Gieson procedures, which reveal collagen and elastin content, respectively (Figs. 5A and 5C).

We found that, in AAV-LacZ-treated animals, collagen occupied 83.5% ± 1.28 of the neointimal layer at 2 weeks after transduction; collagen deposition did not change significantly over a 2-week period in this control group (73.7% ± 6.49 at day 28; $P$ nonsignificant). In contrast, collagen content in the AAV-Timp1-transduced arteries was decreased by 22.9 and 42.6% at 2 and 4 weeks, respectively (83.5% ± 1.28 vs 64.8% ± 3.92; $P = 0.009$ and 73.7% ± 6.49 vs 42.2% ± 7.64; $P = 0.03$; the decrease between 2 and 4 weeks in the AAV-Timp1 group was also statistically significant; $P < 0.01$). These results demonstrate an important effect in the modulation of collagen deposition by AAV-Timp1 transduction (Fig. 5B). We found no significant differences in collagen content in the medial layers (data not shown).

Contrary to collagen, elastin fibers, as evaluated after staining with Weigert–Van Gieson, were more abundant in the neointimal areas of the AAV-Timp1-transduced arteries compared to those treated with AAV-LacZ at both 2 (16.5% ± 1.36 vs 26.9% ± 4.46 of neointima; $P = 0.01$) and 4 weeks (23% ± 4.4 vs 42.3% ± 10.59; $P = 0.04$; 63.1

FIG. 1. Transduction of vascular SMCs with AAV vectors. (A) Transduction of vascular SMC from human coronary artery with high-titer AAV-GFP [43]. Cell fluorescence was analyzed by flow cytometry, showing 18.9% positive cells at 5 days after infection (counts in the upper right). (B) Schematic representation of the AAV-Timp1 expression vector used in this study. TR, AAV terminal repeat sequences; CMV, constitutive cytomegalovirus immediate early promoter; pA, polyadenylation site. Cloning restriction sites are indicated. (C) Immunocytochemistry on transduced vascular SMCs showing expression of TIMP1. (D) Effect of TIMP1 overexpression on SMC migration across a Matrigel barrier. A suspension of SMCs, transduced with either AAV-LacZ or AAV-Timp1, was placed in the upper chamber and medium with chemoattractants was placed in the lower compartment. The bars show the number of cells that migrated in response to chemoattraction. The invasion activity is expressed as the mean number of cells that had migrated per microscopic field (400×) ± SEM for triplicate determinations. The asterisk denotes statistical significance ($P = 0.0005$) using the Student $t$ test, one tailed.

FIG. 2. Transduction of rat carotid artery by AAV vectors. (A) Transduction of rat carotid arteries with AAV-LacZ at day 14 after balloon injury. The left shows immunohistochemistry with an antibody against α-actin of VSMCs to show the SMC phenotype of neointima cells. The right shows β-galactosidase reactivity of the transduced smooth muscle cells in the media and the neointima. Few adventitial cells also appeared positive for β-galactosidase expression. (B) Immunohistochemistry of carotid arteries at 2 weeks after transduction with either AAV-LacZ (left) or AAV-Timp1 (right) using an antibody against TIMP1, to show expression of the transgene in the transduced cells. (C) Quantification of hTIMP1 expression *in vivo* by real-time PCR. Balloon-injured rat carotid arteries (three animals per time point) were transduced with AAV-Timp1. At the indicated time points, total RNA was extracted and subjected to real-time PCR amplification. In each sample, the expression of transduced hTIMP1 was normalized to the levels of the housekeeping 18s gene. The results are expressed relative to the expression at 1 week; shown are the means ± SEM. No statistical difference was detected among the different time points.

doi:10.1016/j.ymthe.2004.02.020

and 84% increase, respectively). As for collagen, the elastin content within the media was similar at both time points in both treated and control arteries (data not shown).

Taken together, these observations suggest that the reduction of neointimal thickness determined by MMP blockage after AAV-Timp1 transduction is paralleled by the inhibition of extensive collagen accumulation and the promotion of elastin deposition in the neointimal lesion.

## DISCUSSION

In this work we demonstrate the *in vitro* and *in vivo* efficacy of recombinant AAV vectors for vascular SMC transduction and show the therapeutic potential of *TIMP1* gene transfer for the prevention of restenosis. After balloon injury of rat carotid arteries followed by AAV-LacZ transduction, the expression of the β-gal transgene was visualized through the arterial wall, with special intensity in the media and neointima layers and with particular localization at the sites of maximal damage, in agreement with a recent study [22]. In our experiments, the overall efficiency of transduction varied widely from 10 to 50% of the entire vascular wall. This variability may be secondary to the unequal conditions in intravascular delivery, the extent of balloon injury, and the cell types infected at the moment of injury when neointimal cells are not present. On average, the efficiency of AAV vectors for gene transfer to the damaged arterial wall is lower than that obtained using first-generation adenoviral vectors, but this is largely outweighed by the lack of undesirable inflammatory effects and the long-term expression of the therapeutic genes [19,22]. In addition, this rate of *in vivo* transduction appears satisfactory, especially when the transferred gene encodes a secreted protein (such as TIMP1), which exerts effects not only on transduced cells, but also on neighboring cells, which may not have undergone gene transduction. This paracrine action may be of great importance in achieving a significant therapeutic effect.

AAV vectors are of interest not only for their potential therapeutic applications, they also represent valuable tools to assess the *in vivo* effects of gene overexpression. The possibility of delivering and expressing a suitable gene within the arterial wall for prolonged periods of time might facilitate the molecular understanding of the disease process and the implementation of new therapeutic strategies without systemic side effects. In this context, the inhibition of intimal hyperplasia in injured rat carotid arteries by AAV-Timp1 underscores the importance of extracellular matrix remodeling in the pathogenesis of this process (reviewed in Refs. [23,24]). This outcome is consistent with biochemical studies that have revealed MMP overexpression after coronary angioplasty [25] or other procedures that have damaged the vascular endothelium [26,27], with recent genetic studies that have highlighted the role of MMP2 and MMP9 polymorphisms on the rate of restenosis [28], with the outcome of studies performed in MMP2- [29] and MMP9-knockout animals [30–32], and with the therapeutic role of pharmacological inhibition of MMP activity on the stenotic process [8,33,34]. Contrary to systemic therapy with nonspecific inhibitors of MMP activity in the minipig model—which were shown to affect constrictive arterial remodeling but not neointima formation [8]—in our experiments the local overexpression of TIMP1 in the arterial wall markedly reduced the neointimal area. This effect might be related to the advantages of local gene delivery and expression compared to systemic treatment.

What is the actual molecular mechanism by which local overexpression of TIMP1 in the arterial wall reduces neointimal thickness? This outcome correlates with the modulation of extracellular matrix content and with a marked reduction in the number of proliferating cells migrated to the neointima. Much experimental evidence indicates that MMPs are overexpressed in the early phases of the stenotic process and that their activity is essential

FIG. 4. Inhibition of intimal hyperplasia by AAV-Timp1. (A–C) Inhibition of neointima formation by AAV-Timp1 at different times after injury. Arterial morphometric analysis was performed in control animals at 2, 4, and 8 weeks after injury ($n = 11$, 6, and 5, respectively) and in animals treated with AAV-Timp1 at the same time points ($n = 5$ for all groups). Shown are the mean values and SEM of the (A) neointima and (B) media areas and of the (C) intima:media ratio; at least three sections per animal were evaluated. The asterisk denotes statistical significance between AAV-Timp1 and AAV-LacZ ($P < 0.01$) using the Student *t* test, one tailed. (D) Neointima formation in two carotid arteries transduced with AAV-LacZ (left) or AAV-Timp1 (right) at 2 weeks after injury. The arteries were visualized by staining with nuclear fast red.

FIG. 5. Modification of collagen and elastin content of the arterial wall after AAV-Timp1 transduction. (A) Effects of AAV-Timp1 transduction on collagen content as assessed by Azan–Mallory staining. Shown are enlargements of the arterial wall at 4 weeks after transduction with AAV-Timp1 or AAV-LacZ. Collagen is visualized by blue staining; muscle cells appear in orange. (B) Quantification of collagen content at 2 and 4 weeks after transduction. The histogram shows the percentage of collagen in the neointima expressed as number of pixels per area (see Materials and Methods). Shown are the mean values and SEM. Quantification was performed in four animals per group, analyzing at least three sections per animal. The asterisks indicate statistical significance ($P < 0.05$). (C) Effects of AAV-Timp1 transduction on elastin content as visualized by Weigert–Van Gieson staining. Shown are the images of two arteries and of the respective enlargements at 4 weeks after transduction with AAV-Timp1 or AAV-LacZ. Elastin is visualized as dark fibers by staining with Weigert resorcin fuchsin; collagen stains in red. (D) Quantification of elastin content at 2 and 4 weeks after transduction. The histogram shows the percentage of elastin in the neointima expressed as number of pixels per area (see Materials and Methods). Shown are the mean values and SEM. Quantification was performed in four animals per group, analyzing at least three sections per animal. The asterisks indicate statistical significance ($P < 0.05$).

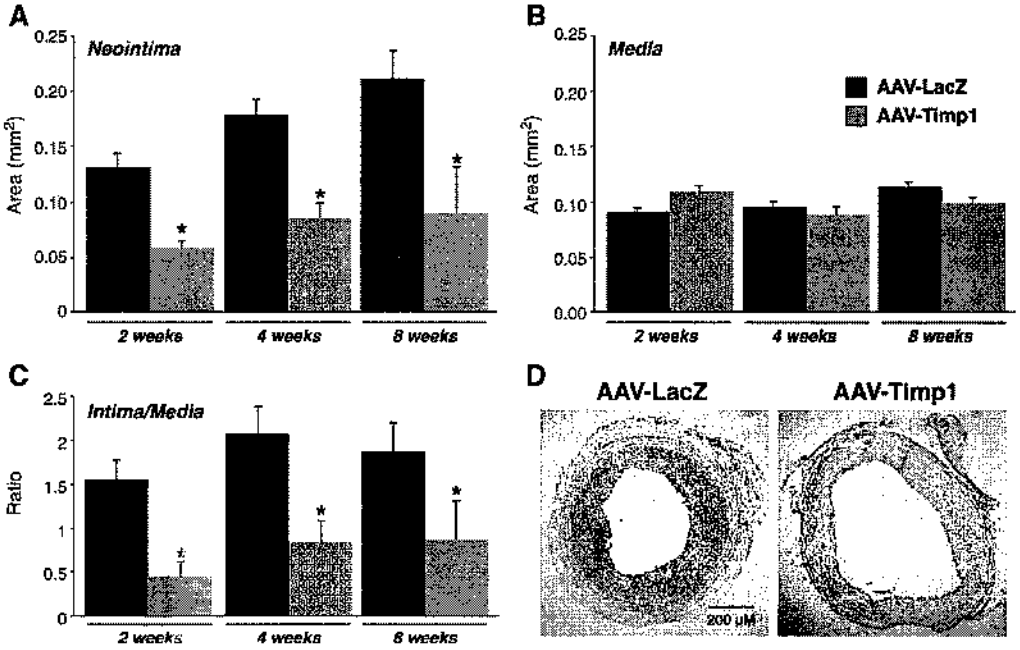


FIG. 4.

for neointima formation [7–9]. In this respect, it is worth noting that restenosis and constrictive remodeling are positively correlated with endothelial dysfunction and collagen accumulation, whereas elastin density is inversely correlated with neointimal growth [35]. Consistent with these findings, other groups have also observed that col-

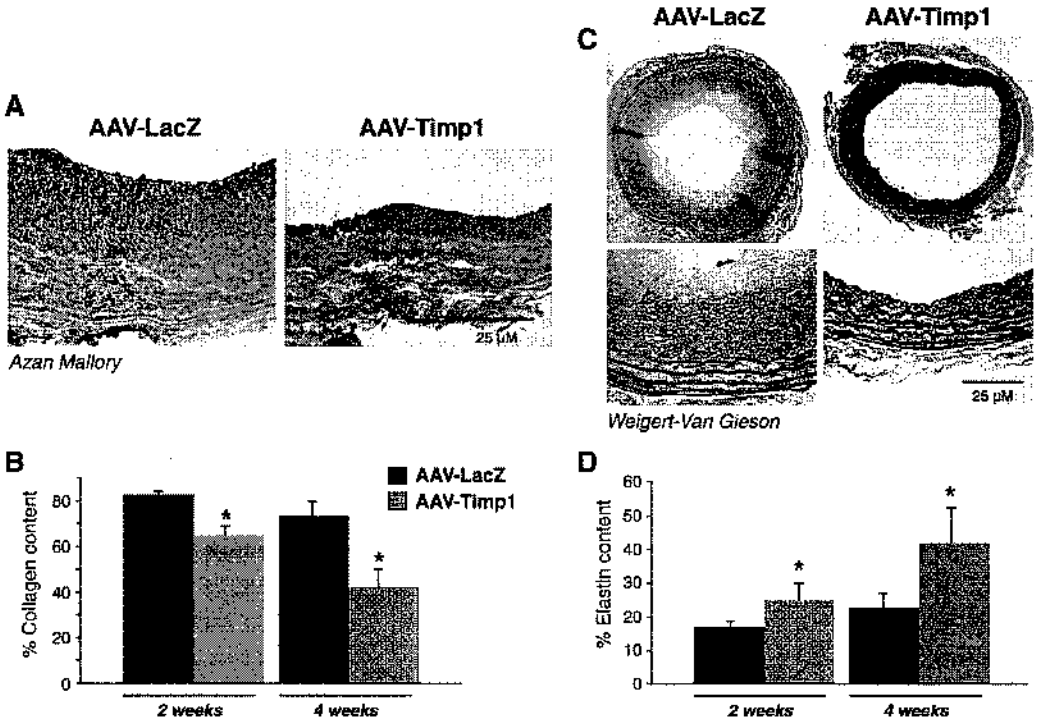


FIG. 5.

doi:10.1016/j.ymthe.2004.02.020

lagen content was altered after balloon injury in normolipemic rabbits and pigs and that pharmacological inhibition of MMPs resulted in diminished collagen accumulation [10,36]. Furthermore, Johnson *et al.* have found that MMP9 is necessary for collagen organization by SMCs [32]. Our findings, showing decreased collagen deposition and increased elastin content after AAV-mediated *TIMP1* gene transfer, are in perfect agreement with these observations, as well as with the conclusions of the work of Forough *et al.*, who have shown that local overexpression of TIMP1 increases elastin accumulation through a posttranslational processing mechanism [21]. Most likely, the overall outcome of the modifications induced by TIMP1 overexpression is the reduction of passive tensile strength (less collagen) and the maintenance of the elastic properties of the arterial wall (more elastin).

The activity of MMPs is essential to permit SMC migration and invasion of the neointima, as also confirmed by the results of our *in vitro* chemoinvasion assay. Although TIMP1 does not seem able to affect SMC proliferation directly [11,37], recent experimental evidence indicates that the composition of the extracellular matrix regulates the responsiveness of SMCs to mitogenic stimuli, allowing their transition from a contractile to a proliferative phenotype [38–41]. Accordingly, both SMC migration and proliferation are significantly impaired in MMP9-knockout mice [31]. Thus, TIMP1 might affect SMC proliferation indirectly by interfering with the remodeling of the extracellular matrix. In a consistent manner, in our *in vivo* experiments we observed that *TIMP1* gene transfer determined a marked reduction in the total number of cells in the neointima and lowered the fraction of proliferating cells, as shown by reactivity to PCNA immunostaining (data not shown). The overall result of the earlier organization of the neointimal matrix and the inhibition of SMC migration and proliferation is the reduction in neointimal thickness. This conclusion is consistent with the higher efficacy of AAV-Timp1 gene transfer in the early phases of the stenotic response (2 weeks compared to 1 or 2 months), when MMPs are overexpressed [9]. The slightly reduced effect of TIMP1 at the later time points could also be ascribed to the development of an immune response against the transferred human TIMP1. However, the high similarity between the human and the rat proteins, the persistence of human TIMP1 expression over time, and the absence of inflammation at histological examination indicate indirectly that the animals did not raise an important immune response against the transgene-expressing cells. Nevertheless, we cannot exclude the presence of neutralizing antibodies against the human TIMP1, which might account for a partial reduction in the therapeutic effect over time.

Taken together, the results described in this work suggest that MMPs contribute to the restenosis process favoring SMC migration from the media to the intima and inducing extensive remodeling of extracellular matrix, which in turn might be essential for SMC accommodation within the neointima. Up-regulation of MMP expression—especially of MMP2 and MMP9—was shown to be even higher after stent implantation than after balloon angioplasty [7]. Thus, AAV-Timp1 gene delivery might find an application as an approach to avoid neointima formation in the process of in-stent restenosis, which depends mostly on intimal hyperplasia. The development of a gene therapy strategy for this condition might be of great interest as an alternative approach to the implantation of drug-coated stents.

## Materials and Methods

***Production, purification, and characterization of rAAV vectors.*** pAAV-Timp1 was constructed by cloning the human TIMP1 cDNA, which was obtained by RT-PCR amplification from HeLa cell total RNA, to substitute for the GFP and neomycin-resistance genes in plasmid pTR-UF5, kindly provided by N. Muzyczka (University of Florida, Gainesville, FL, USA). pAAV-LacZ was again obtained by inserting the *LacZ* gene from plasmid pCH110 (Pharmacia, Uppsala, Sweden) [42] into the pTR-UF5 backbone.

The cloning and propagation of AAV plasmids was carried out in the JC 8111 *Escherichia coli* strain. Infectious AAV2 vector particles were generated and titered exactly as described previously [42,43]. Viral preparations used for this work had titers of $\sim 1 \times 10^{12}$ viral genome particles per milliliter.

***Evaluation of smooth muscle cell transduction by AAV vectors.*** To define the permissivity of smooth muscle cells to AAV vectors *in vitro*, a preparation of AAV-GFP (obtained from plasmid pTR-UF5; $1 \times 10^{11}$ genome particles) was used to transduce $1 \times 10^5$ coronary artery smooth muscle cells (purchased from Clonetics, BioWhittaker, Walkersville, MD, USA). After 5 days, flow cytometric analysis of GFP-expressing cells was performed using a FACScalibur instrument (Becton–Dickinson, San Jose, CA, USA) acquiring $1 \times 10^4$ events for each sample.

The efficiency of the AAV transduction of the arterial wall *in vivo* was evaluated by intraluminal delivery of rAAV-LacZ for 40 min. After 2 and 4 weeks from treatment, the carotid arteries were harvested, fixed, and stained for X-gal reactivity as described [22]. Five to eight 5-μm sections were counterstained with nuclear fast red.

***Chemoinvasion assay.*** To assay the ability of SMCs to invade matrix, $1 \times 10^5$ human coronary artery SMCs were transduced with either AAV-Timp1 or AAV-LacZ ($1 \times 10^{11}$ genome particles) for 48 h and then seeded in serum-free medium into the cell culture inserts of 8-μm pore size invasion chambers coated with Matrigel (BioCoat Matrigel Invasion Chambers; Becton–Dickinson). The same medium supplemented with serum and chemoattractants (hEGF 0.5 ng/ml, insulin 2.5 μg/ml, hFGF-B 1 ng/ml, FBS 5%) was placed in the lower chamber. After 22 h incubation, cells that migrated to the lower side of the filter were fixed in methanol, stained with Giemsa solution, and counted in eight fields per membrane at 400× magnification. Each assay was carried out in triplicate. Results are given as the mean number of migrated cells ± standard error of mean (SEM).

***Balloon injury and AAV application.*** Animal care and treatment were conducted in conformity with institutional guidelines issued in compliance with national and international laws and policies (EEC Council Directive 86/609, OJL 358, December 12, 1987). Male Wistar rats weighing

300–400 g were anesthetized and the right common and external carotid arteries were exposed and isolated. A 2F Fogarty catheter (Baxter–Edwards Healthcare, Irvine, CA, USA) was introduced into the common carotid artery through an arteriotomy in the external carotid artery and inflated to 1.5–2 atm. Injury was induced as described by Clowes *et al.* [2], covering a total length of 1 cm. After balloon removal, rAAV vectors were injected through an Intramedic PE50 (Becton–Dickinson) polyethylene cannula and allowed to incubate in the injured segment in the absence of flow for 40 min. The external carotid was then tied and the blood flow was restored through the common carotid artery.

The AAV-Timp1-treated group consisted of 15 animals, whereas the control group was composed of 22 animals; animals were randomly exposed to AAV-Timp1, PBS, or AAV-LacZ after an appropriate curve of learning on a previous set of animals. The treated group received 100 μl of rAAV-Timp1 ($1 \times 10^{11}$ total viral particles); the control group received 100 μl of rAAV-LacZ ($1 \times 10^{11}$ particles) or PBS ($n = 16$ and $n = 6$, respectively). Animals were sacrificed after 2, 4, and 8 weeks (Timp1 group, $n = 5$ at each time point; control group, $n = 11$, $n = 6$, $n = 5$ at 2, 4, and 8 weeks, respectively).

***Quantification of transduced hTIMP1 by real-time RT-PCR.*** Total RNA from injured arteries at different times after transduction was extracted according the guanidinium thiocyanate–phenol–chloroform extraction procedure [44]. After reverse transcription with random hexameric primers, real-time quantitative PCR was performed on a 7000 ABI Prism instrument (Applied Biosystems, Foster City, CA, USA). In the same tubes, a multiplex reaction was carried out for the simultaneous amplification of the hTIMP1 cDNA and the housekeeping gene 18s as a standard. The TaqMan probe and primers were purchased from Applied Biosystems as an Assay-on-Demand for hTIMP1 and as a Predevelopment Assay Reagent for the 18s.

***Zymography and reverse zymography.*** Three days after balloon injury, rat carotid arteries were harvested and kept in culture in serum-free medium. The 3-day conditioned medium was used for substrate gel electrophoresis under nonreducing conditions on a 0.1% gelatin and 10% SDS–polyacrylamide gel. After extensive washing in 2.5% Triton to remove SDS, the gel was incubated for 16 h at 37°C with shaking in collagenase buffer (50 mM Tris–HCl, pH 7.4, 150 mM NaCl, 5 mM $CaCl_2$, and 0.2% Triton X-100). Finally, the gel was stained in 0.1% Coomassie brilliant blue; clear zones against the blue background indicate the presence of gelatinolytic activity [45].

The activity of human TIMP1 on rat MMP activity was assessed by reverse gel zymography [45]. 293 cells transfected with pAAV-Timp1 or a control plasmid were cultured for 24 h in serum-free medium; supernatants were harvested, filtered, and concentrated prior to loading onto a 0.6% gelatin and 12% polyacrylamide gel. The gel was then incubated for 2 h in the medium of cultured rat carotid arteries (used as a source of rat MMPs) mixed 1:1 with the collagenase buffer. Functional TIMP1 appeared as a dark band at approximately $M_r$ 28,000.

***Histology and immunohistochemistry.*** For histological analysis, a segment of each harvested artery was fixed in 2% formaldehyde, embedded in paraffin, sectioned at 5 μm, and processed for microscopic examination after hematoxylin staining.

The intima and media areas and the intima-to-media ratio were calculated by digital planimetry of tissue sections, by an investigator blinded for treatment regimen. For each animal, at least four individual sections (at 350-μm intervals), obtained from the middle portion of the treated segment, were analyzed.

Protocols for immunohistochemistry were undertaken according to the Vectastain Elite ABC Kit (universal or goat) from Vector Laboratories using primary antibodies against TIMP1 (NeoMarkers, Fremont, CA, USA) and α-SMA (1A4; Sigma Chemical Co., St. Louis, MO, USA). After treatment, slides were rinsed in PBS and signal was developed using 3,3′-diaminobenzidine as substrate for the peroxidase chromogenic reaction (Lab Vision Corp., Fremont, CA, USA).

***Collagen and elastin content quantification.*** The collagen and elastin content was assessed by Azan–Mallory and Weigert–Van Gieson staining. Briefly, for Azan–Mallory staining rehydrated sections were consecutively stained in Azocarmin and Azan solutions, using phosphotungstic acid as a mordant, and a careful differentiation was completed in anilin. For Weigert–Van Gieson staining, rehydrated sections were first stained in Weigert resorcin fuchsin solution at 60°C, rinsed in water, differentiated in acid alcohol, and counterstained in Van Gieson solution.

For each animal analyzed, at least three individual sections (at 350-μm intervals) were stained with Azan–Mallory or Weigert–Van Gieson to evaluate collagen (cyan) and elastin (black), respectively. Histological quantification was performed by transforming the respective colors into monochrome with a 255-level gray scale (NIH Image J 1.29 software, Bethesda, MD, USA), followed by the evaluation of the relative number of pixels after adjustment of the individual thresholds for each color, thus permitting a binary analysis [35]. Results are expressed as the number of pixels per area classified as collagen or elastin divided by total number of pixels in each area.

***Statistical analysis.*** Results are expressed as means ± SEM. The Student *t* test was used to compare cell migration, media (M) and neointima (I) mean areas, and I/M ratios. The nonparametric Mann–Whitney test was used to compare collagen and elastin content in treated and control groups. Values were considered statistically different when $P < 0.05$. Two occluded arteries were excluded from the AAV-Timp1 group at 14 days and one from AAV-LacZ group at 28 days.

## ACKNOWLEDGMENTS

*This work was supported by grants from the Progetto Finalizzato "Genetica Molecolare" of the Italian National Research Council and from the Fondazione Cassa di Risparmio of Trieste, Italy. The authors are grateful to Sara Tomasi for technical support and to Suzanne Kerbavcic for editorial assistance.*

RECEIVED FOR PUBLICATION JULY 4, 2003; ACCEPTED FEBRUARY 29, 2004.

## REFERENCES

1. Topol, E. J., and Serruys, P. W. (1998). Frontiers in interventional cardiology. *Circulation* **98:** 1802–1820.
2. Clowes, A. W., and Schwartz, S. M. (1985). Significance of quiescent smooth muscle migration in the injured rat carotid artery. *Circ. Res* **56:** 139–145.
3. Serruys, P. W., *et al.* (1994). A comparison of balloon-expandable-stent implantation with balloon angioplasty in patients with coronary artery disease. Benestent Study Group. *N. Engl. J. Med.* **331:** 489–495.
4. Hoffmann, R., *et al.* (1996). Patterns and mechanisms of in-stent restenosis: a serial intravascular ultrasound study. *Circulation* **94:** 1247–1254.
5. Loscalzo, J. (2000). Vascular matrix and vein graft failure: is the message in the medium? *Circulation* **101:** 221–223.
6. Libby, P., and Lee, R. T. (2000). Matrix matters. *Circulation* **102:** 1874–1876.
7. Feldman, L. J., *et al.* (2001). Differential expression of matrix metalloproteinases after stent implantation and balloon angioplasty in the hypercholesterolemic rabbit. *Circulation* **103:** 3117–3122.
8. de Smet, B. J., *et al.* (2000). Metalloproteinase inhibition reduces constrictive arterial remodeling after balloon angioplasty: a study in the atherosclerotic Yucatan micropig. *Circulation* **101:** 2962–2967.
9. Bendeck, M. P., Zempo, N., Clowes, A. W., Galardy, R. E., and Reidy, M. A. (1994). Smooth muscle cell migration and matrix metalloproteinase expression after arterial injury in the rat. *Circ. Res.* **75:** 539–545.
10. Strauss, B. H., *et al.* (1996). In vivo collagen turnover following experimental balloon angioplasty injury and the role of matrix metalloproteinases. *Circ. Res.* **79:** 541–550.
11. George, S. J., Johnson, J. L., Angelini, G. D., Newby, A. C., and Baker, A. H. (1998). Adenovirus-mediated gene transfer of the human TIMP-1 gene inhibits smooth muscle cell migration and neointimal formation in human saphenous vein. *Hum. Gene Ther.* **9:** 867–877.
12. Lijnen, H. R., Soloway, P., and Collen, D. (1999). Tissue inhibitor of matrix metalloproteinases-1 impairs arterial neointima formation after vascular injury in mice. *Circ. Res.* **85:** 1186–1191.
13. Dollery, C. M., Humphries, S. E., McClelland, A., Latchman, D. S., and McEwan, J. R. (1999). Expression of tissue inhibitor of matrix metalloproteinases 1 by use of an adenoviral vector inhibits smooth muscle cell migration and reduces neointimal hyperplasia in the rat model of vascular balloon injury. *Circulation* **99:** 3199–3205.

14. Turunen, M. P., *et al.* (2002). Peptide-retargeted adenovirus encoding a tissue inhibitor of metalloproteinase-1 decreases restenosis after intravascular gene transfer. *Mol. Ther.* **6:** 306–312.
15. Morishige, K., *et al.* (2003). Overexpression of matrix metalloproteinase-9 promotes intravascular thrombus formation in porcine coronary arteries in vivo. *Cardiovasc. Res.* **57:** 572–585.
16. Silence, J., Collen, D., and Lijnen, H. R. (2002). Reduced atherosclerotic plaque but enhanced aneurysm formation in mice with inactivation of the tissue inhibitor of metalloproteinase-1 (TIMP-1) gene. *Circ. Res.* **90:** 897–903.
17. Lemaitre, V., Soloway, P. D., and D'Armiento, J. (2003). Increased medial degradation with pseudo-aneurysm formation in apolipoprotein E-knockout mice deficient in tissue inhibitor of metalloproteinases-1. *Circulation* **107:** 333–338.
18. Forough, R., *et al.* (1996). Overexpression of tissue inhibitor of matrix metalloproteinase-1 inhibits vascular smooth muscle cell functions in vitro and in vivo. *Circ. Res.* **79:** 812–820.
19. Monahan, P. E., and Samulski, R. J. (2000). AAV vectors: is clinical success on the horizon? *Gene Ther.* **7:** 24–30.
20. Arsic, N., *et al.* (2003). Induction of functional neovascularization by combined VEGF and angiopoietin-1 gene transfer using AAV vectors. *Mol. Ther.* **7:** 450–459.
21. Forough, R., *et al.* (1998). Metalloproteinase blockade by local overexpression of TIMP-1 increases elastin accumulation in rat carotid artery intima. *Arterioscler. Thromb. Vasc. Biol.* **18:** 803–807.
22. Rolling, F., Nong, Z., Pisvin, S., and Collen, D. (1997). Adeno-associated virus-mediated gene transfer into rat carotid arteries. *Gene Ther.* **4:** 757–761
23. Ward, M. R., Pasterkamp, G., Yeung, A. C., and Borst, C. (2000). Arterial remodeling: mechanisms and clinical implications. *Circulation* **102:** 1186–1191.
24. Galis, Z. S., and Khatri, J. J. (2002). Matrix metalloproteinases in vascular remodeling and atherogenesis: the good, the bad, and the ugly. *Circ. Res.* **90:** 251–262.
25. Hojo, Y., Ikeda, U., Katsuki, T., Mizuno, O., Fujikawa, H., and Shimada, K. (2002). Matrix metalloproteinase expression in the coronary circulation induced by coronary angioplasty. *Atherosclerosis* **161:** 185–192.
26. Kranzhofer, A., Baker, A. H., George, S. J., and Newby, A. C. (1999). Expression of tissue inhibitor of metalloproteinase-1, -2, and -3 during neointima formation in organ cultures of human saphenous vein. *Arterioscler. Thromb. Vasc. Biol.* **19:** 255–265.
27. Godin, D., Ivan, E., Johnson, C., Magid, R., and Galis, Z. S. (2000). Remodeling of carotid artery is associated with increased expression of matrix metalloproteinases in mouse blood flow cessation model. *Circulation* **102:** 2861–2866.
28. Cho, H. J., *et al.* (2002). Functional polymorphism in the promoter region of the gelatinase B gene in relation to coronary artery disease and restenosis after percutaneous coronary intervention. *J. Hum. Genet.* **47:** 88–91.
29. Kuzuya, M., *et al.* (2003). Deficiency of gelatinase a suppresses smooth muscle cell invasion and development of experimental intimal hyperplasia. *Circulation* **108:** 1375–1381.
30. Galis, Z. S., *et al.* (2002). Targeted disruption of the matrix metalloproteinase-9 gene impairs smooth muscle cell migration and geometrical arterial remodeling. *Circ. Res.* **91:** 852–859.
31. Cho, A., and Reidy, M. A. (2002). Matrix metalloproteinase-9 is necessary for the regulation of smooth muscle cell replication and migration after arterial injury. *Circ. Res.* **91:** 845–851.
32. Johnson, C., and Galis, Z. S. (2003). Matrix metalloproteinase-2 and -9 differentially regulate smooth muscle cell migration and cell-mediated collagen organization. *Arterioscler. Thromb. Vasc. Biol.*
33. Bendeck, M. P., Conte, M., Zhang, M., Nili, N., Strauss, B. H., and Farwell, S. M. (2002). Doxycycline modulates smooth muscle cell growth, migration, and matrix remodeling after arterial injury. *Am. J. Pathol.* **160:** 1089–1095.
34. Wentzel, J. J., *et al.* (2001). Shear-stress and wall-stress regulation of vascular remodeling after balloon angioplasty: effect of matrix metalloproteinase inhibition. *Circulation* **104:** 91–96.
35. Lafont, A., *et al.* (1999). Endothelial dysfunction and collagen accumulation: two independent factors for restenosis and constrictive remodeling after experimental angioplasty. *Circulation* **100:** 1109–1115.
36. Sierevogel, M. J., *et al.* (2002). Matrix metalloproteinase inhibition reduces adventitial thickening and collagen accumulation following balloon dilation. *Cardiovasc. Res.* **55:** 864–869.
37. Baker, A. H., Zaltsman, A. B., George, S. J., and Newby, A. C. (1998). Divergent effects of tissue inhibitor of metalloproteinase-1, -2, or -3 overexpression on rat vascular smooth muscle cell invasion, proliferation, and death in vitro: TIMP-3 promotes apoptosis. *J. Clin. Invest.* **101:** 1478–1487.
38. Raines, E. W., Koyama, H., and Carragher, N. O. (2000). The extracellular matrix dynamically regulates smooth muscle cell responsiveness to PDGF. *Ann. N. Y. Acad. Sci.* **902:** 39–51, discussion 51–32.
39. Davenpeck, K. L., *et al.* (2001). Regional differences in integrin expression: role of alpha(5)beta(1) in regulating smooth muscle cell functions. *Circ. Res.* **88:** 352–358.
40. Stegemann, J. P., and Nerem, R. M. (2003). Altered response of vascular smooth muscle cells to exogenous biochemical stimulation in two- and three-dimensional culture. *Exp. Cell Res.* **283:** 146–155.
41. Ross, J. J., and Tranquillo, R. T. (2003). ECM gene expression correlates with in vitro tissue growth and development in fibrin gel remodeled by neonatal smooth muscle cells. *Matrix Biol.* **22:** 477–490.
42. Deodato, B., *et al.* (2002). Recombinant AAV vector encoding human VEGF165 enhances wound healing. *Gene Ther.* **9:** 777–785.
43. Zentilin, L., Marcello, A., and Giacca, M. (2001). Involvement of cellular double-strand DNA break-binding proteins in processing of recombinant adeno-associated virus (AAV) genome. *J. Virol.* **75:** 12279–12287.
44. Chomczynski, P., and Sacchi, N. (1987). Single-step method of RNA isolation by acid guanidinium thiocyanate–phenol–chloroform extraction. *Anal. Biochem.* **162:** 156–159.
45. Zacchigna, S., *et al.* (2004). AAV-mediated gene transfer of tissue inhibitor of metalloproteinases-1 inhibits vascular tumor growth and angiogenesis in vivo. *Cancer Gene Ther.* **11:** 73–80.

# Pentraxin 3 Inhibits Fibroblast Growth Factor 2–Dependent Activation of Smooth Muscle Cells In Vitro and Neointima Formation In Vivo

Maura Camozzi, Serena Zacchigna, Marco Rusnati, Daniela Coltrini, Genaro Ramirez-Correa, Barbara Bottazzi, Alberto Mantovani, Mauro Giacca, Marco Presta

***Objective***—The fibroblast growth factor (FGF)/FGF receptor system plays an important role in smooth muscle cell (SMC) activation. Long-pentraxin 3 (PTX3) is a soluble pattern recognition receptor with non-redundant functions in inflammation and innate immunity. PTX3 is produced by different cell types of the vessel wall, including SMCs. PTX3 binds FGF2 and inhibits its angiogenic activity on endothelial cells. We investigated the capacity of PTX3 to affect FGF2-dependent SMC activation in vitro and in vivo.

***Methods and Results***—When added to human coronary artery SMCs, human PTX3 inhibits cell proliferation driven by endogenous FGF2 and the mitogenic and chemotactic activity exerted by exogenous recombinant FGF2. Accordingly, PTX3 prevents $^{125}$I-FGF2 interaction with FGF receptors on the same cells. Also, PTX3 overexpression after recombinant adeno-associated virus-*PTX3* gene transfer inhibits human coronary artery SMC proliferation and survival promoted by FGF2 in vitro. Consistently, a single local endovascular injection of recombinant adeno-associated virus-*PTX3* gene inhibits intimal thickening after balloon injury in rat carotid arteries.

***Conclusions***—PTX3 is a potent inhibitor of the autocrine and paracrine stimulation exerted by FGF2 on SMCs. Local PTX3 upregulation may modulate SMC activation after arterial injury. (***Arterioscler Thromb Vasc Biol.* 2005;25:0-0.**)

**Key Words:** smooth muscle cells ■ arterial injury ■ gene therapy ■ fibroblast growth factor ■ pentraxin 3

Excessive growth of vascular smooth muscle cells (SMCs) is an important component in atherosclerosis and restenosis. Fibroblast growth factors (FGFs), a family of pleiotropic heparin-binding growth factors,[1] exert their activity by interacting with tyrosine-kinase receptors (FGFRs) on target cells.[2] The FGF/FGFR system plays an important role in SMC activation in vitro and in vivo after arterial injury. Indeed, FGF2 promotes survival, proliferation, and migration of SMCs[3–6] that express FGFRs.[7] FGFs are expressed in injured arteries and contribute to intimal thickening.[8,9] Accordingly, arterial injury leads to FGFR upregulation in SMCs.[8,10] Also, most of the cell types found in the restenotic area, eg, endothelial cells, macrophages, T-cells, and SMCs themselves, synthesize FGFs,[11] the production and release of which is modulated by inflammatory mediators,[12,13] hypoxia,[14] and cell damage.[15]

Pentraxin 3 (PTX3) is the prototypic member of the long-pentraxin family.[16] PTX3 is a glycosylated protein whose C-terminal pentraxin domain shares homology with the entire sequence of the classic short-pentraxins C-reactive protein and serum amyloid P (SAP) component, whereas its $NH_2$-terminal portion does not show homology with any other known protein. PTX3 is a soluble pattern recognition receptor with unique non-redundant functions in various physiopathological conditions and may serve as a mechanism of amplification of inflammation and innate immunity.[16] Unlike short-pentraxins produced by the liver in response to inflammatory mediators, PTX3 is synthesized at the inflammatory site by monocytes and endothelial cells in response to inflammatory cytokines.[16] In endothelial cells, PTX3 upregulates tissue factor expression, possibly acting as an endothelial regulator during thrombogenesis and ischemic vascular disease.[17] Also, PTX3 is upregulated during vasculitis,[18] and increased plasma level of PTX3 predicts 3-month survival in patients with acute myocardial infarction.[19,20]

Recent observations have shown that PTX3 is present in atherosclerotic plaques[21] and is expressed by SMCs isolated from human arterial specimens.[22] Moreover, PTX3 binds FGF2 and inhibits its angiogenic activity on endothelial cells.[23] On this basis, we investigated the capacity of PTX3 to affect FGF2-dependent SMC activation in vitro and the impact of recombinant adeno-associated virus (rAAV)-*PTX3* gene transfer on neointimal hyperplasia after arterial injury in vivo.

Original received January 24, 2005; final version accepted June 30, 2005.

From the Unit of General Pathology (M.C., M.R., M.P.) and Unit of Histology (D.C.), Department of Biomedical Sciences and Biotechnology, School of Medicine, University of Brescia; Molecular Medicine Laboratory, International Center for Genetic Engineering and Biotechnology, Trieste (S.Z., G.R.-C., M.G.); Mario Negri Institute, Milan (B.B., A.M.); and the Institute of General Pathology, University of Milan, Milan (A.M.), Italy.

Correspondence to Marco Presta, General Pathology & Immunology, Department of Biomedical Sciences and Biotechnology, viale Europa 11, 25123 Brescia, Italy. E-mail presta@med.unibs.it



*Arterioscler Thromb Vasc Biol.* is available at http://www.atvbaha.org DOI: 10.1161/01.ATV.0000177807.54959.7d

# Methods

## Chemicals

Human recombinant FGF2 and PTX3 were produced as described.[24,25] SAP, epidermal growth factor (EGF), and insulin were from Sigma. Neutralizing anti-FGF2 antibodies were from UBI. The recombinant soluble extracellular domain of FGFR-1 (xcFGFR-1) was provided by A. Isacchi (Pharmacia-Upjohn, Nerviano, Italy).

## Cell Cultures and rAAV Transduction

Human coronary artery SMCs (HCASMCs) were grown in complete smooth muscle cell growth medium-2 (PBI International) containing 5% fetal calf serum (FCS). pAAV-*PTX3* was constructed by cloning the human *PTX3* cDNA in pTR-UF5 plasmid (provided by N. Muzyczka, University of Florida, Miami, Fla) to replace the *GFP* and neomycin-resistance genes. pAAV-*LacZ* was obtained by inserting the *LacZ* gene from plasmid pCH110 (Amersham) in the pTR-UF5 backbone.[26] The cloning and propagation of AAV plasmids was carried out in the JC 8111 *Escherichia coli* strain. Infectious AAV2 vector particles were generated and titered as described.[26] HCASMCs were transduced with AAV-*PTX3* or *AAV-LacZ*, and PTX3 and FGF2 protein levels were evaluated in the cell extracts and conditioned media by ELISA (see supplemental Methods, available online at http://atvb.ahajourn.ls.org).

## Cell Proliferation and Caspase-3 Activation Assays

Parental or AAV-infected HCASMCs were seeded at 5000 cells/cm$^2$ in complete smooth muscle cell growth medium-2. After overnight incubation, fresh basal medium containing 0.5% FCS was added and cells were incubated at 37°C in the presence of selected molecules. At selected periods of time, cells were trypsinized and counted in a Burker chamber. The experiments were repeated 3 to 6 times in duplicate. Parallel cell cultures were acetone-fixed and incubated overnight at 4°C with anti-cleaved caspase-3 antibody (Cell Signaling Technology) and then with goat anti-rabbit immunoglobulin G-fluorescein isothiocyanate antibody for 1 hour. Nuclei were stained with DAPI. Next, the percentage of cleaved caspase-3 positive cells was assessed under a fluorescence microscope in 10 random ×400 fields per sample.

For $^3$H-thymidine incorporation, HCASMCs in basal medium containing 0.5% FCS were added with FGF2 (1.7 nmol/L) in the absence or presence of 220 nmol/L of PTX3 or SAP. After 14 hours, cells were incubated for 10 hours with $^3$H-thymidine (2 μCi/mL). Radioactivity incorporated in trichloroacetic acid-insoluble material was determined by scintillation counting and data were expressed as cpm/μg of DNA. The experiments were repeated twice in triplicate. Cell viability evaluated at the end of incubation by Trypan blue exclusion was higher than 98% under all experimental conditions.

## Chemotaxis Assay

HCASMCs (1x10$^6$ cells/mL) were seeded in serum-free medium in the upper compartment of a Boyden chamber containing a gelatin-coated 5 μm PVP free polycarbonate filter (Costar). FGF2s with or without PTX3 or SAP were placed in the lower compartment. After 4 hours at 37°C, cells that migrated to the lower side of the filter were stained with Diff-Quik (Dade-Behring) and 5 random fields were counted for each experimental condition. The experiments were repeated 3 times in triplicate.

## $^{125}$I-FGF2 Cell Binding and Solid Phase Binding Assays

Confluent HCASMCs were incubated at 4°C in serum-free medium containing $^{125}$I-FGF2 (0.11 nmol/L, specific radioactivity of 800 cpm/fmol), 0.15% gelatin, and 20 mmol/L Hepes buffer (pH 7.5), with or without PTX3. After 2 hours, the amount of $^{125}$I-FGF2 bound to FGFRs was evaluated.[27] For solid phase binding assay, ELISA microplates were coated with PTX3 and incubated with $^{125}$I-FGF2 (1.6 nmol/L) in the presence of increasing concentrations of soluble extracellular domain of FGFR-1 (xcFGFR-1). PTX3-bound radioactivity was then measured (see supplemental Methods). The experiments were repeated 3 times in duplicate.

## Reverse Transcription-Polymerase Chain Reaction Assay

Total RNA was isolated by the TRIzol method from HCASMCs ($3\times10^4$ cells/well in 24-well plates). Total RNA (2 μg) was retrotranscribed with Ready-To-Go You-Prime First Strand Beads (Amersham). Then, 1/10$^{th}$ of the reaction was amplified in a final volume of 25 μL using the primers for human PTX3, FGF2, or FGFR-1 (see supplemental Methods). After polymerase chain reaction, 5-μL aliquots were separated on a 1.5% agarose gel and visualized by ethidium bromide staining.

## Balloon Injury and rAAV Vector Application

A 2F Fogarty catheter was introduced into the common carotid artery of anesthetized male Wistar rats, inflated to 1.5 to 2.0 atmospheres, and a 10-mm injury was induced (see supplemental Methods). After balloon removal, 100-μL aliquots of phosphate-buffered saline containing no viral particles (n=6), AAV-*LacZ* ($1\times10^{11}$ particles, n=11), or AAV-*PTX3* ($1\times10^{11}$ particles, n=12) were injected through a cannula and allowed to incubate in the injured segment for 40 minutes. The external carotid was then tied and the blood flow was restored. Animals were euthanized after 2 and 4 weeks. Media and neointima areas of injured arteries were quantified and intima-to-media ratios were calculated. PTX3 immunostaining of paraffin-embedded carotid sections was performed 4 weeks after injury using a rabbit polyclonal anti-PTX3 antibody (see supplemental Methods).

## Statistical Analysis

Results are expressed as mean±SEM. Student *t* test was used for statistical analysis and $P<0.05$ was considered significant.

# Results

## PTX3 Inhibits FGF2-Induced Proliferation and Chemotaxis in SMCs

SMCs produce FGF2 that, in turn, stimulates their proliferation and migration[3,4] by interacting with FGFRs.[28] Accordingly, HCASMCs express FGF2 and FGFR-1 transcripts (Figure 1A, inset), and anti-FGF2 antibodies (60 nmol/L) inhibit the proliferation of HCASMCs when grown in 0.5% FCS (Figure 1A). These data demonstrate the existence of a FGF2-dependent autocrine loop of stimulation in HCASMCs. Under the same experimental conditions, addition of 220 nmol/L of PTX3 to HCASMCs caused a similar inhibitory effect (Figure 1A). SAP, which shares a high homology with the PTX3 C-terminus,[29] was ineffective (data not shown).

HCASMCs respond to exogenously added FGF2 with an increase in proliferation rate and DNA synthesis that were suppressed by anti-FGF2 antibodies and PTX3 but not SAP (Figure 1B and 1C). PTX3 did not affect the mitogenic activity of insulin, EGF, or serum, confirming the specificity of its FGF2-antagonist activity (Figure 1D). FGF2 also exerted a chemotactic activity on HCASMCs (Figure 2A) which was inhibited by PTX3 but not by SAP (Figure 2B).

These data suggest that PTX3 inhibits FGF2-driven stimulation by preventing FGF2 interaction with HCASMCs. Indeed, PTX3 inhibits the binding of $^{125}$I-FGF2 to FGFRs expressed on HCASMCs at doses similar to those required to inhibit the mitogenic and chemotactic activity of FGF2 (Figure 3A). To confirm that the interactions of FGF2 with PTX3 or FGFRs are mutually exclusive, plastic-immobilized PTX3 was incubated with $^{125}$I-FGF2 in the presence of

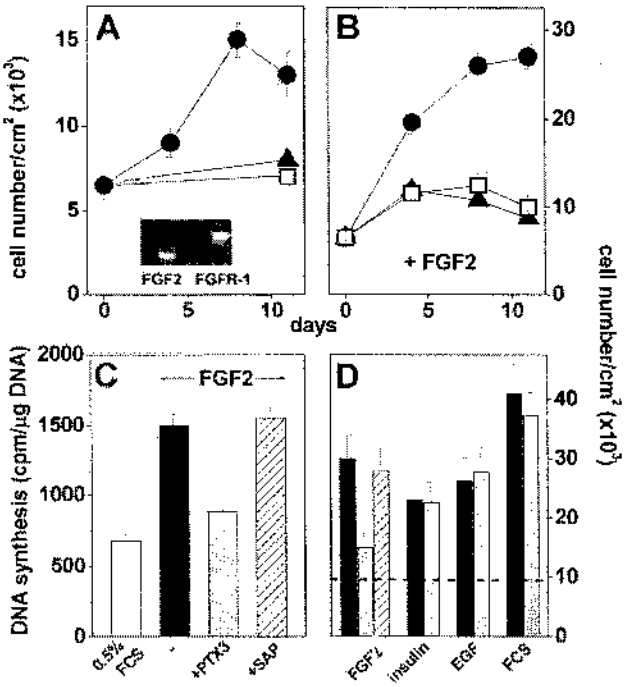


**Figure 1.** Effect of PTX3 on the mitogenic activity of FGF2 in HCASMCs. A, Proliferation of HCASMCs treated with 0.5% FCS alone (●), PTX3 (220 nmol/L) (□), or anti-FGF2 antibodies (60 nmol/L) (▲); inset, real-time polymerase chain reaction analysis of FGF2 and FGFR-1 mRNA expression in HCASMCs. B, The experiment was performed as in A but in the presence of 1.7 nmol/L FGF2. C, $^{3}$H-thymidine incorporation in HCASMCs treated with FGF2 (1.7 nmol/L) in the absence (black bar) or presence of 220 nmol/L of PTX3 (gray bar) or SAP (dashed bar). D, Proliferation of HCASMCs treated for 4 days with FGF2 (1.7 nmol/L), insulin (0.83 μmol/L), EGF (5.0 nmol/L), or 5% FCS in the absence (black bars) or in the presence of PTX3 (gray bars) or SAP (dashed bar) (both at 220 nmol/L). All mitogens induced a significant increase in cell proliferation when compared with cells grown in 0.5% FCS (dashed line).

xcFGFR-1. As anticipated, xcFGFR-1 prevented the binding of $^{125}$I-FGF2 to immobilized PTX3 (Figure 3B).

## *AAV-PTX3* Transduction Inhibits FGF2-Induced SMC Proliferation and Survival

PTX3 is expressed by vascular SMCs under defined conditions.[21,22] To assess the effect of endogenous PTX3 on SMC behavior, HCASMCs were infected with an rAAV harboring the human *PTX3* cDNA, generating AAV-*PTX3* HCASMCs. Preliminary experiments performed with cells transduced with *LacZ*-AAV (AAV-*LacZ* HCASMCs) showed that the infection efficiency was higher than 70% (data not shown).

AAV-*PTX3* infection resulted in the upregulation of PTX3 mRNA in AAV-*PTX3* HCASMCs when compared with AAV-*LacZ* HCASMCs (Figure 4A, inset). This was paralleled by an increase of PTX3 protein produced and released by AAV-*PTX3*–infected cells (PTX3 levels in the conditioned medium of AAV-*PTX3* and AAV-*LacZ* HCASMCs were equal to 100 pmol/L and 8 pmol/L, respectively). AAV infection and consequent PTX3 upregulation did not affect FGF2 expression. Indeed, AAV-*PTX3* and AAV-*LacZ* HCASMCs showed similar levels of cell-associated (4.4 versus 5.0 fmol/μg) and released (2.2 versus 2.7 pmol/L)

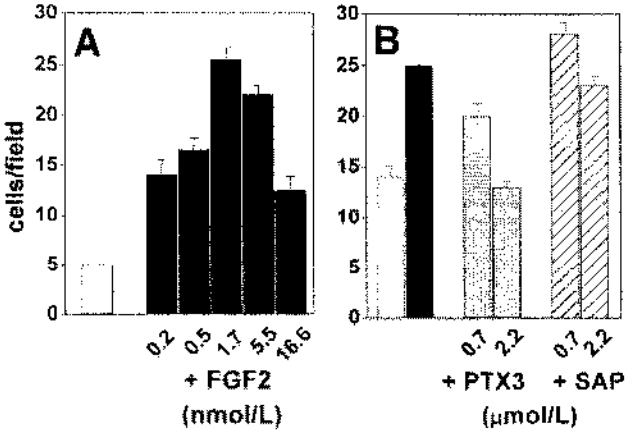


**Figure 2.** Effect of PTX3 on the chemotactic activity of FGF2 in HCASMCs. Cells were seeded in the upper compartment of a Boyden chamber. A, Serum-free medium alone (white bar) or added with the indicated concentrations of FGF2 (black bars) was placed in the lower compartment. B, FGF2 (1.7 nmol/L) was placed in the lower compartment in the presence of PTX3 (gray bars) or SAP (dashed bars), and migrated cells were counted 4 hours thereafter.

FGF2 protein. Nevertheless, AAV-*PTX3* transduction blocked the proliferation of HCASMCs maintained in 0.5% FCS when compared with AAV-*LacZ* HCASMCs (Figure 4A, open symbols). Also, AAV-*PTX3* HCASMCs were unable to respond to exogenously added recombinant FGF2. The inhibitory effect was specific because the growth factor maintained its mitogenic activity in control AAV-*LacZ* HCASMCs (Figure 4A).

FGF2 represents an important SMC survival factor.[5,6] Deprivation of endogenous FGF2 after PTX3 upregulation caused caspase-3 activation in AAV-*PTX3* HCASMCs that was drastically reduced by recombinant FGF2 treatment to values similar to those observed in AAV-*LacZ* HCASMCs (Figure 4B and 4C; Figure I, available online at http://atvb.ahajournals.org). Accordingly, cell number was reduced

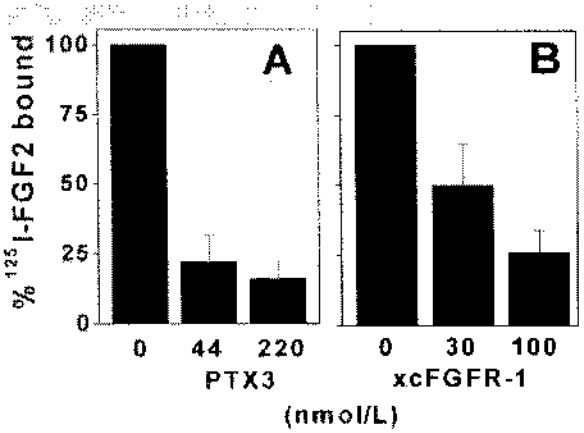


**Figure 3.** Effect of PTX3 on $^{125}$I-FGF2 binding to FGFRs. A, HCASMCs were incubated with $^{125}$I-FGF2 in the presence of PTX3. The amount of $^{125}$I-FGF2 bound to FGFRs is expressed as percent of radioactivity measured in cells incubated in the absence of PTX3. B, PTX3-coated wells were incubated with $^{125}$I-FGF2 in the presence of soluble xcFGFR-1. PTX3-bound radioactivity was expressed as percent of the binding measured in the absence of the competitor.

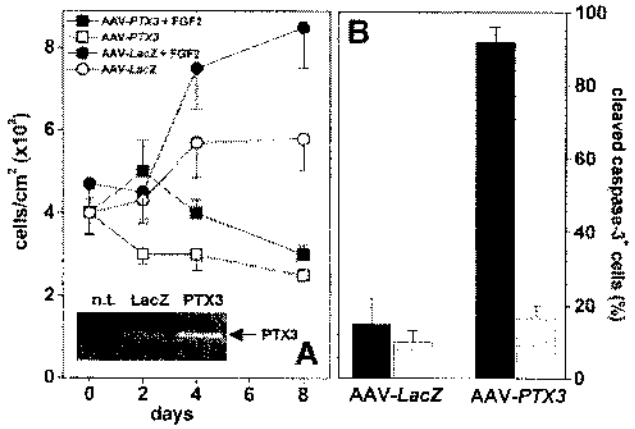


**Figure 4.** Effect of PTX3 overexpression in HCASMCs. A, Proliferation of AAV-*PTX3*- (squares) and AAV-*LacZ*-transduced (circles) HCASMCs incubated in the absence (open symbols) or presence (closed symbols) of FGF2 (1.7 nmol/L); inset, real-time polymerase chain reaction analysis of PTX3 mRNA expression in AAV-*LacZ* and AAV-*PTX3* HCASMCs. n.t. indicates no template. B, Caspase-3 activation in AAV-*LacZ* and AAV-*PTX3* HCASMCs. The percentage of cleaved caspase-3 positive cells was calculated 2 days after treatment with vehicle (black bars) or FGF2 (gray bars).

overtime in PTX3-overexpressing HCASMCs (Figure 4A). Similarly, PTX3 protein treatment, like anti-FGF2 antibodies, caused caspase-3 activation in AAV-*LacZ* HCASMCs (Figure II, available online at http://atvb.ahajournals.org).

## Efficacy of *AAV-PTX3* in the Reduction of Intimal Hyperplasia

To explore the effects of PTX3 expression in vivo, we evaluated its ability to prevent intimal hyperplasia after arterial injury. Rat carotid arteries infected with AAV-*LacZ* immediately after balloon injury express β-galactosidase with a peak 2 weeks after infection that persists over the following weeks. The marker gene is expressed throughout the vessel wall, maximally in the neointima (Figure 5D), including infiltrating SMCs.[30] Therefore, the rat carotid artery of 12 rats was exposed to AAV-*PTX3* for 40 minutes immediately after balloon injury. A matched group of control animals received either AAV-*LacZ* or phosphate-buffered saline. Immunostaining of carotid sections demonstrates that PTX3 is expressed in the intima and media of AAV-*PTX3*-treated animals both at 2 weeks (data not shown) and 4 weeks after infection when compared with control animals (Figure 5C). At these time points, the stenotic response was quantified by measuring the intima and media areas. The thickness of the media of the injured rat carotids was similar in control and AAV-*PTX3*-treated groups (0.09±0.01 versus 0.11±0.01 mm² at 2 weeks; 0.10±0.01 versus 0.12±0.01 mm² at 4 weeks), whereas the neointimal area of the treated group was significantly reduced both at 2 and 4 weeks (0.13±0.01 versus 0.08±0.02 mm² at 2 weeks, $P<0.05$; 0.18±0.01 versus 0.15±0.03 mm² at 4 weeks, $P<0.05$) (Figure 5A and 5B). Accordingly, the intima-to-media ratio, a more sensitive parameter for assessing relative changes in intima and media thickness, was significantly reduced in the AAV-*PTX3*-treated group

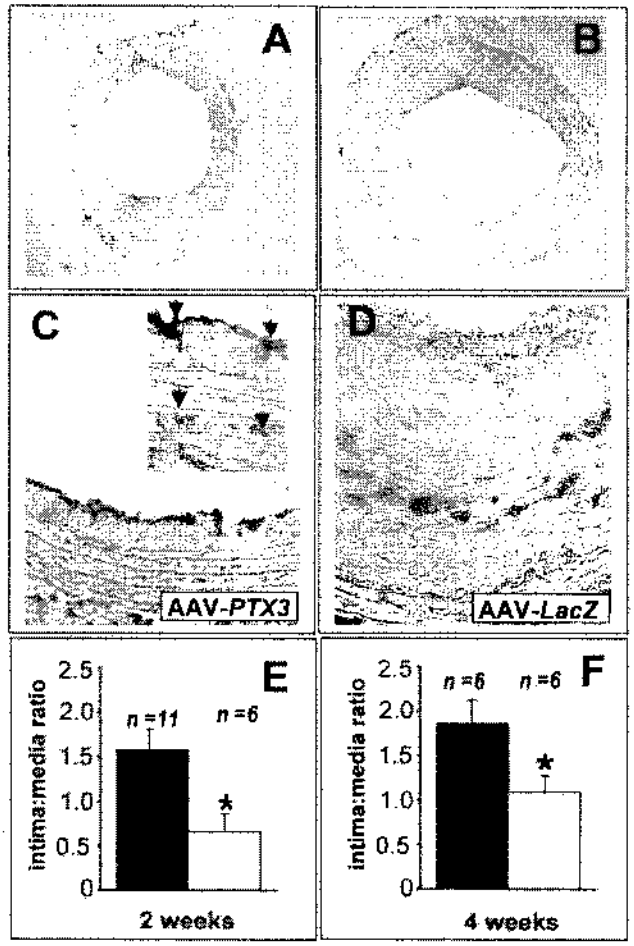


**Figure 5.** AAV-*PTX3* transduction in balloon-injured rat carotids. Neointima formation in 2 carotid arteries transduced with AAV-*PTX3* (A) or AAV-*LacZ* (B) at 2 weeks after injury. At 4 weeks, immunostaining shows an intense PTX3 immunoreactivity (arrows in inset) in an AAV-*PTX3*-transduced carotid (C) compared with an AAV-*LacZ*-transduced vessel counterstained for β-galactosidase (D). Morphometric analysis of rat carotid intima-to-media ratio was performed at 2 weeks (E) and 4 weeks (F) after balloon injury in control animals that received either AAV-*LacZ* or phosphate-buffered saline (black bars) and in animals treated with AAV-*PTX3* (open bars). *$P<0.05$. Original magnification in C and D, ×200; inset in C, ×400. Nonspecific staining of adventitia (detectable also by omitting primary antibody [not shown]) is observed in both C and D.

compared with controls (55% and 44% inhibition at 2 and 4 weeks, respectively) (Figure 5E and 5F).

## Discussion

The FGF/FGFR system plays a key role in SMC proliferation, migration, and survival in vitro[3–6] and neointimal thickening after arterial injury.[8,9] Accordingly, in vivo abrogation of FGF2 activity or FGFR signaling inhibits SMC proliferation after intimal injury.[9,10,28] Here we demonstrate that PTX3 exerts a potent FGF2 antagonist activity by suppressing cell proliferation, survival, and migration in HCASMCs and by inhibiting intimal thickening after carotid injury.

HCASMCs express both FGF2 and FGFR1 transcripts. Anti-FGF2 antibodies suppress the proliferation of HCASMCs maintained under low serum concentrations,

demonstrating the existence of an autocrine FGF2 signaling in these cells, as already shown for SMCs of different origin.[5] Exogenously added PTX3 and endogenously overexpressed PTX3 both inhibit this autocrine loop of stimulation. Also, PTX3 fully abolishes the activity of exogenous recombinant FGF2 protein. The short pentraxin SAP, however, does not affect FGF2-dependent cell proliferation and chemotaxis, and PTX3 does not inhibit HCASMC proliferation triggered by insulin, EGF, and serum, underlining the specificity of the FGF2-antagonist effect exerted by PTX3.

The antagonist activity of PTX3 depends on its capacity to bind FGF2 with high affinity,[23] thus acting as a "FGF2 decoy" that sequesters the growth factor in an inactive form. Accordingly, PTX3 prevents the binding of $^{125}$I-FGF2 to FGFRs expressed on HCASMCs. Also, the interactions of FGF2 with PTX3 or soluble xc-FGFR1 are mutually exclusive. Thus, PTX3 affects the activity of both endogenous and exogenous FGF2 by binding the growth factor and preventing FGFR occupancy in SMCs.

SMCs are permissive to rAAV transduction.[31] Accordingly, we successfully infected HCASMCs with an AAV-*PTX3* vector. This resulted in high levels of expression and secretion of PTX3, with the consequent inhibition of the activity exerted in vitro by endogenous and exogenous FGF2. Noticeably, PTX3 produced endogenously after rAAV transduction exerts a more potent FGF2-antagonist activity when compared with PTX3 administered as a single bolus of purified protein (the FGF2-antagonist activity being observed at 100 pmol/L versus 220 nmol/L of PTX3, respectively). This indicates that the continuous production of PTX3 and its release in the microenvironment surrounding the FGF2-target cell, an experimental condition that mimics more closely the in vivo situation, results in an increased ability to interact with the growth factor and to antagonize its activity, further supporting the efficacy of the rAAV gene transfer approach.

In injured rat carotid arteries transduced in vivo with AAV-*LacZ*, expression of β-galactosidase peaks ≈2 weeks after infection and persists for several weeks. The marker gene is expressed throughout the vessel wall, maximally in the neointima, with an overall efficiency of transduction equal to approximately 10% of the entire vascular wall (Figure 5).[30] Consistently, in vivo AAV-*PTX3* transduction results in PTX3 protein expression in the vessel wall. This was paralleled by a significant decrease in the intima-to-media ratio at 2 and 4 weeks after injury. FGF2 is produced by SMCs and other cell types in the restenotic area, including endothelial cells, macrophages, and T-cells.[12] Thus, FGF2 may exert autocrine and/or paracrine functions on FGFR-expressing SMCs of the injured vessel.[5,32] The bulk of our observations strongly suggests that the inhibition of neointimal thickening exerted by rAAV-delivered *PTX3* is attributable to its FGF antagonist activity, in keeping with previous studies about the capacity of FGF2 antisense or dominant negative FGFR gene transfer to prevent restenosis.[9,10]

PTX3 is produced at the inflammatory site in response to cytokines and bacterial components.[29,33,34] Several cellular components of the blood vessel wall express PTX3, including endothelial cells,[29] macrophages,[34] dendritic cells,[35] adipocytes,[36] fibroblasts[33] and myoblasts.[37] Also, limited levels of PTX3 mRNA and protein are detected in HCASMCs in vitro (present work). Interestingly, PTX3 expression is upregulated by modified atherogenic lipoproteins in SMCs isolated from human arterial specimens.[22] Our observations suggest that PTX3 may exert a modulatory function on SMCs after blood vessel injury by limiting the activity of FGF2. However, this does not seem to be sufficient to prevent the pro-stenotic action of the growth factor, and higher levels of PTX3 expression, like those achieved after rAAV gene transfer, are required to limit neointimal thickness.

Twenty-three members of the FGF family exist that interact with the products of 4 FGFR genes, underlying the complexity of the FGF/FGFR system.[1] Here we have shown that PTX3 affects FGF2/FGFR-1 interaction in HCASMCs. Also, PTX3 can bind FGF8 but not FGF1 or FGF4.[23] Recently, FGF9/FGFR-2 interaction has been implicated in the proliferation of neointimal SMCs after arterial injury.[8] Further studies are required to assess the capacity of PTX3 to affect the activity exerted by different members of the FGF family on SMCs.

## Acknowledgments

This work was supported by grants from MIUR (Centro di Eccellenza IDET, FIRB 2001, Cofin 2004), Fondazione Berlucchi and AIRC to M.P.; from MIUR (Cofin 2003) to M.R.; and from CNR (Progetto Finalizzato "Genetica Molecolare") and MIUR (FIRB) to M.G.

## References

1. Itoh N, Ornitz DM. Evolution of the Fgf and Fgfr gene families. *Trends Genet.* 2004;20:563–569.
2. Klint P, Claesson-Welsh L. Signal transduction by fibroblast growth factor receptors. *Front Biosci.* 1999;4:D165–D177.
3. Koyama H, Olson NE, Dastvan FF, Reidy MA. Cell replication in the arterial wall: activation of signaling pathway following in vivo injury. *Circ Res.* 1998;82:713–721.
4. Jackson CL, Reidy MA. Basic fibroblast growth factor: its role in the control of smooth muscle cell migration. *Am J Pathol.* 1993;143:1024–1031.
5. Miyamoto T, Lecoute J, Swain JL, Fox JC. Autocrine FGF signaling is required for vascular smooth-muscle cell survival in vitro. *J Cell Physiol.* 1998;177:58–67.
6. Fox JC, Shanley JR. Antisense inhibition of basic fibroblast growth factor induces apoptosis in vascular smooth muscle cells. *J Biol Chem.* 1996;271:12578–12584.
7. Segev A, Aviezer D, Safran M, Gross Z, Yayon A. Inhibition of vascular smooth muscle cell proliferation by a novel fibroblast growth factor receptor antagonist. *Cardiovasc Res.* 2002;53:232–241.
8. Agrotis A, Kanellakis P, Kostolias G, Di Vitto G, Wei C, Hannan R, Jennings G, Bobik A. Proliferation of neointimal smooth muscle cells after arterial injury: dependence on interactions between fibroblast growth factor receptor-2 and fibroblast growth factor-9. *J Biol Chem.* 2004;279:42221–42229.
9. Hanna AK, Fox JC, Neschis DG, Safford SD, Swain JL, Golden MA. Antisense basic fibroblast growth factor gene transfer reduces neointimal thickening after arterial injury. *J Vasc Surg.* 1997;25:320–325.
10. Casscells W, Lappi DA, Olwin BB, Wai C, Siegman M, Speir EH, Sasse J, Baird A. Elimination of smooth muscle cells in experimental restenosis: targeting of fibroblast growth factor receptors. *Proc Natl Acad Sci U S A.* 1992;89:7159–7163.
11. Lindner V, Reidy MA. Expression of basic fibroblast growth factor and its receptor by smooth muscle cells and endothelium in injured rat arteries: an en face study. *Circ Res.* 1993;73:589–595.
12. Cozzolino F, Torcia M, Lucibello M, Morbidelli L, Ziche M, Platt J, Fabiani S, Brett J, Stern D. Interferon-alpha and interleukin 2 synergistically enhance basic fibroblast growth factor synthesis and induce release, promoting endothelial cell growth. *J Clin Invest.* 1993;91:2504–2512.

13. Ziche M, Parenti A, Ledda F, Dell'Era P, Granger HJ, Maggi CA, Presta M. Nitric oxide promotes proliferation and plasminogen activator production by coronary venular endothelium through endogenous bFGF. *Circ Res*. 1997;80:845–852.
14. Kuwahara K, Ogawa S, Matsumoto M, Koga S, Clauss M, Pinsky DJ, Lyn P, Leavy J, Witte L, Joseph-Silverstein J, et al. Hypoxia-mediated induction of acidic/basic fibroblast growth factor and platelet-derived growth factor in mononuclear phagocytes stimulates growth of hypoxic endothelial cells. *Proc Natl Acad Sci U S A*. 1995;92:4606–4610.
15. Gajdusek CM, Carbon S. Injury-induced release of basic fibroblast growth factor from bovine aortic endothelium. *J Cell Physiol*. 1989;139:570–579.
16. Mantovani A, Garlanda C, Bottazzi B. Pentraxin 3, a non-redundant soluble pattern recognition receptor involved in innate immunity. *Vaccine*. 2003;21(suppl 2):S43–S47.
17. Napoleone E, Di Santo A, Bastone A, Peri G, Mantovani A, de Gaetano G, Donati MB, Lorenzet R. Long pentraxin PTX3 upregulates tissue factor expression in human endothelial cells: a novel link between vascular inflammation and clotting activation. *Arterioscler Thromb Vasc Biol*. 2002;22:782–787.
18. Fazzini F, Peri G, Doni A, Dell'Antonio G, Dal Cin E, Bozzolo E, D'Auria F, Praderio L, Ciboddo G, Sabbadini MG, Manfredi AA, Mantovani A, Querini PR. PTX3 in small-vessel vasculitides: an independent indicator of disease activity produced at sites of inflammation. *Arthritis Rheum*. 2001;44:2841–2850.
19. Peri G, Introna M, Corradi D, Iacuitti G, Signorini S, Avanzini F, Pizzetti F, Maggioni AP, Moccetti T, Metra M, Cas LD, Ghezzi P, Sipe JD, Re G, Oliveti G, Mantovani A, Latini R. PTX3, a prototypical long pentraxin, is an early indicator of acute myocardial infarction in humans. *Circulation*. 2000;102:636–641.
20. Latini R, Maggioni AP, Peri G, Gonzini L, Lucci D, Mocarelli P, Vago L, Pasqualini F, Signorini S, Soldatesch D, Tarli L, Schweiger C, Fresco C, Cecere R, Tognoni G, Mantovani A. Prognostic significance of the long pentraxin PTX3 in acute myocardial infarction. *Circulation*. 2004;110:2349–2354.
21. Rolph MS, Zimmer S, Bottazzi B, Garlanda C, Mantovani A, Hansson GK. Production of the long pentraxin PTX3 in advanced atherosclerotic plaques. *Arterioscler Thromb Vasc Biol*. 2002;22:e10–e14.
22. Klouche M, Peri G, Knabbe C, Eckstein HH, Schmid FX, Schmitz G, Mantovani A. Modified atherogenic lipoproteins induce expression of pentraxin-3 by human vascular smooth muscle cells. *Atherosclerosis*. 2004;175:221–228.
23. Rusnati M, Camozzi M, Moroni E, Bottazzi B, Peri G, Indraccolo S, Amadori A, Mantovani A, Presta M. Selective recognition of fibroblast growth factor-2 by the long pentraxin PTX3 inhibits angiogenesis. *Blood*. 2004;104:92–99.
24. Isacchi A, Statuto M, Chiesa R, Bergonzoni L, Rusnati M, Sarmientos P, Ragnotti G, Presta M. A six-amino acid deletion in basic fibroblast growth factor dissociates its mitogenic activity from its plasminogen activator-inducing capacity. *Proc Natl Acad Sci U S A*. 1991;88:2628–2632.
25. Bottazzi B, Vouret-Craviari V, Bastone A, De Gioia L, Matteucci C, Peri G, Spreafico F, Pausa M, D'Ettorre C, Gianazza E, Tagliabue A, Salmona M, Tedesco F, Introna M, Mantovani A. Multimer formation and ligand recognition by the long pentraxin PTX3: similarities and differences with the short pentraxins C-reactive protein and serum amyloid P component. *J Biol Chem*. 1997;272:32817–32823.
26. Deodato B, Arsic N, Zentilin L, Galeano M, Santoro D, Torre V, Altavilla D, Valdembri D, Bussolino F, Squadrito F, Giacca M. Recombinant AAV vector encoding human VEGF165 enhances wound healing. *Gene Ther*. 2002;9:777–785.
27. Moscatelli D. High and low affinity binding sites for basic fibroblast growth factor on cultured cells: absence of a role for low affinity binding in the stimulation of plasminogen activator production by bovine capillary endothelial cells. *J Cell Physiol*. 1987;131:123–130.
28. Yukawa H, Miyatake SI, Saiki M, Takahashi JC, Mima T, Ueno H, Nagata I, Kikuchi H, Hashimoto N. In vitro growth suppression of vascular smooth muscle cells using adenovirus-mediated gene transfer of a truncated form of fibroblast growth factor receptor. *Atherosclerosis*. 1998;141:125–132.
29. Breviario F, d'Aniello EM, Golay J, Peri G, Bottazzi B, Bairoch A, Saccone S, Marzella R, Predazzi V, Rocchi M, et al. Interleukin-1-inducible genes in endothelial cells: cloning of a new gene related to C-reactive protein and serum amyloid P component. *J Biol Chem*. 1992;267:22190–22197.
30. Ramirez Correa GA, Zacchigna S, Arsic N, Zentilin L, Salvi A, Sinagra G, Giacca M. Potent inhibition of arterial intimal hyperplasia by TIMP1 gene transfer using AAV vectors. *Mol Ther*. 2004;9:876–884.
31. Rohr UP, Kronenwett R, Grimm D, Kleinschmidt J, Haas R. Primary human cells differ in their susceptibility to rAAV-2-mediated gene transfer and duration of reporter gene expression. *J Virol Methods*. 2002;105:265–275.
32. Peoples GE, Blotnick S, Takahashi K, Freeman MR, Klagsbrun M, Eberlein TJ. T lymphocytes that infiltrate tumors and atherosclerotic plaques produce heparin-binding epidermal growth factor-like growth factor and basic fibroblast growth factor: a potential pathologic role. *Proc Natl Acad Sci U S A*. 1995;92:6547–6551.
33. Lee GW, Lee TH, Vilcek J. TSG-14, a tumor necrosis factor- and IL-1-inducible protein, is a novel member of the pentaxin family of acute phase proteins. *J Immunol*. 1993;150:1804–1812.
34. Vouret-Craviari V, Matteucci C, Peri G, Poli G, Introna M, Mantovani A. Expression of a long pentraxin, PTX3, by monocytes exposed to the mycobacterial cell wall component lipoarabinomannan. *Infect Immun*. 1997;65:1345–1350.
35. Doni A, Peri G, Chieppa M, Allavena P, Pasqualini F, Vago L, Romani L, Garlanda C, Mantovani A. Production of the soluble pattern recognition receptor PTX3 by myeloid, but not plasmacytoid, dendritic cells. *Eur J Immunol*. 2003;33:2886–2893.
36. Abderrahim-Ferkoune A, Bezy O, Chiellini C, Maffei M, Grimaldi P, Bonino F, Moustaid-Moussa N, Pasqualini F, Mantovani A, Ailhaud G, Amri EZ. Characterization of the long pentraxin PTX3 as a TNFalpha-induced secreted protein of adipose cells. *J Lipid Res*. 2003;44:994–1000.
37. Introna M, Alles VV, Castellano M, Picardi G, De Gioia L, Bottazzai B, Peri G, Breviario F, Salmona M, De Gregorio L, Dragani TA, Srinivasan N, Blundell TL, Hamilton TA, Mantovani A. Cloning of mouse ptx3, a new member of the pentraxin gene family expressed at extrahepatic sites. *Blood*. 1996;87:1862–1872.

Neoplasia • Vol. 6, No. 4, July/August 2004, pp. 364–373 

www.neoplasia.com

# Evidence for a Proangiogenic Activity of TNF-Related Apoptosis-Inducing Ligand[1]

*Paola Secchiero*, Arianna Gonelli*, Edvige Carnevale†, Federica Corallini*, Clara Rizzardi‡, Serena Zacchigna†, Mauro Melato‡ and Giorgio Zauli†*

*Human Anatomy Section, Department of Morphology and Embryology, University of Ferrara, Via Fossato di Mortara 66, Ferrara 44100, Italy; †Department of Normal Human Morphology, University of Trieste, Via Manzoni 16, Trieste 34138, Italy; ‡Unit of Pathology, University of Trieste, Via Stuparich 1, Trieste 34125, Italy

**Abstract**

**Starting from the observation that tumor necrosis factor–related apoptosis-inducing ligand (TRAIL)/Apo-2L protein is expressed in both malignant and inflammatory cells in some highly vascularized soft tissue sarcomas, the angiogenic potential of TRAIL was investigated in a series of *in vitro* assays. Recombinant soluble TRAIL induced endothelial cell migration and vessel tube formation to a degree comparable to vascular endothelial growth factor (VEGF), one of the best-characterized angiogenic factors. However, the proangiogenic activity of TRAIL was not mediated by endogenous expression of VEGF. Although TRAIL potentiated VEGF-induced extracellular signal–regulated kinase (ERK) phosphorylation and endothelial cell proliferation, the combination of TRAIL + VEGF did not show additive effects with respect to VEGF alone in inducing vessel tube formation. Thus, although TRAIL has gained attention as a potential anticancer therapeutic for its ability to induce apoptosis in a variety of cancer cells, our present data suggest that TRAIL might also play an unexpected role in promoting angiogenesis, which might have therapeutic implications.**

*Neoplasia* (2004) **6**, 364–373

**Keywords:** TRAIL, VEGF, signal transduction, angiogenesis, endothelial cells.

## Introduction

Tumor necrosis factor–related apoptosis-inducing ligand (TRAIL)/Apo-2L is a member of the TNF family of cytokines, which is broadly expressed at the mRNA level in many normal tissues and tumor cell lines [1]. TRAIL is a type II membrane protein, which can be proteolytically cleaved by cysteine proteases to a soluble form [2] as previously shown also for TNF-α and CD95 (Apo-1/Fas) ligand. The unique feature of TRAIL, compared to other members of the TNF family, is its ability to induce apoptosis in a variety of malignant cells both *in vitro* and *in vivo*, displaying minimal or absent toxicity on normal cells and tissues [3,4].

TRAIL interacts with four high-affinity transmembrane receptors belonging to the apoptosis-inducing TNF-R family. TRAIL-R1 (DR4) and TRAIL-R2 (DR5) transduce apoptotic signals on binding of TRAIL, whereas TRAIL-R3 (DcR1) and TRAIL-R4 (DcR2) are homologous to DR4 and DR5 in their cysteine-rich extracellular domain, but lack intracellular death domain and apoptosis-inducing capability and have been proposed to function as decoy receptors, protecting normal cells, including endothelial cells, from apoptosis [5,6]. Although little is known about possible nonapoptotic effects induced by TRAIL, it has been shown that endothelial cells express all TRAIL-Rs [6–8], whereas TRAIL protein is expressed in the medial smooth cell layer of the aorta and pulmonary artery [9]. Whereas cleavage of Fas ligand from the cell surface requires the action of zinc-dependent metalloproteases, generation of soluble TRAIL involves the action of cysteine proteases [2]. Notably, the vessel wall is a rich source of cysteine proteases [10], which suggests that the TRAIL/TRAIL-R system likely plays a physiological role in vascular biology. In this respect, we have recently demonstrated that addition of TRAIL to human umbilical vein endothelial cells induces the rapid phosphorylation and activation of extracellular signal–regulated kinase (ERK) and Akt [7,8]. Because these intracellular pathways are known to be involved in endothelial cell survival, proliferation, and migration [11,12], in this study, we have investigated whether TRAIL induced angiogenesis by using various *in vitro* assays. Taking into consideration that several recent studies have confirmed the hypothesis that tumor growth, in general, is dependent on angiogenesis [13,14], we have also analyzed the expression of TRAIL protein in soft tissue sarcomas because these tumors are often highly vascularized [15].

## Materials and Methods

### *Reagents and Cells*

Recombinant histidine6-tagged TRAIL was produced in bacteria and purified by chromatography on $Ni^{2+}$ affinity resin,

Address all correspondence to: Giorgio Zauli, MD, PhD, Department of Normal Human Morphology, University of Trieste, Via Manzoni 16, Trieste 34138, Italy. E-mail: zauli@units.it

[1]This research was supported by AIRC and FIRB grants.

Received 2 November 2003; Revised 9 December 2003; Accepted 11 December 2003.



DOI 10.1593/neo.03421

as described [7]. The concentration of TRAIL used in most assays (10 ng/ml) was determined in preliminary dose–response (0.1–1000 ng/ml) experiments. For neutralization experiments, TRAIL was preincubated with TRAIL-R1-Fc and/or TRAIL-R2-Fc chimeras, according to the supplier's instructions (R&D, Minneapolis, MI). Vascular endothelial growth factor (VEGF; Peprotec, London, UK), was used at the final concentration of 10 ng/ml. Polymyxin B (Calbiochem, La Jolla, CA), was used at the final concentration of 10 μg/ml. A pharmacological inhibitor of the ERK pathway (PD98059; final concentration: 10 μM) was from Calbiochem.

Primary human umbilical vein endothelial cells (HUVECs) were obtained as described previously [8] and were used between the third and sixth passages *in vitro*. Cells were grown on 0.2% gelatin-coated tissue culture plates in M199 endothelial growth medium (BioWhittaker, Walkersville, MD) supplemented with 20% fetal bovine serum (FBS), 10 μg/ml heparin, and 50 μg/ml Endothelial Cell Growth Factor (ECGF) (Sigma, St. Louis, MO).

*Neoplastic Samples and Immunohistochemistry*

Formalin-fixed and paraffin-embedded tissues of human sarcomas were obtained from 10 surgically treated patients. The tumors consisted of five liposarcomas, two leiomyosarcomas, one rhabdomyosarcoma, one angiosarcoma, and one Kaposi's sarcoma. Immunohistochemical study was performed on 4 μm sections using a streptavidin–biotin complex immunoperoxidase technique with a polyclonal anti–TRAIL antibody (Ab; clone H-257; Santa Cruz Biotechnology, Santa Cruz, CA). Isotype-matched irrelevant antibodies, used as negative control, gave absence of background. For the evaluation of tumor vascularization, sections were stained with Ab anti-CD31 (clone JC/70A; BioGenex, San Ramon, CA) and angiogenesis was quantified by assessment of microvessel density using previously described techniques [16,17]. Briefly, the number of vessel was counted throughout the entire core specimen in serial sections. Consecutive per ×20 high-power fields were examined, a median count per field was calculated, and a simple high-density/low-density score was used. Microvessel density was analyzed blinded toward the result of the TRAIL staining.

*Cell Migration and Cell Invasion Assays*

Cell migration was analyzed using a modified Boyden chamber assay, as described previously [18], by using 24-well plates with inserts containing 8 μm pore size gelatinized polycarbonate membranes separating the two chambers of each well (Transwell; Costar, New York, NY).

Cell invasion was investigated by using the Chemicon Cell Invasion Assay kit (Chemicon International, Temecula, CA) according to the manufacturer's instruction. This assay is performed in an invasion chamber, a 24-well tissue culture plate with cell culture inserts containing an 8-μm pore size polycarbonate membrane, over which a thin layer of extracellular matrix (ECM) is dried.

For the assays, exponentially growing cells were harvested with trypsin, centrifuged, resuspended at 0.5 $\times 10^6$ cells/ml in migration buffer [M199 medium, 10 mM HEPES, pH 7.4, and 0.5% bovine serum albumin (BSA)], and placed in the upper compartment of the chambers. TRAIL or VEGF, used alone or in combination, was added in the lower chambers. After 4 hours (for the migration assay) or 48 hours (for the invasion assay) of incubation at 37°C, cells on the upper face of the membrane were scraped using a cotton swab and cells on the lower face were fixed and stained with Mayer's hematoxylin solution. The number of migrated cells on the lower face of the filters was counted in five fields under ×100 magnification. Assays were done in triplicates.

*Tube Formation Assays*

*In vitro* formation of tubular structures was studied on BioCoat Matrigel tissue culture plates (BD Biosciences, Bedford, MA). Briefly, HUVECs were plated at 3.5 $\times 10^5$ cells/well in 24-well plates precoated with a solution of Matrigel basement membrane matrix, and left untreated or exposed to TRAIL or VEGF. After 48 hours of incubation at 37°C, the cell 3D organization was examined under an inverted photomicroscope and photographed (×40). Each treatment was performed in triplicate.

*In vitro* angiogenesis was assessed as formation of capillary-like structures of HUVECs cocultured with matrix-producing cells that had been UV-irradiated before plating of primary HUVECs (TCS Biologicals, Buckingham, UK) [19]. Briefly, cultures were left untreated or stimulated with TRAIL or VEGF, used alone or in combination, at day 3. When indicated, PD98059 or the vehicle (0.25% DMSO), previously diluted in medium, was added to the cultures 45 minutes before exposure to TRAIL or VEGF. Medium and treatments were replaced every 2 to 3 days. At day 12, the cells were fixed and HUVECs were stained using an anti–CD31 Ab (TCS Biologicals, Buckingham, UK), according to the instructions provided with the kit. Images were captured and analyzed. In particular, to measure the formation of the capillary network, the number of connections between three or more capillary-like structures and the total length of tubes were quantified by image analysis at ×40 magnification. Four-six different fields were analyzed per well.

*Western Blot Analysis*

For Western blots, HUVECs were plated in 10-cm dishes and grown at subconfluence before treatments. In order to minimize activation by serum, HUVECs were subject to partial fetal calf serum (FCS) reduction (to 0.5%) and complete growth factor withdrawal for 18 hours prior to the addition of TRAIL or VEGF, used alone or in combination. Cells were harvested in lysis buffer containing 1% Triton X-100, Pefablock (1 mM), aprotinin (10 μg/ml), pepstatin (1 μg/ml), leupeptin (10μg/ml), NaF (10 mM), and $Na_3VO_4$ (1 mM). Protein determination was performed by Bradford assay (Bio-Rad, Richmond, CA). Equal amounts of protein (50 μg) for each sample were migrated in acrylamide gels and blotted onto nitrocellulose filters. Blotted filters were probed with antibodies for the phosphorylated ERK1/2 and p38/MAPK (all from New England Biolaboratories, Beverly, MA). After incubation with peroxidase-conjugated

anti–rabbit or anti–mouse IgG (Sigma), specific reactions were revealed with the Enhanced Chemiluminescence (ECL) Western blotting detection reagent. Membranes were stripped by incubation in Re-Blot 1 × Ab stripping solution (Chemicon International) and reprobed for the respective total protein kinase content or β-actin (New England Biolaboratories) for verifying loading evenness.

Densitometric values, expressed in arbitrary units, were estimated by the ImageQuant software (Molecular Dynamics, Piscataway, NJ). Multiple film exposures were used to verify the linearity of the samples analyzed and avoid saturation of the film.

### *[$^3$H]Thymidine Incorporation*

HUVECs were plated onto 96-well plates at a density of $5 \times 10^3$ cell/well. On the next day, the medium was changed to endothelial cell basal medium containing 0.5% FBS and 0.1% BSA (starvation medium). The cells were then pretreated with PD98059 for 1 hour and incubated with TRAIL or VEGF, used alone or in combination, for 30 hours. [$^3$H]thymidine (1 μCi) was added to each well during the last 6 hours of incubation. [$^3$H]thymidine-labeled DNA was then measured using a Beckman (Fullerton, CA) model LS6000IC liquid scintillation counter.

### *Statistical Analysis*

Data were analyzed using the two-tailed, two-sample *t*-test (statistical analysis software; Minitab, State College, PA). Values of $P < .05$ were considered significant.

## Results

### *TRAIL Is Expressed in Highly Vascularized Soft Tissue Sarcomas*

Having previously demonstrated that TRAIL activates intracellular signal transduction pathways [7,8], which have been involved in promoting angiogenesis [13,14], in the first group of experiments, we have investigated the expression of TRAIL in some cases of malignant mesenchymal tumors because these tumors are often highly vascularized [15,20]. As shown in Figure 1*A*, the cells of a low-grade gastric leiomyosarcoma stained negative for TRAIL and were poorly vascularized. However, the malignant neoplastic cells of a high-grade leiomyosarcoma showed a strong expression of TRAIL and were characterized by prominent neovascularity. To ascertain that TRAIL expression was not confined to leiomyosarcomas, we have also analyzed TRAIL expression in some cases of angiogenetic liposarcomas (Figure 1*B*). In these sarcomas, a clear-cut positivity for TRAIL was noticed in both malignant cells as well as in tumor-infiltrating lymphocytes and plasma cells (Figure 1*B*). Finally, a high expression of TRAIL was documented also in tumors characterized by tumultuous angiogenesis, such as malignant vascular sarcomas (Kaposi's sarcoma; Figure 1*C*).

### *TRAIL Promotes Endothelial Cell Migration and Invasion*

Because angiogenesis is a tightly regulated process, which involves the coordinated migration, differentiation, and morphogenetic organization of endothelial cells into new capillary structures [18], these aspects of angiogenesis were next examined in a series of *in vitro* assays.

To test whether recombinant soluble TRAIL could affect endothelial cell motility, HUVECs were incubated in a modified Boyden chamber with recombinant soluble TRAIL (10 ng/ml). For comparison, cells were treated also with VEGF (10 ng/ml). TRAIL significantly ($P < .01$) increased HUVEC migration (Figure 2*A*). The increase in the number of migrated cells detected with TRAIL (approximately two-fold) was similar to that observed in the presence of VEGF (2.5-fold). Interestingly, however, the simultaneous addition of optimal concentrations of TRAIL and VEGF did not show additive effects on endothelial cell migration (data not shown).

To form new blood vessels, endothelial cells have to migrate and cross basement membranes. This invasive capacity of HUVECs in response to TRAIL was investigated by measuring the invasion of an ECM layer. Addition of recombinant TRAIL significantly ($P < .01$) increased HUVEC invasion through ECM (Figure 2*B*). Again, maximal stimulation, corresponding to a 1.5-fold increase in the number of migrated cells in response to TRAIL, was similar to that observed in response to VEGF. The specificity of these biological effects was confirmed by preincubation of TRAIL with TRAIL-R1-Fc (Figure 2, *A* and *B*) or TRAIL-R2-Fc (data not shown) chimeric proteins, which completely ($P < .01$) abrogated the ability of TRAIL to promote cell migration and invasion (Figure 2, *A* and *B*), without exhibiting, by themselves, any effect on endothelial cell migration or invasion (data not shown). These data demonstrate, for the first time, that TRAIL induces endothelial cell migration and invasion through the basement membrane. Importantly, the TRAIL concentration used in these assays was in the range reported to be present in the plasma of patients affected by hematological malignancies (1–10 ng/ml) [21].

### *TRAIL Induces Morphological Endothelial Differentiation*

To examine whether TRAIL induces morphogenetic changes resembling capillary-like structure tube formation, HUVECs were plated on 3D Matrigel plates. After 48 hours, untreated endothelial cultures showed both cells with small round shape (that remained isolated) and elongated shape, forming connections but an incomplete network of tubes (Figure 3*A*). However, cultures exposed to TRAIL (10 ng/ml) exhibited a distinct phenotype by assuming a more elongated shape, forming thin cords of interconnecting cells (Figure 3*A*). Similar effects were also observed with VEGF (10 ng/ml) (Figure 3*A*). Morphometric quantitation of the vessel-like structures in the 3D cultures revealed that Fc-TRAIL-R1 completely abrogated this response to TRAIL (Figure 3*B*). These data demonstrate that TRAIL, like VEGF, is able to mediate morphogenetic effects leading to differentiation into vascular structures, which represent an obligatory step for the sprouting of endothelial cells and tube formation.

Because tubules formed in standard Matrigel assays are short and relatively homogeneous, the ability of TRAIL to induce angiogenesis was further investigated by using the

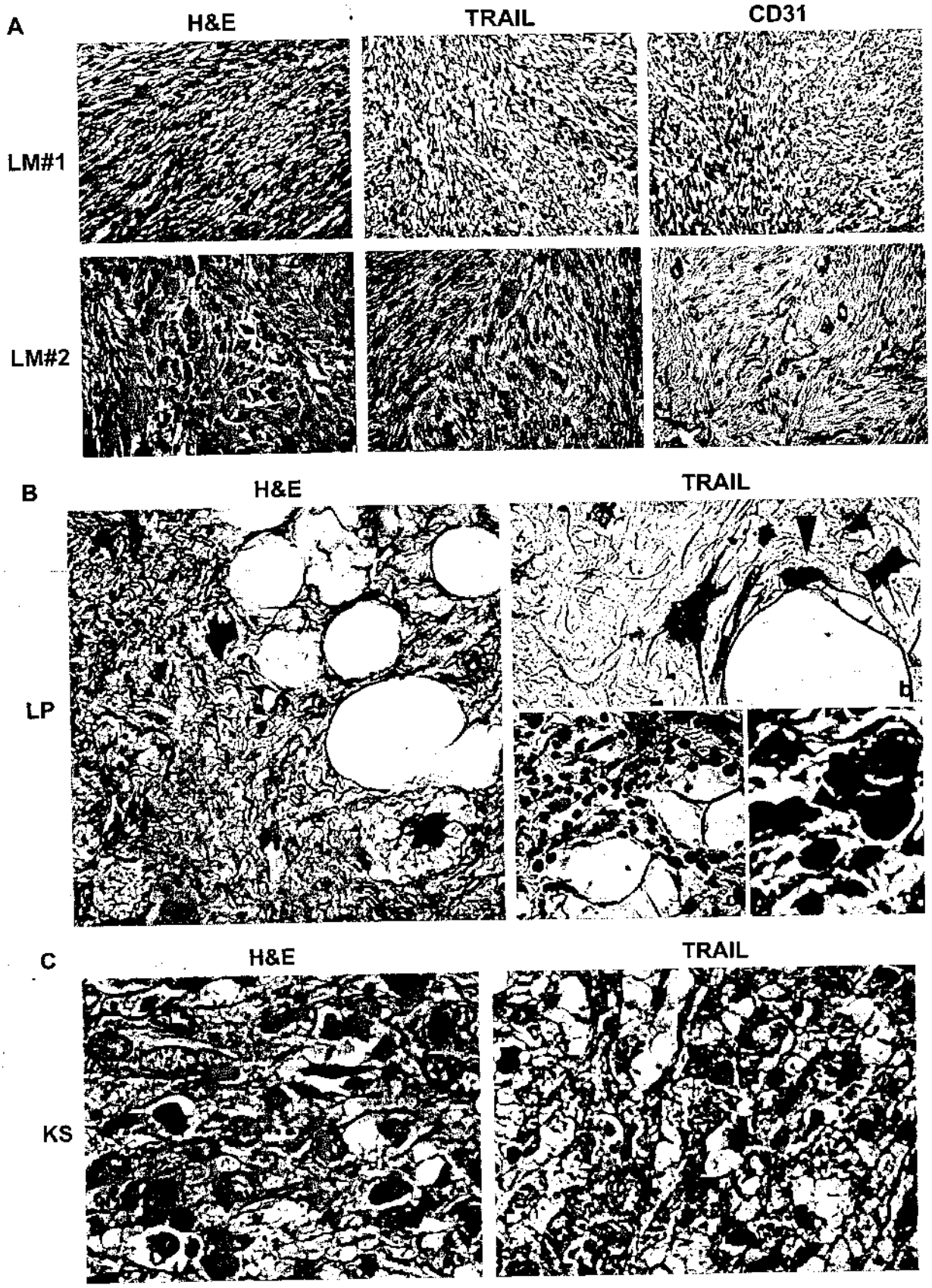


**Figure 1.** *Expression of TRAIL in human sarcomas. Sections of sarcomas were examined immunohistochemically by using an anti–TRAIL Ab. (A) Representative sections of leiomyosarcomas at low (LM 1) and high vascularity (LM 2) are shown. Stainings with anti–CD31 Ab to detect endothelial cells and vascular structures, and hematoxylin and eosin (H&E) are also shown. Original magnification, ×20. (B) Liposarcoma (panel a, H&E staining, ×40) showing TRAIL expression in malignant neoplastic cells (arrowhead in panel b; ×40), tumor-infiltrating lymphocytes (panel c; ×40), and plasma cells (arrowhead in panel c; ×100). (C) Kaposi's sarcoma showing diffuse expression of TRAIL. Original magnification, ×40.*

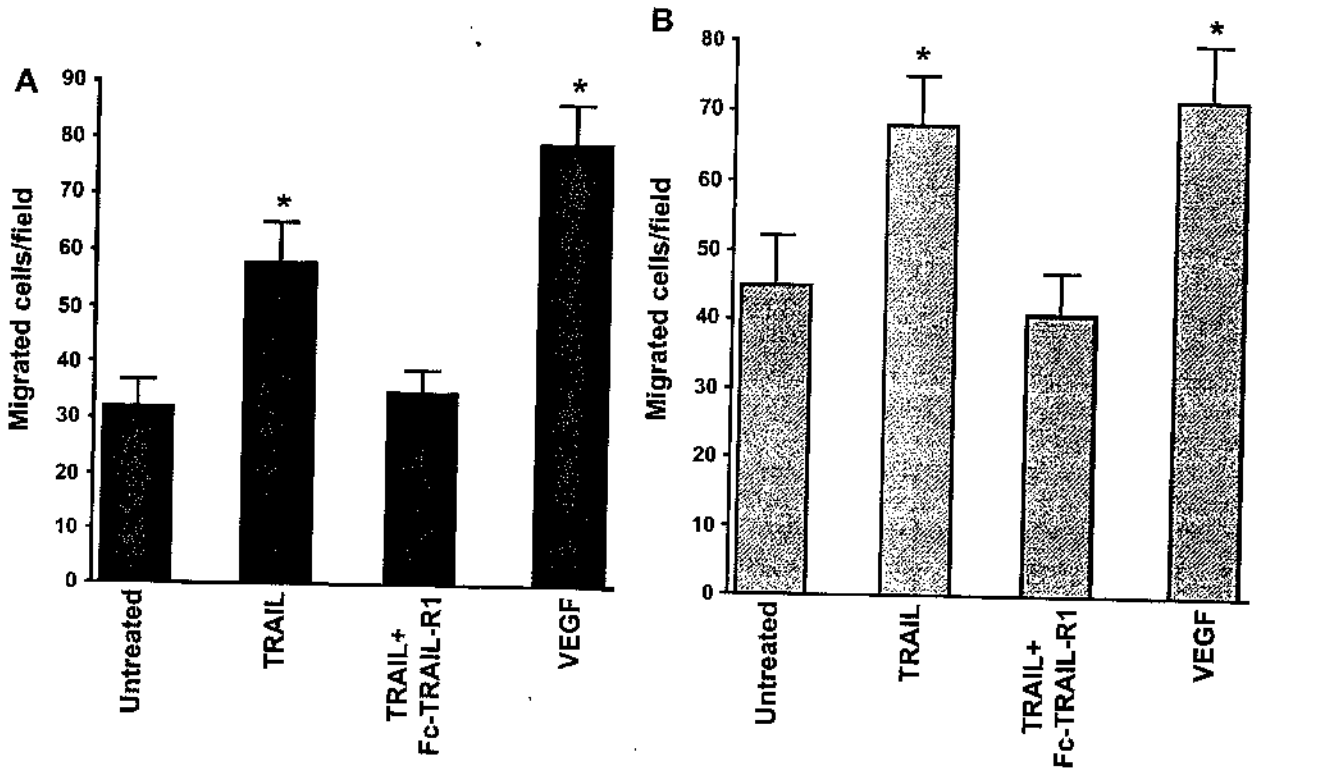


**Figure 2.** *Effect of TRAIL on HUVEC migration and invasion. Cell migration (A) and cell invasion (B) assays were performed in 24-well Transwell plates, as described in Materials and Methods section. Endothelial cells were seeded in the upper compartments, whereas TRAIL or VEGF was added in the lower compartments. For neutralization experiments, TRAIL was preincubated with TRAIL-R-Fc chimera. Cells migrated through the gelatinized membranes and ECM-coated membranes were counted after 4 hours (A) and 48 (B) hours, respectively. Data are expressed as the number of migrated cells in 10 high-power fields and are mean ± SD of results from four experiments each performed in triplicate. *P < .01 compared to untreated cells.*

angiogenesis coculture assay, which appeared significantly heterogeneous, consisting of both short and long interconnecting tubules that more closely resembled capillaries (Figure 4). In this assay, vessels develop where they are well protected (e.g., between layers of fibroblasts) and morphogenetic processes of tubule formation occur in HUVECs completely surrounded by stromal cells, as *in vivo*. The ability of fibroblasts to support tubule formation has been attributed to their capacity of producing considerable quantities of collagen, fibronectin, and other matrix molecules [19].

To rule out the possibility that the angiogenic activity of TRAIL might be mediated by upregulation of endogenous VEGF, the production of VEGF released in the culture medium was analyzed by enzyme-linked immunosorbent assay (ELISA) in both untreated and TRAIL-treated cultures. In HUVECs, VEGF was not detected in the culture supernatants of both untreated and TRAIL-treated cultures analyzed up to 72 hours (data not shown). In angiogenesis coculture assay, VEGF was endogenously produced, but the levels were similar in untreated (256 ± 36 pg/ml) and TRAIL-treated (240 ± 45 pg/ml) cultures.

We next performed a quantitative analysis by calculating both the total length of tubes and the number of capillary connections per field in cocultures left untreated or exposed to VEGF, TRAIL, and combination of the two cytokines (10 ng/ml each). As shown in Figure 5, the basal formation of capillary-like structures was significantly ($P < .01$) increased after stimulation with either TRAIL or VEGF, and TRAIL-R1-Fc chimeric protein significantly ($P < .01$) inhibited TRAIL-induced total tube length and capillary connections. Moreover, preincubation of TRAIL with 5 μg/ml polymyxin B, which complexes and inactivates endotoxin, did not abrogate the angiogenetic activity of TRAIL, further indicating that these responses to TRAIL are specific. However, the simultaneous addition of TRAIL + VEGF did not show any additive or synergistic effect, and it was not statistically different from VEGF alone (Figure 5).

### *TRAIL Potentiates VEGF-Induced ERK1/2 But Not p38/MAPK Phosphorylation*

The findings illustrated above suggest that TRAIL and VEGF might compete for the same intracellular signal transduction pathways. Therefore, in the next group of experiments, we have investigated the effect of TRAIL and VEGF, used alone or in combination, on mitogen-activated protein (MAP) kinase family members, which have been involved in different aspects of angiogenesis. Although ERK1 and ERK2 are strongly activated on stimulation of cells with mitogens [11], p38/MAPK plays a complex role in angiogenesis by promoting cell migration and inhibiting endothelial cell survival [21–24]. After exposure to either TRAIL or VEGF, induction of phospho-ERK1/2 was observed starting at 5 minutes of treatment (Figure 6*A*). Remarkably, the

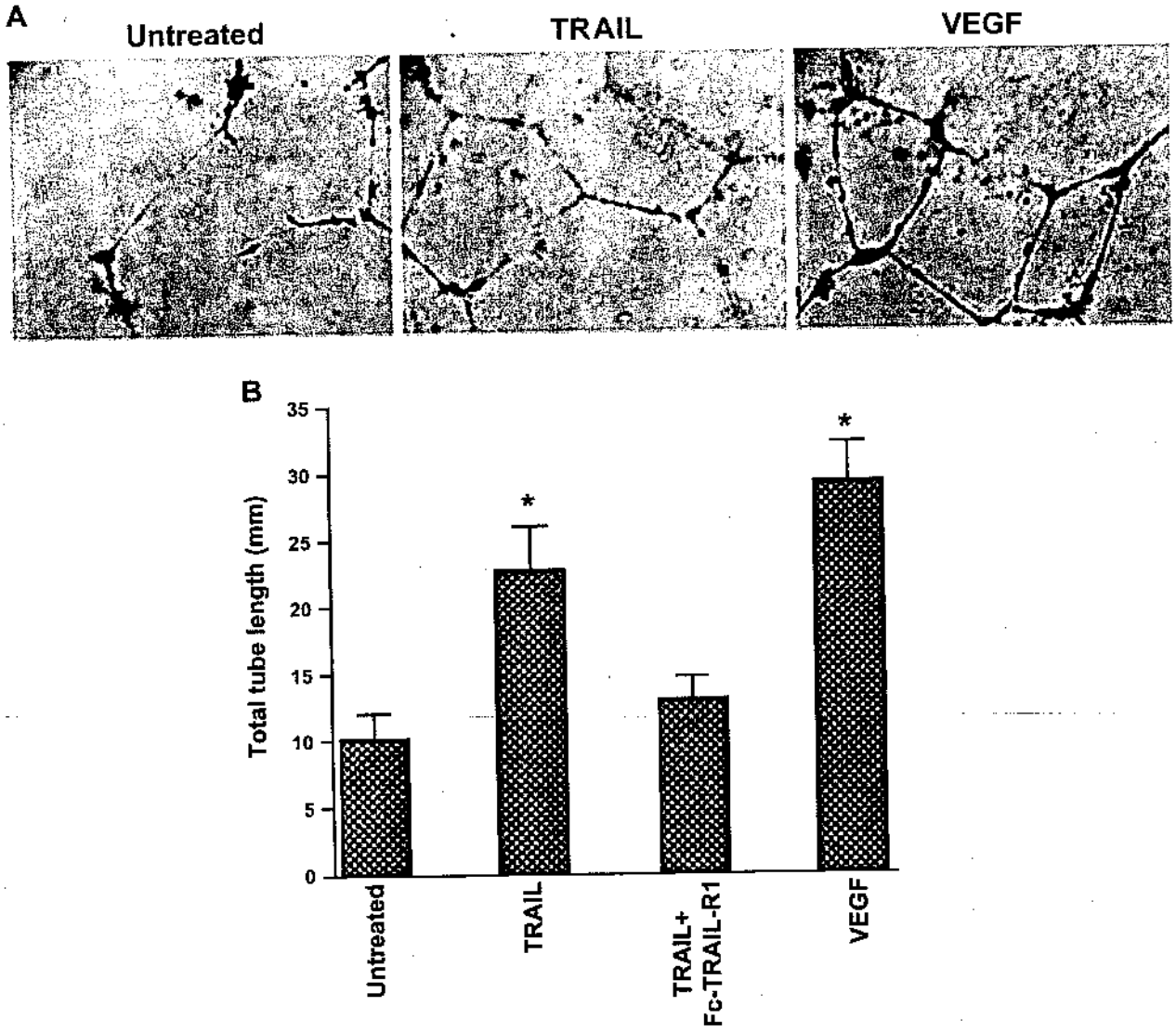


**Figure 3.** *Effect of TRAIL on in vitro tube formation. HUVECs were seeded into 24 wells containing 3D Matrigel in the absence and presence of TRAIL ± TRAIL-R-Fc or VEGF. (A) Photographs (×40) were taken at 48 hours of cultures. Representative images of at least five experiments with similar results are shown. (B) Five to seven random fields were photographed and recorded, and tube length was quantified by measuring the total cell projection length and individual tubular structure. Tubular length per field is reported as mean ± SD. *P < .01 compared to untreated cells.*

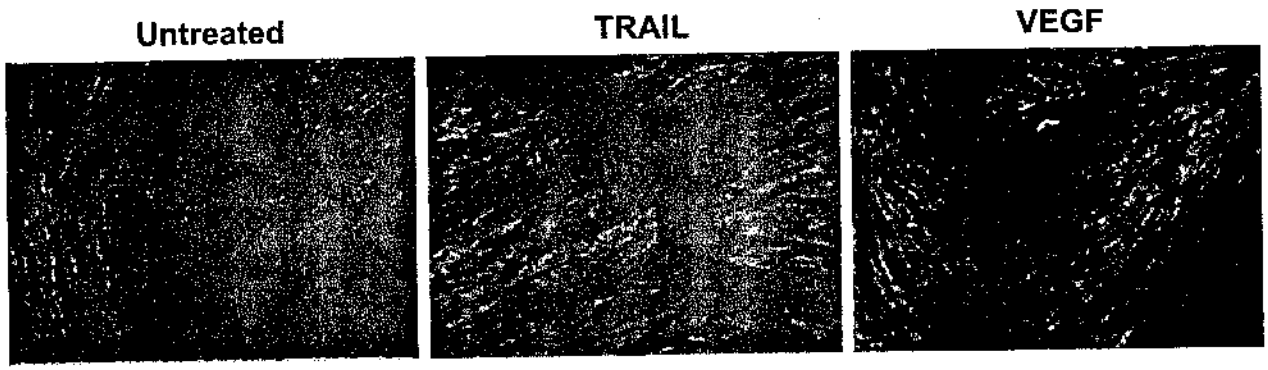


**Figure 4.** *Effect of TRAIL on the capillary-like network in a coculture angiogenesis assay. Formation of capillary-like structures of HUVECs cultured with matrix-producing cell types was analyzed after 12 days of culture treatment as indicated. Representative example of the morphology endothelial structures was detected after staining with anti–CD31 Ab in the in vitro angiogenesis assay. Rare capillary structures were observed in the angiogenesis assay left untreated, whereas both TRAIL and VEGF induced a diffuse network of capillary structures. Original magnification, ×10.*

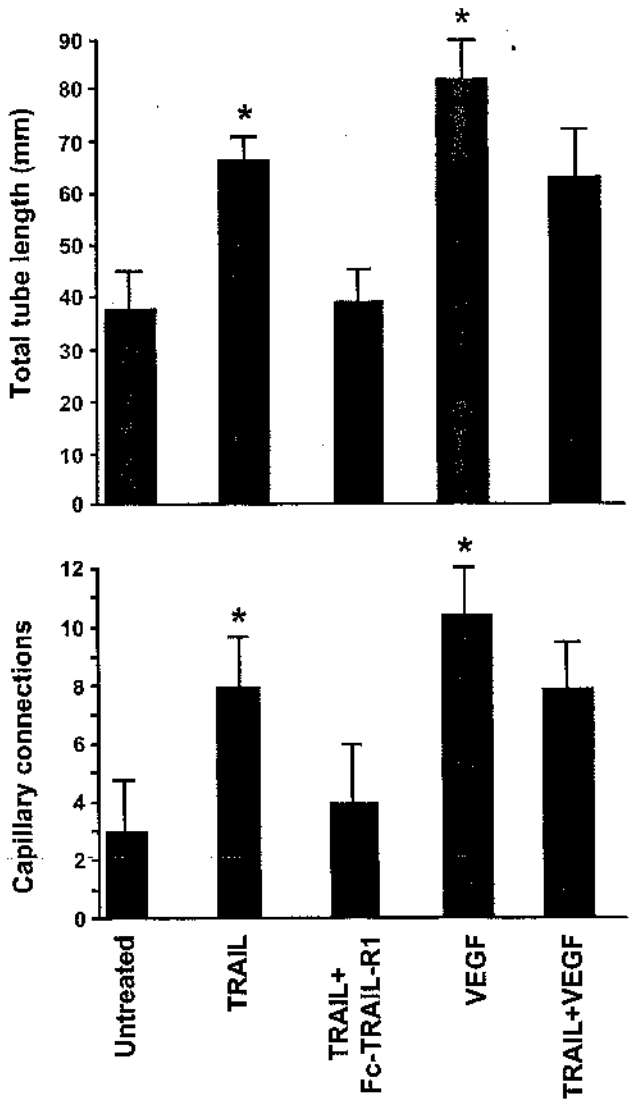


**Figure 5.** *Lack of additive effect of TRAIL + VEGF on the capillary-like network in coculture angiogenesis assay. Cultures treated as indicated were observed after 12 days and results were recorded for quantitative analysis of the total length of tubes per field and the number of capillary connections per field. Data are expressed as mean ± SD of results from at least five experiments each performed in duplicate. *P < .01 compared to untreated cells.*

simultaneous addition of TRAIL + VEGF resulted in a prolonged activation of ERK phosphorylation with respect to each cytokine used alone (Figure 6*A*). However, although TRAIL was unable to induce p38 phosphorylation, it decreased somewhat the VEGF-induced phosphorylation of p38/MAPK (Figure 6*B*). Consistent with a key role of the ERK pathway in endothelial proliferation, thymidine incorporation assay showed that the combination of VEGF + TRAIL showed an additive effect ($P < .01$) with respect to VEGF or TRAIL used alone (Table 1). Preincubation with the cell-permeable PD098059 compound (20 μM), a commonly used inhibitor of the ERK pathway, completely inhibited thymidine uptake induced by any cytokine combination (Table 1), clearly confirming that the activity of ERK is required for TRAIL- and VEGF-induced mitogenesis.

Moreover, PD098059 treatment strongly suppressed the total tube length and number of tube interconnections in control, TRAIL-treated, and VEGF-treated cocultures (Figure 7), underscoring the key role of ERK pathway in the whole process of tube formation evaluated in the angiogenesis assay.

## Discussion

The growth of microvessels is an integral component of tissue remodeling during a variety of normal and pathological events, such as the female reproductive cycle, fetal development, wound healing, inflammation, diabetic retinopathy, and tumor progression [13,14]. The way in which vessels form is being intensively studied because this complex morphogenetic process is very important in medicine. Although a true understanding of the morphogenetic processes involved in tubule formation is still lacking, all these angiogenic events are orchestrated by a network of extracellular factors, including several classes of cytokines, ECM, and integrins, and by their cognate receptors. Several cytokines have been involved in angiogenesis and, in particular, in tumor-associated angiogenesis [13,14]. Besides its involvement in vascular development, VEGF has been demonstrated to play a key role in both physiologic and tumor angiogenesis in adult mammals [25].

It has also been shown in previous studies that some angiogenic regulators belong to the TNF family [26]. Ligands of this family trigger biological activities by binding and signaling through their corresponding receptors in the TNF receptor family. The majority of the TNF family members mediate host defense, inflammation, and immunological regulation, but some of these ligands also regulate endothelial cell functions [26]. For instance, it has been demonstrated that TNF-α modulates endothelial cell behavior; however, its effects are complex. TNF-α inhibits endothelial cell growth yet induces capillary tube formation *in vitro* [27,28]. It also can be antiangiogenic in the context of solid tumors, or angiogenic in corneal settings *in vivo* [27–29]. In a recent study, we have demonstrated that TRAIL functions as an anti–apoptotic factor for endothelial cells [7], and we have hypothesized that TRAIL may contribute to endothelial cell integrity by acting as a survival factor for newly formed blood vessels.

In this study, we have demonstrated for the first time that TRAIL induces a proangiogenic phenotype in human endothelial cells. This phenotype includes both early (increase in migration, invasion, and proliferation) and late (differentiation into vascular cords) angiogenic events. More importantly, TRAIL is angiogenic in a variety of *in vitro* and *in vivo* assays to a degree comparable to VEGF. However, the interplay between TRAIL and VEGF appears rather complex, with TRAIL unable to potentiate VEGF activity in most assays. In fact, TRAIL increased VEGF-induced ERK phosphorylation and HUVEC proliferation; however, TRAIL did not potentiate VEGF-induced p38/MAPK phosphorylation or capillary formation in the

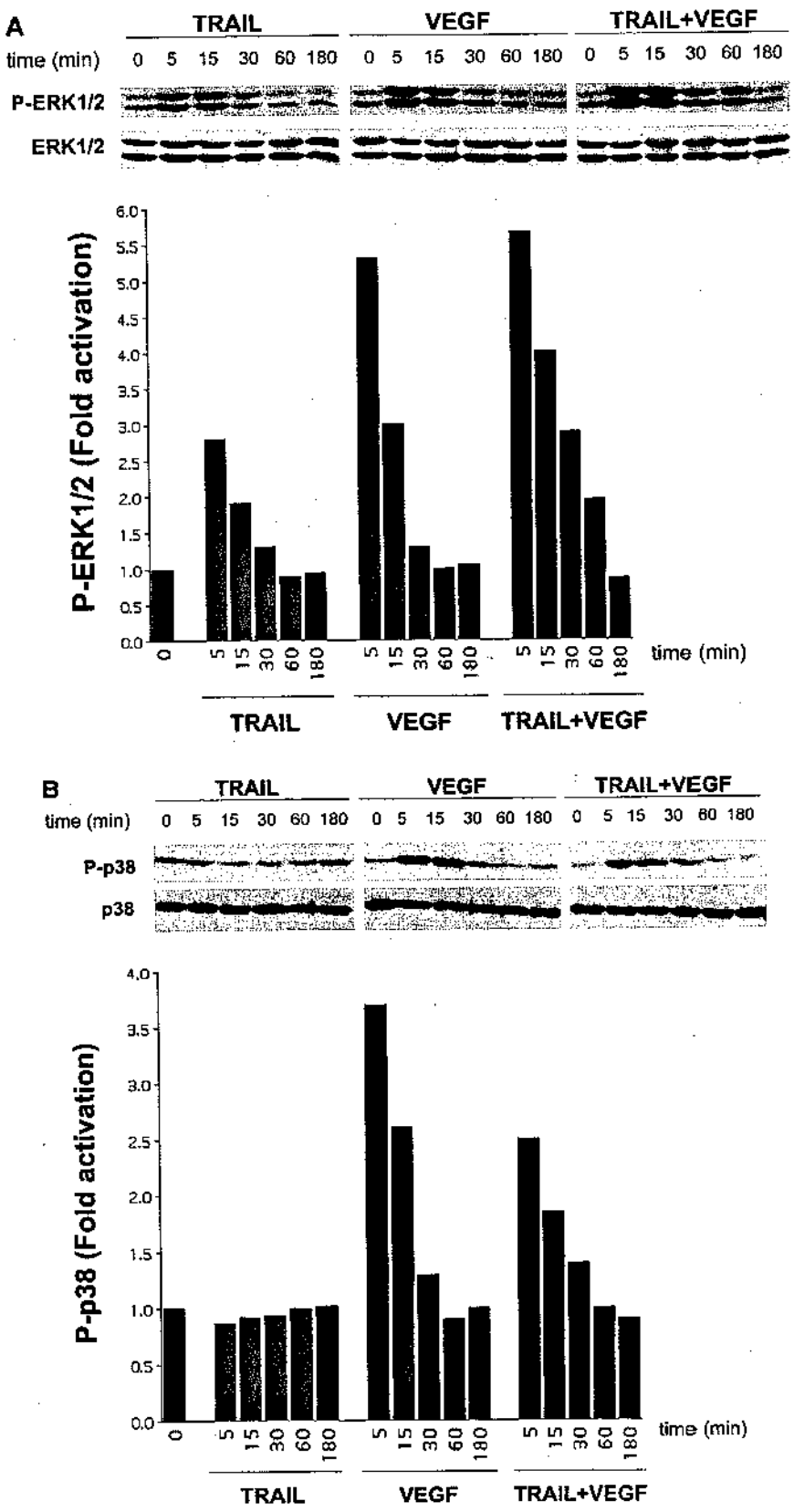


**Figure 6.** *Phosphorylation of ERK1/2 and p38/MAPK in response to TRAIL and VEGF. Quiescent HUVECs were stimulated with either TRAIL, VEGF, or VEGF + TRAIL for 0 to 180 minutes. Cell lysates were analyzed for ERK1/2 (A) and p38/MAPK (B) activation by Western blot analysis of total and phosphorylated (P) proteins using specific antibodies. Protein bands were quantified by densitometry, and levels of P-ERK1/2 and P-p38 were calculated for each time point, after normalization to ERK1/2 and to p38/MAPK, respectively. Unstimulated basal expression was set as unity. Results are representative of four separate experiments.*

coculture assay. Of note, we have also demonstrated that a clear-cut expression of TRAIL was observed in highly vascularized soft tissue sarcomas. At the moment, we have analyzed a small number of sarcomas; experiments aimed to analyze a high number of tumors and a wide variety of tumors, with the aim to quantitatively evaluate potential correlations between microvessel density and the levels of TRAIL expression, are ongoing.

Besides malignant sarcoma cells, TRAIL was expressed also by tumor-infiltrating lymphocytes and plasma cells. Similar findings were obtained by previous authors describing that TRAIL was expressed by tumor-infiltrating lymphocytes as well as by metastatic gastric cancer cells [30]. Although the most frequent hypothesis to explain the expression of TRAIL by cancer cells is a strategy of immune evasion by which TRAIL-positive malignant cells counterattack against activated T lymphocytes [30,31], our data suggest the alternative—not mutually exclusive—hypothesis that TRAIL expression by cancer cells, and, perhaps also by infiltrating lymphocytes, may play a key role in tumor angiogenesis. Consistent with this hypothesis, it has been shown that mouse BALB/c mammary adenocarcinoma cells engineered to express human TRAIL on their membrane grow faster than the parental cell line in both syngeneic and allogeneic mice [32]. In this respect, it has been clearly established that any significant increase in tumor mass must be preceded by an increase in the vascular supply to deliver nutrients and oxygen to the tumor. The ability of a tumor to induce angiogenesis represents an essential step for tumor growth beyond 2 to 3 mm [13]. Consistent with a potentially important role of TRAIL in tumor angiogenesis not confined to soft tissue sarcomas, it has been demonstrated that all primary astrocytic brain tumors analyzed by immunohistochemistry, including astrocytomas and glioblastomas, express TRAIL protein *in vivo* [33,34]. Similarly, TRAIL is expressed by a subset of lymphomas [35], malignant plasmocytoma cells [36], and ovarian carcinomas [37], in which TRAIL expression has been correlated to the degree of malignancy. Therefore, although recombinant TRAIL protein offers great promise as a cancer therapeutic [38], our current demonstration that TRAIL exerts a potent proangiogenic effect adds a cautionary note to the prolonged treatment of cancer patients with pharmacological concentrations of recombinant TRAIL protein or TRAIL-expressing vectors.

**Table 1.** Thymidine Incorporation Assay in HUVEC Cultures.

| | Vehicle | PD098059 |
|---|---|---|
| Untreated | 2700 ± 350 | 570 ± 80 |
| TRAIL | 3850 ± 600 | 588 ± 98 |
| VEGF | 4200 ± 470 | 550 ± 90 |
| VEGF + TRAIL | 5400 ± 550 | 600 ± 105 |

Values are expressed as counts per minute (cpm) per well and are mean±SD of three separate experiments.

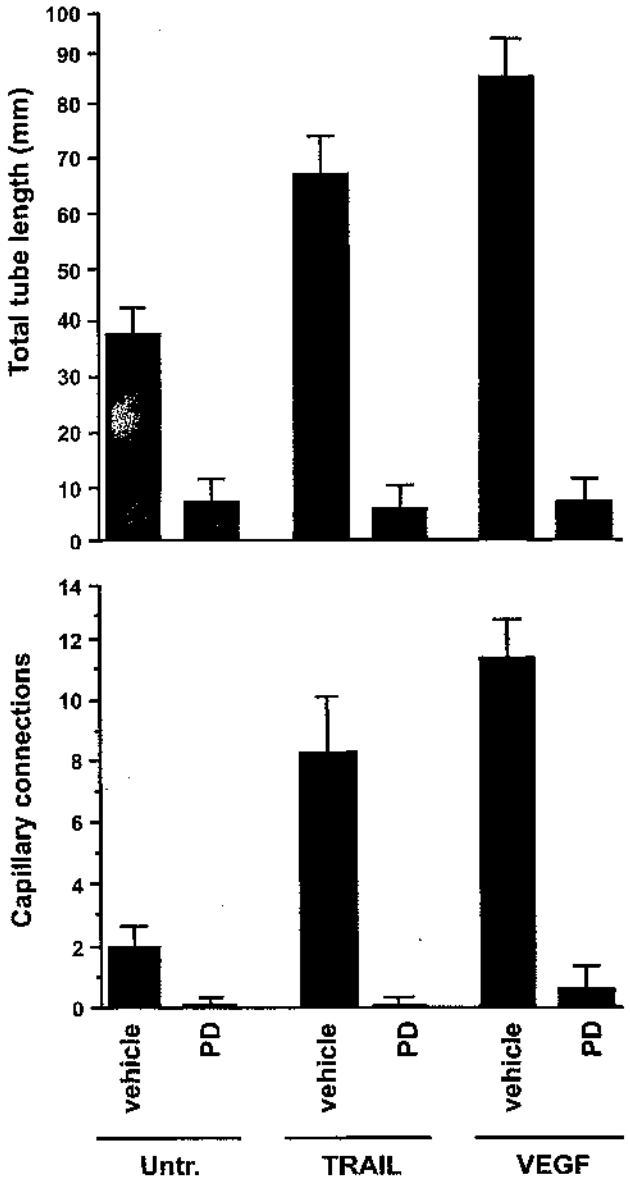


**Figure 7.** *Role of ERK pathway in capillary-like network formation in the coculture angiogenesis assay. Cultures treated as indicated were observed after 12 days and results were recorded for quantitative analysis of the total length of tubes per field and the number of capillary connections per field. PD, PD98059. Data are expressed as mean ± SD of results from at least five experiments each performed in duplicate.*

## References

[1] Ashkenazi A (2002). Targeting death and decoy receptors of the tumour-necrosis factor superfamily. *Nat Rev Cancer* **2**, 420–430.

[2] Mariani SM and Krammer PH (1998). Differential regulation of TRAIL and CD95 ligand in transformed cells of the T and B lymphocyte lineage. *Eur J Immunol* **28**, 973–982.

[3] Walczak H, Miller RE, Ariail K, Gliniak TS, Griffith B, Kubin M, Chin W, Jones J, Woodward A, Le T, Smith C, Smolak P, Goodwin RG, Rauch CT, Schuh JC, and Lynch DH (1999). Tumoricidal activity of tumor necrosis factor–related apoptosis-inducing ligand *in vivo*. *Nat Med* **5**, 157–163.

[4] Ashkenazi A, Pai RC, Fong S, Leung S, Lawrence DA, Marsters SA, Blackie C, Chang L, McMurtrey AE, Hebert A, DeForge L, Koumenis IL, Lewis D, Harris L, Bussi J, Koeppen H, Shahrokh Z, and Schwall RH (1999). Safety and antitumor activity of recombinant soluble Apo2 ligand. *J Clin Invest* **104**, 155–162.

[5] Sheridan JP, Marsters SA, Pitti PM, Gurney A, Skubatch M, Baldwin D,

Yagita H, Gray CL, Baker K, Wood WI, Goddard AD, Godowski P, and Ashkenazi A (1997). Control of TRAIL-induced apoptosis by a family of signaling and decoy receptors. *Science* **277**, 818–822.

[6] Zhang XD, Nguyen T, Thomas WD, Sanders JE, and Hersey P (2000). Mechanisms of resistance of normal cells to TRAIL induced apoptosis vary between different cell types. *FEBS Lett* **482**, 193–199.

[7] Secchiero P, Gonelli A, Carnevale E, Milani D, Pandolfi A, Zella D, and Zauli G (2003). TRAIL promotes the survival and proliferation of primary human vascular endothelial cells by activating the Akt and ERK pathways. *Circulation* **107**, 2250–2256.

[8] Zauli G, Pandolfi A, Gonelli A, Di Pietro R, Guarnieri S, Ciabattoni G, Rana R, Vitale M, and Secchiero P (2003). Tumor necrosis factor–related apoptosis-inducing ligand (TRAIL) sequentially upregulates nitric oxide and prostanoid production in primary human endothelial cells. *Circ Res* **92**, 732–740.

[9] Gochuico BR, Zhang J, Ma BJ, Marshak-Rothstein A, and Fine A (2000). TRAIL expression in vascular smooth muscle. *Am J Physiol Lung Cell Mol Physiol* **278**, L1045–L1050.

[10] Chapman HA, Riese RJ, and Shi GP (1997). Emerging roles for cysteine proteases in human biology. *Annu Rev Physiol* **59**, 63–88.

[11] Yu Y and Sato JD (1999). MAP kinases, phosphatidylinositol 3-kinase, and p70 S6 kinase mediate the mitogenic response of endothelial cells to vascular endothelial growth factor. *J Cell Physiol* **178**, 235–246.

[12] Morales-Ruiz M, Fulton G, Sowa G, Languino LR, Fujio Y, Walsh K, and Sessa WC (2000). Vascular endothelial growth factor–stimulated actin reorganization and migration of endothelial cells is regulated via the serine/threonine kinase Akt. *Circ Res* **86**, 892–896.

[13] Folkman J (2001). Angiogenesis-dependent diseases. *Semin Oncol* **28**, 536–542.

[14] Carmeliet P (2003). Angiogenesis in health and disease. *Nat Med* **9**, 653–660.

[15] Dirix LY, Vermeulen P, De Wever I, and Van Oosterom AT (1997). Soft tissue sarcoma in adults. *Curr Opin Oncol* **9**, 348–359.

[16] Weidner N (1995). Intratumor microvessel density as a prognostic factor in cancer. *Am J Pathol* **147**, 9–19.

[17] Vermeulen PB, Gasparini G, Fox SB, Toi M, Martin L, McP Culloch F, Pezzella F, Viale G, Weidner N, Harris AL, and Dirix LY (1996). Quantification of angiogenesis in solid human tumor: an international consensus in the methodology and criteria of evaluation. *Eur J Cancer* **32A**, 2474–2484.

[18] Passaniti A, Tylor RM, Pili R, Guo Y, Long PV, Haney A, Pauly RR, Grant DS, and Martin GR (1992). A simple, quantitative method for assessing angiogenesis and antiangiogenic agents using reconstituted basement membrane, heparin and fibroblast growth factor. *Lab Invest* **67**, 519–528.

[19] Donovan D, Brown NJ, Bishop ET, and Lewis CE (2001). Comparison of three *in vitro* human angiogenesis assays with capillaries formed *in vivo*. *Angiogenesis* **4**, 113–121.

[20] Mentzel T, Brown LF, Dvorak HF, Kuhnen C, Stiller KJ, Katenkamp D, and Fletcher CDM (2001). The association between tumour progression and vascularity in myxofibrosarcoma and myxoid/round cell liposarcoma. *Virchows Arch* **438**, 13–22.

[21] Llabakk NB, Sundan A, Torp S, Aukrust P, Froland SS, and Espevik T (2002). Development, characterization and use of monoclonal antibodies against sTRAIL: measurement of sTRAIL by ELISA. *J Immunol Methods* **259**, 119–128.

[22] Rousseau S, Houle F, Kotanides H, Witte L, Waltenberger J, Landry J, and Huot J (2000). Vascular endothelial growth factor (VEGF)–driven actin-based motility is mediated by VEGFR2 and requires concerted activation of stress-activated protein kinase 2 (SAPK2/p38) and geldanamycin-sensitive phosphorylation of focal adhesion kinase. *J Biol Chem* **275**, 10661–10672.

[23] Gratton JP, Morales-Ruitz M, Kureishi Y, Fulton D, Walsh K, and Sessa W (2001). Akt down-regulation of p38 signaling provides a novel mechanism of vascular endothelial growth factor–mediated cytoprotection in endothelial cells. *J Biol Chem* **276**, 30359–30365.

[24] Matsumoto T, Turesson I, Book M, Gerwins P, and Claesson-Welsh L (2002). p38 MAP kinase negatively regulates endothelial cell survival, proliferation and differentiation in FGF-2–stimulated angiogenesis. *J Cell Biol* **156**, 149–160.

[25] Ferrara N, Gerber HP, and LeCouter J (2003). The biology of VEGF and its receptors. *Nat Med* **9**, 669–676.

[26] Locksley RM, Killeen N, and Lenardo MJ (2001). The TNF and TNF receptor superfamilies. Integrating mammalian biology. *Cell* **104**, 487–501.

[27] Frater-Schroder M, Risau W, Hallmann R, Gautschi P, and Bohlen P (1987). Tumor necrosis factor type $\alpha$, a potent inhibitor of endothelial cell growth *in vitro*, is angiogenic *in vivo*. *Proc Natl Acad Sci USA* **84**, 5277–5281.

[28] Yoshida S, Ono M, Shono T, Izumi H, Ishibashi T, Suzuki H, and Kuwano M (1997). Involvement of interleukin-8, vascular endothelial growth factor, and basic fibroblast growth factor in tumor necrosis factor alpha–dependent angiogenesis. *Mol Cell Biol* **17**, 4015–4023.

[29] Ruegg C, Yilmaz A, Bieler G, Bamat J, Chaubert P, and Lejeune FJ (1998). Evidence for the involvement of endothelial cell integrin alphaV-beta3 in the disruption of the tumor vasculature induced by TNF and IFN-gamma. *Nat Med* **4**, 408–414.

[30] Koyama S, Koike N, and Adachi S (2002). Expression of TNF-related apoptosis-inducing ligand (TRAIL) and its receptors in gastric carcinoma and tumor-infiltrating lymphocytes: a possible mechanism of immune evasion of the tumor. *J Cancer Res Clin Oncol* **128**, 73–79.

[31] Takeda K, Smyth MJ, Cretney E, Hayakawa Y, Kayagaki N, Yagita H, and Okumura K (2002). Critical role for tumor necrosis factor–related apoptosis-inducing ligand in immune surveillance against tumor development. *J Exp Med* **195**, 161–169.

[32] Giovarelli M, Musiani P, Garotta G, Ebner R, Di Carlo E, Kim Y, Cappello P, Rigamonti L, Bernabei P, Novelli F, Modesti A, Coletti A, Ferrie AK, Lollini PL, Ruben S, Sakcedi T, and Forni G. A "Stealth Effect": adenocarcinoma cells engineered to express TRAIL elude tumor-specific and allogeneic T cell reactions. *J Immunol* **163**, 4886–4893.

[33] Rieger J, Ohgaki H, Kleihues P, and Weller M (1999). Human astrocytic brain tumors express APO2L/TRAIL. *Acta Neuropathol* **97**, 1–4.

[34] Frank S, Kohler U, Schackert G, and Schackert HK (1999). Expression of TRAIL and its receptors in human brain tumors. *Biochem Biophys Res Commun* **257**, 454–459.

[35] Zhao S, Asgary Z, Wang Y, Goodwin R, Andreeff M, and Younes A (1999). Functional expression of TRAIL by lymphoid and myeloid tumor cells. *Br J Haematol* **106**, 827–832.

[36] Silvestris F, Cafforio P, Tucci M, and Dammacco F (2002). Negative regulation of erythroblast maturation by Fas-L(+)/TRAIL(+) highly malignant plasma cells: a major pathogenetic mechanism of anemia in multiple myeloma. *Blood* **99**, 1305–1313.

[37] Lancaster JM, Sayer R, Blanchette C, Calingaert B, Whitaker R, Schildraut J, Marks J, and Berchuck A (2003). High expression of tumor necrosis factor–related apoptosis-inducing ligand is associated with favorable ovarian cancer survival. *Clin Cancer Res* **9**, 762–767.

[38] Smyth MJ, Takeda K, Hayakawa Y, Peschon JJ, van den Brink MRM, and Yagita H (2003). Nature's TRAIL—on a path to cancer immunotherapy. *Immunity* **18**, 1–6.

*Cancer Gene Therapy (2004) 11, 73–80*

*www.nature.com/cgt*

# AAV-mediated gene transfer of tissue inhibitor of metalloproteinases-1 inhibits vascular tumor growth and angiogenesis *in vivo*

**Serena Zacchigna,[1] Lorena Zentilin,[1] Monica Morini,[2] Raffaella Dell'Eva,[2] Douglas M Noonan,[2] Adriana Albini,[2] and Mauro Giacca[1,3]**

*[1]Molecular Medicine Laboratory, International Centre for Genetic Engineering and Biotechnology (ICGEB), Trieste, Italy; [2]Istituto Nazionale per la Ricerca sul Cancro (IST), Genova, Italy; and [3]Laboratorio di Biologia Molecolare, Scuola Normale Superiore, Pisa, Italy.*

The activity of matrix metalloproteinases (MMPs) is a universal feature of cellular invasion, tumor angiogenesis and metastasis, which is counterbalanced and regulated by the natural tissue inhibitors of MMPs (Timps). Here we show that Timp1 gene transfer delivered by an adeno-associated virus (AAV) vector inhibits tumor growth in a murine xenotransplant model. A human Kaposi's sarcoma cell line, forming highly vascularized tumors *in vivo* and having a high natural permissivity to AAV gene transfer, was transduced to express the Timp1 cDNA. AAV-Timp1-transduced cells secreted high levels of Timp1 that inhibited MMP2 and MMP9 gelatinolytic activity. Following subcutaneous inoculation in nude mice, the AAV-Timp1-transduced cells showed significantly reduced tumor growth when compared to control AAV-LacZ-transduced cells. In addition, direct intratumoral injection of AAV-Timp1 into pre-existing tumors significantly impaired the further expansion of the tumor mass. Histological analyses showed that the AAV-Timp1-transduced tumors had limited development of vascular structures and extensive areas of cell death, suggesting that Timp1 overexpression had an antiangiogenic effect. To further support this conclusion, we demonstrated that AAV-Timp1 transduction significantly reduced endothelial cell migration and the invasion of a Matrigel barrier and strongly inhibited angiogenesis in the chick chorioallantoic membrane assay. These results indicate that transfer and overexpression of the Timp1 gene is a promising therapeutic strategy to target tumor-associated angiogenesis in cancer gene therapy.
*Cancer Gene Therapy* (2004) **11,** 73–80. doi:10.1038/sj.cgt.7700657

***Keywords: angiogenesis; tumor growth; AAV; MMPs***

Extracellular matrix integrity is maintained by a delicate balance between the synthesis and degradation of its structural components, involving the concerted actions of numerous enzymes, as well as those of specific inhibitors that keep their activity in check. A general aspect of malignancies is a shift of this balance in favor of the proteolysis, promoting cellular proliferation and invasion. Tumor cells can directly secrete proteolytic enzymes or induce the normal neighboring cells to elaborate proteases.[1] In addition to invasion and metastasis, high proteolytic activity also has a crucial role in the induction of tumor angiogenesis, an event that is essential for tumor survival, expansion and dissemination.[2]

The members of the matrix metalloproteinases (MMP) family are zinc-dependent proteases that function at neutral pH and collectively degrade most of the proteins in the extracellular matrix. They have been subgrouped into four broad categories, according to their substrate preference and structural similarity: interstitial collagenases, gelatinases, stromelysins and membrane-type MMPs (MT-MMPs).[3,4] The expression and activity of the MMPs are tightly controlled at several levels.[5] The secreted inactive zymogens must undergo proteolytic cleavage to become catalytically active, and natural inhibitor proteins, such as the tissue inhibitor of metalloproteinases (TIMPs), can block the latent or the active MMPs.[6] Timp1, the first discovered member of the TIMP family,[7] is a glycoprotein that forms an inhibitory complex with a broad spectrum of activated MMPs, including the basement membrane-degrading enzymes MMP2 (gelatinase A, 72-kDa type IV collagenase) and MMP9 (gelatinase B, 94-kDa type IV collagenase). These MMPs have been particularly implicated in tumor progression, regulation of growth factor availability and angiogenesis.[8] The antineoplastic activity of Timp1 has been to date demonstrated in relatively few tumor models following different experimental approaches including transfection,[9–12] adenovirus gene transfer[13] and retroviral tranduction.[14] The molecular mechanisms by which the

*Received 17 March 2003.*
*Address correspondence and reprint request to: Professor Mauro Giacca, Head, Molecular Medicine Laboratory, ICGEB, Padriciano, 99 34012 Trieste, Italy. E-mail: giacca@icgeb.org*

antitumoral activity of Timp1 is exerted might involve direct inhibition of tumor cell growth, invasion or tumor angiogenesis.

To investigate the role of Timp1 in modulating tumor cell growth and tumor vessel formation, and to explore the therapeutic potential of Timp1 gene transfer, we exploited an adoptive tumorigenesis model based on tumor formation by KS-IMM cells. This immortal cell line was originally isolated from a Kaposi's sarcoma (KS) lesion[15] and retains most of the properties of KS, including induction of endothelial cell migration and invasion *in vitro*[16] and strong angiogenic responses *in vivo*.[17,18] Inoculation of these cells in nude mice results in the formation of aggressive and highly vascularized tumors that bear a striking resemblance to human KS lesions. These characteristics, coupled with an exquisite permissivity to adeno-associated virus (AAV) vectors, which provide sustained and long-term gene expression, make this cell line an ideal experimental system to assess the role of single factor expression in modulating tumor growth and angiogenesis. We show that Timp1 significantly suppresses tumor growth *in vivo* and demonstrate that Timp1 negatively regulates the angiogenic process both *in vitro* and *in vivo*.

## Results

### *Construction and characterization of AAV-Timp1*

To attain a constitutive, high-level expression of Timp1, its cDNA was cloned under the control of the cytomegalovirus (CMV) promoter to obtain the pAAV-Timp1 plasmid, in which the expression cassette is flanked by the AAV inverted terminal repeats (Fig 1a). This same construct was then used to produce an AAV vector by a standard packaging system based on cotransfection of AAV and adenovirus helper functions. After purification on a $CsCl_2$ gradient, the viral titer was determined by a competitive PCR assay, as previously described.[19] Similarly, high-titer viral preparations were obtained for AAV vectors expressing the marker genes $\beta$-galactosidase (AAV-LacZ) and GFP (AAV-GFP), which were used as control vectors in several experiments.

The expression of human Timp1 in hamster cells was assessed after transfection with the pAAV-Timp1 plasmid or transduction with the recombinant AAV-Timp1 vector. As shown in Figure 1b, in both cases exogenous Timp1 was detected as a 23 kDa polypeptide in the total cell lysates and as a 28 kDa polypeptide in the concentrated cell supernatants of treated cells, indicating that the protein was properly produced, processed, secreted and glycosylated.

To assess the permissivity of KS-IMM cells to AAV vectors, these cells were transduced with a preparation of AAV-GFP and the transduction efficiency was evaluated by flow cytometry. As shown in Figure 1c, these cells were found to be highly sensitive to AAV transduction, without or after treatment with hydroxyurea, an agent that increases AAV infectivity (producing 20 and 63% GFP-positive cells, respectively).[19] After transduction with AAV-Timp1, KS-IMM cells clearly expressed the transgene as shown by immunocytochemistry (Fig 1d).

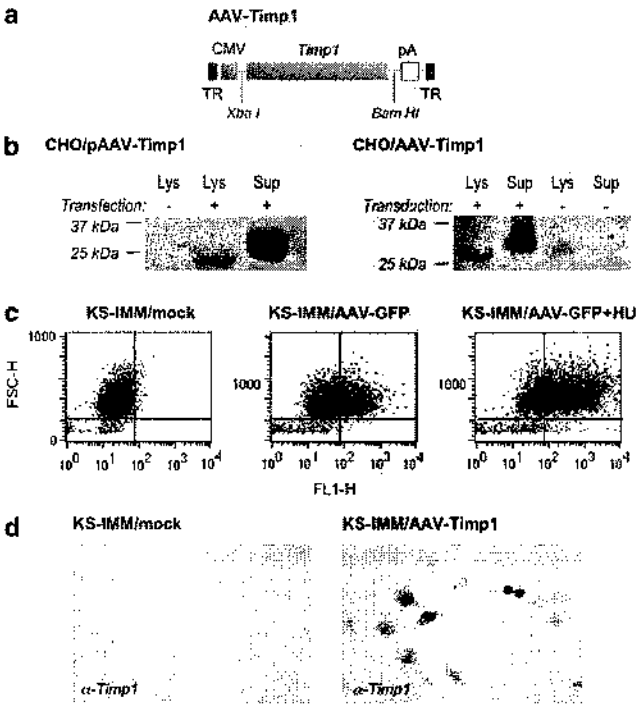


**Figure 1** Characterization of AAV-Timp1 gene transfer and expression. (**a**) Schematic representation of the AAV-Timp1 expression vector used in this study. *TR*, AAV terminal repeat sequences; *CMV*, constitutive CMV immediate early promoter; *pA*, polyadenylation site. Cloning restriction sites are indicated. (**b**) Expression of Timp1 by CHO cells transiently transfected with plasmid pAAV-Timp1 DNA (panel on the left) or transduced with the AAV-Timp1 viral vector. Total cell lysates (*Lys*) and supernatants (*Sup*) were analyzed by Western blotting using anti-Timp1 antibodies. (**c**) Flow cytometry profiles of KS-IMM cells transduced for 48 hours with AAV-GFP ($10^3$ viral particles/$10^6$cells) with or without overnight treatment with 1 mM hydroxyurea (*HU*). The percentages of fluorescent cells (upper right panels in each profile) were 0.3% (mock), 20.2% (AAV-GFP, no hydroxyurea) and 63.3% (AAV-GFP, hydroxyurea). Treatment with hydroxyurea alone had no effect on cell fluorescence (not shown). (**d**) Immunocytochemistry of KS-IMM cells mock transduced (panel on the left side) or transduced with AAV-Timp1 (panel on the right side); × 400 magnification.

### *Protease inhibitory activity of AAV-Timp1-transduced cells*

To visualize the presence of intrinsic gelatinolytic activity produced by the KS-IMM and EAhy.926 cells, serum-free conditioned medium was collected and tested by *in vitro* zymography (Fig 2a). Two major areas of proteolysis, corresponding to the molecular weights of MMP9 and MMP2, were observed in KS-IMM cell supernatants. Only the lower band, corresponding to MMP2 activity, was present in EAhy.926 cell supernatants. In both cases, transduction with AAV-Timp1 essentially did not alter the levels of expression and secretion of either MMP.

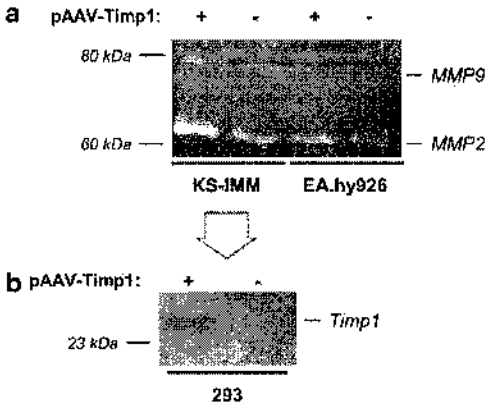


**Figure 2** Protease inhibitory activity of AAV-Timp1. (**a**) MMP expression by KS-IMM and EAhy.926 cells. Supernatants from mock-transfected and pAAV-Timp1-transfected cells were analyzed by gelatin zymography. Clear bands indicate MMP activity in a background of gelatin. *MMP2*: gelatinase A, 72-kDa type IV collagenase; *MMP9*: gelatinase B, 94-kDa type IV collagenase. (**b**) Antigelatinolytic activity of Timp1. Supernatants from 293 cells transfected with pAAV-Timp1 were concentrated and resolved by reverse zymography, using KS-IMM conditioned medium as a source of MMPs. The dark band in the pAAV-Timp1 lane represents MMP inhibitory activity.

To ascertain the effect of Timp1 on MMP2 and MMP9 activity, reverse zymography was performed using KS-IMM cell supernatants as a source of MMPs. Serum-free media conditioned for 48 hours were collected from Timp1 and mock-transfected 293 cells, concentrated, resolved by gelatin SDS-PAGE and incubated in the presence of KS-IMM supernatant for 16 hours. A clear band at 28 kDa (Fig 2b), absent in the control lane, showed that AAV-Timp1-transduced cells synthesize and secrete a fully processed recombinant Timp1 that efficiently inhibits gelatinolytic activity.

### *AAV-Timp1 inhibits tumor growth* in vivo

We then investigated whether Timp1 could function as a suppressor of tumor growth of KS-IMM cells *in vivo*. In an initial set of experiments, KS-IMM cells were transduced with either the AAV-Timp1 or the AAV-LacZ vectors, collected as a pool after 48 hours, mixed with Matrigel, and inoculated subcutaneously in nude mice ($5 \times 10^6$ cells/animal, groups of six animals). In all cases, cell implantation induced the formation of tumors that became evident and palpable after 5 days. However, as shown in Figure 3a, the tumors derived from AAV-Timp1-transduced cells grew at a significantly slower rate than control tumors, resulting in an ~50% reduction in tumor mass at 5 weeks after cell implantation ($0.61 \pm 0.18$ *versus* $1.15 \pm 0.27\,cm^3$; $P < .01$). The histological analysis of tumors recovered upon termination of the experiment showed that tumors from AAV-Timp1-transduced cells exhibited clear signs of regression, such as limited development of vascular structures and extensive areas of cell death (Fig 3b). In contrast, the control KS-IMM tumors transduced with AAV-LacZ showed massive proliferation of spindle-shaped cells and the presence of

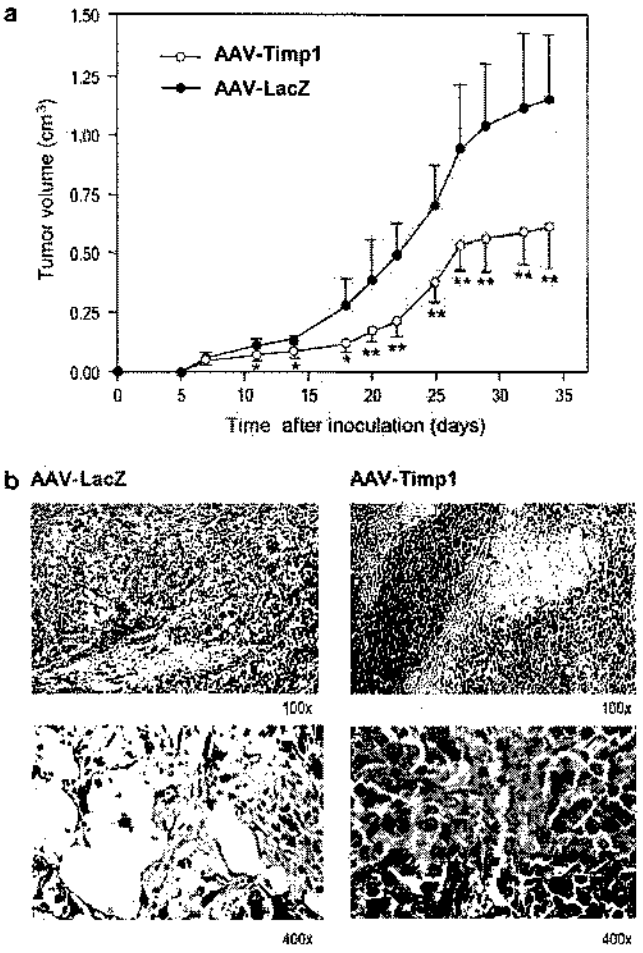


**Figure 3** Inhibition of tumor growth by Timp1 overexpression after *in vitro* transduction with AAV-Timp1. (**a**) Effects of AAV-Timp1 on KS-IMM tumor growth *in vivo*. KS-IMM cells ($5 \times 10^5$), transduced with either AAV-Timp1 or AAV-LacZ ($10^3$ viral particles/$10^6$cells), were injected subcutaneously in nude mice. AAV-Timp1-transduced cells grew at a significantly slower rate than mock-transduced cells, resulting in a 50% reduction in tumor volume at 35 days. The means and standard deviations of tumor mass are shown (groups of six animals), with indications of statistical significance (*$P < .05$; **$P < .01$). (**b**) Histological features of tumors formed by KS-IMM cells transduced with either AAV-Timp1 or AAV-LacZ at day 35 after inoculation, after staining of tissue sections with hematoxylin and eosin ( × 100 and × 400 magnification). Tumor growth inhibition was accompanied by histological signs of regression, including limited development of vascular structures and the presence of a large number of cells with picnotic nuclei. In contrast, control AAV-lacZ-transduced KS-IMM lesions were highly vascularized, with massive spindle-cell infiltration, erythrocyte extravasation and edema.

numerous blood vessels, with the formation of vascular lacunae and erythrocyte extravasation.

These data clearly indicated that the transduction of KS-IMM cells with AAV-Timp1 represents an efficient method to impair the growth of this kind of tumor. To explore possible therapeutic potentials of this vector in cancer gene therapy, we performed a second set of experiments, in which we injected established KS-IMM xenograft tumors with either the AAV-Timp1 or the

AAV-LacZ vectors. The experimental design for these experiments is shown in Figure 4a. The intratumoral injection of AAV-Timp1 induced marked growth suppression and initial regression of the tumors, particularly evident after the last vector injection on day 21 (tumor mass fold increase 9.1±4.2 *versus* 4.0±2.0 fold for the AAV-LacZ- and AAV-Timp1-transduced tumors, respectively, at day 35; $P<.05$; Fig. 4b). The long-term effect of AAV-Timp1 injection is likely to be due to the delayed appearance of transgene expression after AAV gene transfer. Similar to the inoculation of *in vitro*-transduced cells, histological analysis of the tumors showed massive KS-IMM cell proliferation interspersed with many blood vessels in the AAV-lacZ-injected tumors. In contrast, the tumors treated with AAV-Timp1 presented large necrotic areas and numerous inflammatory cells (Fig 4c).

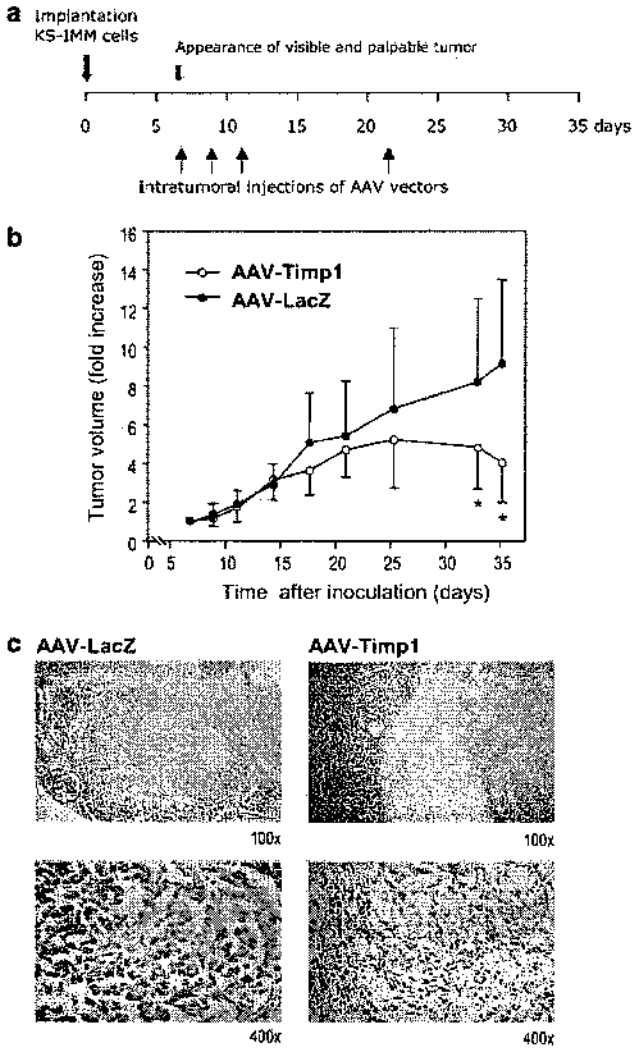


**Figure 4** Growth suppression of pre-existiting KS-IMM xenografts after intratumoral inoculation of AAV-Timp1. (**a**) Experimental design of the therapy study. KS-IMM cells ($4 \times 10^6$) were injected subcutaneously in nude mice at day 0. At day 7, all mice presented a small but visible and palpable tumor. From that day onward, intratumoral injections of AAV-Timp-1 and AAV-LacZ were performed every second day, three times. A fourth dose of each vector was administered on day 21. (**b**) Treatment with AAV-Timp1 significantly reduced the growth rate of the KS-IMM xenografts compared to AAV-LacZ. For each animal (five animals per group) the tumor volume was measured repeatedly during 5 weeks following cell implantation, and normalized against the initial volume on day 7. Results are presented as mean and standard deviation for both vectors at each time point, with indication of statistical significance ($P<.05$). (**c**) Histology of preimplanted KS-IMM tumors, transduced with either AAV-Timp1 or AAV-LacZ at day 7 after inoculation, and harvested at day 35. Hematoxylin staining of tissue sections ($\times 100$ and $\times 400$ magnification) shows several histological signs of tumor regression after AAV-Timp1 inoculation, such as a lower number of blood vessels, large areas of fibrosis and necrosis, and the presence of numerous inflammatory cells.

### *Timp1 inhibits cell migration across a basement membrane*

The histology of the tumors described above, together with the biological and clinical hallmarks of KS, suggested that the inhibition of tumor growth by Timp1 could be largely due to a direct repression of tumor angiogenesis. Therefore the capacity of Timp1 to modulate the endothelial response to angiogenic factors *in vitro* was investigated in the chemoinvasion assay. Previous studies have shown that KS-IMM cells release several chemoattractants and angiogenic factors, including VEGF and b-FGF, which stimulate the motility and invasiveness of endothelial cells.[20,21] The EAhy.926 cells produce a gelatinase activity at 72 kDa, corresponding to MMP2 (Fig 2a), whose activity is important in angiogenic growth factor-induced invasion.[22] To ascertain the effect of Timp1 overexpression on endothelial cell migration through a reconstituted basement membrane, the supernatant harvested from transfected 293 cells, which contains Timp1 activity (Fig 2b), was added to EA.hy926 cells in the upper compartment of invasion chambers. After a 1-hour incubation, chemoattractants were placed in the lower compartment. This preincubation had no significant effect on the adhesion of the cells to the Matrigel (not shown). However, this treatment significantly reduced ($P=.026$) the ability of the endothelial cells to invade and migrate across the Matrigel barrier (Fig 5).

This finding indicates that the levels of Timp1 expressed by AAV-transduced KS-IMM cells significantly interfere with the invasive capacity of endothelial cells, suggesting that the biological effects of Timp1 gene transfer extend beyond the cells actually producing the factor.

### *Antiangiogenic activity of AAV-Timp1*

To examine whether the inhibitory activity of Timp1 on endothelial cell migration might directly affect angiogenesis, we set up a chick chorioallantoic membrane (CAM) assay, using 50 ng of recombinant VEGF as a proangiogenic stimulus. Transduced cells ($3 \times 10^4$) were seeded on a foamy sponge on top of the CAM of chick eggs, and the extent of the new developing vasculature was assessed by microscopic inspection. The presence of control rhVEGF induced the development of new blood vessels sprouting in a radial pattern around the sponge and frequently

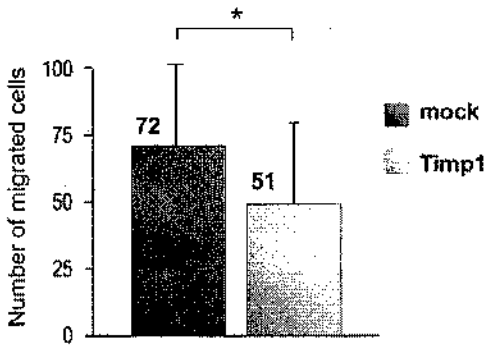


**Figure 5** Timp1 significantly inhibits endothelial cell invasion. Effect of Timp1 on invasion of EAhy.926 endothelial cells through a Matrigel barrier. Preincubation with the supernatant of 293 cells transfected with pAAV-Timp1 (Fig. 2b) determined a clear inhibitory effect on cellular invasion. Results are shown as the mean number of migrated cells per high-power microscopic field (×400) ±SD for triplicate determinations. *Statistical significance ($P<.05$).

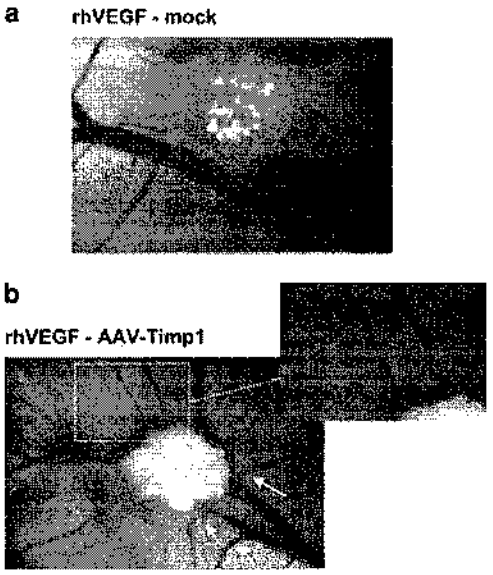


**Figure 6** Antiangiogenic effect of AAV-Timp1 on the chick CAM. (**a**) CAM of a 12-day-old chick embryo incubated with a sponge adsorbed with 50 ng of rhVEGF and a suspension of mock-infected CHO cells. Note the presence of a large number of blood vessels in a radial pattern around the implant (×20 magnification). (**b**) CAM of a 12-day-old chick embryo incubated with a sponge adsorbed with 50 ng of rhVEGF and a suspension of AAV-Timp1-transduced CHO cells. No blood vessels penetrate the sponge. Arrows indicate arc-like structures formed by sprouting vessels in the proximity of Timp1-expressing cells (×20 magnification). The inset shows a magnification of some vessels exhibiting signs of regression, including irregular morphology and several discontinuities.

penetrating into it. Seeding of mock-transduced cells on the sponge did not interfere with this effect (Fig 6a). In contrast, no blood vessels penetrated the sponges in which AAV-Timp1-transduced cells had been seeded. Instead, developing vessels seemed to turn away from the sponge, forming arc-like structures as indicated by the arrows in Figure 6b. Furthermore, some vessels close to the sponge exhibited degenerative features, such as irregular morphology and several interruptions (shown in the higher magnification inset). These observations clearly indicate that secretion of Timp1 by AAV-Timp1-transduced cells is able to markedly impair the angiogenic process.

## Discussion

In this study, we show that overexpression of Timp1 represses tumor growth in an animal model of adoptive tumorigenesis based on KS-IMM cell implantation in nude mice. A significant therapeutic effect was obtained either by transduction of cultured cells before implantation or by direct injection into pre-existing tumors. Timp1 gene transfer was obtained by exploiting the high sensitivity of the KS-IMM cells, higher than that observed with other cell types under the same conditions, to infection with AAV vectors. In contrast to other gene delivery systems, the expression of genes delivered by AAV vectors is not subjected to progressive silencing over time *in vivo*. As a consequence, these vectors offer the unique possibility to study the biological and therapeutic effects of factor expression and release in experimental animal models over relative long periods of time.[23,25] Furthermore, cells transduced with AAV do not express any viral proteins and thus do not become immunogenic or elicit inflammatory responses. This might be crucial in a clinical setting, and, in particular, in cancer gene therapy, where prolonged expression of the therapeutic gene might be required in order to achieve a therapeutic response.

MMPS are involved in a wide range of phenomena associated with tumor progression.[4] In addition, a growing body of evidence indicates that endogenous inhibitors of MMPs exert biological effects that extend beyond the inhibition of MMP enzymatic activity, being able to affect directly basic cellular functions, such as proliferation and survival.[14,26]

In our model, the histology of AAV-Timp1-transduced tumors revealed several signs of regression, including the presence of cells with picnotic nuclei, suggesting that Timp1 overexpression could have a direct proapoptotic activity on the tumor cells *in vivo*. However, we did not observe differences in either the growth rate or the apoptotic death rate of Timp1-expressing KS-IMM cells as compared to controls (not shown), indicating that Timp1 did not affect KS-IMM cell survival *in vitro*. It appears that Timp1 causes tumor cell death and tumor growth inhibition *in vivo* indirectly, most probably through the inhibition of angiogenesis. Previous studies have shown divergent effects of Timp1 overexpression in EBV-negative Burkitt's lymphoma: an initial antiapoptotic effect stimulating tumor growth, followed by an antiangiogenic effect that caused tumor regression.[14]

New blood vessel formation is a hallmark of solid tumor progression, since both local expansion and metastatic dissemination depend on vascularization of the primary tumor mass. Among human tumors, KS shows an impressively abundant neovascularization,

accompanied by spindle-shaped cell growth, inflammation and edema. The pathogenesis of KS has long been debated, but several lines of evidence suggest that KS most probably develops from reactive endothelial cells as a result of a "hit and run" mechanism of the KS-associated herpesvirus HHV8 producing uncontrolled angiogenic factor release and inflammation.[27] KS-IMM cells display a strong angiogenic activity, and the tumors they generate show tumor cell proliferation and vascular structure formation, probably due to massive endothelial cell recruitment.[21] Our experiments provide two-fold evidence of the specific antiangiogenic potential of Timp1. First, Timp1 was able to inhibit significantly endothelial cell migration in response to the angiogenic factors secreted by KS-IMM cells in the chemoinvasion assay. Second, Timp1 had a profound effect on new blood vessel development in the CAM assay, an established *in vivo* assay measuring angiogenesis. Thus, Timp1 inhibition of angiogenesis and host endothelial cell recruitment might represent a primary mechanism of the inhibition of KS tumor growth.

Blocking endothelial cell invasion is the basis of several current antiangiogenic and antitumor therapies.[28,29] Endothelial cells invasion requires the degradation of the basement membrane by MMP2 produced by endothelial cells themselves in response to angiogenic factors. MMP2 is known to be highly expressed in human KS and other tumors,[30] substantially contributing to tumor cell invasion and dissemination into tissues. Our experiments confirm secretion of MMP2 by endothelial cells and show that this metalloproteinase is also constitutively produced by KS-IMM cells, thus possibly contributing to direct tumor expansion and invasion of these cells *in vivo*.

The concept of inhibiting MMP activity for cancer treatment is a very attractive one given the broad involvement of these enzymes in most steps of tumor cell biology, including tissue invasion, metastasis and induction of angiogenesis. The hopes raised by small synthetic MMP inhibitors were dashed by poor performance in most clinical trials, which disclosed the existence of several drawbacks associated with enzyme specificity, drug delivery and stability, and the occurrence of serious side effects.[31] More important may be the timing of administration of the different inhibitory drugs.[4,32] The possibility to obtain better therapeutic efficacy by Timp1 gene transfer and overexpression might provide several advantages as compared to systemic drug administration. Among these advantages, our *in vivo* data underscore the possibilities to achieve a higher local concentration of the therapeutic molecule through direct intratumoral administration, thus avoiding serious side effects at distant sites, and to obtain sustained and prolonged expression of this molecule by single gene administration.

## Materials and methods

### *Cell cultures*

The human Eahy.926 cells, of endothelial origin, were derived from the fusion of human umbilical vein endothelial cells with the A549 carcinoma cell line,[33] and still retain endothelial characteristics.[34] KS-IMM is an immortalized cell line derived from a human KS lesion, which forms highly vascularized tumors *in vivo*.[15] Human HEK 293 and hamster CHO cells were purchased from the American Type Culture Collection, Manassas, VA. All cells were cultured in D-MEM, supplemented with 10% FCS, 100 U/ml penicillin, 100 $\mu$g/ml streptomycin, and maintained at 37°C under a mixture of 95% air and 5% $CO_2$.

### *Western blotting for Timp1*

To analyze Timp1 levels in cell-associated and conditioned media fractions, cells were washed after infection with AAV-Timp1 and maintained in serum-free media for 24 hours. Conditioned media were collected and concentrated using Centricon-10 filter units (Amicon, Inc., Stonehouse). Immunoreactive proteins were visualized using the mouse monoclonal antibody 102D1 against Timp1 (NeoMarkers, Fremont, CA) and a chemiluminescence assay (ECL, Amersham Pharmacia Biotech, Little Chalfont).

### *Zymography and reverse zymography*

KS-IMM and Eahy.926 total cell lysates were harvested and used for substrate gel electrophoresis. Samples were normalized for protein content and resolved in nonreducing conditions on a 0.1% gelatin (Sigma Chemical Co., St Louis, MO) and 12% SDS-polyacrylamide gel. After electrophoresis, the gel was washed at room temperature for 30 minutes in 2.5% Triton X-100 to remove SDS and incubated for 16 hours at 37°C with shaking in the developing buffer (50 mM Tris-HCl, pH 7.4, 10 mM $CaCl_2$ and 0.05% Brij 35). The gel was stained in 0.1% Coomassie brilliant blue. Clear zones against the blue background indicate the presence of gelatinolytic activity.

Functional activity of secreted Timp1 was assessed by reverse gel zymography. 293 cells transfected with pAAV-Timp1 were cultured for 24 hours in serum-free D-MEM and culture supernatants were harvested, filtered, concentrated by ultrafiltration through Centricon-10 filter units (Amicon, Inc., Stonehouse) and loaded onto a 0.2% gelatin and 12.5% SDS-polyacrylamide gel. The gel was then incubated for 16 hours in the supernatant from KS-IMM cells, used as a source of MMPs. Functional Timp1 appeared as a dark band at approximately Mr 28,000.

### *Matrigel invasion assay*

To visualize and quantify cellular invasion, $1 \times 10^5$ Eahy.926 cells were incubated for 1 hour in conditioned medium from Timp1- or mock-transfected cells and seeded in the upper chamber of 8 $\mu$m pore size 24-well plate invasion chambers coated with Matrigel Matrix (Biocoat Matrigel Invasion Chamber, Becton Dickinson, San Jose, CA). Supernatant from KS-IMM cells, which contains numerous chemoattractants, was placed in the lower compartment of the chamber. After 24 hours, the cells on the upper surface of the filter were removed by

gentle scraping with a cotton bud, whereas those that had migrated to the lower side were fixed in methanol and stained with Giemsa solution. Five random 400 × fields were counted per section. Each sample was performed in triplicate. Data are presented as mean number of invaded cells/400 × field.

### *Chick embryo chorioallantoic membrane assay*

CAMs of fertilized chicken eggs were maintained at 37°C. On day 3 of incubation, 2 ml of albumin was removed to detach the developing CAM from the shell and an oval window was opened in the upper side of the shell. After 5 days, 5 $\mu$l of AAV-Timp1- or mock-transduced CHO cells, together with 50 ng of recombinant hVEGF, were loaded onto 1 $mm^3$ gelatin sponges (Gelfoam; Pharmacia-Upjohn, Kalamazoo, MI), previously applied onto the top of the CAM. Sponges adsorbed with wt CHO cells and hVEGF alone were used as negative and positive controls respectively. CAMs were examined daily under a stereomicroscope and photographed at day 12, when the angiogenic response peaked.

### *AAV vectors*

The rAAV vector used in this study is based on the pTR-UF5 construct that was kindly provided by N Muzyczka (University of Florida, Gainesville, FL), which expresses the GFP gene under the control of the human CMV immediate early promoter. The coding sequence of the human Timp1 cDNA was obtained by RT-PCR amplification and cloned in the vector to substitute the GFP and neomycin-resistance genes. Cloning and propagation of AAV plasmids was carried out in the JC 8111 *Escherichia coli* strain. Infectious AAV2 vector particles were generated in 293 cells, cultured in 150 mm-diameter Petri dishes, by cotransfecting each plate with 15 $\mu$g of each vector plasmid together with 45 $\mu$g of the packaging/helper plasmid, pDG (kindly provided by JA Kleinschmidt, Heidelberg, Germany), expressing AAV and adenovirus helper functions. Viral stocks were obtained by $CsCl_2$ gradient centrifugation as previously described.[19,35] rAAV titers were determined by measuring the copy number of viral genomes in pooled, dialyzed gradient fractions using a competitive PCR procedure with primers and competitors mapping in the CMV promoter region common to all vectors.[19] The titers of all the viral preparations used in this study were in the range between $\sim 1 \times 10^{12}$ and $\sim 1 \times 10^{13}$ particles/ml. The efficiency of transduction of KS-IMM cells by AAV vectors was evaluated with or without overnight treatment with 1 mM hydroxyurea, an agent that increases transduction of different cell types.[19]

### *Flow cytometry*

Flow cytometric analysis of GFP-expressing cells after transduction with AAV-GFP was performed on a FACScalibur (Becton Dickinson, San Jose, CA) instrument acquiring $1 \times 10^4$ events for each sample.

### *Immunocytochemistry*

Protocols for immunocytochemistry were according to the Vectastain Elite ABC Kit (universal or goat) from Vector Laboratories using an antibody against Timp1 from NeoMarkers, Fremont, CA. After treatment, slides were rinsed in PBS and signal was developed using 3,3′-diaminobenzidine as substrate for the peroxidase chromogenic reaction (Lab Vision Corporation, Fremont, CA).

### *Tumor growth* in vivo

Animal care and treatment were conducted in conformity with institutional guidelines in compliance with national and international laws and policies (EEC Council Directive 86/609, OJL 358, December 12, 1987). In a first set of experiments, after 48 hours transduction with the AAV-Timp1 and AAV-LacZ vectors, $5 \times 10^6$ KS-IMM cells were resuspended in Matrigel (10 mg/ml) and injected subcutaneously in the flanks of healthy nude (nu/nu) mice (six animals per group). In a second set of experiments, to measure the therapeutic potential of AAV-Timp1 into established tumors, $4 \times 10^6$ KS-IMM cells resuspended in Matrigel were injected into the subcutaneous tissue of nude (nu/nu) mice (five animals per group). After 1 week, intratumoral injections of AAV-Timp1 or AAV-LacZ ($5 \times 10^{11}$ viral particles) were performed every second day, three times. An additional administration of each vector was performed on day 21, when the tumors became substantially larger, thus allowing easier injection into the center of the tumor mass and, most likely, the transduction of a greater number of cells. Tumor size was measured over time with a caliber following standard procedures. After 35 days, the animals were killed and tumor specimens were taken from the injection sites. Each sample was fixed in formalin, embedded in paraffin, sectioned and histologically analyzed by hematoxylin and eosin staining.

### *Statistical analysis*

Statistical analysis was performed with a nonparametric Mann–Whitney test to compare variables between groups using the StatView 4.5 statistical software package for Macintosh (Abacus Concepts, Berkeley, CA).

## Acknowledgments

This work was supported by grants from the Progetto Finalizzato "Genetica Molecolare" of the Consiglio Nazionale delle Ricerche, Italy, from the Fondazione Cassa di Risparmo of Trieste, Italy, from the Associazione Italiana per la Ricerca sul Cancro, Italy and from the Istituto Superiore di Sanità-AIDS project. Raffaella dell'Eva is recipient of a Federazione Italiana Sclerosi Multipla (FISM) fellowship. We are very grateful to Barbara Boziglav and Mauro Sturnega for excellent technical support and to Suzanne Kerbavcic for editorial assistance.

## References


1. Brinckerhoff CE, Rutter JL, Benbow U. Interstitial collagenases as markers of tumor progression. *Clin Cancer Res*. 2000;6:4823–4830.
2. Folkman J, Watson K, Ingber D, Hanahan D. Induction of angiogenesis during the transition from hyperplasia to neoplasia. *Nature*. 1989;339:58–61.
3. Nagase H, Woessner Jr JF. Matrix metalloproteinases. *J Biol Chem*. 1999;274:21491–21494.
4. Egeblad M, Werb Z. New functions for the matrix metalloproteinases in cancer progression. *Nat Rev Cancer*. 2002;2:161–174.
5. Stetler-Stevenson WG, Yu AE. Proteases in invasion: matrix metalloproteinases. *Semin Cancer Biol*. 2001;11:143–152.
6. DeClerck YA, Imren S, Montgomery AM, et al. Proteases and protease inhibitors in tumor progression. *Adv Exp Med Biol*. 1997;425:89–97.
7. Murphy G, Cawston TE, Reynolds JJ. An inhibitor of collagenase from human amniotic fluid. Purification, characterization and action on metalloproteinases. *Biochem J*. 1981;195:167–170.
8. Stetler-Stevenson WG. Matrix metalloproteinases in angiogenesis: a moving target for therapeutic intervention. *J Clin Invest*. 1999;103:1237–1241.
9. Bloomston M, Shafii A, Zervos EE, Rosemurgy AS. TIMP-1 overexpression in pancreatic cancer attenuates tumor growth, decreases implantation and metastasis, and inhibits angiogenesis. *J Surg Res*. 2002;102:39–44.
10. Kawamata H, Kawai K, Kameyama S, et al. Overexpression of tissue inhibitor of matrix metalloproteinases (TIMP1 and TIMP2) suppresses extravasation of pulmonary metastasis of a rat bladder carcinoma. *Int J Cancer*. 1995;63:680–687.
11. Li G, Fridman R, Kim HR. Tissue inhibitor of metalloproteinase-1 inhibits apoptosis of human breast epithelial cells. *Cancer Res*. 1999;59:6267–6275.
12. Yamauchi K, Ogata Y, Nagase H, Shirouzu K. Inhibition of liver metastasis from orthotopically implanted colon cancer in nude mice by transfection of the TIMP-1 gene into KM12SM cells. *Surg Today*. 2001;31:791–798.
13. Rigg AS, Lemoine NR. Adenoviral delivery of TIMP1 or TIMP2 can modify the invasive behavior of pancreatic cancer and can have a significant antitumor effect *in vivo*. *Cancer Gene Ther*. 2001;8:869–878.
14. Guedez L, Courtemanch L, Stetler-Stevenson M. Tissue inhibitor of metalloproteinase (TIMP)-1 induces differentiation and an antiapoptotic phenotype in germinal center B cells. *Blood*. 1998;92:1342–1349.
15. Albini A, Paglieri I, Orengo G, et al. The beta-core fragment of human chorionic gonadotrophin inhibits growth of Kaposi's sarcoma-derived cells and a new immortalized Kaposi's sarcoma cell line. *AIDS*. 1997;11:713–721.
16. Bussolino F, Arese M, Montrucchio G, et al. Platelet activating factor produced *in vitro* by Kaposi's sarcoma cells induces and sustains *in vivo* angiogenesis. *J Clin Invest*. 1995;96:940–952.
17. Marchisone C, Del Grosso F, Masiello L, et al. Phenotypic alterations in Kaposi's sarcoma cells by antisense reduction of perlecan. *Pathol Oncol Res*. 2000;6:10–17.
18. Cassoni P, Sapino A, Deaglio S, et al. Oxytocin is a growth factor for Kaposi's sarcoma cells: evidence of endocrine-immunological cross-talk. *Cancer Res*. 2002;62:2406–2413.
19. Zentilin L, Marcello A, Giacca M. Involvement of cellular double-strand DNA break-binding proteins in processing of recombinant adeno-associated virus (AAV) genome. *J Virol*. 2001;75:12279–12287.
20. Albini A, Fontanini G, Masiello L, et al. Angiogenic potential *in vivo* by Kaposi's sarcoma cell-free supernatants and HIV-1 tat product: inhibition of KS-like lesions by tissue inhibitor of metalloproteinase-2. *AIDS*. 1994;8:1237–1244.
21. Albini A, Marchisone C, Del Grosso F, et al. Inhibition of angiogenesis and vascular tumor growth by interferon-producing cells: a gene therapy approach. *Am J Pathol*. 2000;156:1381–1393.
22. Cai T, Fassina G, Morini M, et al. *N*-acetylcysteine inhibits endothelial cell invasion and angiogenesis. *Lab Invest*. 1999;79:1151–1159.
23. Fisher KJ, Jooss K, Alston J, et al. Recombinant adeno-associated virus for muscle directed gene therapy. *Nat Med*. 1997;3:306–312.
24. Snyder RO, Spratt SK, Lagarde C, et al. Efficient and stable adeno-associated virus-mediated transduction in the skeletal muscle of adult immunocompetent mice. *Hum Gene Ther*. 1997;8:1891–1900.
25. Monahan PE, Samulski RJ. AAV vectors: is clinical success on the horizon? *Gene Therapy*. 2000;7:24–30.
26. Jiang Y, Goldberg ID, Shi YE. Complex roles of tissue inhibitors of metalloproteinases in cancer. *Oncogene*. 2002;21:2245–2252.
27. Cesarman E, Mesri EA, Gershengorn MC. Viral G protein-coupled receptor and Kaposi's sarcoma: a model of paracrine neoplasia? *J Exp Med*. 2000;191:417–422.
28. Harris AL. Antiangiogenesis for cancer therapy. *Lancet*. 1997;349:SII13–SII15.
29. Tosetti F, Ferrari N, De Flora S, Albini A. Angioprevention: angiogenesis is a common and key target for cancer chemopreventive agents. *FASEB J*. 2002;16:2–14.
30. Toschi E, Barillari G, Sgadari C, et al. Activation of matrix-metalloproteinase-2 and membrane-type-1-matrix-metalloproteinase in endothelial cells and induction of vascular permeability *in vivo* by human immunodeficiency virus-1 Tat protein and basic fibroblast growth factor. *Mol Biol Cell*. 2001;12:2934–2946.
31. Zucker S, Cao J, Chen WT. Critical appraisal of the use of matrix metalloproteinase inhibitors in cancer treatment. *Oncogene*. 2000;19:6642–6650.
32. Bergers G, Javaherian K, Lo KM, et al. Effects of angiogenesis inhibitors on multistage carcinogenesis in mice. *Science*. 1999;284:808–812.
33. Edgell CJ, McDonald CC, Graham JB. Permanent cell line expressing human factor VIII-related antigen established by hybridization. *Proc Natl Acad Sci USA*. 1983;80:3734–3737.
34. Marchisone C, Benelli R, Albini A, et al. Inhibition of angiogenesis by type I interferons in models of Kaposi's sarcoma. *Int J Biol Markers*. 1999;14:257–262.
35. Deodato B, Arsic N, Zentilin L, et al. Recombinant AAV vector encoding human VEGF165 enhances wound healing. *Gene Therapy*. 2002;9:777–785.

# Acknowledgements

*There are people in life who leave a mark on you. Once you have met them, you can't be as you were before. Have you become better? This is a hard question... life is probably the most difficult experiment you will ever have to carry on. There are no protocols and guidelines. I have got only a few smart suggestions so far: be yourself and, sometimes, take it easy.*

*To those special people go my special thanks.*